TESIS DE LA UNIVERSIDAD DE ZARAGOZA

2019

87

Clara Aguilar Pérez

Antimicrobial activity and mode of action of bacteriocin AS-48 against Mycobacterium tuberculosis

Departamento
Microbiología, Medicina Preventiva y Salud Pública

Director/es
AINSA CLAVER, JOSE ANTONIO

ISSN 2254-7606

Prensas de la Universidad
Universidad Zaragoza

ISSN 2254-7606

Universidad Zaragoza
1542

Tesis Doctoral

ANTIMICROBIAL ACTIVITY AND MODE OF ACTION OF BACTERIOCIN AS-48 AGAINST MYCOBACTERIUM TUBERCULOSIS

Autor

Clara Aguilar Pérez

Director/es

AINSA CLAVER, JOSE ANTONIO

UNIVERSIDAD DE ZARAGOZA

Microbiología, Medicina Preventiva y Salud Pública

2019

Antimicrobial activity and mode of action of bacteriocin AS-48 against *Mycobacterium tuberculosis*

Clara
Aguilar Pérez

Tesis doctoral
2019

Universidad Zaragoza
1542

INDEX

CHAPTER 2

CHAPTER 3

CONCLUSIONS

ANNEXES

ABSTRACT

The increasing incidence of multi-drug resistant strains of *Mycobacterium tuberculosis* and the very few drugs available for treatment are promoting the development of a new line of drugs that try to solve these problems. Following this idea, we explored the antibacterial peptide AS-48, produced by *E. faecalis*, which is targeting the bacterial membrane, and it is active against several Gram-positive bacteria. We demonstrated that AS-48 has a bactericidal action against *M. tuberculosis* including H37Rv and other clinical and reference strains, and also against some non-tuberculous clinical mycobacterial species. We highlight the synergistic effect of the combination of AS-48 with either lysozyme or ethambutol (commonly used in the treatment of tuberculosis), two compounds that increase antimicrobial action of AS-48. Under these conditions, AS-48 kills *M. tuberculosis* at a lower dose, and exhibits a MIC (Minimal Inhibitory Concentration) close to some of the first line anti-TB agents.

In addition, we assayed cytotoxicity of AS-48 against THP-1, MHS and J774 macrophage cell lines, and found that at concentrations close to the MIC of AS-48 we could not detect any cytotoxic effect. The activity of AS-48 for inhibiting *M. tuberculosis* growth was also observed within the infected macrophages; in this model, synergy was also observed for combinations of AS-48 and ethambutol.

We have explored the mechanism of action of bacteriocin AS-48 against *M.tuberculosis* showing that, AS-48 is affecting the membrane, which is one of the unexplored targets that would reduce the incidence of new resistant strains. In addition, some mechanism related with the appearance of persistent strains seems to be altered after treating *M. tuberculosis* with AS-48. We have assayed transcriptomics analysis in order to better understand the As-48 mode of action.

Interestingly, we have demonstrated that, AS-48 is also targeting the mobility of the DNA, probably affecting other molecular process. Therefore, we can consider AS-48 as a multitarget drug reducing the probabilities to develop a resistant mutant strain.

In vivo toxicity studies, have been performed showing that the BALB/c strain is lesser sensitive to AS-48 than C57BL/6. The subchronic toxicity assays shows that mice are keeping healthy in treatments of ten days with doses of 2-1 mg/Kg body weight of AS-48.

However, in the efficacy assay, AS-48 does not exhibit the antitubercular activity observed in the *in vitro* assays, even along with ethambutol was not shown to reduce bacterial burden in *M. tuberculosis* infected mice.

In summary, we consider that combination of ethambutol and the bacteriocin AS-48 has an interesting potential in antituberculosis therapy, due to its activity against mycobacterial species and its low cytotoxicity against cell lines.

RESUMEN

La creciente incidencia de cepas multirresistentes de *Mycobacterium tuberculosis* y los pocos medicamentos disponibles para su tratamiento están promoviendo el desarrollo de una nueva línea de medicamentos que tratan de resolver estos problemas. Siguiendo esta idea, exploramos el péptido antibacteriano AS-48, producido por *E. faecalis*, cuya diana es la membrana bacteriana y, además, es activo contra varias bacterias grampositivas. Demostramos que AS-48 tiene una acción bactericida contra *M.tuberculosis*, incluyendo H37Rv y otras cepas clínicas y de referencia, también contra algunas especies micobacterianas clínicas no tuberculosas. Destacamos el efecto sinérgico de la combinación de AS-48 con lisozima o etambutol (comúnmente utilizado en el tratamiento de la tuberculosis), dos compuestos que aumentan la acción antimicrobiana de AS-48. En estas condiciones, AS-48 mata a *M. tuberculosis* a una dosis más baja y muestra una CIM (Concentración Inhibitoria Mínima) cercana a algunos de los agentes anti-TB de primera línea.

Además, ensayamos la citotoxicidad de AS-48 contra las líneas celulares de macrófagos THP-1, MHS y J774, y encontramos que a concentraciones cercanas a la CIM de AS-48 no pudimos detectar ningún efecto citotóxico. La actividad de AS-48 para inhibir el crecimiento de *M. tuberculosis* también se observó dentro de los macrófagos infectados; en este modelo, también se observó sinergia para las combinaciones de AS-48 y etambutol.

Hemos explorado el mecanismo de acción de la bacteriocina AS-48 contra *M. tuberculosis* que muestra que AS-48 está afectando la membrana, que es una de las dianas menos exploradas, y que reduciría la incidencia de nuevas cepas resistentes. Además, algunos mecanismos relacionados con la aparición de cepas persistentes parecen estar alterados después de tratar *M. tuberculosis* con AS-48. Hemos realizado un análisis transcriptómico para comprender mejor el modo de acción AS-48.

Curiosamente, hemos demostrado que AS-48 también tiene como diana la movilidad del ADN, probablemente afectando a otros procesos moleculares. Por

lo tanto, podemos considerar que AS-48 es un fármaco multidiana que reduce las probabilidades de desarrollar una cepa mutante resistente.

Se han realizado estudios de toxicidad *in vivo* que muestran que la cepa BALB/c es menos sensible a AS-48 que C57B/6. Los ensayos de toxicidad subcrónica muestran que los ratones se mantienen saludables en tratamientos de diez días con dosis de 2-1 mg/Kg de peso corporal de AS-48.

Sin embargo, en el ensayo de eficacia, el AS-48 no muestra la actividad antituberculosis observada en los ensayos *in vitro*, incluso junto con etambutol no demostró reducir la carga bacteriana en ratones infectados con *M. tuberculosis*.

En resumen, consideramos que la combinación de etambutol y bacteriocina AS-48 tiene un potencial interesante en el tratamiento antituberculoso, debido a su actividad contra las especies micobacterianas y su baja citotoxicidad contra las líneas celulares.

LIST OF ABREVIATIONS

ADC	Albumin, Dextrose and Catalase
ADME	Absortion, Distribution, Metabolism and Excretion
AMP	Antimicrobial Peptides
BCG	Bacilluss Calmette-Guérin
CETAB	Cetyl Trimetyl Ammonium Bromide
CFU	Colony Forming Unid
DEG	Differentially Expressed Genes
DNA	Desoxiribonucleic Acid
EDTA	Ethylene Diamine Tetr-Acetic
EMB	Ethambutol
EMSA	Electrophoretic Mobility Shift Assay
ETH	Ethionamide
ETOH	Ethanol
FBS	Fetal Bovine Serum
FDA	Food and Drug Administration
FC	Fold Change
FIC	Fractional Inhibitory Concentration
FICI	Fractional Inhibitory Concentration Index
FPKM	Fragments Per Kilobase of transcript per Million mapped reads
FSC	Forward scatter
GFP	Green Fluorescent Protein
Gran	Granulocytes
GRAS	Generally Regarded As Safe
HCT	Hematocrit
HCU	Hosputal Clínico Universitario Lozano Blesa
HE	Hematoxylin-eosin
HGB	Hemoglobin
HIV	Human Immunodeficiency virus
HMS	Hospital Miguel servet
IN	Intranasal
INH	Isoniazid
IP	Intraperitoneal
LAB	Lactic Acid Bacteria
LAM	lipoarabinomanan
Lym	Lymphocytes
MAP	Mitogen-Activated Protein
MCH	Mean Corpuscular Hemoglobin
MCHC	Mean Corpuscular Hemoglobin Concentration
MCV	Mean Corpuscular Volumne
MDR	Multi-drug Resistant
MIC	Minimum Inhibitory Concentration
Mon	Monocytes
MPV	Mean Platelet Volumne
MTBVAC	Mycobacterium Tuberculosis Vaccine candidate

MTT	3-(4,5-dimetiltiazol-2-il)-5-(3-carboximetoxifenil)-2-(4-sulfofenil)-2H-tetrazolio
NHP	Non-Human Primate
NR	Neutral Red
NTM	Non-Tunerculous Mycobacteria
OADC	Oleic, Albumin, Dextrose and Catalase
OECD	Organisation for Economic Co-operation and Development
PAS	Para-aminosalicylic acid
PBS	Phosphate Buffer Saline
PCR	Polymerase Chain Reaction
PCT	Procalcitonin
PDW	Platelet Distribution Width
PIM	Phosphatidylinositol-mannosides
PLT	Platelet count
PZA	Pyrazinamide
RBC	Red Blood Cells
RDW	Red cell Distribution Width
RIF	Rifampicin
RiPPs	Ribosomally synthesized and Post-translationally modified Peptides
RNA	Ribonucleic Acid
RQ	Relative Quantification
SDS	Sodium Dodecyl Sulfate
SEM	Scanning electron Microscopy
SSC	Side Scatter
TA	Toxin-Antitoxin System
TDR	Totally-Drug Resistant
TFA	Trifluoroacetic
WBC	White Blood Cells
WGS	Whole-Genome Sequencing
WHO	World Health Organization
XDR	Extensively drug resistant

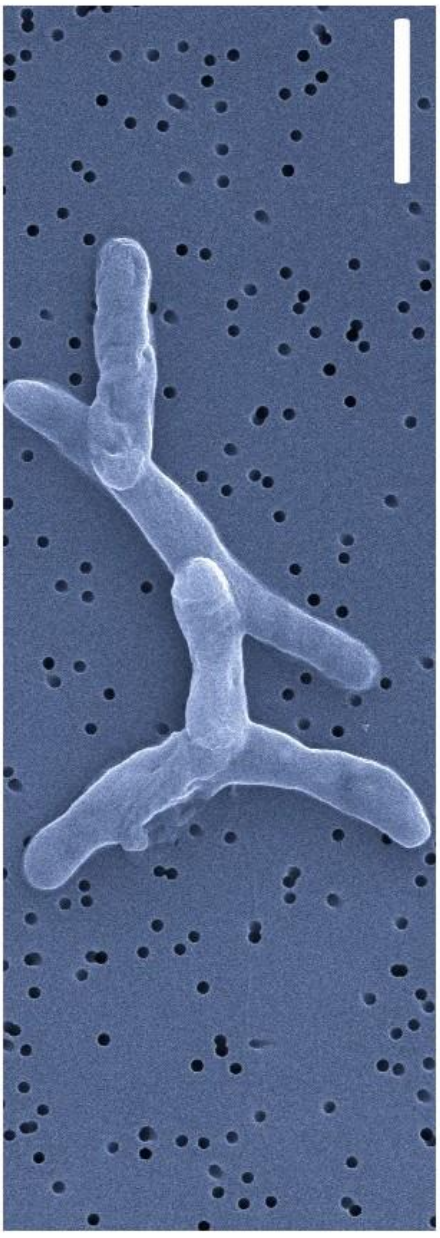

Introdution

HISTORY OF TUBERCULOSIS DISEASE

TUBERCULOSIS, A PANDEMIC STILL IN 21ST CENTURY

Tuberculosis is the most lethal infectious disease in our days, according to the WHO 2018 report (1) causing 1.4 million deaths per year. It has caused through history a great amount of deaths, taking a huge importance not only in the field of medicine but also in the literature, art and music. It is thought that tuberculosis could be the oldest disease in the history of humanity, it is thought that an early progenitor of *M. tuberculosis* was present in East Africa as around 3 million years ago, infecting early hominids (2). In Egypt, mummies of humans affected by tuberculosis infection dated from the 3rd Intermediate Period (1064-656 BC) have been found (3, 4). In the false door of a *mastaba* tomb of the Old Kingdom date(4th or 5th Dynasty, 2900 B.C.) has been discovered the representation of two humane figures with a deformity in the back, in the upper thoracic region, which is indicative of the Pott's disease (5), a form of tuberculosis outside the lungs and affecting the spine (**Figure 1**).

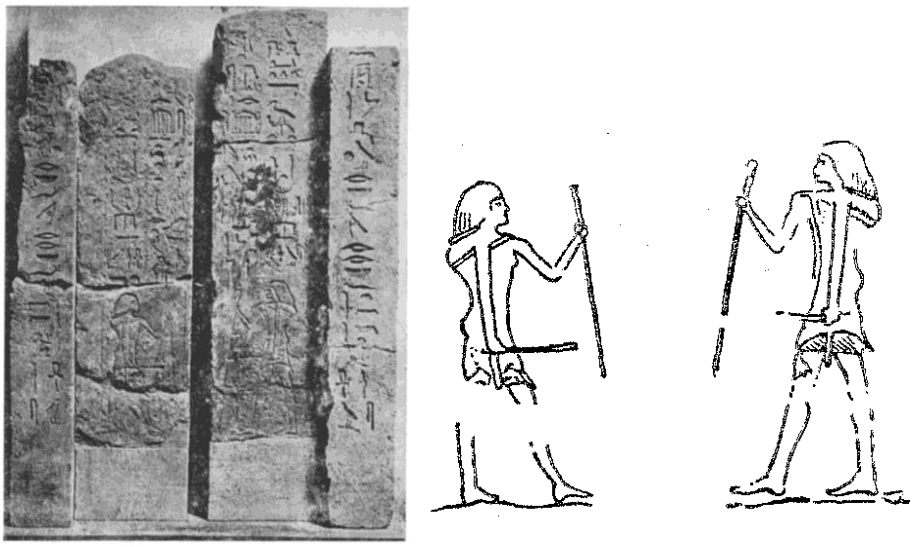

Figure 1: False door of a *mastaba* tomb (Glyptotek NY Carlsberg, Copenhagen). Detail of the human figure showing deformity due to tuberculous upper thoracic spine.

In ancient Greece, the disease of tuberculosis was cited in the *Book I, Of the Epidemics* wrote by Hippocrates (460-370 B.C.); tuberculosis was known as phtisis and described in this book as "comsumption was the most considerable of the

disease which then prevailed, and the only one which proved fatal to many persons" (6).

Tuberculosis was also an important disease in the Middle Ages and in Modern Era, having a high incidence across the centuries. The epidemic of tuberculosis was called "The White Plague", increased notably in the 17th century, and persisted for the following 200 years. The industrialization process triggered the migration of the population to the cities, where the high population density, poorly ventilated housing, malnutrition and the bad sanitary conditions make most of Europe and America the best environment for the spread of the disease (7). The huge amount of deaths that happened in the 18th century defined tuberculosis as "Captain of All These Men of Death" (7, 8).

During the 20th century, the development of a vaccine (BCG) (9) and the finding of several antituberculosis drugs, resulted in a decrease in the incidence of this disease; also patients had not to be hospitalized and the success of the treatment was high. Because of these factors, tuberculosis seemed to be a disease under control; in fact, in the earliest 80's tuberculosis was thought to be almost extinct. However, during this decade, the rising incidence of HIV infection and a general relaxation in measures for prevention, diagnosis and treatment of tuberculosis resulted in an upturn of this disease. In this way, the coinfection with HIV in tuberculosis patients was one of the key factors behind the increase of the incidence of tuberculosis, predominantly in those countries where both diseases are endemic (10).

THE CAUSATIVE AGENT OF TUBERCULOSIS

It was at the end of 19th century (1882) when Robert Koch identified the etiologic agent of tuberculosis as a bacterium that was named *Mycobacterium tuberculosis*. He performed new innovative methods to cultivate bacteria, in this case using potato and agar to get a pure culture of *M. tuberculosis*. Robert Koch also demonstrated that the origin of this disease was the presence of the bacilli of *M. tuberculosis* in animals or humans (4, 6). This was part of the Henle-Koch postulates that settle the basis for the study of the rest of the infectious diseases. Moreover, Robert Koch presented the "tuberculin" as a therapeutic for curing tuberculosis, but the results were not what expected. Even though, nowadays, tuberculin is still in use as a test for tuberculosis diagnosis (Mantoux test).

Image 2: Timeline summary of the history of tuberculosis.

THE GENUS MYCOBACTERIUM

Species in genus *Mycobacterium* are mostly free-living bacteria and do not to infect humans or cause any disease commonly. Classically, they have been divided according to their growth rate, hence being distinguished between fast-growing mycobacteria with a generation time between 2 and 5 hours, like *M. smegmatis*, and slow-growing mycobacteria like *M. tuberculosis,* that takes around 14-15 hours in completing a duplication round. In addition, slow-growing mycobacteria were classified based on the production of pigments and photoreactivity. Those species that produce carotenoid pigments when they are exposed to light, like *M. kansasii* and *M. marinum,* are named photochromogenic. The scotochromogenic mycobacteria produce orange or yellow colonies independently of the presence of light, like *M. gordonae* or *M. paraffinicum*. Finally, those mycobacteria that do not produce any pigments are known as non-chromogenic, like *M. tuberculosis* and *M. bovis*. This classification of mycobacteria is known as the Runyon classification and dates from 1959 (11).

In our days, however, mycobacterial species have been classified according to their genetic and evolutionary relationships, in particular those species belonging to the *M. tuberculosis* complex. This has been possible because *Mycobacterium tuberculosis* has a low mutation rate, and this has allowed to date the possible origin of modern ancestor of *M. tuberculosis* around 20,000-35,000 years ago (2). According to the study presented by Gutierrez MC, *et al*. (2), *Mycobacterium canetti* could correspond to a lineage from which the *M. tuberculosis* complex was evolved. More recently, Riojas MA, *et al*.(12) have observed that all the *Mycobacterium* species analysed are extremely close related indicating that they belong to the same specie (*Mycobacterium tuberculosis*) (**Image 3**), and they propose the use of a variants to define the current *Mycobactium* species (i.e. *M. tuberculosis* var *bovis*).

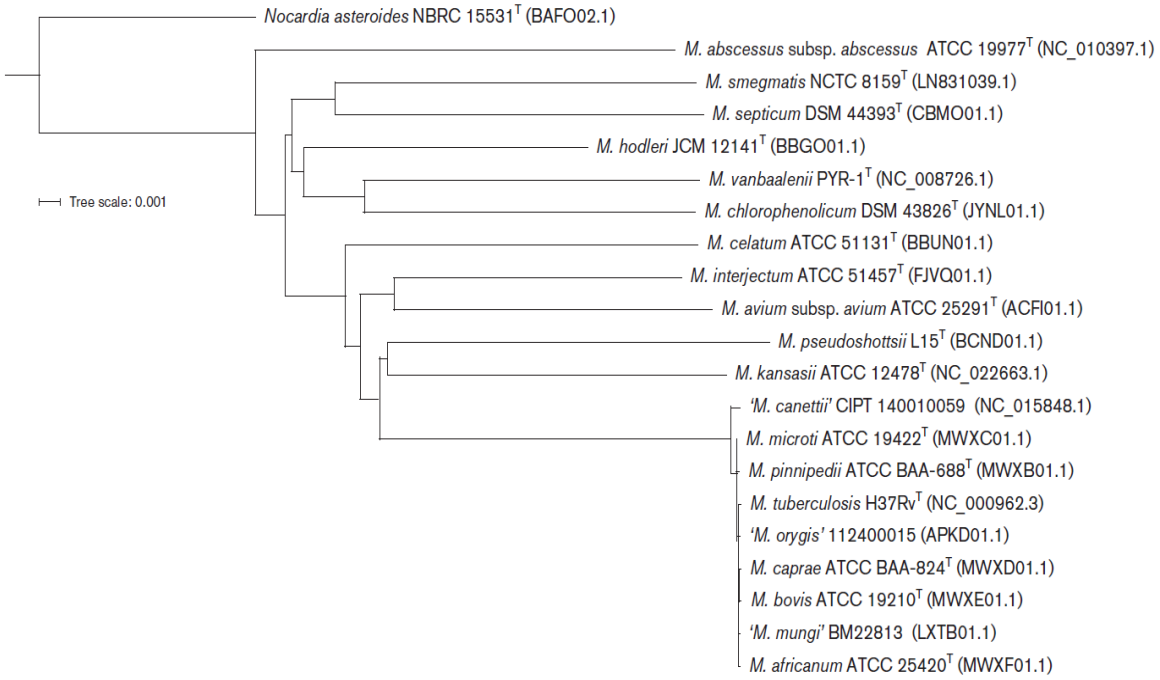

Image 3: Phylogenomic tree showing the relationship between the whole genomes of type strains of species of MTBC and the type strains of various other species of the genus Mycobacterium with Nocardia asteroides as an outgroup (12).

CHARACTERISTICS OF *M. TUBERCULOSIS*

Mycobacterium tuberculosis is an aerobic bacteria, so it grows in well aerated tissues, with a high oxygen tension, as it is the case of the lungs, where they grow mainly in the upper lobes. In laboratory conditions, an atmosphere of a 5-10% of carbon dioxide is provided since this promotes growth (13). Also, *M. tuberculosis* is neutrophilic and mesophilic, the best conditions to keep *M. tuberculosis* in culture are at 37ºC and neutral pH. Among the most common culture media used for M. tuberculosis, we find Middlebrook 7H9 (broth) and 7H10 and 7H11 (solid agar-containing media), and Coletsos and Lowenstein-Jensen (egg-based solid media). Middlebrook media must be supplemented with ADC (Albumin, Dextrose and Catalase) or OADC (Oleic, Albumin, Dextrose and Catalase) supplements. Giving that the hydrophobic mycobacterial envelope cause bacteria to clump when using liquid media, detergents or other dispersing agents are used to avoid clumps formation (14).

GENERAL FEATURES OF MYCOBACTERIAL CELLS

The mycobacteria are acid-fast, non-motile, non-spore forming and aerobic bacilli that belong to the phylum Actinobacteria. Then, phylogenetically, they belong to the group of Gram positive bacteria but present notable differences compared with the vast majority of other Gram positive bacteria, as detailed below. Mycobacteria have a high content of guanine cytosine (65.6%) in its DNA (15), and a high content of lipids in their cell wall. In fact, the 6.6%, of the total of 4111 genes described for *M. tuberculosis* (Mycobrowser database https://mycobrowser.epfl.ch/), are involved in lipid metabolism. Indeed, one of the most remarkable aspects of mycobacterial physiology is the composition and structure of their cell envelope.

MYCOBACTERIAL ENVELOPE: THE MEMBRANE, THE CELL WALL, AND THE CAPSULE

As in other bacteria, the membrane (16) is where many essential metabolic processes take place, such us transport of nutrients and wastes, communication with other cells in the microbial community, the respiratory chain and other metabolic process. The membrane must to keep its structure for the survival even when they are in non-replicating forms.

Mycobacterial cell wall (17-20) contains peptidoglycan, arabinogalactan, and an outermost layer of mycolic acids that confers a cover similar to wax. This is one of the aspects that makes mycobacterial envelope so impermeable and hence resistant to external agents. The structure and composition of the cell wall seems to be related with the slow growth rate of mycobacterial cells, given that the production of all complex components of the cell wall represents a high metabolic cost for the bacteria.

The peptidoglycan covers all the surface of bacterial membrane but differs from peptidoglycan present in other Gram positive bacteria in that, first, the muramic acid moiety has an N-glycolyl substituent instead of an N-acetyl group, and second, the number of cross-links between two peptidoglycan chains is higher than in other Gram positive bacteria.

The arabinogalactan is composed by D-arabinofuranosyl and D-galactofuranosyl sugars and keeps linked to the peptidoglycan through phosphodiester links.

The mycolic acids are hydrophobic hydrocarbon α-branched, β-hydroxylated fatty acids with around 90 carbon atoms with a high molecular weight. Mycolic acids are bond to the arabinose terminal residue of the arabinogalactan, in the external side of the cell wall, creating a hydrophobic layer that looks like the external membrane typically described in Gram negative bacteria, and that is frequently referred to as the mycomembrane. The length of mycolic acids is thought to be related with the virulence of the strain and the

survival of bacilli intracellularly (21). The mycomembrane also contains phospholipids, glycolipids, trehalose dimycolate, trehalose monomycolate, phosphatidylinositol-mannosides, and the lipoarabinomanan (LAM) that is a polysaccharide present in all kind of actinomycetales. The mycomembrane also contains porins, which create hydrophilic channels that allow the passive transport of hydrophilic molecules and other proteins.

The high content of lipids in mycobacterial cell wall contributes not only to its low permeability but also the innate resistance of mycobacteria to dehydration and consequently to their great resistance to antibacterial substances, and to its virulence. In fact, during the Gram staining, mycobacterial cells stain slightly blue due to colorants that cannot penetrate into the cell. For microscopy, giving they are resistant to de-coloration by acids and alcohols, they can be stained with acid-fast staining such as Ziehl-Neelsen or auramine-rhodamine fluorochrome stain (22).

Finally, mycobacteria also have a capsule, composed by proteins, polysaccharides and other lipids that are considered as virulence factor such us, the cord factor, a glycolipid also present in the cell wall. Cord factor is a trehalose 6,6'-dimycolate; this molecule is responsible for the characteristic chain formation of mycobacterial cells and their adhesion to the respiratory tract. This factor is also thought to be associated to the pathogenicity of *M. tuberculosis* and considered responsible of the inhibition of the acidification of the phagosome and granuloma formation (23).

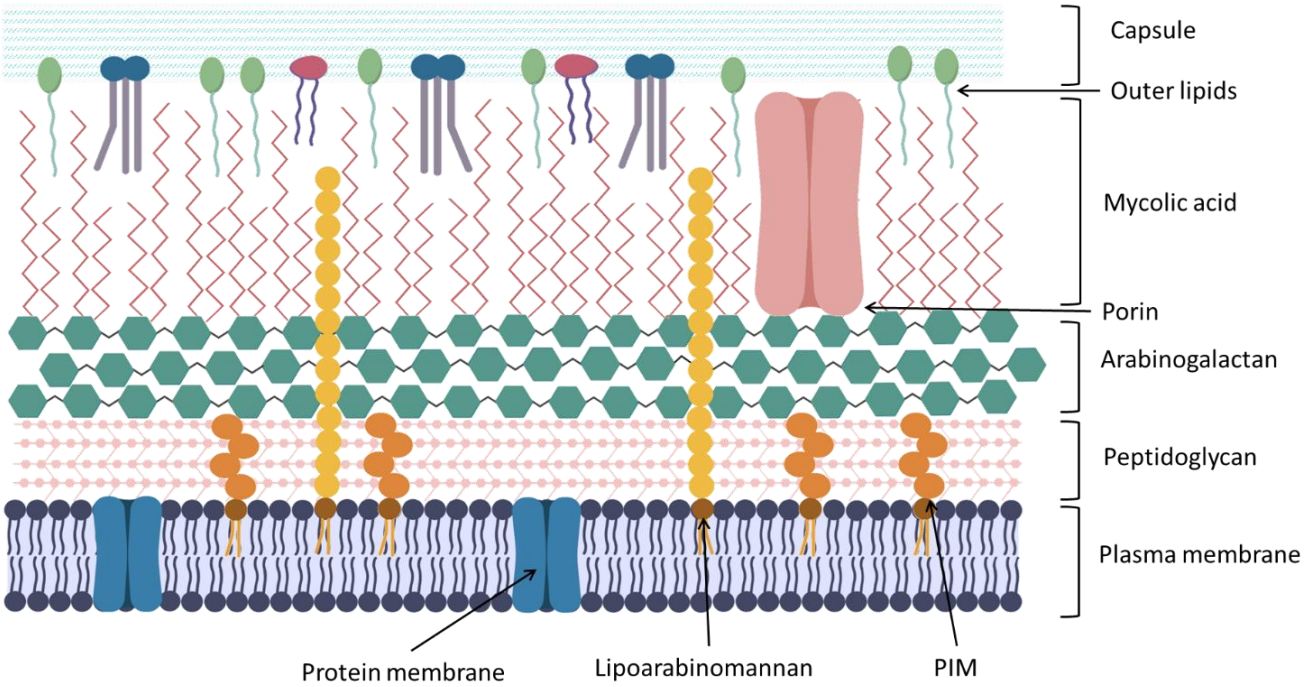

Image 4: Schematic representation of the cell wall structure.

PATHOGENICITY AND VIRULENCE OF M. TUBERCULOSIS

Humans are the unique reservoir of *M. tuberculosis*, and it seems that we, humans and *M. tuberculosis*, evolved together through years. *M. tuberculosis* is an obligate intracellular pathogen that is adapted to live within the pulmonary macrophages. *M. tuberculosis* is able to colonize also other tissues, developing other extra-pulmonary diseases, which are less common than the pulmonary tuberculosis (24, 25).

The success of the colonization in lungs implies the inhibition of numerous processes within the macrophages, which finally allows the intracellular proliferation of the bacilli. For example, *M. tuberculosis* blocks the fusion between the phagosome (the compartment where it resides, after having been phagocytosed) and the lysosomes; it also inhibits the antigen presentation, the beginning of the apoptotic cascade and the stimulation of the bactericide response mediated by MAP kinases, γ-interferon and calcium signals (26).

At the cellular level, the infection can be contained in a special structure called granuloma (**Image 5**).

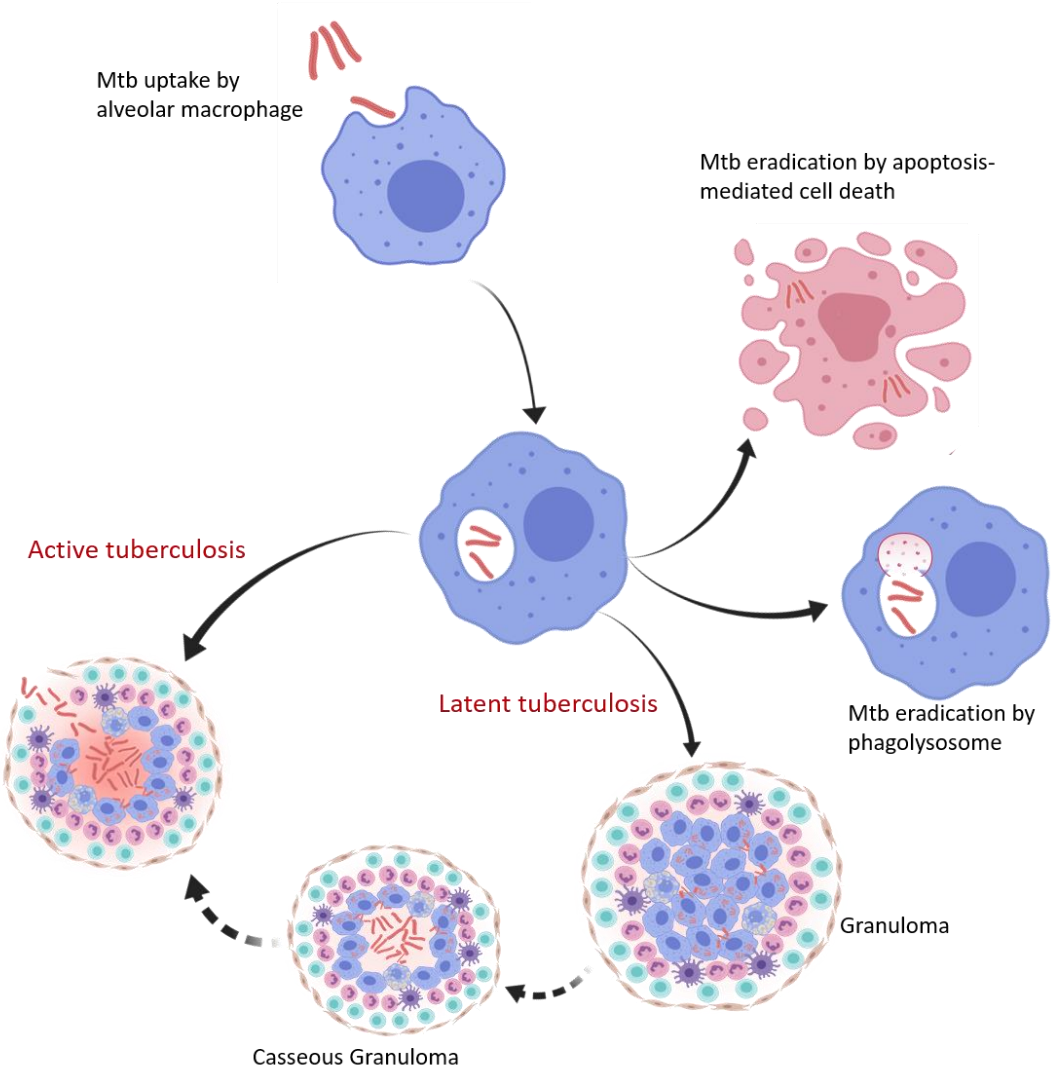

Image 5: Process of macrophage infection and granuloma formation.

It is composed by macrophages containing the bacilli, epithelioid cells, dendritic cells, neutrophils, fibroblast, and lymphocytes B and T. In some lesions, the granuloma can content an extracellular and fibrous matrix surrounding the cells that compose the granuloma. It is thought that the granuloma keeps the infection controlled, concentrating the immune response to this localized area, but it has been demonstrated that mycobacteria can escape from the granuloma and colonize other areas (25, 27). The 90% of the population infected with *M. tuberculosis* are able to control the infection within the granuloma and will not present any symptomatology of the disease; in this case, we say that tuberculosis

is in latent form. When the bacilli multiply uncontrolledly, the macrophage lyse and the bacilli that are released could be internalized by other macrophages or could escape from the granuloma. When this happens, an inflammation, calcification and colonization of the lymphatic nodules occurs creating the named Ghon complex. After the Ghon complex formation, the liquefaction process could happen in the bronchioles and the bacilli goes out through the respiratory tract, where it can be incorporated into small contagious particles that will be released in form of aerosol when the patient coughs of sneezes. If the liquefaction happens in a blood vessel, the infection could be spread throughout the organism. The granuloma could evolve into a necrotizing granuloma, which commonly begins by the centre of the granuloma forming a caseum core that eventually spread all around generating serious damage in the lung tissue. The bacilli are mainly found within the macrophage away of the immune system but it could be allocated in all kind of cells and type of lesion (27, 28).

Given that during infection, *M. tuberculosis* can go through a diversity of intra and extracellular locations, one factor contributing to the complexity of tuberculosis disease is that different subpopulations of bacteria are present during the infection, and there are numerous barriers that difficult the penetration of the different drugs to reach their targets.

CONFRONTING *M. TUBERCULOSIS* INFECTIONS

Similar to other microbial infections, the three major approaches to control tuberculosis disease are based on prevention, diagnostics and treatment.

PREVENTION

After the success obtained in the development of a smallpox vaccine by Edward Jenner, efforts concentrated in developing a vaccine for protecting against tuberculosis. Albert Calmette and Camile Guérin selected a *Mycobacterium bovis* strain, the etiological agent responsible of the tuberculosis infection in cattle, although it was discovered that also can cause the disease in humans. Calmette and Guérin subcultivated it for 230 times until they got an attenuated bacillus, named Bacille Calmette-Guérin (BCG). Since 1921, BCG has been the unique vaccine to prevent tuberculosis infection.

On recent decades, lack of protection conferred by BCG vaccine has been pointed out as one of the reasons for the increased incidence of tuberculosis. This has promoted a world wide effort to develop novel vaccines against tuberculosis, with improved protection than BCG. The University of Zaragoza is developing MTBVAC (**Image 6**), an attenuated live vaccine candidate based on the disruption of a transcriptional regulator that controls several virulence factors (29-31). Currently this vaccine candidate is in clinical phase II in adults and newborns.

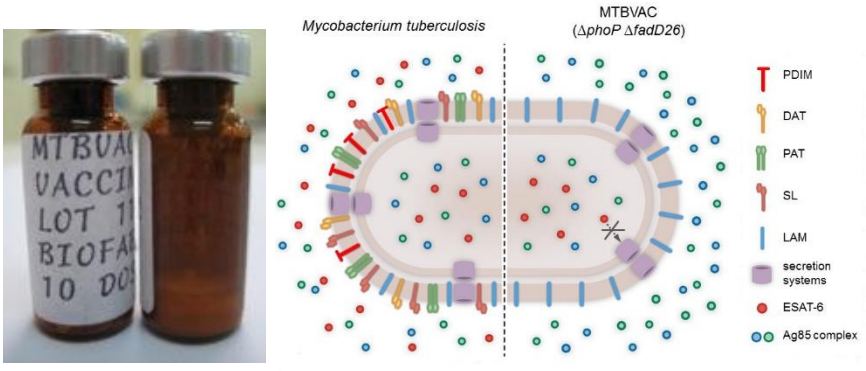

Image 6: MTBVAC candidate, live attenuated vaccine. Developed in the University of Zaragoza and produced by Biofabri.

DIAGNOSTICS

Classical methods to diagnose(32) whether a patient has tuberculosis, include chest X-ray (**Image 7**) since it allows to see the pulmonary lesions; however, this technique is not specific for tuberculosis and other infectious (or even, non-infectious) diseases may lead to a wrong diagnostic. Then, normally, it has to be confirmed with a microscopic examination of a sputum sample (after, for example, a Zielh-Neelsen stain (**Image 7**)), as well as a bacteriological culture test. However, cultivation of *M. tuberculosis* takes between 2 and 6 weeks to show a positive result on conventional tuberculosis culture media (although this time can be importantly reduced by using fluorescent detection of mycobacterial growth, using automated systems such as the MGIT-960 (Becton Dickinson)). The tuberculosis skin test (Mantoux test) has been also widely used, and consists on the injection of a small amount of tuberculin subcutaneously (33). If a skin reaction is observed at the site of injection (**Image 7**), it is assumed to reveal the presence of *M. tuberculosis* in the organism, but it cannot distinguish between latent and active forms. Moreover, Mantoux test cannot distinguish neither between vaccinated and infected patients, and previous immunization by environmental non-tuberculous mycobacteria also can lead to false positive results.

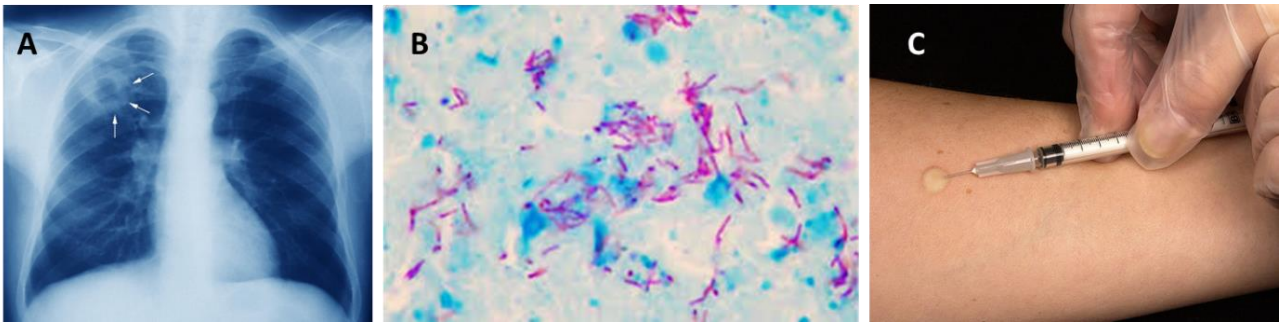

Image 7: A) Thorax x-Ray showing lesions produced by tuberculosis (arrows). B) Zielh-Neelsen stain, the bacilli of *M. tuberculosis* are in pink. C) Mantoux test.

Given the uncertainty associated to most classical diagnostic methods, novel methods based on molecular analysis (34) have been developed in recent years, which frequently are complementary to one or several of the classical methods described above. The Interferon Gamma Release Assay (IGRAs) is an

immunological assay that measures the production of the cytokine interferon gamma in blood samples when stimulated with specific *M. tuberculosis* antigens. Other molecular methods, more specific and sensitive, are those based on nucleic acid amplification through the PCR technique, frequently combined with hybridization on strip, for easy detection of amplification products. Most of these methods have been automatized and are adapted for convenient and fast diagnosis of tuberculosis in clinical microbiology laboratories, such as the GeneXpert® (Cepheid) system (35).

TREATMENT AND DRUG RESISTANCE

The different treatments used to cure tuberculosis have been changing along history, from bathing in human urine, eating wolf liver, avoid eating, doing exercise or having rest in the mountains. Indeed, the sanatoriums in the mountains, far away from the cities, became very popular during 19th century and the first half of 20th century to treat tuberculosis. The medical prescription was to rest in sanatorium, and take fresh air and good nutrition; the fact is that some patients cured spontaneously from the disease (33, 36).

In 1943, Selman Waksman discovered the antibiotic streptomycin from a *Streptomyces griseus* isolate; this was the first antimicrobial used in the treatment of tuberculosis, although resistance to streptomycin arose frequently (37). One year later, para-aminosalicylic acid (PAS), a derivative from aspirin, showed great results in tuberculosis treatment, and seemed to be less prone to select resistance than streptomycin. At that time, it was observed that, when applying a combination of both antimicrobials, patients had more probabilities to recover than when they were treated with only one of these drugs. This was the beginning of the combined therapy, a key factor in tuberculosis treatment.

Isoniazid was the third antibiotic discovered to have antitubercular activity and included in the combined treatment. With these three drugs, tuberculosis became a disease completely curable, but the treatment still has to be administered

during a long period, 18-24 months. In the decade of the 60s PAS was substituted by ethambutol and timing was reduced to 18 months. After introducing rifampicin and pyrazinamide, treatment was reduced up to six months (38). Nowadays, the antitubercular therapy include always a combined treatment of isoniazid, rifampicin, pyrazinamide and ethambutol during two months, and is followed by four months taking only rifampicin and isoniazid. Since then, combined therapy was established as the only way to cure tuberculosis infection. It was clear that applying one single drug as monotherapy forced the selection of those bacilli that are drug resistant, which could proliferate again without curing the infection (39).

Over the years, other antitubercular drugs have been discovered. Antitubercular drugs can be classified as first, second and third line drugs depending on the preference for treatment, which is based on efficacy of antitubercular activity as well as toxicity. First-line drugs are rifampicin, isoniazid, pyrazinamide, streptomycin and ethambutol. Belonging to the group of second line drugs are kanamycin, amikacin, capreomycin, ethionamide and fluoroquinolones.

In 1990, in New York, it was isolated the so called "W strain" as being the first strain resistant to isoniazid, rifampicin, ethambutol and streptomycin. In three years, this strain had spread to eleven other hospitals and had affected 367 people. The patients infected with this strain had a death rate of 83%, due to the difficulty to use an appropriate treatment (40).

Over the years, other *M. tuberculosis* strains resistant to main antituberculosis drugs have been isolated world-wide. Investigation of molecular basis of drug resistance have revealed that in *M. tuberculosis*, the major mechanism of drug resistance is mediated through the acquisition of chromosomal mutations in genes encoding either drug target proteins or drug activating enzymes. Extensive reports of mutations found in drug resistant isolates have allowed the development of molecular methods for detecting drug resistant isolates (41-45). Most methods are based on PCR, frequently in combination with chromatographic detection on strips with immobilized oligonucleotides containing the most

popular mutations that result in drug resistance; in such devices (like for example the Line Probe Assay (46)) hybridization of the PCR amplification product on the strip results in a pattern indicative of drug resistance.

Globally, a strain in considered as MDR (multi-drug resistant) when it is resistant to rifampicin and isoniazid at least; XDR (extensively drug resistant) strains are those MDR strains that also show resistance to fluoroquinolone, and one of the injectable second-line drugs (amikacin, kanamycin or capreomycin). In light of the increase of the MDR and XDR prevalence, there is an urgent need for developing new antimicrobials against tuberculosis.

Since the 1970s, only bedaquiline (47) and delamanid (48) have reached the market of novel drugs against tuberculosis, which seems insufficient for confronting the tuberculosis epidemic and their resistant variants. New strategies that pursue the reduction of the treatment, by using combined therapy (as it has been proved useful in the past for reducing tuberculosis treatment) need to be investigated.

REFERENCES

1. Organization WH. 2018. Global tuberculosis report 2018.
2. Gutierrez MC, Brisse S, Brosch R, Fabre M, Omais B, Marmiesse M, Supply P, Vincent V. 2005. Ancient origin and gene mosaicism of the progenitor of Mycobacterium tuberculosis. PLoS Pathog 1:e5.
3. Lalremruata A, Ball M, Bianucci R, Welte B, Nerlich AG, Kun JF, Pusch CM. 2013. Molecular identification of falciparum malaria and human tuberculosis co-infections in mummies from the Fayum depression (Lower Egypt). PLoS One 8:e60307.
4. Barberis I, Bragazzi NL, Galluzzo L, Martini M. 2017. The history of tuberculosis: from the first historical records to the isolation of Koch's bacillus. J Prev Med Hyg 58:E9-E12.
5. Cave A. 1939. The evidence for the incidence of tuberculosis in ancient Egypt. British Journal of Tuberculosis 33:142-152.
6. Daniel TM. 2006. The history of tuberculosis. Respir Med 100:1862-70.
7. Condrau F. 2001. "Who is the captain of all these men of death?" the social structure of a tuberculosis sanatorium in postwar Germany. J Interdiscip Hist 32:243-62.
8. Grange J, Mwaba P, Dheda K, Hoelscher M, Zumla A. 2010. World TB Day 2010--new innovations are required for enhancing the global fight against tuberculosis: the 'captain of all these men of death'. Trop Med Int Health 15:274-6.
9. Calmette A. 1928. On preventive vaccination of the new-born against tuberculosis by B.C.G. The British Journal of Tuberculosis XXII.
10. Bruchfeld J, Correia-Neves M, Kallenius G. 2015. Tuberculosis and HIV Coinfection. Cold Spring Harb Perspect Med 5:a017871.
11. Runyon EH. 1959. Anonymous mycobacteria in pulmonary disease. Med Clin North Am 43:273-90.
12. Riojas MA, McGough KJ, Rider-Riojas CJ, Rastogi N, Hazbon MH. 2018. Phylogenomic analysis of the species of the Mycobacterium tuberculosis complex demonstrates that Mycobacterium africanum, Mycobacterium bovis, Mycobacterium caprae, Mycobacterium microti and Mycobacterium pinnipedii are later heterotypic synonyms of Mycobacterium tuberculosis. Int J Syst Evol Microbiol 68:324-332.
13. Schaefer WB. 1957. Studies on the inhibiting effect of carbon dioxide on the growth of two mutant strains of Mycobacterium tuberculosis. J Bacteriol 73:52-5.
14. Larsen MH, Biermann K, Jacobs WR, Jr. 2007. Laboratory maintenance of Mycobacterium tuberculosis. Curr Protoc Microbiol Chapter 10:Unit 10A 1.
15. Cole ST, Brosch R, Parkhill J, Garnier T, Churcher C, Harris D, Gordon SV, Eiglmeier K, Gas S, Barry CE, 3rd, Tekaia F, Badcock K, Basham D, Brown D, Chillingworth T, Connor R, Davies R, Devlin K, Feltwell T, Gentles S, Hamlin N, Holroyd S, Hornsby T, Jagels K, Krogh A, McLean J, Moule S, Murphy L, Oliver K, Osborne J, Quail MA, Rajandream MA, Rogers J, Rutter S, Seeger K, Skelton J, Squares R, Squares S, Sulston JE, Taylor K, Whitehead S, Barrell BG. 1998. Deciphering the biology of Mycobacterium tuberculosis from the complete genome sequence. Nature 393:537-44.

16. Chen H, Nyantakyi SA, Li M, Gopal P, Aziz DB, Yang T, Moreira W, Gengenbacher M, Dick T, Go ML. 2018. The Mycobacterial Membrane: A Novel Target Space for Anti-tubercular Drugs. Front Microbiol 9:1627.

17. Alderwick LJ, Harrison J, Lloyd GS, Birch HL. 2015. The Mycobacterial Cell Wall--Peptidoglycan and Arabinogalactan. Cold Spring Harb Perspect Med 5:a021113.

18. Chiaradia L, Lefebvre C, Parra J, Marcoux J, Burlet-Schiltz O, Etienne G, Tropis M, Daffe M. 2017. Dissecting the mycobacterial cell envelope and defining the composition of the native mycomembrane. Sci Rep 7:12807.

19. Bhat ZS, Rather MA, Maqbool M, UL Lah H, Yousuf SK, Ahmad Z. 2017. Cell wall: A versatile fountain of drug targets in Mycobacterium tuberculosis. Biomedicine & Pharmacotherapy 95:1520-1534.

20. Marrakchi H, Laneelle MA, Daffe M. 2014. Mycolic acids: structures, biosynthesis, and beyond. Chem Biol 21:67-85.

21. Gotoh K, Mitsuyama M, Imaizumi S, Kawamura I, Yano I. 1991. Mycolic acid-containing glycolipid as a possible virulence factor of Rhodococcus equi for mice. Microbiol Immunol 35:175-85.

22. Holani AG, Ganvir SM, Shah NN, Bansode SC, Shende I, Jawade R, Bijjargi SC. 2014. Demonstration of mycobacterium tuberculosis in sputum and saliva smears of tuberculosis patients using ziehl neelsen and flurochrome staining- a comparative study. J Clin Diagn Res 8:ZC42-5.

23. Lee WB, Yan JJ, Kang JS, Chung S, Kim LK. 2017. Mycobacterial cord factor enhances migration of neutrophil-like HL-60 cells by prolonging AKT phosphorylation. Microbiol Immunol 61:523-530.

24. Kirschner DE, Young D, Flynn JL. 2010. Tuberculosis: global approaches to a global disease. Curr Opin Biotechnol 21:524-31.

25. Silva Miranda M, Breiman A, Allain S, Deknuydt F, Altare F. 2012. The tuberculous granuloma: an unsuccessful host defence mechanism providing a safety shelter for the bacteria? Clin Dev Immunol 2012:139127.

26. Schorey JS, Cooper AM. 2003. Macrophage signalling upon mycobacterial infection: the MAP kinases lead the way. Cell Microbiol 5:133-42.

27. Davis JM, Ramakrishnan L. 2009. The role of the granuloma in expansion and dissemination of early tuberculous infection. Cell 136:37-49.

28. Dartois V. 2014. The path of anti-tuberculosis drugs: from blood to lesions to mycobacterial cells. Nat Rev Microbiol 12:159-67.

29. Aguilo N, Gonzalo-Asensio J, Alvarez-Arguedas S, Marinova D, Gomez AB, Uranga S, Spallek R, Singh M, Audran R, Spertini F, Martin C. 2017. Reactogenicity to major tuberculosis antigens absent in BCG is linked to improved protection against Mycobacterium tuberculosis. Nat Commun 8:16085.

30. Arbues A, Aguilo JI, Gonzalo-Asensio J, Marinova D, Uranga S, Puentes E, Fernandez C, Parra A, Cardona PJ, Vilaplana C, Ausina V, Williams A, Clark S, Malaga W, Guilhot C, Gicquel B, Martin C. 2013. Construction, characterization and preclinical evaluation of MTBVAC, the first live-attenuated M. tuberculosis-based vaccine to enter clinical trials. Vaccine 31:4867-73.

31. Marinova D, Gonzalo-Asensio J, Aguilo N, Martin C. 2017. MTBVAC from discovery to clinical trials in tuberculosis-endemic countries. Expert Rev Vaccines 16:565-576.

32. Lyon SM, Rossman MD. 2017. Pulmonary Tuberculosis. Microbiol Spectr 5.

33. Martini M, Besozzi G, Barberis I. 2018. The never-ending story of the fight against tuberculosis: from Koch's bacillus to global control programs. J Prev Med Hyg 59:E241-E247.

34. Abubakar I, Drobniewski F, Southern J, Sitch AJ, Jackson C, Lipman M, Deeks JJ, Griffiths C, Bothamley G, Lynn W, Burgess H, Mann B, Imran A, Sridhar S, Tsou CY, Nikolayevskyy V, Rees-Roberts M, Whitworth H, Kon OM, Haldar P, Kunst H, Anderson S, Hayward A, Watson JM, Milburn H, Lalvani A, Team PS. 2018. Prognostic value of interferon-gamma release assays and tuberculin skin test in predicting the development of active tuberculosis (UK PREDICT TB): a prospective cohort study. Lancet Infect Dis 18:1077-1087.

35. Stevens WS, Scott L, Noble L, Gous N, Dheda K. 2017. Impact of the GeneXpert MTB/RIF Technology on Tuberculosis Control. Microbiol Spectr 5.

36. Pezzella AT. 2019. History of Pulmonary Tuberculosis. Thorac Surg Clin 29:1-17.

37. Jones D, Metzger HJ, Schatz A, Waksman SA. 1944. Control of Gram-Negative Bacteria in Experimental Animals by Streptomycin. Science 100:103-5.

38. Anonymous. 2007. Tuberculosis 2007. From basic science to patient care.

39. Kerantzas CA, Jacobs WR, Jr. 2017. Origins of Combination Therapy for Tuberculosis: Lessons for Future Antimicrobial Development and Application. MBio 8.

40. Munsiff SS, Nivin B, Sacajiu G, Mathema B, Bifani P, Kreiswirth BN. 2003. Persistence of a highly resistant strain of tuberculosis in New York City during 1990-1999. J Infect Dis 188:356-63.

41. de Welzen L, Eldholm V, Maharaj K, Manson AL, Earl AM, Pym AS. 2017. Whole-Transcriptome and -Genome Analysis of Extensively Drug-Resistant Mycobacterium tuberculosis Clinical Isolates Identifies Downregulation of ethA as a Mechanism of Ethionamide Resistance. Antimicrob Agents Chemother 61.

42. Comas I. 2017. Genomic Epidemiology of Tuberculosis. Adv Exp Med Biol 1019:79-93.

43. Comas I, Borrell S, Roetzer A, Rose G, Malla B, Kato-Maeda M, Galagan J, Niemann S, Gagneux S. 2011. Whole-genome sequencing of rifampicin-resistant Mycobacterium tuberculosis strains identifies compensatory mutations in RNA polymerase genes. Nat Genet 44:106-10.

44. Gygli SM, Borrell S, Trauner A, Gagneux S. 2017. Antimicrobial resistance in Mycobacterium tuberculosis: mechanistic and evolutionary perspectives. Fems Microbiology Reviews 41:354-373.

45. Gygli SM, Keller PM, Ballif M, Blochliger N, Homke R, Reinhard M, Loiseau C, Ritter C, Sander P, Borrell S, Loo JC, Avihingsanon A, Gnokoro J, Yotebieng M, Egger M, Gagneux S, Bottger EC. 2019. Whole genome sequencing for drug resistance profile prediction in Mycobacterium tuberculosis. Antimicrob Agents Chemother doi:10.1128/AAC.02175-18.

46. Nathavitharana RR, Cudahy PG, Schumacher SG, Steingart KR, Pai M, Denkinger CM. 2017. Accuracy of line probe assays for the diagnosis of pulmonary and multidrug-resistant tuberculosis: a systematic review and meta-analysis. Eur Respir J 49.

47. Mahajan R. 2013. Bedaquiline: First FDA-approved tuberculosis drug in 40 years. Int J Appl Basic Med Res 3:1-2.

48. Matsumoto M, Hashizume H, Tomishige T, Kawasaki M, Tsubouchi H, Sasaki H, Shimokawa Y, Komatsu M. 2006. OPC-67683, a nitro-dihydro-imidazooxazole derivative with promising action against tuberculosis in vitro and in mice. Plos Medicine 3:2131-2144

.

1 Chapter

Activity, Synergy and Toxicity of AS-48 *in vitro*

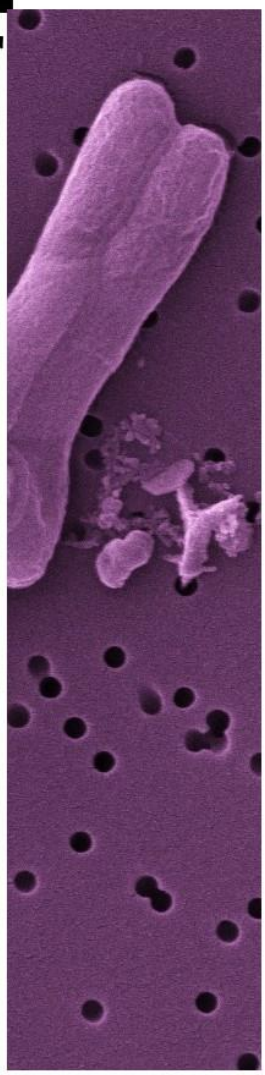

INTRODUCTION

APPROACHES FOR ANTIMICROBIAL DRUG DISCOVERY

There are different experimental approaches for the discovery of new antimicrobial drugs, the two major ones are target-based and whole cell-based screenings. Both methods have advantages and disadvantages; the whole cell screening (also known as phenotypic screening) is used to identify new molecules that directly kill the bacterial cells, and this may lead to the discovery of drugs with novel modes of action but that may have important issues on cytotoxicity on mammalian cells. Most of the screens focused on the inhibition of the enzymatic activity of the target have resulted in the identification of compounds with a known mechanism of action, that sometimes may have a poor permeation through the bacterial cell wall (1). All the drugs commonly used in tuberculosis treatment were discovered by phenotypic approaches. Phenotypic assays (in comparison with target based approaches) reintroduce biological complexity into the screening model system and allow the study of disease-relevant pathways in a more physiological context (2). This approach may offer the possibility to find new drug targets or vulnerable pathways, as long as drugs with complex mechanisms of action or even with a multi-mode of action (3, 4).

ANTIMICROBIAL PEPTIDES

In the context of antimicrobial drug discovery, not only in *M. tuberculosis* but also in many other bacterial pathogens, antimicrobial peptides (AMPs) may have a great potential use in treatment, either used by themselves or in combination with other antimicrobial drugs. They seem to be a good alternative to the actual treatments that have become inefficient against MDR strains.

AMPs can be produced by eukaryotic or prokaryotic cells; they are mostly cationic and have an amphiphilic nature. Those AMPs produced by bacterial cells

are called bacteriocins, and exhibit antimicrobial activity mostly against those species that are phylogenetically close related with the producer species.

Bacteriocins

Bacteriocins are ribosomally synthetized small peptides with bactericidal activity against a range of closely related species. They are capable of interacting with different pathways and targets in the bacterial cells; some bacteriocins may affect the same target as common antibiotics, and some others may inhibit new targets; moreover, bacteriocins can affect several targets simultaneously (5).

Bacteriocins are being widely used in the field of food preservation; they are generally regarded as safe (GRAS), so that in the case of nisin (a product of *Lactococcus lactis*), this bacteriocin has been accepted by the FDA as a food additive in Title 21 of the Code of Federal Regulations (21 CFR 184). Nisin preparation from *Lactococcus lactis* Lancefield Group N for use as an antimicrobial agent to inhibit the outgrowth of *Clostridium botulinum* spores and toxin formation in pasteurized cheese spreads (21 CFR 184.1538) (6). It has been suggested antimicrobial activity of bacteriocin could be useful in other fields, such as the fight against clinically relevant microorganisms. The main restrictions for using bacteriocins for therapeutic applications are that, due to their peptidic nature, they are susceptible to proteolytic degradation in the gut and that proteolysis-resistant bacteriocins may alter or even arrest the growth of the natural microbiota. Despite of this, the fact is that many bacteriocins have been isolated from bacteria commonly found in human sources, suggesting that they are naturally present in our bodies. Some strategies such as nano-encapsulation would provide bacteriocins with a more suitable way to be delivered orally, avoiding the degradation by proteolytic enzymes (7). The broad spectrum antimicrobial activity and the potential to enhance the effect of other antimicrobials are the best advantages of the use of bacteriocins against infectious diseases. In addition, bacteriocins are equally active

against antibiotic susceptible or antibiotic resistant strains (8), so that bacteriocins may have an important role in antimicrobial drug discovery.

It is accepted a recently classification of bacteriocins (9) where Class I (less than 10 kDa), encompasses all the peptides that undergo enzymatic modification during biosynthesis, which provides molecules with uncommon amino acids and structures, having an impact on their properties. Thus, there are lanthipeptides (Class Ia), head-to-tail cyclic peptides (Class Ib), sactibiotics that are sulphur-to-α -carbon-containing peptides (Class Ic) and linear azol (in)e-containing peptides (Class Id). Class II (less than 10 kDa) includes unmodified bacteriocins that do not require enzymes for their maturation; and finally, Class III that consists of heat-labile bacteriocins without modifications, larger than 10 kDa and with bacteriolytic or non-lytic mechanism of action. The prototype of the ribosomally synthesized and post-translationally modified peptides (RiPPs) by head-to-tail cyclization to render a circular molecule is the bacteriocin AS-48 (Class Ib). All these cyclic peptides are synthesized as a linear precursor containing a leader sequence with a high molecular weight, and then are post-translationally modified.

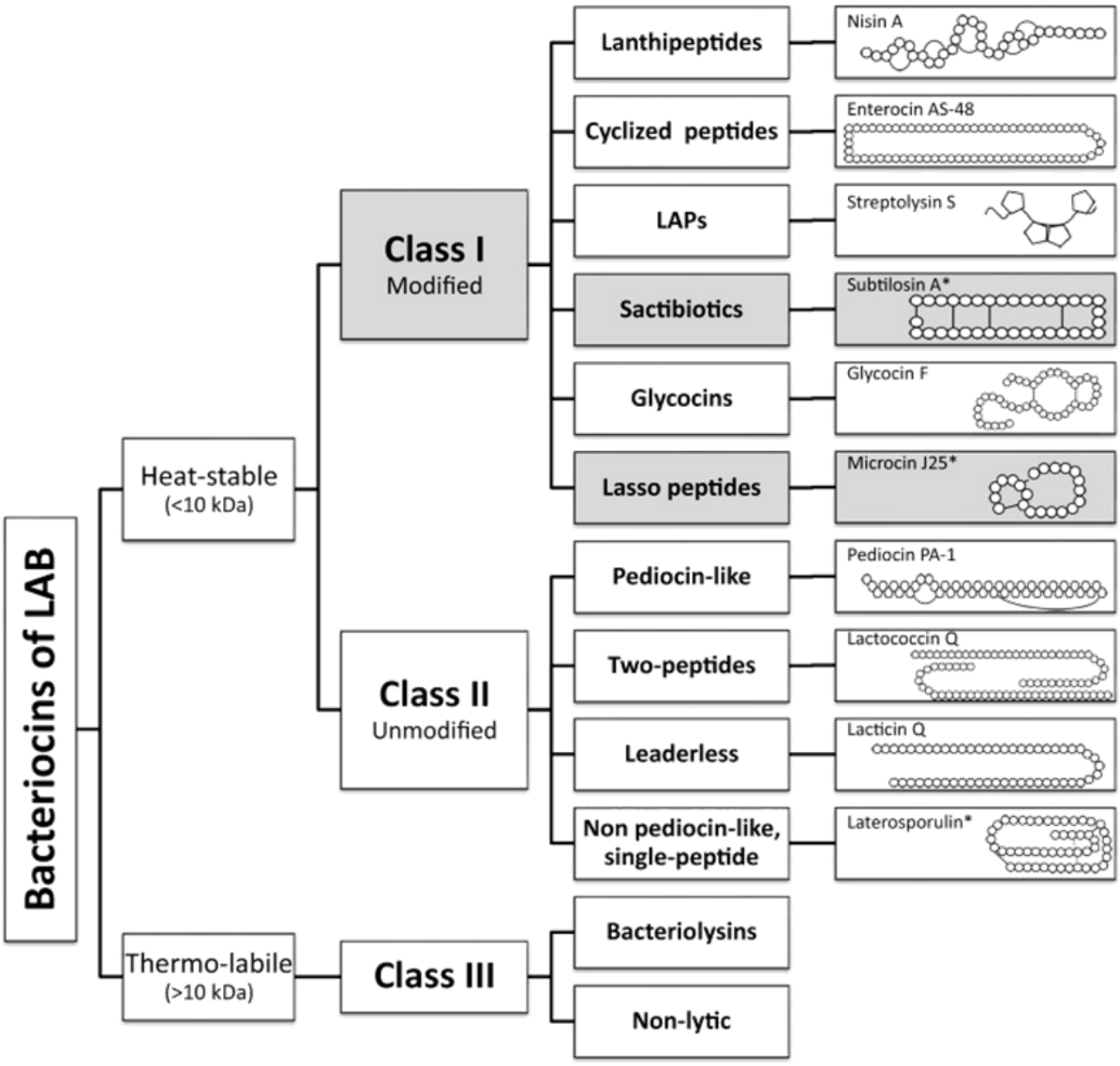

Image 8: Bacteriocins of Lactic Acid Bacteria (LAB) classification proposed by Alvarez-Sieiro, *et al*. (9).

AS-48, a bacteriocin with a great potential

The bacteriocin AS-48 is a 70 amino acid, alpha-helical membrane-interacting peptide (**Image 9**) produced by *Enterococcus faecalis*, which displays a broad antimicrobial spectrum against Gram-positive and Gram-negative bacteria. The mechanism of AS-48 antibacterial activity involves the accumulation of positively charged molecules at the membrane surface leading to a disruption of the membrane potential (10, 11). Its antimicrobial activity has already been proven in food products (12) and has been observed against numerous Gram-positive bacteria including *Listeria monocytogenes* and enterotoxic *Staphylococcus aureus* (13).

Most of the studies on bacteriocins focus on their potential application as food preservatives and only a few of them are focused on their potential biomedical applications and, specifically, in antimicrobial or antituberculosis activity. Nisin and lacticin 3147 activity has been proved against *Mycobacterium* strains such as: *M. kansasii*, *M. avium paratuberculosis* and *M. tuberculosis* H37Ra; in particular, lacticin 3147 exhibit greater antimycobacterial activity than nisin (14). The antimycobacterial activity of several bacteriocins was found to be similar to rifampicin against *M. tuberculosis* (15).

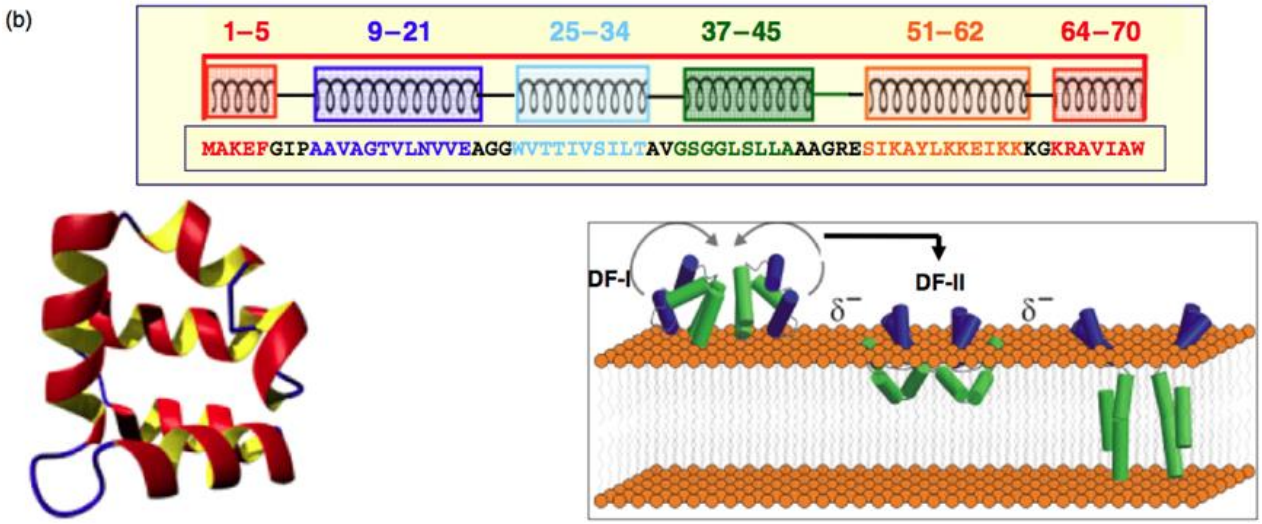

Image 9: AS-48 aminoacidic composition, structure and possible interaction with the plasmatic membrane (16).

BACTERIOCIN ENGINEERING

One of the strategies that can be followed to improve properties such as antimicrobial activity of bacteriocins is to modify its chemical structure, and this can be easily accomplished by genetically modifying the structural gene encoding the bacteriocin. The improvement of the activity, solubility and stability of current bacteriocins at broad pH ranges has increased the probabilities for a further therapeutic application of bacteriocins. In the case of Microcin B17, a DNA gyrase inhibitor, it has been found that the derivative molecule Mcc[Gly46-Ile69] is much more stable than the original molecule, while retaining a similar gyrase inhibitory activity (17). Engineered modifications have also improved the production rate of, for example, the nisin mutants D19A, F18H, F18M, L16D, L16K and L16A (18). There are other examples in which structural modifications have not resulted in a significant improvement of the activity; this is the case of AS-48, the bacteriocin featured in this study: all several mutants resulting from engineering modifications had the same or lower antimicrobial activity than the wild type molecule (11).

SYNERGY AND COMBINATION THERAPIES INCLUDING BACTERIOCINS

Antimicrobial peptides, and in particular bacteriocins, have a great potential as alternatives for common antimicrobials because of their innate antimicrobial activity. In addition to consider their use as antimicrobials by themselves, they can be considered as helper compounds that could enhance the antimicrobial activity of other antimicrobial peptides or antibiotic-based therapies, as long as they have a synergistic interaction. A combined therapy has some advantages in comparison with those based on single drugs. First, a synergistic relationship reduces considerably the concentration of the components needed for the same antibacterial effect, and consequently, reduces also their potential side-effects. Second, a synergistic combination of antimicrobial compounds reduces considerably the probability of arising and selecting resistant mutants.

The molecular interaction profile of a drug describes its interactions with other biomolecules, pathways or processes attributable to its pharmacodynamics, toxicological, pharmacokinetic and combination effects. A combination of drugs is synergistic, with no interaction, or antagonistic if its effect is greater than, equal to, or lower than the summed effects of the individual drugs, respectively. We refer also to synergy when the therapeutic activity of one drug is enhanced by another drug, via regulation of its absorption, distribution, metabolism and excretion (ADME) (19). According to Jia *et al*. (20) there are three situations in which synergy combinations act. First, an effect anti-counteractive in the drugs combined, reduce the side effects that one of the drugs could have or with a compensatory activity (21). In the second group, the drugs have complementary actions to reach one target or pathway site (22). The third group, involves facilitating actions: one drug enhance the activity of another drug, for example when combining gentamicin and vancomycin: the alterations in the cell wall caused by the action of vancomycin increases the accession of gentamicin to reach the ribosome (23). Despite this, a recent report concluded that antagonism is more common than synergy and occurs almost exclusively between drugs that target different cellular processes (24). Cokol *et al*. (25) also have reported a higher prevalence of antagonism combinations in antifungal drugs.

Validating *in vitro* observed synergy may provide a synergistic outcome *in vivo*, as have been observed in the case of an experimental therapy based in a combination of spectinamide and clarithromycin against tuberculosis infection in animal models (26).

Commonly, synergy is defined for a combination of two drugs but synergy also can be considered when several (more than two) drugs are included in a treatment (27).

AMP's have shown synergy together with common drugs against *M. smegmatis* either in axenic culture or within the infected macrophages (28). Also, the combination of the AMP HNP-1 with isoniazid and rifampicin decreased the MIC of the drugs (rifampicin and isoniazid) and reduced the mycobacterial load

in vivo (29). Then, we consider synergy strategy for AMPs as a simple and effective approach that would help to find new alternatives to conventional antimicrobial compounds.

In this chapter we present the antimicrobial activity of AS-48 against several *M.tuberculosis* strains and Non-tuberculous Mycobacteria, we have explored the differences of activity in porins mutants strains and also with some variants of the bacteriocin AS-48 engineered for improving the antimicrobial activity. Moreover, we assayed the cytotoxicity of the bacteriocin in human and murine macrophages. And finally, its antimicrobial activity in a model of infected macrophages.

OBJECTIVES

Given the high concern raised globally on the increase of drug resistant variants of *M. tuberculosis*, to characterise novel compounds with new bacterial targets is a priority of biomedical research in our days. Bacteriocin AS-48 is an AMP with great biotechnological applications, although its potential biomedical uses have been little explored. For this, the objectives of this work have been the following:

1) To characterise antimycobacterial activity of AS-48 *in vitro*
2) To identify and characterise potential synergistic combinations of AS-48 and drugs or hydrolytic enzymes
3) To assess cytotoxicity of AS-48 against macrophage cell lines
4) To determine the antituberculosis activity of AS-48 against intracellular mycobacteria.

MATERIALS AND METHODS

BACTERIAL STRAINS AND CULTURE CONDITIONS

Mycobacterial strains used in this work for *in vitro* tests are listed in **Table 1 and Table 2**. All strains were cultured in Middlebrook 7H9 media (Difco™) supplemented with 10% ADC (BD) and 0.05% Tween 80 in 25 cm^2 flasks. For drug susceptibility testing, Tween 80 was replaced by 0.5% glycerol. Cultures on solid media were performed in Middlebrook 7H10 agar (Difco™) supplemented with 10% ADC and 0.05% Tween 80. All cultures were incubated at 37°C until visible growth.

Table 1: *Mycobacterium tuberculosis* complex strains used.

Strain	Source or reference
***M. tuberculosis* H37Rv**	(30)
***M. tuberculosis* H37Ra**	(31)
***M. bovis* BCG Pasteur 1173**	Laboratory collection
***M. tuberculosis* Mt103**	(32)
***M. tuberculosis* CDC 1551**	(33)
***M. tuberculosis* GC 1237**	(34)
***M. tuberculosis* H37RvPhoP**	(35)
***M. tuberculosis* SS18b**	(36)
HMS 1500	HMS
HMS 1555	HMS
HMS 1531	HMS
HMS 1536	HMS
HMS 1546	HMS
HMS 1547	HMS
HMS 1548	HMS
HMS 1292	HMS
HMS 1543	HMS
HMS 1278	HMS

[a]= fast-growing strains, the rest of the strains have a slow growth. HMS= Clinical isolates provided by Hospital Miguel Servet, Zaragoza.

Table 2: Non-Tuberculous Mycobacteria used.

Strain	Source or reference
M. fortuitum [a]	HCU
M. mucogenicum [a]	HCU
M. xenopi	HCU
M. gordonae	HCU
M. avium [a]	HCU
M. abcesus [a]	HCU
M. lentiflavum	HCU
M. smegmatis mc²155 [a]	(37)
M. smegmatis SMR5 [a]	(38)
M. smegmatis MN01 [a]	(39)
M. smegmatis ML10 [a]	(39)

Note: [a]= fast-growing mycobacteria. HCU= Clinical isolates provided by the Hospital Clínico Universitario Lozano Blesa, Zaragoza.

MINIMAL INHIBITORY CONCENTRATION (MIC)

Serial broth microdilutions were made to determine the MIC of AS-48, lysozyme (Sigma-Aldrich L 3790) and other antimicrobials (isoniazid, rifampicin, moxifloxacin, streptomycin and ethambutol; Sigma-Aldrich). Bacteriocin AS-48, and its derivative mutants E4A, E20A, E49A, W70A, G13K, and L40K were purified to homogeneity from *Enterococcus faecalis* UGRA 10 strain (40) according to (41) (**Annex I**).

Two-fold dilutions of compounds were made in 100 µl of culture medium for mycobacterial strains in sterile 96-well polypropylene flat bottom plates. Wells

were inoculated with $1x10^5$ CFU in 100 µl of culture medium and incubated at 37°C during 7 days for slow-growing mycobacteria or 4 days for fast-growing species. Then, 30 µl of 0.1 mg/ml filter-sterilized resazurin (Sigma-Aldrich) was added. The colour change from blue (indicative of no bacterial growth) to pink (indicative of bacterial growth) was recorded after 48 hours in the case of slow-growing mycobacteria or after 24 hours for fast-growing species. The MIC was defined as the lowest concentration of compound capable of inhibiting bacterial growth. Positive and negative growth controls were added in all the experiments and moxifloxacin (Sigma) at 0.5 mg/ml was used in all the assays as a control (42).

SYNERGY TEST

This assay blends gradients of concentration of two compounds to evaluate their antimicrobial activity and the interaction between them. In fresh medium for culturing mycobacteria, solutions at 4x the highest concentration to be tested were prepared for each compound. Then, both compounds were serially two-fold diluted in a sterile 96-well flat bottom plates, one of the compounds was diluted along the columns and the other in rows. The MIC of one of the compounds alone will be tested in column one, and the MIC of the second compound will be tested in row H; the rest of the plate is a matrix of both gradients. Finally, wells were inoculated as described above, and incubated and treated with resazurin as in a conventional MIC assay (**Image 10**).

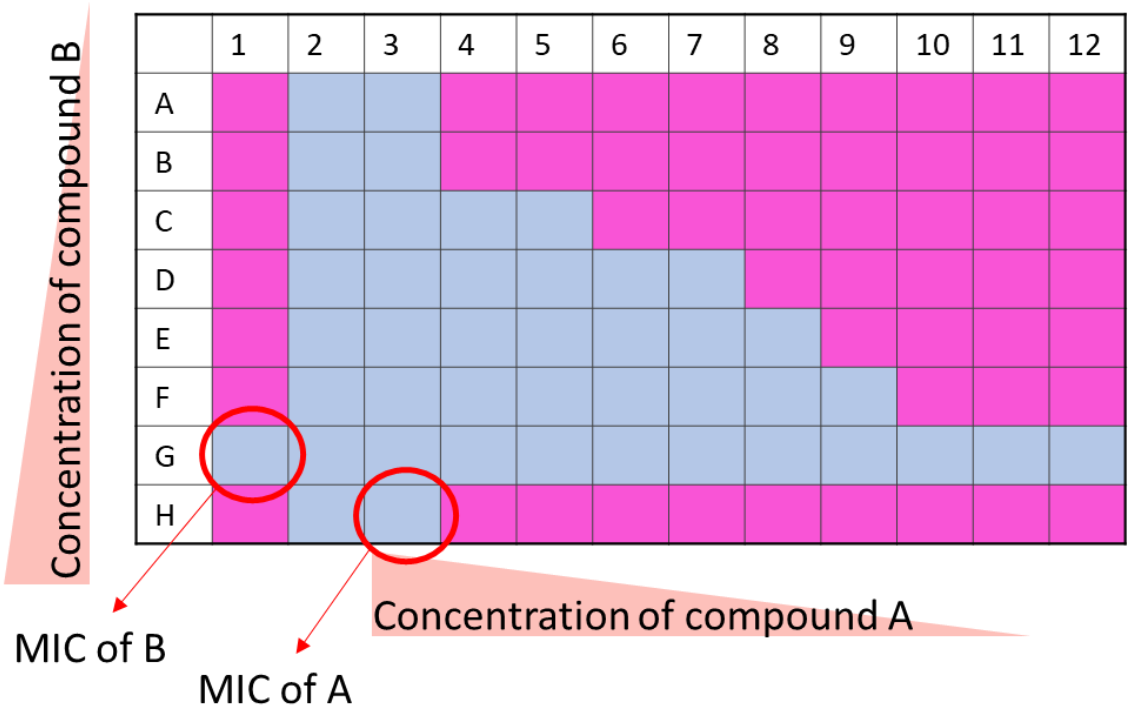

Image 10: Example of a 96-well plate for checkerboard assay. The illustration represents a hypothetical result of synergy.

FRACTIONAL INHIBITORY CONCENTRATION INDEX ANALYSES

After a synergy test is done, the determination of Fractional Inhibitory Concentration (FIC) index allows objective identification of any interaction between two compounds against a particular bacterial strain, indicating whether there is synergy, no interaction or antagonism.

For each well in which there is no growth next to a well with bacterial growth, the FIC for each of the two compounds must be calculated using the following formula:

FIC_X = MIC of X in presence of Y / MIC de X alone.

FIC_Y = MIC de Y in presence X / MIC de Y alone.

Both values, together with other points of inhibition can be represented graphically and a concave line will be indicative of synergy. Alternatively (or

additionally), the addition of FIC $_X$ and FIC $_Y$ results in the FICI value (Fractional Inhibitory Concentration Index). A FICI value up to 0.5 indicates synergy, when it is between 0.5 and 4 indicates there is no interaction between the compounds, and a FICI value over 4 indicates antagonism (43, 44). The relation between the two compounds could be represented graphically as is shown in the **Image 11**:

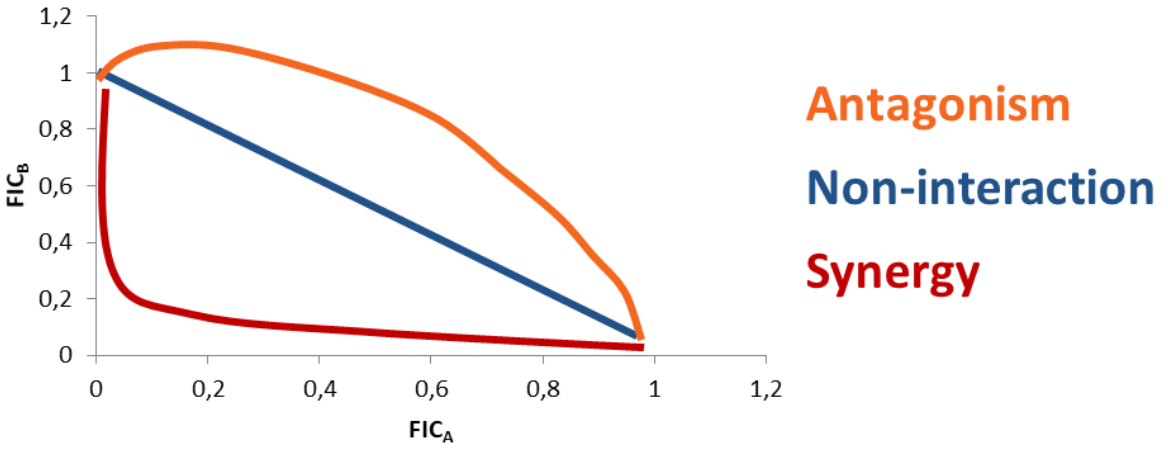

Image 11: Graphic representation of the interaction between two compounds in the checkerboard assay.

CELL CULTURES

The following cell lines were used: murine macrophages MHS (HPA Culture Collections, 95090612), J774.2 (ECACC, 85011428), Raw 264.7 (TIB-71) and human monocytes THP-1 (ECACC, 88081201). MHS cells were cultured in DMEM and the rest were cultivated in RPMI-1640 Glutamax medium (Gibco) containing 10% heat-inactivated Fetal Bovine Serum (FBS, Gibco). When cells were going to be used for cytotoxicity assays, antibiotics (penicillin, streptomycin and ciprofloxacin) were added to cell pre-cultures. Cells were cultured in a controlled 5% CO_2 atmosphere at 37°C.

CYTOTOXICITY ASSAYS

The MTT assay and Neutral Red assay (45) were carried out to determine AS-48 cytotoxicity in MHS and J774.2 murine macrophages, and THP-1 human macrophages. Cells were cultured in 96-well flat bottom plates with the appropriate media. THP-1 monocytes were differentiated to macrophages by using 10 ng/ml of phorbol 12-myristate 13-acetate (PMA, Sigma Aldrich ref P1585-1MG) for 72 hours. The concentrations of cells used for cytotoxicity assays for mouse lung macrophages were 15000 cells/well (MH-S) and 20000 cells/well (J774.2), and for human lung macrophages were 50000 cells/well (THP-1). They were cultured for 24 hours and then the compounds were added dissolved in fresh culture media and incubated, together with the cells, during 24 hours.

After the time of incubation of cells with compounds, media was removed and 100 µl of MTT (1 mg/ml) or 100 µl of NR (0.05 mg/ml) was added. MTT and NR were incubated during 3 hours. Plate was centrifuged with a short spin, then media was removed and crystals of MTT were dissolved in 200 µl of pure isopropyl alcohol. After removing the NR media, cells were washed with PBS and finally NR was dissolved in ETOH/water/acetic acid 50:49:1 (v/v). Absorbance was measured in MTT assay at 570 and 650 nm and fluorescence in the case of NR at 530 and 645 nm excitation and emission wavelengths respectively. Percent of cell viability in comparison with untreated controls was determined, and treatments were considered to be cytotoxic or not according to (13). To check the absence of statistically significant differences between samples treated with lower concentrations of AS-48, we performed one-way ANOVA test.

M. TUBERCULOSIS MACROPHAGE INFECTION ASSAY

For infection assays, a recombinant strain of *M. tuberculosis* H37Rv (ATCC#27294) constitutively expressing a green fluorescent protein (H37Rv-GFP) was used as a reporter for the intracellular mycobacterial replication assay (46). This strain was grown in Middlebrook 7H9 medium supplemented with 10% of oleic acid-albumin-dextrose-catalase (OADC, Difco), 0.05% of Tween 80 (Sigma-Aldrich), 0.5% of glycerol (Euromedex) and 50 µg/ml of hygromycin B (Invitrogen). Cultures were maintained at 37°C in static conditions for up to 14 days before being used for the intracellular mycobacterial replication assay, to reach the exponential phase of bacterial growth. Cultures of H37Rv-GFP were maintained under stirring during three days before the infection to ensure that bacterial cells were in exponential growth. Then, bacterial cells were washed twice with PBS without Mg^{2+} and Ca^{2+}, followed by a third wash with RPMI supplemented with 10% FBS and centrifuged at 70 g during 2 min to pellet bacterial clumps; the supernatant corresponds to a homogenous suspension of bacteria.

Bacterial titre was determined by measuring the optical density at 600 nm and by measuring EGFP fluorescence on a Victor Multilabel Counter (Perkin Elmer), and further diluted in RPMI 1640 supplemented with 10% FBS (RPMI-FBS) prior to infection. Raw 264.7 macrophages were used for the intracellular mycobacterial replication assay and harvested by using Versene solution (LifeTechnologies). Macrophages were prepared at a concentration of $5 \cdot 10^5$ cells/ml, infected with a 1:2 MOI with *M. tuberculosis* H37Rv-GFP and incubated in RPMI-FBS cell culture media at 37°C under stirring at 120 rpm. After 2 hours, cells were centrifuged at 160 g during 5 min, resuspended in the same volume of fresh medium containing 50 µg/ml of amikacin to kill extracellular bacteria, and incubated during 1 hour at 37°C with shaking at 120 rpm. Cells were washed and resuspended in the same volume of fresh medium. Infected cells were seeded in 384-wells plates (Greiner Bio-One) at $2 \cdot 10^4$ cells/well containing the compounds

(AS-48, ethambutol and lysozyme diluted in water). Plates were incubated for 5 days at 37°C, 5% CO_2.

Infected cells were stained during 30 min with Syto60 dye (Invitrogen) at a final concentration of 5 µM. Finally, images were acquired (as described below), then cells were lysed with DPBS-0.1% Triton X-100 buffer for 1 min for releasing intracellular bacteria. The number of viable bacterial cells was determined by serially plate dilutions on Middlebrook 7H11 (Difco) agar plates, supplemented with 0.5% glycerol, 10% OADC and 50 µg/mL hygromycin B. After 3-weeks of incubation at 37°C with 5% CO_2, the number of viable bacteria (CFUs) were calculated.

IMAGE ACQUISITION AND ANALYSIS

Images were performed on an automated fluorescent confocal microscope (Opera, PerkinElmer), using a 20X- water immersion lens. Syto60-labeled cells were detected using a 640 nm excitation laser coupled with a 690/70 detection filter and GFP-bacteria were detected using a 488 nm laser coupled with a 540/75 detection filter. A series of 6 images was taken by well and each one was analysed using the image-analysis software Columbus system (version 2.5.1, PerkinElmer). Briefly, the images were processed to determine the output image of GFP mask and remove background in that channel. Then, the output images corresponding to the Syto60 values were processed similarly to assess morphological parameters of cells. Properties of intensity and morphology were filtered to select the correct nuclei population. Spots corresponding to the bacteria that are infecting the cells were detected, and bacterial number and area in pixels were determined for each cell. The intracellular bacterial growth was quantified by the total intracellular bacterial area (pixel) per well. In order to consider a cell as infected, the number of bacteria within the cell area should be ≥1. Efficiency of infection and effectivity of treatment with compounds was determined in terms of percentage of infected cells and mean of *M. tuberculosis* area per infected cell.

RESULTS

BACTERIOCIN AS-48 SHOWED BACTERICIDAL ACTIVITY AGAINST *M. TUBERCULOSIS* COMPLEX

The activity of AS-48 was determined against several mycobacteria including *M. tuberculosis* complex reference strains, clinical isolates, and other clinically relevant non-tuberculous mycobacteria (NTM). First of all, we tested AS-48 activity against *M. tuberculosis* complex clinical and reference strains. The MIC of AS-48 was quite uniform, between 16 and 64 µg/ml (**Table 3 and 4**), and there was no difference in the MICs of AS-48 between active replicating cells and the non-replicative strain SS18b of *M. tuberculosis*. We observed a similar MIC of AS-48 in *M. smegmatis* and the other NTM (see below).

Table 3: MICs of AS-48 and lysozyme of *M. tuberculosis* complex strains and clinical strains.

Strain	MIC AS48 (µg/ml)	MIC lysozyme (µg/ml)
***M. tuberculosis* H37Rv**	32-64	200-400
***M. tuberculosis* H37Ra**	32	400
***M. bovis* BCG Pasteur 1173**	32	200-400
***M. tuberculosis* Mt103**	64	400
***M. tuberculosis* CDC 1551**	64	400
***M. tuberculosis* GC 1237**	16-32	400
***M. tuberculosis* H37RvPhoP**	64	400
***M. tuberculosis* SS18b**	32-64	>1200
HMS 1500	32	100-200
HMS 1555	32	>400
HMS 1531	8	50-100
HMS 1536	32	200-400
HMS 1546	32	100
HMS 1547	32	200
HMS 1548	32	400
HMS 1292	32	100-200
HMS 1543	>32	>400
HMS 1278	32	200

Table 4: MICs of AS-48 and lysozyme of NTM and porins mutans of *M. smegmatis*.

Strain	MIC AS48 (µg/ml)	MIC lysozyme (µg/ml)
M. fortuitum [a]	64	>1200-1200
M. mucogenicum [a]	64	200-400
M. xenopi	<2	< 9.375
M. gordonae	<2	<9.375
M. avium [a]	64	>1200
M. abcesus [a]	64	>1200
M. lentiflavum	> 256	>1200
***M. smegmatis* mc²155** [a]	64	400
***M. smegmatis* SMR5** [a]	64	400
***M. smegmatis* MN01** [a]	128	>800
***M. smegmatis* ML10** [a]	64	50

Note: [a]= fast-growing mycobacteria.

The kill curve kinetics indicated that bacteriocin AS-48 is bactericidal since concentrations equal to the MIC and 2xMIC were capable of reducing the number of live bacteria in a culture of *M. tuberculosis* H37Rv. First, after one or two days of treatment, the number of CFU was reduced by almost 2 log in comparison with untreated cultures. After 6 days of treatment with 128 or 64 µg/ml of AS-48, no live bacteria could be detected (**Image 12**) and this was found to be statistically significant by linear regression test (p-value of 0.0005 and <0.0001 respectively).

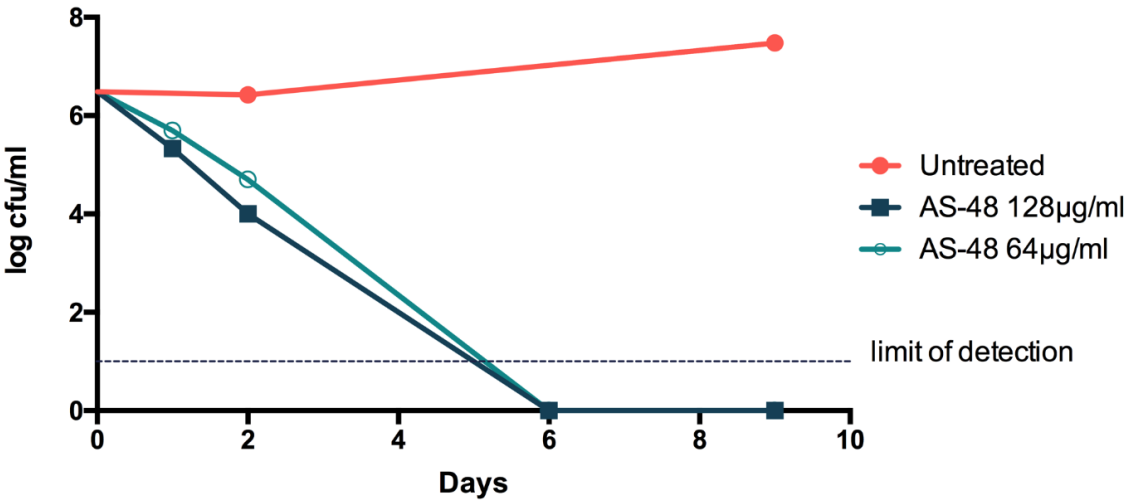

Image 12: Kill curve kinetics of bacteriocin AS-48 at 64 and 128 µg/ml against cultures of *M. tuberculosis* H37Rv. Untreated cultures have been used as a control.

SYNERGY BETWEEN BACTERIOCIN AS-48 AND OTHER ANTIMICROBIAL COMPOUNDS

Synergy interaction between lysozyme and the bacteriocin nisin was already observed in Gram-positive bacteria (47, 48). Similarly, we have observed that the presence of lysozyme resulted in an increase in the *M. tuberculosis* susceptibility to AS-48. First, we tested lysozyme activity against mycobacterial strains and found that different mycobacterial strains or species have more variability in the MIC of lysozyme (**Table 1 and Table 2**) than that obtained for AS-48. Notably, the non-replicating strain SS18b of *M. tuberculosis* was found to be greatly resistant to lysozyme. Secondly, we tested the susceptibility of mycobacterial strains to AS-48 in the presence of lysozyme. We found that, for most strains, susceptibility to AS-48 greatly increased (between 64 and 16-fold) in the presence of subinhibitory concentrations of lysozyme. In order to quantify the effect of lysozyme on growth inhibition by AS-48, we calculated the Fractional Inhibitory Concentration Index (FICI). The results of all strains assayed are indicated in **Table 5**. For reference strains, maximum synergism was observed for H37Rv and to a lesser extent to BCG, H37Ra, H37RvPhoP, GC 1237 (Beijing genotype), CDC1551, Mt103. Although technically the synergism is defined when

the FICI≤0.5, for the strains Mt103 and HMS 1548, which resulted in a FICI slightly over 0.5, we can consider it as a weak synergistic interaction. Even though, the synergy effect occurred in all the *M. tuberculosis* complex strains analysed.

Table 5: MIC of AS-48 in the presence of different concentrations of lysozyme and the Fractional Inhibitory Concentration Index (FICI).

Strain[a]	MIC of AS-48 (µg/ml) for mycobacterial strains in the presence of lysozyme						FICI[b]
Lysozyme concentration (µg/ml)	400	200	100	50	25	12.5	
H37Rv	<0.0312	0.0625	1	4	>32		**0.25**
H37Ra	<0.0312	2	4	16	>32		**0.375**
***M. bovis* BCG Pasteur**		<0.125	2	16	>32		**0.312**
Mt103	<0.125	4	32	32	64	>64	**0.562**
CDC 1551		<0.125	16	32	64	>64	**0.5**
GC 1237	<0.0312	4	8	>32			**0.375**
H37RvPhoP		<0.125	8	32	64	>64	**0.375**
M. smegmatis mc²155	<0.125	32	64	>64			1
M. smegmatis SMR5	<0.125	16	64				0.75
M. smegmatis ML10				<0.125	0.5	16	**0.5**
HMS 1500		<0.0312	8	>32			**0.375**
HMS 1531			<0.0312	0.5	4	8	**0.375**
HMS 1536		<0.0312	8	>32			**0.5**
HMS 1546			<0.0312	2	8	>32	**0.5**
HMS 1548	<0.03125	2	16	>32			**0.531**
HMS 1292			<0.03125	4	16	>32	**0.312**
HMS 1278		<0.03125	2	8	>32		**0.5**

[a]: unless indicated, all strains are *M. tuberculosis*

[b]: the fractional inhibitory index (FICI) is calculated as follows: FICI= ($MIC_{AS\text{-}48\ in\ presence\ of\ lysozyme}$ /$MIC_{AS\text{-}48\ alone}$) + ($MIC_{lysozyme\ in\ presence\ of\ AS\text{-}48}$ /$MIC_{lysozyme\ alone}$); FICI≤ 0.5 indicates synergism; FICI= 0.5-4, indicates no interaction and FICI> 4.0, indicates antagonism

ANTITUBERCULOSIS ACTIVITY OF VARIANTS OF AS-48

A series of variants of AS-48 were obtained previously by site-directed mutagenesis within the structural *as-48A* gene. These mutants were performed with the aim of improving their activity and stability (49-51).

We first tested antituberculosis activity of these mutant variants of AS-48 and results are given in **Table 6**. The results were that no one of the mutants exhibit a greater MIC against *M. tuberculosis* than the wild type, AS-48. Only the mutants, G13K and L40K, have the same MIC value as AS-48.

Table 6: MIC of each AS-48 mutant against *M. tuberculosis*.

Mutant name	MIC AS-48 mutant (µg/ml)
E4A	>64
E20A	>64
E49A	>64
W70A	>64
G13K	64
L40K	32

Additionally, synergy with lysozyme was assessed for AS-48 mutants. Synergy was observed only for the same mutants that have the same MIC of AS-48, L40K and G13K, and the extent of the synergy effect was comparable to that of the wild type AS-48, reaching a FICI of 0.312. **Image 13** represents the FIC of AS-48 and lysozyme for these two mutants and for AS-48

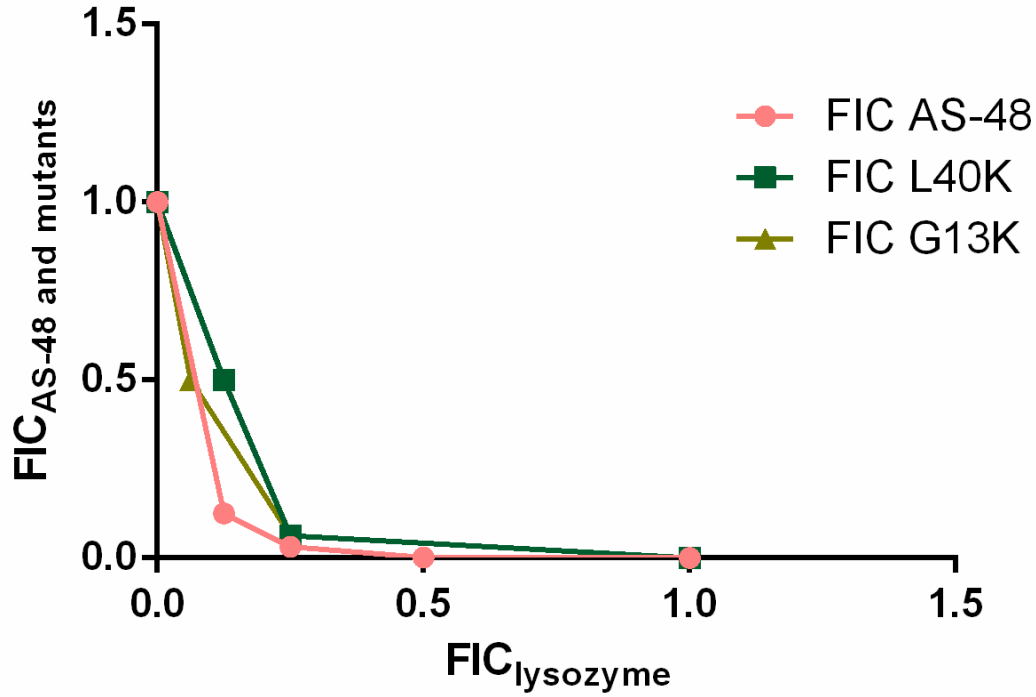

Image 13: FIC representation of AS-48, and the mutants L40K and G13K, with the FIC representation of lysozyme.

A PORIN MUTANT OF *M. SMEGMATIS* ARE LESS SENSITIVE TO AS-48

We have assayed three *M. smegmatis* mc² porins mutants: ML10, MN01 and MNR5. In the **Table 4,** we show the results of the MIC of AS-48 against the mutants SMR5, MN01 and ML10. The SMR5 comes from the *M. smegmatis* mc²155 but Streptomycin resistant due to a mutation in the *rpsL* gene, in this case the result of the MIC is exactly the same as *M. smegmatis* mc²155 as expected. We also have assayed the activity of AS-48 against two porin mutants strains derived from SMR5, which are MN01 (ΔmspA) and ML10 (ΔmspA ΔmspC). In the case of the double mutant the MIC for AS-48 are the same as in the wildtype and lower in the case of lysozyme. However, in the case of the simple mutant the MIC is higher than the range assayed.

We analysed the synergy effect in strains with the cell wall altered, which is the case of the porins mutants (MN01 and ML10). The result was that for the wild type, *M. smegmatis* MNR5, the relation between lysozyme and AS-48 was of no-interaction (FICI=0.75); for the double mutant, ML10 there is synergy (FICI=0.5) but, for the single mutant, MN01, we could not reach a clear relation between the two components (**Image 14**). We could expect that as much modifications in the cell wall as much sensitive would be the strain to the effect of AS-48. The possible mode of action of AS-48 would not be related with the presence or absence of porins.

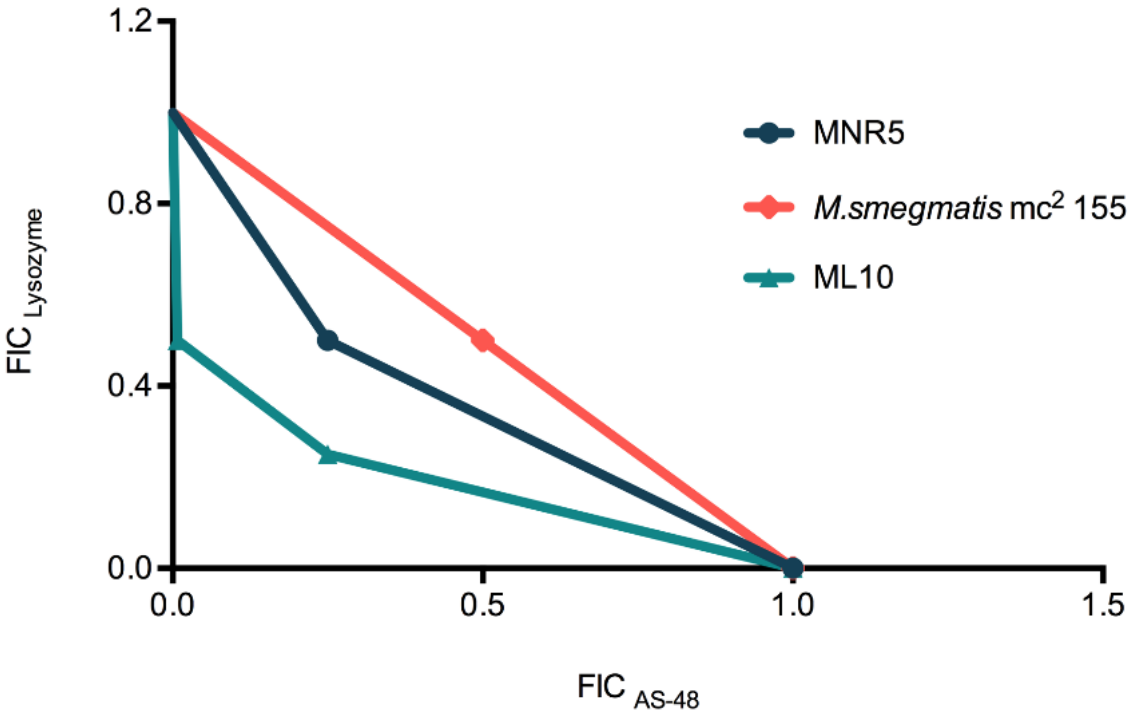

Image 14: FIC representation of AS-48 and lysozyme against *M. smegmatis* porins mutants.

BACTERIOCIN AS-48 HAS VARIABLE ACTIVITY AGAINST NTM

In most NTM, the MIC of AS-48 is the same as for *M. tuberculosis,* (*i.e.* 64 µg/ml) with the exception of the slow-growing mycobacterial species such as *M. xenopi*, *M. lentiflavum* and *M. gordonae*. In *M. xenopi* and *M. gordonae* the value of the MIC of AS-48 was <2 µg/ml, and the MIC of lysozyme is < 9.375 µg/ml. In contrast, the MIC of AS-48 against *M. lentiflavum* was higher than 256 µg/ml and the MIC of lysozyme was also higher than 1200 µg/ml, being the mycobacterial species less susceptible to AS-48 and to the lysozyme (**Table 4**).

SYNERGY TEST BETWEEN AS-48 AND FIRST-LINE ANTITUBERCULOSIS DRUGS

AS-48 has been tested also in combination with the main first-line antituberculosis drugs, ethambutol, isoniazid, streptomycin and rifampicin. The combination of AS-48 and ethambutol was the only one to present synergistic relation with a FICI of 0.09375, being the lowest FICI obtained in all the assays (**Image 15**).

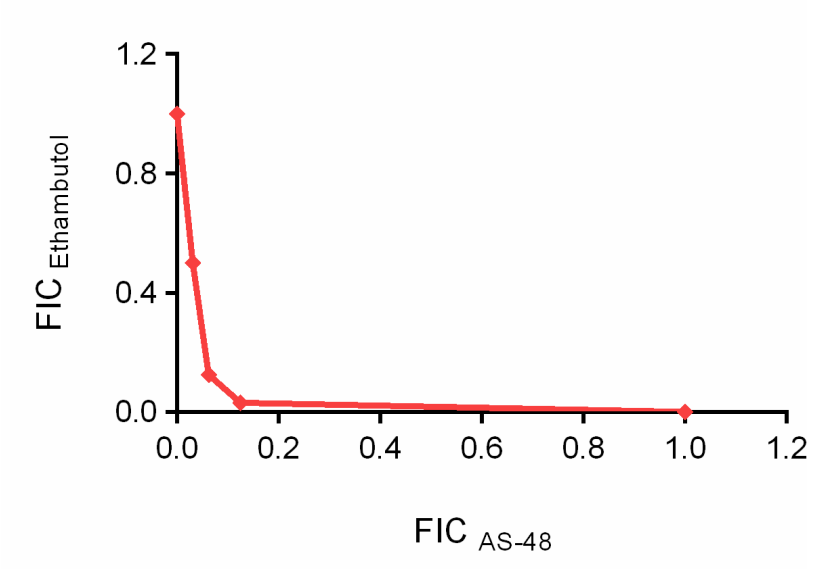

Image 15: Synergism between AS-48 and ethambutol in H37Rv *M. tuberculosis*. For the reference strains: CDC1551, Mt103, H37Ra and H37Rv phoP, the synergy relationship between AS-48 and ethambutol was almost the same.

ANTIMICROBIAL CONCENTRATIONS OF AS-48 ARE NOT CYTOTOXIC FOR MACROPHAGE CELL LINES.

The cytotoxicity of AS-48 on human and mouse lung macrophages cell lines was carried out by MTT and Neutral Red assays.

In both protocols, > 70% cell viability was observed at concentrations of AS-48 below 128 µg/ml which is considered as no cytotoxic effect by standard international protocols (52). Even when slight differences in cell viability were observed below 32 µg/ml of AS-48, they were no significant (**Image 16**). We did not observe a concentration-dependent cytotoxic effect in none of the cell lines assayed. At 128 µg/ml, <40% cell viability was observed (**Image 16**; p-value <0.0001).

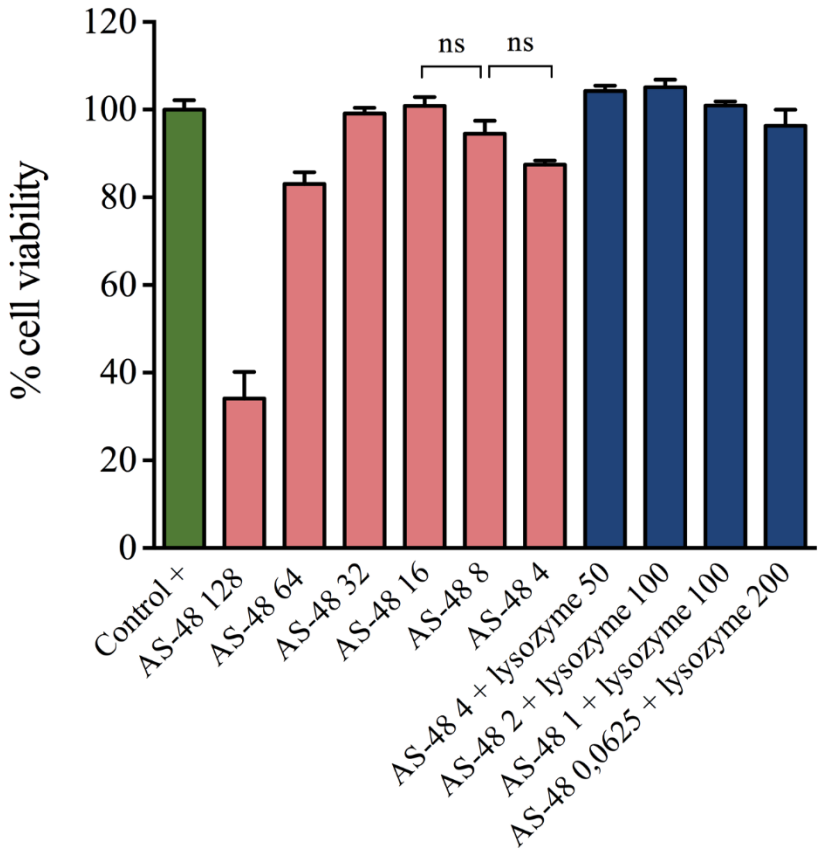

Image 16: Representative results of the cytotoxicity assays, as determined by Neutral Red Uptake technique in cell cultures of J774.2 murine macrophages. Concentration of compounds are expressed in µg/ml. Cell suspensions with no compounds added were used as a positive control.

Lysozyme cytotoxicity was also analysed and, as expected, no cytotoxicity was observed in these cell lines. Finally, we assayed cytotoxicity of some of those synergistic combinations of AS-48 and lysozyme that showed great antimicrobial effect in *M. tuberculosis*, and we found that these combinations did not cause any significant cytotoxic effect (**Image 16**).

SYNERGY BETWEEN ETHAMBUTOL AND AS-48 IN THE INFECTED MACROPHAGES.

In the model of Raw 264.7 cells infected with *M. tuberculosis* H37Rv-GFP, we observed low FICI values (**Table 7**) ranging from 0.5 and 0.18, which is indicative of synergism. These FICI values were similar to those obtained in the *in vitro* antimycobacterial assays. The combination of 2 µg/ml AS-48 and 2 µg/ml ethambutol against *M. tuberculosis* infected macrophages resulted in the lowest FICI value, that was 0.18, and it is worth to remark that this concentration of AS-48 (2 µg/ml) is well below the doses that were found to be toxic in macrophage cell lines.

Other combinations also resulted in synergistic FICI values in infected macrophages, but to a lesser extent (**Table 5**). The determination of viable bacteria after treatment with ethambutol and AS-48 resulted in a reduction of CFUs between 90 and 99.9% in comparison with untreated controls. The efficacy of AS-48 for killing intracellular pathogens was already proven by Abengózar *et al.*(53), when they showed the anti-leishmanial activity of AS-48 in Raw 264.7 infected macrophages. Despite the fact that the infection mechanism is different between *Leishmania* and mycobacteria, these experiments show that the AS-48 is active *versus* pathogens residing intracellularly in macrophages.

Table 7: Intracellular MICs of AS-48, ethambutol, and three combinations, related FIC values, and FICI data in Raw 264.7 cells infected with M. tuberculosis H37Rv-GFP.

MIC (μg/ml)				
AS-48	EMB	FIC AS-48	FIC EMB	**FICI[a]**
32	-	-	-	**-**
16	0.125	0.5	0.007	**0.50**
8	0.5	0.25	0.03	**0.28**
2	2	0.06	0.12	**0.18**
-	16	-	-	**-**

[a]: the fractional inhibitory index (FICI) is calculated as follows: FICI= ($MIC_{AS\text{-}48\ in\ presence\ of\ ethambutol}$ /$MIC_{AS\text{-}48\ alone}$) + ($MIC_{ethambutol\ in\ presence\ of\ AS\text{-}48}$ /$MIC_{ethambutol\ alone}$); FICI$\leq$ 0.5 indicates synergism; FICI= 0.5-4, indicates no interaction and FICI> 4.0, indicates antagonism. EMB: Ethambutol.

DISCUSSION

Bacteriocins have been highlighted as potential antimicrobial compounds in antituberculosis treatment, and in fact, several works have reported the antituberculosis activity of certain bacteriocins (14, 54, 55). Howerver, although antimicrobial and antiparasital activity of bacteriocin AS-48 has also reported in the literature (12, 13, 40, 48, 53, 56-64), to date, its antituberculosis activity had never been characterized before.

Susceptibility of *M. tuberculosis* strains to bacteriocin AS-48 ranged from 16 to 64 µg/ml, including reference strains and several clinical isolates of *M. tuberculosis* selected by their different spoligotype and RFLP profile. We found that AS-48 is bactericidal against *M. tuberculosis*. Several other bacteriocins have been reported as effective against *M. tuberculosis* in *in vitro* assays (14, 54, 65, 66): colistin has an MIC of 16 µg/ml (55), and nisin showed an MIC >60µg/ml against *M. tuberculosis* H37Ra (14). These authors described variants of nisin with an enhanced antimicrobial activity (65) against *M. tuberculosis* as well as other naturally occurring bacteriocin such as lacticin 3147 (MIC_{90} = 7.5 µg/ml) (14). In conclusion, when comparing antituberculosis activity of AS-48 with that of other bacteriocins, most values are in the range of 7.5 – 64 µg/ml. However other bacteriocins, such as B602, OR7, S760 and E50-52, have a stronger effect in inhibiting growth of *M. tuberculosis* at 0.1 µg/ml concentration, than the same concentration of rifampicin (15).

The success in the improvement of antituberculosis activity of nisin derivatives (65) prompted us to explore whether variants of AS-48 (altered in residues important for maturation, conformation stability, etc.) could have reduced MICs in comparison with wild-type AS-48. However, none of these variants resulted in a significant change of their MICs against *M. tuberculosis*, similarly to what has been described for other bacterial species (11). The only two mutants that exhibit a similar inhibitory activity against *M. tuberculosis* were G13K

and L40K, they also have almost the same activity against the majority of the gram-positive bacteria assayed (51). According to Maqueda M., *et al*. (67) the active site, where the maximum positive electrostatic potential (that will promote the peptide to its first approach to the membrane) is in the opposite site of the lysine residues of mutants G13K and L40K. The addition of an extra positive charge in mutants G13K and L40K did not improve the activity or stability of these mutants (11). From this experiments, we decided to continue exploring the activity of the wild-type, AS-48, since these mutants do not exhibit a great advantage in the activity against *M. tuberculosis*. Nevertheless, other aspects could be considered for further studies, such us the cytotoxicity of the mutants or the bioavailability for *in vivo* experiments.

We have also explored susceptibility of other mycobacterial species to AS-48 and found that for some species (*M. smegmatis, M. fortuitum* and *M. mucogenicum;* all three fast-growing mycobacteria) the MIC of AS-48 does not change significantly in comparison with that of *M. tuberculosis*. Carroll *et al.* (65) also described a rather uniform susceptibility of nisin derivatives between *M. tuberculosis, M. kansasii, and M. avium*. For other mycobacterial species (slow-growing and chromogenic species), however, we obtained either very low MICs (<2 μg/ml for *M. xenopi* and *M. gordonae*) or we could not detect any inhibition of growth up to 256 μg/ml (*M. lentiflavum*).

Lysozyme is an enzyme present in respiratory tract secretions as a part of the body defense mechanisms against microbes. It has been reported that the combination of lysozyme and bacteriocins such as nisin results in a synergistic effect against many bacterial pathogens such as *C. difficile* (68). This synergistic effect of lysozyme has also been described for AS-48 (48). The lysozyme, acting in the cell wall, could facilitate the access of AS-48 into the bacteria and increase its bactericidal effect. Through synergy tests, we have found that AS-48 strongly synergizes with lysozyme, as it has been reported for other bacterial species (48). Moreover, the combination of drugs with cell wall hydrolytic enzymes (i.e.

lysozyme) augment the efficacy of the drugs, and reveal a synergistic effect and an enhancement of the bactericidal activity in mycobacterial strains (69).

From the early dates of antituberculosis treatment, it became evident that monotherapy results in the selection of drug-resistant strains, so a combination therapy was established as a gold-standard for antituberculosis treatment with decreased probabilities to develop resistance. Then, for any new antituberculosis agent, it is interesting to investigate not only its own antimicrobial activity but also how it may interact with other drugs in use against tuberculosis. We have investigated the interaction between AS-48 and first-line antituberculosis drugs by using the checkerboard assay, considered as an accurate drug-combination analysis method (20), that has been used for demonstrating synergism of drugs and drug candidates in *M. tuberculosis* (70, 71). We found that there is a synergism between AS-48 and ethambutol. In fact, the synergism between AS-48 and ethambutol was stronger than that of AS-48 and lysozyme. We can hypothesize that ethambutol, by inhibiting biosynthesis of arabinogalactan in cell wall, this would increase the permeability of mycobacterial cells, and this could facilitate the access of AS-48 to its potential target, the mycobacterial membrane. The work by Kalita *et al.* (29) reported synergism between the antimicrobial human neutrophil peptide 1 (HNP-1) and the antituberculosis drugs isoniazid and rifampicin, and hence proposed the use of this AMP as an adjuvant in antituberculosis chemotherapy.

In the intracellular *M. tuberculosis* growth assays in macrophages, the combination between AS-48 and ethambutol readily shows strong synergism, and the FICI values obtained are similar to the ones found in *in vitro* cultures. However, when we tested the interaction between AS-48 and lysozyme in the intracellular model of infection, no synergistic effect was observed in any of the conditions tested, in contrast with what we have observed in *in vitro* cultures. We can speculate that either lysozyme could not get inside the macrophages, hence it could not reach the intracellular bacteria residing in the phagosome, or it could be degraded by the macrophage.

In summary, we have reported here the antituberculosis activity *in vitro* of circular bacteriocin AS-48, both on extracellular and intracellular bacteria. Interestingly, we have found that in both systems, AS-48 strongly synergizes with ethambutol, hence opening the way to further explore the interaction of other AMPs with antituberculosis drugs and their future potential use as adjuvants of current antituberculosis treatments or as part of a new alternative therapeutic regimen.

REFERENCES

1. Shirude PS, Ramachandran S, Hosagrahara V. 2013. Challenges and opportunities in tuberculosis drug discovery: an industry perspective. Future Med Chem 5:499-501.
2. Cong F, Cheung AK, Huang SM. 2012. Chemical genetics-based target identification in drug discovery. Annu Rev Pharmacol Toxicol 52:57-78.
3. Manjunatha UH, Smith PW. 2015. Perspective: Challenges and opportunities in TB drug discovery from phenotypic screening. Bioorg Med Chem 23:5087-97.
4. Cooper CB. 2013. Development of Mycobacterium tuberculosis whole cell screening hits as potential antituberculosis agents. J Med Chem 56:7755-60.
5. Cavera VL, Arthur TD, Kashtanov D, Chikindas ML. 2015. Bacteriocins and their position in the next wave of conventional antibiotics. Int J Antimicrob Agents 46:494-501.
6. Administration USFD. 2018. Microorganisms & Microbial-Derived Ingredients Used in Food (Partial List). Accessed
7. Fahim HA, Khairalla AS, El-Gendy AO. 2016. Nanotechnology: A Valuable Strategy to Improve Bacteriocin Formulations. Front Microbiol 7:1385.
8. Marr AK, Gooderham WJ, Hancock RE. 2006. Antibacterial peptides for therapeutic use: obstacles and realistic outlook. Curr Opin Pharmacol 6:468-72.
9. Alvarez-Sieiro P, Montalban-Lopez M, Mu D, Kuipers OP. 2016. Bacteriocins of lactic acid bacteria: extending the family. Appl Microbiol Biotechnol 100:2939-51.
10. Sánchez-Barrena MJ, Martínez-Ripoll M, Gálvez A, Valdivia E, Maqueda M, Cruz V, Albert A. 2003. Structure of Bacteriocin AS-48: From Soluble State to Membrane Bound State. Journal of Molecular Biology 334:541-549.
11. Sánchez-Hidalgo M, Montalban-Lopez M, Cebrián R, Valdivia E, Martínez-Bueno M, Maqueda M. 2011. AS-48 bacteriocin: close to perfection. Cell Mol Life Sci 68:2845-57.
12. Abriouel H, Lucas R, Omar NB, Valdivia E, Galvez A. 2010. Potential Applications of the Cyclic Peptide Enterocin AS-48 in the Preservation of Vegetable Foods and Beverages. Probiotics Antimicrob Proteins 2:77-89.
13. Ananou S, Valdivia E, Martinez Bueno M, Galvez A, Maqueda M. 2004. Effect of combined physico-chemical preservatives on enterocin AS-48 activity against the enterotoxigenic Staphylococcus aureus CECT 976 strain. J Appl Microbiol 97:48-56.
14. Carroll J, Draper LA, O'Connor PM, Coffey A, Hill C, Ross RP, Cotter PD, O'Mahony J. 2010. Comparison of the activities of the lantibiotics nisin and lacticin 3147 against clinically significant mycobacteria. Int J Antimicrob Agents 36:132-6.

15. Sosunov V, Mischenko V, Eruslanov B, Svetoch E, Shakina Y, Stern N, Majorov K, Sorokoumova G, Selishcheva A, Apt A. 2007. Antimycobacterial activity of bacteriocins and their complexes with liposomes. J Antimicrob Chemother 59:919-25.

16. Gonzalez C, Langdon GM, Bruix M, Galvez A, Valdivia E, Maqueda M, Rico M. 2000. Bacteriocin AS-48, a microbial cyclic polypeptide structurally and functionally related to mammalian NK-lysin. Proc Natl Acad Sci U S A 97:11221-6.

17. Collin F, Thompson RE, Jolliffe KA, Payne RJ, Maxwell A. 2013. Fragments of the bacterial toxin microcin B17 as gyrase poisons. PLoS One 8:e61459.

18. Plat A, Kluskens LD, Kuipers A, Rink R, Moll GN. 2011. Requirements of the engineered leader peptide of nisin for inducing modification, export, and cleavage. Appl Environ Microbiol 77:604-11.

19. Chou TC. 2006. Theoretical basis, experimental design, and computerized simulation of synergism and antagonism in drug combination studies. Pharmacol Rev 58:621-81.

20. Jia J, Zhu F, Ma X, Cao Z, Cao ZW, Li Y, Li YX, Chen YZ. 2009. Mechanisms of drug combinations: interaction and network perspectives. Nat Rev Drug Discov 8:111-28.

21. Sergina NV, Rausch M, Wang D, Blair J, Hann B, Shokat KM, Moasser MM. 2007. Escape from HER-family tyrosine kinase inhibitor therapy by the kinase-inactive HER3. Nature 445:437-41.

22. Keith CT, Borisy AA, Stockwell BR. 2005. Multicomponent therapeutics for networked systems. Nat Rev Drug Discov 4:71-8.

23. Cottagnoud P, Cottagnoud M, Tauber MG. 2003. Vancomycin acts synergistically with gentamicin against penicillin-resistant pneumococci by increasing the intracellular penetration of gentamicin. Antimicrob Agents Chemother 47:144-7.

24. Brochado AR, Telzerow A, Bobonis J, Banzhaf M, Mateus A, Selkrig J, Huth E, Bassler S, Zamarreno Beas J, Zietek M, Ng N, Foerster S, Ezraty B, Py B, Barras F, Savitski MM, Bork P, Gottig S, Typas A. 2018. Species-specific activity of antibacterial drug combinations. Nature 559:259-263.

25. Cokol M, Weinstein ZB, Yilancioglu K, Tasan M, Doak A, Cansever D, Mutlu B, Li S, Rodriguez-Esteban R, Akhmedov M, Guvenek A, Cokol M, Cetiner S, Giaever G, Iossifov I, Nislow C, Shoichet B, Roth FP. 2014. Large-scale identification and analysis of suppressive drug interactions. Chem Biol 21:541-551.

26. Bruhn DF, Scherman MS, Liu J, Scherbakov D, Meibohm B, Bottger EC, Lenaerts AJ, Lee RE. 2015. In vitro and in vivo Evaluation of Synergism between Anti-Tubercular Spectinamides and Non-Classical Tuberculosis Antibiotics. Sci Rep 5:13985.

27. Bhusal Y, Shiohira CM, Yamane N. 2005. Determination of in vitro synergy when three antimicrobial agents are combined against Mycobacterium tuberculosis. Int J Antimicrob Agents 26:292-7.

28. Gupta K, Singh S, van Hoek ML. 2015. Short, Synthetic Cationic Peptides Have Antibacterial Activity against Mycobacterium smegmatis by Forming Pores in Membrane and Synergizing with Antibiotics. Antibiotics (Basel) 4:358-78.

29. Kalita A, Verma I, Khuller GK. 2004. Role of human neutrophil peptide-1 as a possible adjunct to antituberculosis chemotherapy. J Infect Dis 190:1476-80.

30. Cole ST, Barrell BG. 1998. Analysis of the genome of Mycobacterium tuberculosis H37Rv. Novartis Found Symp 217:160-72; discussion 172-7.

31. Lee JS, Krause R, Schreiber J, Mollenkopf HJ, Kowall J, Stein R, Jeon BY, Kwak JY, Song MK, Patron JP, Jorg S, Roh K, Cho SN, Kaufmann SH. 2008. Mutation in the transcriptional regulator PhoP contributes to avirulence of Mycobacterium tuberculosis H37Ra strain. Cell Host Microbe 3:97-103.

32. Gonzalo Asensio J, Maia C, Ferrer NL, Barilone N, Laval F, Soto CY, Winter N, Daffe M, Gicquel B, Martin C, Jackson M. 2006. The virulence-associated two-component PhoP-PhoR system controls the biosynthesis of polyketide-derived lipids in Mycobacterium tuberculosis. J Biol Chem 281:1313-6.

33. Fleischmann RD, Alland D, Eisen JA, Carpenter L, White O, Peterson J, DeBoy R, Dodson R, Gwinn M, Haft D, Hickey E, Kolonay JF, Nelson WC, Umayam LA, Ermolaeva M, Salzberg SL, Delcher A, Utterback T, Weidman J, Khouri H, Gill J, Mikula A, Bishai W, Jacobs WR, Venter JC, Fraser CM. 2002. Whole-Genome Comparison of Mycobacterium tuberculosis Clinical and Laboratory Strains. Journal of Bacteriology 184:5479-5490.

34. Caminero JA, Pena MJ, Campos-Herrero MI, Rodriguez JC, Garcia I, Cabrera P, Lafoz C, Samper S, Takiff H, Afonso O, Pavon JM, Torres MJ, van Soolingen D, Enarson DA, Martin C. 2001. Epidemiological evidence of the spread of a Mycobacterium tuberculosis strain of the Beijing genotype on Gran Canaria Island. Am J Respir Crit Care Med 164:1165-70.

35. Chesne-Seck ML, Barilone N, Boudou F, Gonzalo Asensio J, Kolattukudy PE, Martin C, Cole ST, Gicquel B, Gopaul DN, Jackson M. 2008. A point mutation in the two-component regulator PhoP-PhoR accounts for the absence of polyketide-derived acyltrehaloses but not that of phthiocerol dimycocerosates in Mycobacterium tuberculosis H37Ra. J Bacteriol 190:1329-34.

36. Zhang M, Sala C, Hartkoorn RC, Dhar N, Mendoza-Losana A, Cole ST. 2012. Streptomycin-starved Mycobacterium tuberculosis 18b, a drug discovery tool for latent tuberculosis. Antimicrob Agents Chemother 56:5782-9.

37. Snapper SB, Melton RE, Mustafa S, Kieser T, Jacobs WR, Jr. 1990. Isolation and characterization of efficient plasmid transformation mutants of Mycobacterium smegmatis. Mol Microbiol 4:1911-9.

38. Sander P, Meier A, Bottger EC. 1995. rpsL+: a dominant selectable marker for gene replacement in mycobacteria. Mol Microbiol 16:991-1000.

39. Stephan J, Stemmer V, Niederweis M. 2004. Consecutive gene deletions in Mycobacterium smegmatis using the yeast FLP recombinase. Gene 343:181-90.

40. Cebrian R, Banos A, Valdivia E, Perez-Pulido R, Martinez-Bueno M, Maqueda M. 2012. Characterization of functional, safety, and probiotic properties of Enterococcus faecalis UGRA10, a new AS-48-producer strain. Food Microbiol 30:59-67.

41. Ananou S, Muñoz A, Gálvez A, Martínez-Bueno M, Maqueda M, Valdivia E. 2008. Optimization of enterocin AS-48 production on a whey-based substrate. International Dairy Journal 18:923-927.

42. Palomino JC, Martin A, Camacho M, Guerra H, Swings J, Portaels F. 2002. Resazurin microtiter assay plate: simple and inexpensive method for detection of drug resistance in Mycobacterium tuberculosis. Antimicrob Agents Chemother 46:2720-2.

43. Odds FC. 2003. Synergy, antagonism, and what the chequerboard puts between them. J Antimicrob Chemother 52:1.

44. (ESCMID) ECfASTEotESoCMaID. 2000. Terminology relating to methods for the determination of susceptibility of bacteria to antimicrobial agents. Clinical Microbiology and Infection 6:503-508.

45. Repetto G, del Peso A, Zurita JL. 2008. Neutral red uptake assay for the estimation of cell viability/cytotoxicity. Nat Protoc 3:1125-31.

46. Christophe T, Jackson M, Jeon HK, Fenistein D, Contreras-Dominguez M, Kim J, Genovesio A, Carralot JP, Ewann F, Kim EH, Lee SY, Kang S, Seo MJ, Park EJ, Skovierova H, Pham H, Riccardi G, Nam JY, Marsollier L, Kempf M, Joly-Guillou ML, Oh T, Shin WK, No Z, Nehrbass U, Brosch R, Cole ST, Brodin P. 2009. High content screening identifies decaprenyl-phosphoribose 2' epimerase as a target for intracellular antimycobacterial inhibitors. PLoS Pathog 5:e1000645.

47. Chun W, Hancock RE. 2000. Action of lysozyme and nisin mixtures against lactic acid bacteria. Int J Food Microbiol 60:25-32.

48. Ananou S, Rivera S, Madrid MI, Maqueda M, Martínez-Bueno M, Valdivia E. 2018. Application of enterocin AS-48 as biopreservative in eggs and egg fractions: Synergism through lysozyme. LWT - Food Science and Technology 89:409-417.

49. Sanchez-Hidalgo M, Martinez-Bueno M, Fernandez-Escamilla AM, Valdivia E, Serrano L, Maqueda M. 2008. Effect of replacing glutamic residues upon the biological activity and stability of the circular enterocin AS-48. J Antimicrob Chemother 61:1256-65.

50. Cebrian R, Maqueda M, Neira JL, Valdivia E, Martinez-Bueno M, Montalban-Lopez M. 2010. Insights into the functionality of the putative residues involved in enterocin AS-48 maturation. Appl Environ Microbiol 76:7268-76.

51. Sanchez-Hidalgo M, Fernandez-Escamilla AM, Martinez-Bueno M, Valdivia E, Serrano L, Maqueda M. 2010. Conformational stability and activity of circular Enterocin AS-48 derivatives. Protein Pept Lett 17:708-14.

52. 10993-5 I. 2009. Biological evaluation of medical devices (Part 5: Test for *in vitro* cytotoxicity). ISO 10993-5:2009(E). (ISO) IOfS,

53. Abengozar MA, Cebrian R, Saugar JM, Garate T, Valdivia E, Martinez-Bueno M, Maqueda M, Rivas L. 2017. Enterocin AS-48 as Evidence for the Use of Bacteriocins as New Leishmanicidal Agents. Antimicrob Agents Chemother 61.

54. Carroll J, J OM. 2011. Anti-mycobacterial peptides: made to order with delivery included. Bioeng Bugs 2:241-6.

55. van Breda SV, Buys A, Apostolides Z, Nardell EA, Stoltz AC. 2015. The antimicrobial effect of colistin methanesulfonate on Mycobacterium tuberculosis in vitro. Tuberculosis (Edinb) 95:440-6.

56. Viedma PM, Abriouel H, Omar NB, Lopez RL, Galvez A. 2009. Antistaphylococcal effect of enterocin AS-48 in bakery ingredients of vegetable origin, alone and in combination with selected antimicrobials. J Food Sci 74:M384-9.

57. Ruiz-Rodriguez M, Martinez-Bueno M, Martin-Vivaldi M, Valdivia E, Soler JJ. 2013. Bacteriocins with a broader antimicrobial spectrum prevail in enterococcal symbionts isolated from the hoopoe's uropygial gland. FEMS Microbiol Ecol 85:495-502.

58. Martinez Viedma P, Sobrino Lopez A, Ben Omar N, Abriouel H, Lucas Lopez R, Valdivia E, Martin Belloso O, Galvez A. 2008. Enhanced bactericidal effect of enterocin AS-48 in combination with high-intensity pulsed-electric field treatment against Salmonella enterica in apple juice. Int J Food Microbiol 128:244-9.

59. Grande Burgos MJ, Pulido RP, Del Carmen Lopez Aguayo M, Galvez A, Lucas R. 2014. The Cyclic Antibacterial Peptide Enterocin AS-48: Isolation, Mode of Action, and Possible Food Applications. Int J Mol Sci 15:22706-22727.

60. Grande Burgos MJ, Kovacs AT, Mironczuk AM, Abriouel H, Galvez A, Kuipers OP. 2009. Response of Bacillus cereus ATCC 14579 to challenges with sublethal concentrations of enterocin AS-48. BMC Microbiol 9:227.

61. Cobo Molinos A, Abriouel H, Lopez RL, Valdivia E, Omar NB, Galvez A. 2008. Combined physico-chemical treatments based on enterocin AS-48 for inactivation of Gram-negative bacteria in soybean sprouts. Food Chem Toxicol 46:2912-21.

62. Caballero Gomez N, Abriouel H, Grande MJ, Perez Pulido R, Galvez A. 2013. Combined treatments of enterocin AS-48 with biocides to improve the inactivation of methicillin-sensitive and methicillin-resistant Staphylococcus aureus planktonic and sessile cells. Int J Food Microbiol 163:96-100.

63. Antonio CM, Abriouel H, Lopez RL, Omar NB, Valdivia E, Galvez A. 2009. Enhanced bactericidal activity of enterocin AS-48 in combination with essential oils, natural bioactive compounds and chemical preservatives against Listeria monocytogenes in ready-to-eat salad. Food Chem Toxicol 47:2216-23.

64. Ananou S, Munoz A, Martinez-Bueno M, Gonzalez-Tello P, Galvez A, Maqueda M, Valdivia E. 2010. Evaluation of an enterocin AS-48 enriched bioactive powder obtained by spray drying. Food Microbiol 27:58-63.

65. Carroll J, Field D, O'Connor PM, Cotter PD, Coffey A, Hill C, Ross RP, O'Mahony J. 2010. Gene encoded antimicrobial peptides, a template for the design of novel anti-mycobacterial drugs. Bioeng Bugs 1:408-12.

66. Montalban-Lopez M, Sanchez-Hidalgo M, Valdivia E, Martinez-Bueno M, Maqueda M. 2011. Are bacteriocins underexploited? Novel applications for old antimicrobials. Curr Pharm Biotechnol 12:1205-20.

67. Maqueda M, Galvez A, Bueno MM, Sanchez-Barrena MJ, Gonzalez C, Albert A, Rico M, Valdivia E. 2004. Peptide AS-48: prototype of a new class of cyclic bacteriocins. Curr Protein Pept Sci 5:399-416.

68. Chai C, Lee KS, Imm GS, Kim YS, Oh SW. 2017. Inactivation of Clostridium difficile spore outgrowth by synergistic effects of nisin and lysozyme. Can J Microbiol 63:638-643.

69. Gustine JN, Au MB, Haserick JR, Hett EC, Rubin EJ, Gibson FC, 3rd, Deng LL. 2019. Cell Wall Hydrolytic Enzymes Enhance Antimicrobial Drug Activity Against Mycobacterium. Curr Microbiol doi:10.1007/s00284-018-1620-z.

70. Makarov V, Lechartier B, Zhang M, Neres J, van der Sar AM, Raadsen SA, Hartkoorn RC, Ryabova OB, Vocat A, Decosterd LA, Widmer N, Buclin T, Bitter W, Andries K, Pojer F, Dyson PJ, Cole ST. 2014. Towards a new combination therapy for tuberculosis with next generation benzothiazinones. EMBO Mol Med 6:372-83.

71. Lechartier B, Hartkoorn RC, Cole ST. 2012. In vitro combination studies of benzothiazinone lead compound BTZ043 against Mycobacterium tuberculosis. Antimicrob Agents Chemother 56:5790-3.

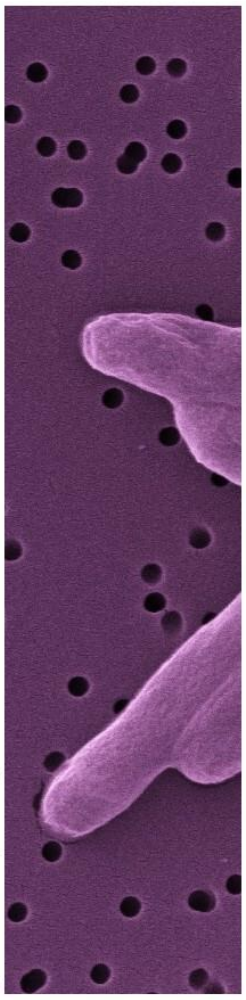

Chapter 2

Strategies for elucidation of AS-48 Mode of Action

INTRODUCTION

In the study of drug discovery, it is crucial to know which are the mechanisms of resistance that microorganism have, either intrinsic or acquired. Knowing this, would help to prevent the development of new resistant strains.

MECHANISMS OF RESISTANCE IN *MYCOBACTERIUM TUBERCULOSIS*

In the search of new antimicrobials to fight tuberculosis, the knowledge of how the different drugs interact with the bacteria, and the strategies that *M. tuberculosis* has to avoid their harmful effect, seem to be crucial for the development of new antituberculosis compounds and new therapeutic strategies. The fast development of drug resistance in *M. tuberculosis* strains, is causing a heavy burden in the global health panorama. Again, it is very important the understanding of the different molecular mechanisms that are involved in the appearance of drug resistance, especially in those cases where a single strain presents resistance against different kinds of antimicrobials, i.e. multi-drug-resistant (MDR), extensively-drug-resistant (XDR) and totally-drug-resistant (TDR) strains (1, 2).

In *M. tuberculosis,* horizontal gene transfer, through plasmids, transposon or phages has not been registered, so the acquired resistance is due to chromosomal mutations. Selection of resistant mutants can be enhanced by the environmental pressure caused by the use of antimicrobial drugs, especially when a non-effective concentration is given (3), or when there is non-adherence to the treatment during such as long periods of regimens that are used in tuberculosis treatment. Under these conditions, most of susceptible populations will be eliminated, and those microorganisms that have got an advantage through the selection of a resistance mutation will survive. With a combined therapy of more than one drug given simultaneously, the appearance of resistance is less probable

but is still possible, and nowadays, multi-drug resistant strains constitute a social problem that has to be solved by different approaches.

Intrinsic resistance

One of the reasons why the number of antimicrobials available for treating tuberculosis is lower than for other pathogens is its intrinsic resistance. Besides, it makes harder to discover or find new strategies or antimicrobials. Cell permeability is a factor contributing to intrinsic resistance, mainly mediated by the existence of the multi-layered cell wall. The intrinsic resistance due to the cell wall has been demonstrated in several occasions by studying mutations that affect the cell wall biosynthesis (4, 5).

Of course, this intrinsic resistance due to the cell wall could be overcame by the existence of porins (proteins causing hydrophilic channels in the cell wall), that could allow the entrance of antimicrobial drugs through them, although this could be compensated with porin mutations or with the efflux of the drug by the efflux pumps. The efflux pumps are transmembrane proteins that have several functions such as transporting wastes or signalling molecules out of the bacterial cell. They transport specifically several antimicrobial drugs outside the cell, even when they could not be structurally related. Mutations in regulators of efflux pump genes confer in some cases antibiotic resistance. For example, in *M. tuberculosis* the transporter Tap, which is regulated by *WhiB7*, is able to export p-aminosalicylic acid (PAS), conferring a low level of resistance to this drug. It has been proposed that an efflux inhibitor could be a valuable tool for fighting tuberculosis as well as infections caused by other multi-drug resistant pathogens (6). It has been demonstrated that the porins MspA and MspC play a role in the resistance to fluoroquinolones and chloramphenicol in *M. smegmatis* (7).

Target alteration

One of the mechanisms of resistance is the modification of the target, which can take place directly by altering the target sequence through gene mutations or indirectly through other mechanisms that control the access of the drug to the target. This is the case of the resistance to capreomycin and viomycin, two peptides that bind 16S and 23S of rRNA in a region methylated by the enzyme TlyA; a loss of function of TlyA confers resistance to capreomycin and viomycin (8, 9).

Target mimicry

The target of fluoroquinolones is the inhibition of DNA replication, transcription and repair by blocking the DNA gyrase. However, *M. tuberculosis* has an interesting mechanism that confers resistance to fluoroquinolones: it consists in producing a protein called MfpA that mimic the structure of the DNA molecule, it is though that MfpA can capture fluoroquinolones avoiding the binding to the natural DNA (10).

Compensatory mutations

The appearance of these mutations implies an energetic (or fitness) cost that may act against the development of the emerging resistance. For this reason, *M. tuberculosis,* as well as other pathogens, is able to compensate this fitness cost with secondary mutations called "compensatory mutations", which allow resistant bacteria to restore their fitness after a long exposure to antimicrobials. Comas *et al*. (11) demonstrate that the fitness of rifampicin-resistant strains of *M. tuberculosis* was recovered when they performed growth competition assays. They concluded that recovering the fitness by compensatory mutations would had allow to some MDR strains to prevail in the population. We can appreciate that *M. tuberculosis* has a great versatility and capability of adaptation to the drug-

mediated aggressions of the environment, and also it has the ability to modify or counteract the external drug attack.

Drug modification

In the resistance against aminoglycosides (such as kanamycin) a protein called Eis plays and important role. This mycobacterial protein is able to inactivate certain aminoglycosides by acetylation of the amine groups (12), also has been demonstrated by Houghton *et al*. (13), that Eis, could also play a role in the inactivation of capreomycin, which is a circular antimicrobial peptide. Also, mutations in the Eis protein turns *M. tuberculosis* resistant to kanamycin A but not in amikacin.

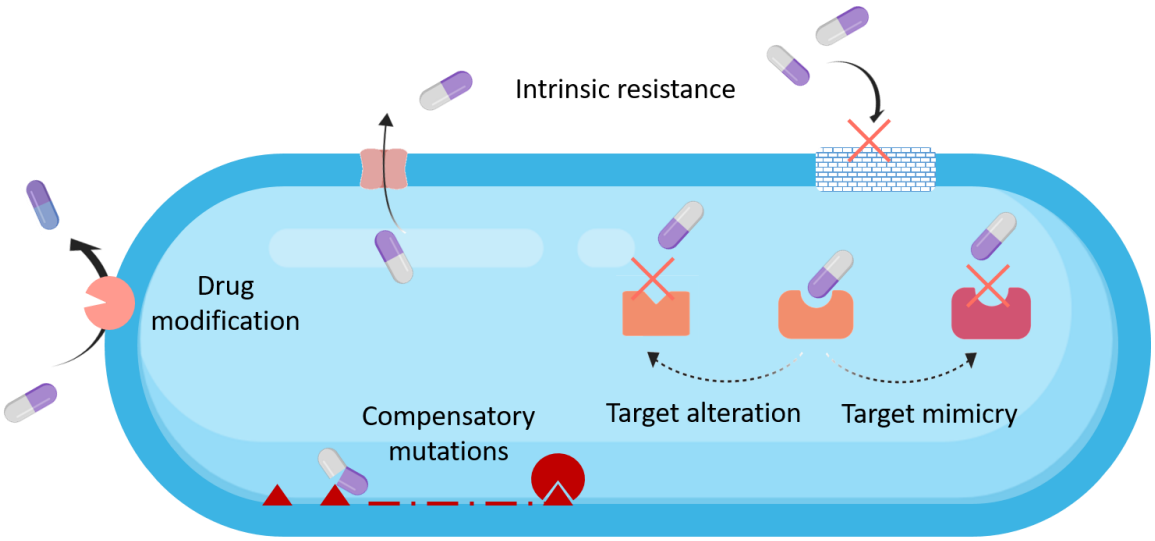

Image 1: Schematic representation of the different mechanisms of resistance in *M. tuberculosis*.

DRUGS, DRUG TARGETS AND MODE OF ACTION

Historically, gene products that are essential for maintaining bacterial structures or contribute to essential metabolic processes like DNA replication, RNA synthesis, protein synthesis, energy metabolism, cell wall synthesis or folate metabolism have been attractive targets for the discovery of new drugs capable of inhibiting them (14). Consequently, antimicrobial drug resistance often arises through the acquisition of mutations in the genes encoding such drug targets. A few well known examples are:

1. Fluoroquinolones are broad-spectrum antimicrobials that interfere with bacterial DNA replication. In the case of *M. tuberculosis*, like in all other bacteria, they block the activity of DNA gyrase, then the DNA is unable to initiate the replication. DNA gyrase is encoded by *gyrA* and *gyrB* genes, and resistance to fluoroquinolones are often due to mutations in the coding region of these genes (15). Currently, fluoroquinolones are used as a second-line drugs for the treatment of MDR tuberculosis.

2. Rifamycins act at the transcription level, since they inhibit the action of RNA polymerase by forming a complex with its β-subunit. Rifampicin (RIF) is one of the most effective drugs used in the treatment of tuberculosis. The most common mutations that produces resistance are located in *rpoB* gen, which encodes the β-subunit of the RNA polymerase. The *M. tuberculosis* strains called multi-drug resistant (MDR) are resistant to RIF (16).

3. Protein synthesis is another classical drug target. Streptomycin, which was the first antitubercular antibiotic discovered, binds to the 30S subunit of the ribosome, thus inhibiting the normal protein synthesis. Mutations in *rpsL* or *rrs* genes, which encode 30S ribosome components, are associated with streptomycin-resistance (17). Currently, streptomycin is used as a first-line drug against tuberculosis. The oxazolidinone drug linezolid binds to the 50S ribosomal subunit altering the protein synthesis and having a bacteriostatic effect. Although resistance to linezolid is not very common, mutations in the 23S rRNA and in the *rplC* gene have been related with resistance to this drug (18); also, the effect of

efflux pumps has been suggested as a possible mechanism of resistance to linezolid in *M. abscessus* (19). Linezolid is very toxic in prolonged treatments; for this reason, it is not commonly used to treat tuberculosis.

4. Pyrazinamide (PZA) is one of the first-line drugs against tuberculosis that plays an important role in the shortening the disease treatment from 9-12 months to 6 months. It is targeting the energy metabolism by disrupting the membrane potential, interfering with the energy production and the synthesis of mycolic acids. The majority of the *M. tuberculosis* resistant strains to PZA has mutations in the gene *pncA*. Also other genes, such as *rpsaA*, *panD* and *hadC* have been reported to play a role in the PZA resistance adquisition. This has suggested that PZA could target the trans-translation process, the acidification of the cytoplasm and the synthesis of coenzyme A in *M. tuberculosis* (20).

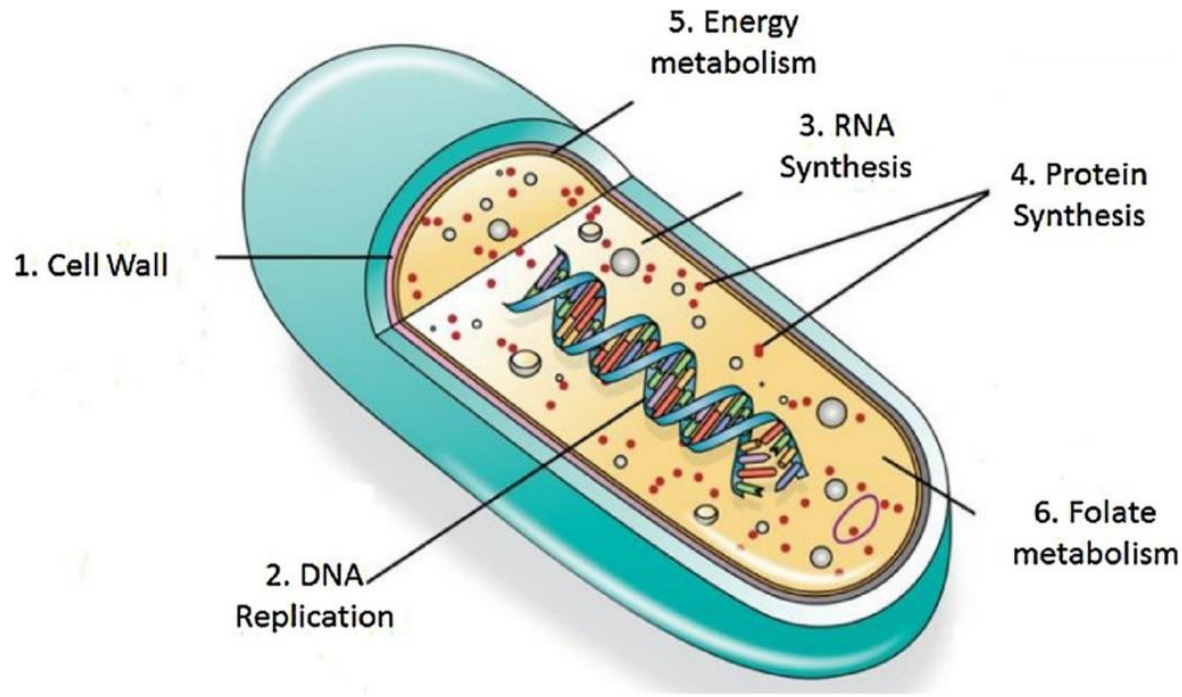

Image 17: Classical targets of antimicrobials against *M. tuberculosis* (14).

DRUGS ACTING AT THE CELL WALL

The bacterial cell wall is one of the most explored drug targets, with several families of drugs acting on it. The mycobacterial cell wall plays an important role in tuberculosis survival, interaction with the host and virulence, and also is a significant barrier for antimicrobial drugs (21). Due to its high content of lipids, most of the hydrophilic agents cannot permeate the cell wall. Some of the drugs that target the cell wall are: isoniazid (INH), ethambutol (EMB), ethionamide (ETH), ethylenediamine, pyrazinamide (PZA) and cycloserine. From these, INH, PZA and EMB are first-line drugs used in combination with RIF in the tuberculosis treatment for drug susceptible strains.

INH is a pro-drug that is activated by catalase-peroxidase and inhibits InhA (enoyl-ACP reductase) that acts in the synthesis of mycolic acids. There are several genes implied in resistance to INH (*katG, inhA, ahpC, kasA* and *ndh*), and efflux pumps are also involved in the acquisition of the resistance to INH (22). EMB is a bacteriostatic agent that has activity against actively replicating bacilli, it is also used for treating infections with *M. avium* and *M. kansasii*. It interferes in the formation of mycolyl-arabinogalactan-peptidoglycan complex by disrupting the synthesis of arabinogalactan, since it inhibits the enzyme arabinosyl transferase. Recently, Pawar A. *et al*, have suggested that EMB is also targeting glutamate racemase (MurI), an enzyme implied in the synthesis of peptidoglycan (23).

The recently discovered antituberculosis drugs delamanid and pretomanid, have an interesting mode of action, since they act in multiple targets, which is an advantage in order to avoid the selection of resistant mutants. In the case of delamanid, it has a strong activity against *M. tuberculosis* including rifampicin resistant and MDR strains (24). Delamanid inhibits the biosynthetic pathways of two mycolic acids, methoxy and ketomycolic acids. It has been recently published that delamanid exert a great activity against dormant tuberculosis *in vitro* and in guinea pig animal model (25). In the case of pretomanid, after being activated by a nitroreductase, it is able to inhibit the protein synthesis and also disrupts the cell wall lipid biosynthesis (26). Despite the fact that, multi-target drugs are less likely

to select resistance, it has been found that a mutation in the *rv3547* gene generate delamanid-resistant strains of *M. tuberculosis* (27), and pretomanid-resistance seems to be caused by the loss of a specific glucose-phosphate dehydrogenase (28).

Moreover, finding new multi-target drugs offer the possibility to reduce the development of resistance (29). Concurrence of multiple targets could be classified as series inhibition: when targets are in the same pathway; parallel inhibition: targets are unrelated; or network inhibition when many targets are in series or in parallel (30).

TARGETING THE MEMBRANE AND MEMBRANE PROTEINS

Recently, the interest on new drugs with unexpected targets has arisen, such as the InhA (enoyl-acyl carrier protein reductase) in methylthiazoles,pirrolydine carboxamides or diaryl ethers; the transmembrane transporter MmpL3 in ethambutol or in adamantly ureas; DprE1 (decaprenylphospho-beta-D-ribofuranose 2-oxidase) in benzothiazoles and the QcrB (ubiquinol-cytrochrome C reductase) in lansoprazole (31). They have in common that they are membrane proteins, thus the membrane could be an underexploited target for the developing of new antituberculosis drugs.

Apart from the drugs that disrupt the function of membrane proteins, there are other agents that interact directly with the structure of the membrane itself. Most of these interactions are due to the charge of the membrane, which is negatively charged due to the phospholipids and polyanionic groups, so that it binds positively charged drugs (32).

In this context, antimicrobial peptides (AMP) interact electrostatically with the mycobacterial membrane and can cross the different layers disrupting some components of the cell envelope. The insertion of AMP in the inner membrane results in a loss of membrane permeability, but also allows pore formation. Pore formation not only affect the permeability of the bacillus membrane; it also alters

the transmembrane potential, and other intracellular processes could result indirectly altered. Targeting the membrane present an advantage: membrane integrity is vital for both replicating and latent bacteria, and this feature is one of the goals for developing new drugs against tuberculosis.

In this work we have explored the activity of AS-48, a circular bacteriocin, that in previous studies has been proposed to have a mode of action by disrupting the plasma membrane (33). However, due to the special composition of the cell wall in *M. tuberculosis* we wanted to explore if the same mode of action that, AS-48 present against other species, is also happening in our microorganism of interest.

THE OMICS IN DRUG RESISTANCE AND DRUG DISCOVERY

In the last years, research on the acquisition of resistance genes has moved from the study of individual genes to the entire genome, the whole-genome sequencing (WGS). The comparative study of different genomes, either resistant strains or not, has become a good tool for the identification of resistance mechanisms. Along with that, further confirmatory studies should be done, such as generation of knockout mutants and phenotypic studies.

In this context, RNAseq analysis seems a very appropriate technique for the evaluation of the interaction of different genes that confer resistance to antimicrobials.

The RNAseq is a quantitative technique, it can provide levels of gene expression more accurately than former microarrays systems. One advantage of RNAseq is the possibility to track gene expression during a dynamic process (34). Other advantages over hybridization-based techniques are the high sensitivity for detecting low abundance transcripts, singles nucleotide resolution and the means to profile gene expression for those strains whose genome sequence is not annotated (35). RNAseq analysis provides the information of differentially

expressed genes (DEG), changes in gene expression under several experimental conditions, etc. This technology is also used to investigate which genes are expressed differentially when an infectious process is happening, and to quantify the levels of expression of each transcript under different conditions (36). DEG identified *in vivo* could help in the design of novel antimicrobials or therapies with different targets (37), this tool could help to avoid the gap between *in vitro* analysis and the *in vivo* approach. By the use of WGS, Winglee *et al*. (38) described the evidence of a mutation in the gene *rv2887*, with a loss of function, in mutants resistant to imidazo[1,2-*a*]pyridine-4-carbonitrile-based (MP-III-71) compounds. By the use of RNAseq analysis, they identified which genes were differentially expressed in the resistant mutant or in the wild type in the presence of MP-III-71. Gene expression analysis have been used not only for understanding the mechanism of action of antimicrobial drugs but also could be an interesting tool for determining new diagnostic biomarkers in the tuberculosis disease (39). By using RNAseq, it was possible to observe the difference of the immune response when the bacilli are adapted to its host. Malone K.M. *et al*. identified the mechanisms of the innate immune response during the early infection of *M. tuberculosis* and differentiated them from the infection of *M. bovis* when they are infecting cows (40, 41). In order to analyse the interaction of cholesterol, palmitic and oleic acids with *M. tuberculosis* during the infectious process, Aguilar-Ayala D.A. *et al*. (42) demonstrated the implications of lipid pathways, efflux pumps and iron and sulphur caption, by RNAseq technique. They suggested that the response to these fatty acids, could be the machinery that confers drug tolerance to drugs and proposed the differentially expressed pathways as a therapeutic target.

Finally, in the fight against tuberculosis exploring new molecules or searching new targets are the best weapon to lead the new emerging resistance and the spread of the multidrug resistance strains.

OBJECTIVE

In the previous chapter, we have characterised the antimicrobial activity of bacteriocin AS-48, against mycobacterial strains, mostly *M. tuberculosis*, and discovered its synergism with a lytic enzyme (lysozyme) and with the first line antituberculosis drug ethambutol. We wanted to get further knowledge on how this bacteriocin acts on mycobacterial cells. For exploring this, we have followed two main approaches: first, assays aimed at determining the integrity and functionality of the bacterial membrane have been done, given that for many other bacteriocins, the bacterial membrane is proposed as a target; in parallel, we have followed a global approach by using transcriptomic techniques, in order to get a complete picture on how the bacterial react to the treatment of AS-48.

The specific objectives have been the following:

1) To determine if mycobacterial cells treated with AS-48 can accumulate increased quantities of ethidium bromide
2) To explore whether AS-48 is able to depolarize the membrane of mycobacterial cells
3) To analyse global transcriptome of *M. tuberculosis* after treatment with AS-48 at several time points
4) To validate candidate genes that could be relevant for the response of mycobacterial cells to treatment with AS-48
5) To build up a hypothesis on how this bacteriocin acts and how the bacteria can response to treatment with AS-48

MATERIALS AND METHODS

ETHIDIUM BROMIDE ACCUMULATION ASSAY

This assay assesses the capacity of *M. smegmatis* cells for accumulating ethidium bromide in the presence of increasing concentrations of bacteriocin AS-48. *M. smegmatis* was cultivated until an $O.D._{600}$ of 0.6-0.8 at 37ºC in Middlebrook 7H9 broth supplemented with Tween 80 at 0.05% and 10% of ADC enrichment. The culture was centrifuged and the pellet washed in PBS buffer supplemented with 0.05% Tween 80, then the $O.D._{600}$ was adjusted to 0.8 in the same buffer further supplemented with glucose 0.4%. The ethidium bromide was used at 1 µg/ml combined with inhibitory and subinhibitory concentrations of AS-48. Verapamil at 75 µg/ml was used as a positive control showing the highest accumulation of ethidium bromide. A control experiment was done with PBS-Tween 80 buffer and no bacterial inoculum, to set the values of fluorescence of the compounds by themselves. Other controls were done without ethidium bromide, to set the values of fluorescence of the bacterial cells. Accumulation of ethidium bromide was measured by recording fluorescence at 530 nm excitation and the 590 nm detection during an hour (43).

ANALYSIS OF THE BACTERIAL MEMBRANE POTENTIAL

M. smegmatis and *M. bovis* BCG membrane potential was measured by the Baclight Bacterial Membrane Potential Kit (BacLight™, B34950, Thermo Fisher Scientific) according to manufacturer instructions; integrity of the membrane potential results in fluorescence due to the accumulation of $DiOC_2(3)$ (Ex/Em of 482/497 nm) inside bacterial cells. Bacterial cells were treated with several concentrations of AS-48 during 24 hours to assess its effect in the membrane potential. The samples were analysed by flow cytometry (Gallios, Beckman Coulter, Inc). Parameters, Forward Scatter (FSC) and side Scatter (SSC), were

adjusted according to the size of bacteria. For detecting $DiOC_2(3)$ a emission laser of 488 nm was used. For collecting the signal the filter FL1 was used that collect the wavelength at 505-545 nm.

SAMPLES FOR SCANNING ELECTRON MICROSCOPY (SEM)

The effect of AS-48 in morphology of *M. tuberculosis* H37Rv was analysed by Scanning Electron Microscopy (SEM). SEM images were acquired using an SEM Inspect™ F50 (FEI Company, Eindhoven, The Netherlands). Bacterial cultures treated with AS-48 at 64 µg/ml or with 8 µg/ml of AS-48 plus 25 µg/ml of lysozyme, were diluted to 10^5 cfu/ml, and samples were firstly fixed with glutaraldehyde. Then, samples were washed three times with 10x PBS and filtered through 0.1 µm filter (Isopore™ Membrane Filters 0.1µm VCTP, Millipore) and finally dehydrated with a graded ethanol series, and kept in 100% ethanol. Finally, ethanol was evaporated at room temperature, and samples were covered with a thin layer of metal (Pt, 15 nm) and examined at 15 keV and at different magnifications.

RNA EXTRACTION

For RNA extraction, *M. tuberculosis* H37Rv was cultured in a minimum of 10 ml volume up to and O.D. of 0.3-0.5. Cultures were then centrifuged at 3220x g during 5 min and supernatants were discarded. Then, 500µl of wash buffer (a solution of 1.5 ml of 8% NaCl and 75µl of Tween 80 in a final volume of 15 ml of nuclease-free water) and 1ml of RNA protect reagent (Quiagen) were added and homogenized. The samples were incubated at room temperature during 5 min and centrifuged at 20817x g during 5 min. The supernatants were discarded and the last drops were removed with a micropipette. At this point, pellets were stored at -80ºC until all samples were collected. Mycobacterial pellets were defrosted and resuspended in 400 µl of fresh lysis buffer (solution of 67 µl of sodium acetate 3M

pH 5.5 (Ambion), 500 µl of SDS 10%, 5 µl EDTA 0.2M in 10 ml of nuclease-free water) and 1 ml of acid-phenol:chloroform (5:1). Mycobacterial cells were lysed in a screw tube with glass beads (lising matrix B, MP Biomedicals™) using Fast-Prep® equipment, with two 45 second cycles at 6.5 m/s. Samples must be cooled on ice for 5 min between pulses. Then, samples were centrifuged at 20817x g during 5 minutes at 4 ºC. The bacterial pellets went again through the Fast-Prep® step in order to recover as much RNA as possible; the upper aqueous phase was recovered and transferred to a fresh tube and extracted with 900 µl of isoamilic:chloroform (24:1). Samples were kept on ice all the time. Again, samples were centrifuged for 5 minutes at 20817x g at 4 ºC. The final supernatant was placed in a new tube with 900 µl of isopropyl alcohol and 90 µl of sodium acetate 3M pH 5.5 for precipitating RNA. Tubes were incubated at -20 ºC over night for RNA precipitation. Up to this point, the experiments were carried out in the BSL3 facilities.

For recovering RNA, tubes were centrifuged at 20817x g during 30 min at 4 ºC. Pellet was washed with 1 ml of 70% ethanol and centrifuged again during 5 min at 20817x g and 4 ºC. Supernatants were discarded and finally the pellets containing RNA were resuspended in 100 µl of nuclease-free water.

Treatment with DNase was done to avoid DNA contamination. Two incubations with Turbo DNA-free DNAse (Ambion) were done at 37 ºC for one hour each of them. A second purification process was performed by adding 200 µl of acid-phenol:chloroform and 50 µl of nuclease-free water, samples were homogenized and centrifuged 5 min at maximum speed. The aqueous phase was precipitated again with 400 µl of isopropyl alcohol and 20 µl of sodium acetate (3M, pH 5.5) and incubated over night at -20 ºC.

After the second purification, RNA pellets were rinsed with 200 µl of ethanol (70%) and resuspended in 50 µl nuclease-free water. RNA integrity was assessed by agarose gel electrophoresis and absence of DNA contamination was checked by PCR amplification.

Concentration of RNA was assessed using ND-1000 spectrophotometer (NanoDrop technologies) reading at 260/280 nm.

RNASEQ ANALYSIS

Bacterial cultures were grown with and without 64 µg/ml of AS-48. RNA extraction was done at time 0, after 4 hours and after 24 hours. RNA samples were sent to FISABIO (*Fundación para el Fomento de la Investigación Sanitaria y Biomédica de la Comunitat Valenciana*) where cDNA libraries were prepared and sequenced by NextSeq RUN High Output 1x150pb by Illumina Technology.

BIOINFORMATIC ANALYSIS

The bioinformatics analysis was performed in FISABIO where the normalized count values were faced for each sample and plotted in a biplot. The relative expression (Sample 1/Sample 2) for each comparison were presented in a distribution in order to show the variability within each comparison. From this distribution, only those values that overcome the quintiles 0.95 and 0.05 of the relative expression were taken into account as a differentially expressed. All statistics have been obtained using The RStatistics software making use of several Open Source libraries such as rtracklayer, GenomicFeatures, etc. Infering the transcripts and its expression has been done using Cufflinks (44) and R libraries: Rsamtools, GenomicFeatures, GenomicAlignments and NOISeq (45) program suite. BAM files from TopHat alignment program has been processed by Cufflinks to assembly transcriptomes from the alignment to reference genome. Computation of gene and transcript expression profiles is given in two formats: count tables and FPKM tables.

Density distribution of expression levels relationship using as reference sample. For samples with different RNA composition, it is expected a different distribution in sequencing reads across genomic features, in such a way that

although a feature had the same number of read counts in both samples, it would not mean that it was equally expressed in both. To check if this bias is present in the data, RNA composition distribution plot and the corresponding diagnostic test can be used. In this case, each sample is compared to the reference sample (which is randomly chosen). To do that, log2 (counts sample / counts reference) are computed. If no bias is present, it should be expected that the median of log2 (counts sample / counts reference) for each comparison is 0. Otherwise, it would be indicating that expression levels in one of the samples tend to be higher than in the other, and this could lead to false discoveries when computing differencial expression.

Therefore, a normalization procedure should be used to correct this effect and make the samples comparable before computing differential expression. Differential expression comparison has been based on relative expression ratio (REi) between normalized reads counts from pairs samples of interest. Normalization of counts are obtained by library or size factor measuring differences between samples in terms of coverage or number of reads and recalibrating counts with this factor to make them comparable (46). Once normalized counts are obtained, relative expression ratio is calculated for each gene as the formula below:

$$REi = \frac{Sample\ 1i}{Sample\ 2i}$$

Being *i* each of consider genes into the analysis. Biplots confronting normalized counts and distribution of relative expression ratios are show bellow for each sample and gene pair considered. Finally, for each comparison high and low relative expressed genes are shown in table format, using quantiles 0.95 (high relative expressed genes: higher sample1 vs lower sample2 normalized counts) and 0.05 (low relative expressed genes: lower sample1 vs higher sample2 normalized counts) of relative expression ratio distributions as threshold criteria.

REAL TIME QUANTITATIVE REVERSE TRANSCRIPTION PCR

A real-time quantitative reverse transcription PCR (qRT-PCR) were carried out to check the expression levels of genes selected after the RNAseq analysis.

First, reverse transcription was done with 500 ng of RNA and 2 µl of Prime Script RT Master Mix (Takara) in a final volume of 10 µl of nuclease-free water. The Mix included Pimer Script Rtase, RNase inhibitor, Random Hexamers, dNTP Mixture and Mg^{2+} buffer. Actinomycin D (Sigma) was added to each sample to avoid second-strand cDNA synthesis during reverse transcription. The reverse transcription reaction was performed at 37 ºC during 15 minutes, 85ºC during 5 seconds and finally kept at 4ºC. Next, the resulting cDNA was diluted 1/10 for the qRT-PCR amplification in presence of the different gene primers (**Table 8**); 5 µl of SYBR green Master Mix (Takara) were added by each cDNA sample. This Mix also contains ROX dye which is used for normalize the non-PCR-related fluctuations in fluorescence signal, 0.2 µl of ROX was added by each cDNA sample.

The qRT-PCR reactions were performed as recommended by the manufacturer (95ºC for 10 minutes, followed by 40 cycles of: 95ºC for 15 seconds and 60ºC for 1 minute, and finished with sample storage at 4ºC). The amplifications were carried out in the StepOne Plus Real Time PCR System (Applied Biosystems). All primers were designed using the Primer Express Software (Applied Biosystems).

Finally, for assessing the specificity and amplification of one single product per each primer pair, a melting curve were done. Two housekeeping genes were used to normalize the gene expression between samples: *sigA* (encoding sigma factor A) and *rrs* (encoding 16S rRNA) because they both have a stable expression level under different experimental conditions.

Table 8: Target genes and primers (5' to 3') for qRT-PCR reactions.

GEN	RV	Forward	Reverse
hycQ	Rv0086	TCTTTGCGCGATGGTTCTG	ACCGTGGTGGCCTCGAT
fadD10	Rv0099	CGGCGGGTTGTGTGTCA	GGTGAGAATCTCCAGCAACGA
hsp	Rv0251c	CGGTGGTCCGTTTGGAACT	GGGTCAAGCTCGACGTTGA
secE2	Rv0379	CGGGTCATTGAGCAGGACAT	CTTGATGCGGTAGGTGATCTTG
mce2D	Rv0592	AGGCGCTCGCGCTGTAC	ACCCGCACACCCATGATC
vapC7	Rv0661c	CTGGGCCGTGTGACTATGC	GGTGGCCTCGATTGATGGT
rpmD	Rv0722	CACTCTGGGCTTACGAAGGATT	CGAGTCGCTGCGTTGTCTT
fadE9	Rv0752c	GCGCATCTTCGAGCAGTTG	ATGTTGTGGATGGACAAAAACG
ephC	Rv1124	CGGCGAACGGGAGTCA	ACGTCAATCCAGTGTGGTTCAG
prpC	Rv1131	CACCGCCATCTCCAAGGT	TCCCCGGTAGGTCAACGA
mbtN	Rv1346	AAGCGCAGGAACGTTTTCC	TCGAATACGCCGCAGACA
cydD	Rv1621c	CGGCTATTTGCCCACGTT	GGCAGTGTGATCACCACAATG
vapB12	Rv1721c	GATGAGCCTGAGCGATTTCC	CCGGTTCTTCCGCGATCT
vapC34	Rv1741	TGATGTCGACGGCGTCATAT	CCCGAAGCGTGTTTCGAT
vapC14	Rv1953	TGCAAGTCGCCGAACAGTT	TCACGCCTCGCTCAATCTC
higB	Rv1955	CCGGCCGGTATTCAAGAAG	GCCCGGGCCTGATCA
parD1	Rv1960c	TGGGTAAGAACACGTCCTTCGT	GCGATCTCGCCGTCGAT
vapC36	Rv1982c	TCTTTCACCGCCGAGCAT	TTGCCGTATCGCAGAAAGG
rpsN2	Rv2056c	AAGAAGTCCAAGATCGTCAAGAATC	GGGATCGGATGATGTCTTTGAG
mazE7	Rv2063	TCCACGACGATTAGGGTTTCA	AGCAGAGCCGACATCGAGAT
vapB16	Rv2231B	CGATGATCGCGAAGTTTGGT	GCAGGCGCCCAGACTTT
cyp121	Rv2276	GGCTCGTCTCCTCGTATGCA	ATGGAAAAACGCCGATCCT
uspB	Rv2317	TCACGCTGTCCCCCTTCTT	GAACTGGTGTGCGGAAGTGAA
lppQ	Rv2341	GTCGACGAAGGCCAGATCTC	CAACCATCGCCGCTTGATA
plcA	Rv2351c	GGTCAGCTGGAAGGTGTACCA	TGATGGGCGTGTTGATGAAT
mbtH	Rv2377c	TTCTTCGTGCTGGTCAACGA	CGGGATATCGGCGAACAC
mbtA	Rv2384	TTCGCTGGAGCTCCGATTAC	ACCACGCCGGTCAAGGTA
accD1	Rv2502c	CCCCGGGTCCCTTACG	GAATTCGCTGCCGTCAACA
fas	Rv2524c	CGTGCACCCGAGTTTGGT	GCAATGATATTCGGCAAGACTTC
vapB17	Rv2526	ATTGAGCTGGACGAAGATCTTGT	ACCGTCGCTCGCAATGTT
vapC42	Rv2759c	GGTCACCGAACTCCCGAAT	TGATCGCGCACAGTTCGA

GEN	RV	Forward	Reverse
vapB22	Rv2830c	TGACCGCTACGGAGGTGAA	CGCCCTGGGCCACTTC
ugpE	Rv2834c	GGGCCGTTGCTGTTCGT	CGCATAGATGTCGGGCTGAT
esxS	Rv3020c	GCCGCCAAGGTCAATACCT	GCGGCCTCACCCAAATT
metA	Rv3341	GCCCGCGACGGAAAG	GCCTGCACCTGGTCACGTA
relK	Rv3358	CCTGGGAGGACTTCTTGTTCTG	ATCCGACGGGCCGTTTT
dppC	Rv3664c	GGATCGATGCGGTGGTTTC	CAACGGCAAGCCGAGAA

MATHEMATICAL ANALYSIS OF QRT-PCR

The data generated by StepOne Plus Real Time PCR System provide the C_T value of each reaction; all gene amplifications were performed in triplicate, and for each gene, arithmetic average of the triplicates was done. For calculating delta C_T, the geometric average of the different arithmetic average of each housekeeping (HK) gene was subtracted from the arithmetic average of the genes of interest (GOI):

$$\Delta CT = arithmetic\ average\ of\ GOI - geometric\ average\ of\ each\ arithmetic\ average\ of\ the\ HK$$

We considered the expression genes of the positive control at time 0 as the calibrator, so for calculating the Delta Delta C_T :

$$\Delta\Delta CT = \Delta CT\ sample - \Delta CT\ calibrator$$

And then the relative quantification (RQ) was calculated as follows from the Delta Delta C_T :

$$RQ = 2^{-\Delta\Delta CT}$$

Finally, the fold change of each gene was calculated as the ratio of the RQ of each gene when the sample was treated with AS-48 and the RQ of each gene when the sample was untreated (positive control):

$$Fold\ Change = \frac{RQ\ sample\ (time)}{RQ\ control\ (time)}$$

Graphic representation of the Fold Change allowed to identify whether any specific gene has been differentially expressed between both conditions.

MYCOBACTERIAL DNA EXTRACTION

The method used for genomic mycobacterial DNA extraction was based on CTAB method (47). Mycobacterial cultures were centrifuged, the pellets resuspended in 400µl of TE (100 mM Tris/HCl, 10 mM EDTA, pH 8) and inactivated by heat during 15 minutes at 85°C. Then, 50µl of lysozyme solution (10 mg/ml) were added and incubated at 37°C at least one hour. Next, 75 µl of the mix composed by SDS (72.5 µl, 10%) and Protein K (2.5 µl, 20mg/ml) were added and mixed by inversion, then incubated at 65°C during 10 minutes. After this, 100 µl of a prewarmed solution of NaCl (5M) and 100 µl of CETAB/NaCl (10% CETAB in 0.7M NaCl) were added and incubated during 10 minutes at 65°C. Then, 750 µl of chloroform/isoamyl alcohol (24:1) were added to extract genomic DNA. After centrifugation (5 minutes at 15294x g) the upper aqueous phase was transferred into a new tube containing 420 µl of isopropanol and kept at -20°C during at least 30 minutes for DNA precipitation. Precipitated DNA was pelleted by centrifugation (5 minutes at15294x g) and washed by 500 µl of ethanol 70%, mixed by inversion. After centrifugation, pellet was vacuum dried and finally resuspended in 50µl of MilliQ water. DNA was quantified by absorbance readings at 260 nm using a ND-1000 spectrophotometer (NanoDrop technologies).

ELECTROPHORETIC MOBILITY SHIFT ASSAY (EMSA)

To evaluate the ability of AS-48 to bind bacterial DNA, an electrophoretic mobility shift assay (EMSA) was done. For this, 250 ng of DNA extracted from *M. tuberculosis* H37Rv were used in a final reaction volume of 12 µl. Serial dilutions of AS-48, from 1300 to 2.5 µg/ml, were incubated during 10 minutes at room temperature with the DNA samples and load in 0.8% agarose gel at 130V and detected by the fluorescence of ethidium bromide. In the first well was loaded the molecular weight marker of 100bp (GeneRuler 100bp Plus DNA Ladder. ThermoFisher).

RESULTS

IS AS-48 TARGETING THE MYCOBACTERIAL MEMBRANE?

In order to explore whether bacteriocin AS-48 could be targeting the mycobacterial membrane, we carried out experiments of ethidium bromide accumulation using *M. smegmatis* mc²155 and we determined the ability of AS-48 for depolarising the mycobacterial membrane.

It is assumed that AS-48 forms pores in the membrane (48), thus making the cell more permeable to compounds such as ethidium bromide. Therefore, in an ethidium bromide accumulation assays, we would expect that the fluorescence detected would be higher in the presence of AS-48, reflecting the increased accumulation of ethidium bromide as a result of the effect of AS-48 in the bacterial membrane. We compared the effect of AS-48 with verapamil, a well-known efflux inhibitor (43), which produces an increase in the accumulation of ethidium bromide. In the presence of AS-48, fluorescence due to accumulated ethidium bromide increased upon time in a concentration dependent manner, although the kinetics of accumulation was rather distinct to that observed with verapamil (**Image 17**).

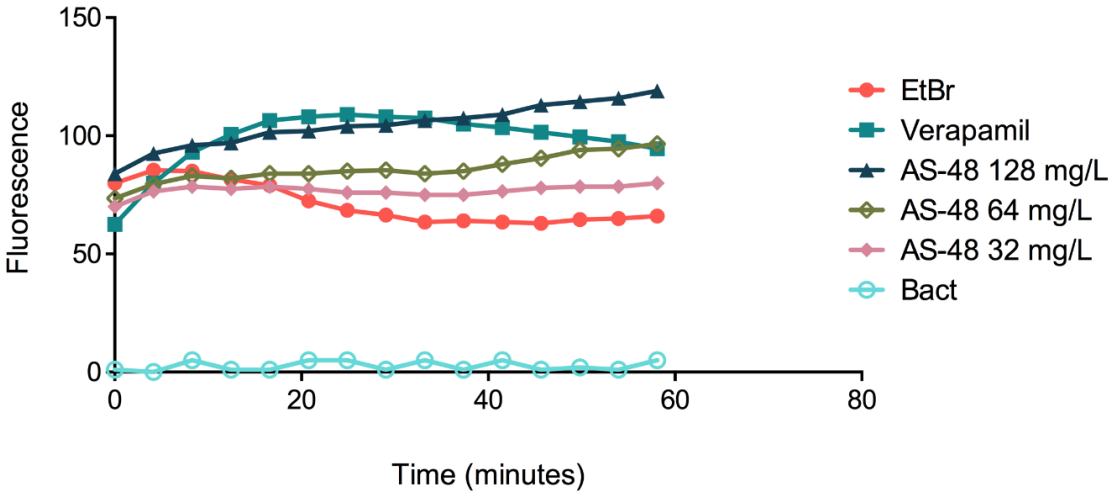

Image 17: Measure of fluorescence in the Ethidium Bromide accumulation assay when treating M. tuberculosis with different AS-48 concentrations and with Verapamil as an efflux inhibitor.

The determination of membrane potential was carried out following the BacLight™ Kit instructions, using *M. smegmatis* mc²155 and *M. bovis* BCG cells. In a representative control experiment, in the untreated cells, a 3.4% of cells were depolarized, whereas in the cells treated with the protonophore CCCP the percentage of depolarized cells was 94.93%. We have assessed the effect of AS-48 in several concentrations and after different times of incubation (1 or 24 hours). We have observed that AS-48 depolarized cells in a concentration-dependent manner, and this effect was much higher in the cells incubated with AS-48 during 24 hours than in those tested after one hour of incubation. **Figure 4** shows that the percentage of depolarized cells after 24 hours is 67.04% in presence of 128 µg/ml of AS-48, 26.34% with 64 µg/ml and, 18.68% with 32 µg/ml. Again, this demonstrate that the depolarization of the cells is dependent on the concentration of AS-48 and increases with time (**Image 18**).

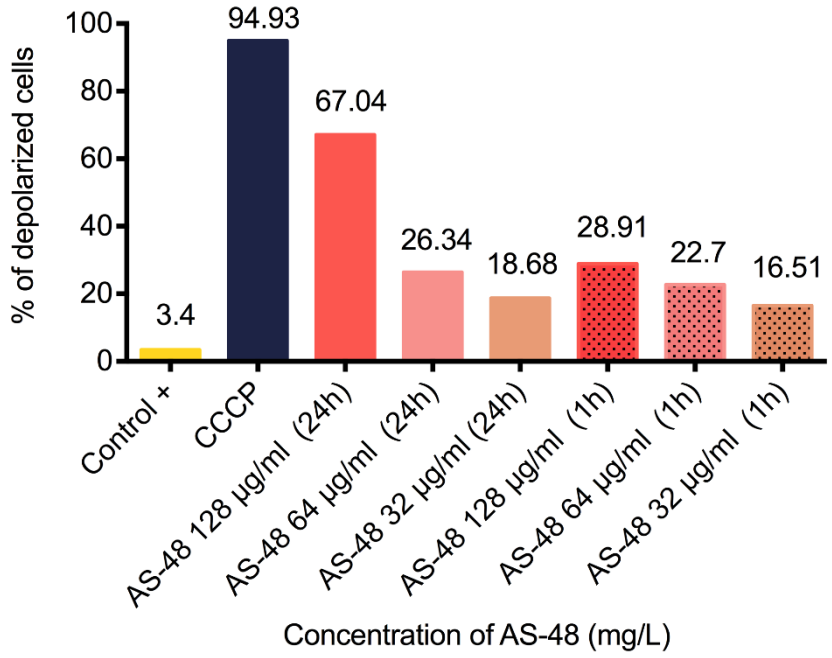

Image 18: Percentage of depolarization when treating *M. smegmatis* with a gradient of AS-48 at different time points. Compared with positive control of depolarization: CCCP (Carbonyl cyanide m-chlorophenyl hydrazone).

TREATMENT WITH AS-48 RESULTS IN MORPHOLOGICAL CHANGES IN *M. TUBERCULOSIS*.

We treated *M. tuberculosis* cells with AS-48, along with untreated cells as a control, and samples were taken at several time points for microscopic observation. We found that after short time exposures (48-72 hours), cells were affected by AS-48 as the morphology of cells treated with a concentration of AS-48 equal to the MIC, were rougher than the control (**Image 19**).

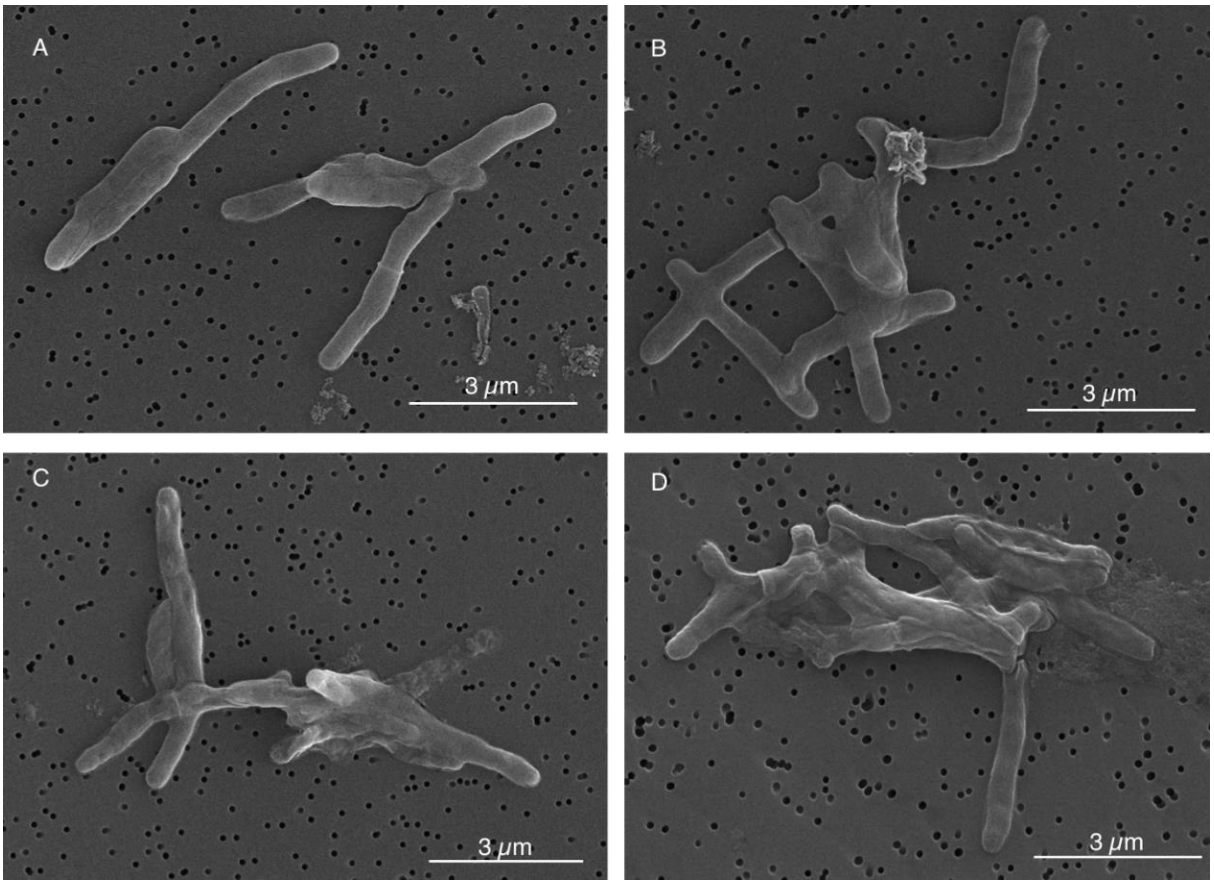

Image 19: Scanning Electron Microscopy (SEM) images of *M. tuberculosis* H37Rv under different conditions. A) Untreated cells after 48 hours of growth. B) Untreated cells after 72 hours of growth. C) Cells treated with 64 µg/ml of AS-48 during 48 hours. D) Cells treated with 64 µg/ml of AS-48 during 72 hours.

Moreover, we analysed the effect of a combination of 8 µg/ml of AS-48 with 25 µg/ml of lysozyme on cell morphology after 24, 48 and 96 hours after treatment. When bacterial cells were treated with a synergistic combination of AS-48 and lysozyme, they exhibited greater morphological damages (**Image 20**), in comparison with cells treated with AS-48 alone (**Image 19**).

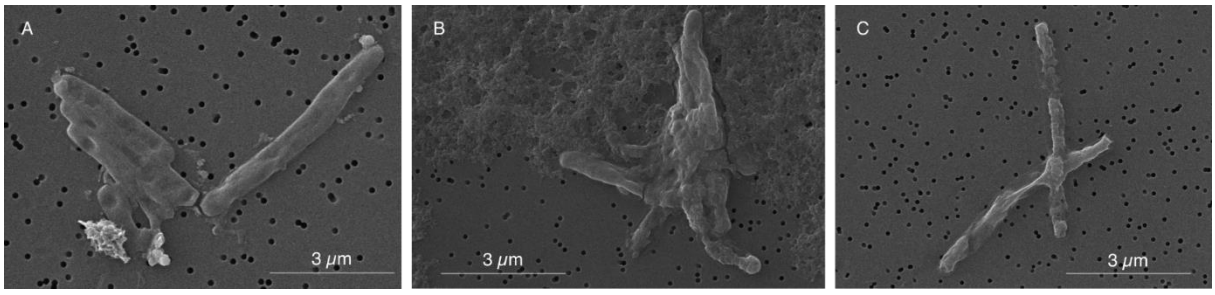

Image 20: Scanning Electron Microscopy (SEM) images of M. tuberculosis H37Rv treated with a synergistic combination of 8 µg/ml of AS-48 and 25 µg/ml of lysozyme; A) after 24 hours of treatment; B) after 48 hours of treatment and C) after 96 hours of treatment.

RESISTANT MUTANTS

For elucidate the mode of action, we have tried to get resistant strains to AS-48 but we could not reach any. We have cultured *M. tuberculosis* under the conditions described in Chapter 1, and treated the inoculum with a concentration of 8 x MIC. After that, we plated the culture and got 57 colonies. The MIC was performed comparing with the wild type strain and the result was that there were not any variation between them.

This suggested that *M. tuberculosis* could present a transitory tolerance to AS-48 but when cultivating again turns into the same susceptibility that we have observed for the MIC determination.

We could not predict which other changes (besides the already described above) AS-48 is causing in *M. tuberculosis*, so, for that reason we decided to perform a transcriptomic assay by RNAseq.

TRANSCRIPTOMICS

In order to get a global impression of the impact of bacteriocin AS-48 on *M. tuberculosis*, we analysed the transcriptome of *M. tuberculosis* H37Rv cultures treated with AS-48 after 4 and 24 hours. We expected that potential mechanisms of resistance or response to the treatment with bacteriocin, or genes related with bacteriocin mode of action would be identified. From the data obtained from the RNAseq analysis, we got a biplot comparison between treated and untreated bacterial cells after the two selected time-points (**Image 21**).

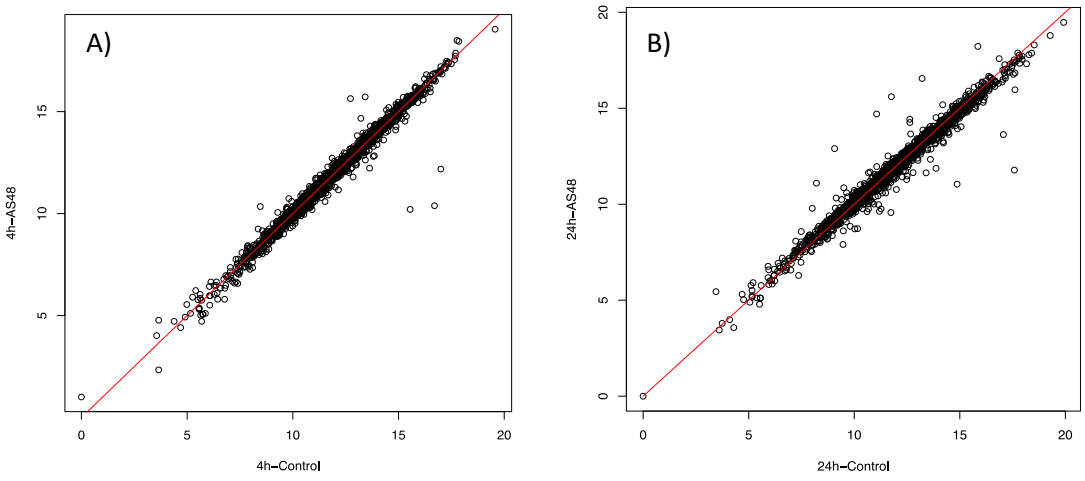

Image 21: Transcriptomics expression bit plots comparisons among treated and untreated cultures after 4hours (A) and 24 hours (B) of treatment with AS-48

The biplot shown in Figure 5 is a density distribution of the relative expression. Those dots that are distant from the diagonal represent genes that change their expression level between treated and untreated cells. It is evident that after 24 hours of treatment, the number of differentially expressed genes is higher than after 4 hours of treatment.

Those genes that have a relative expression values that overcome the quintiles 0.95 (high) and 0.05 (low) were selected for further studies and listed. These are the genes that shows a higher differential expression in the bacteriocin AS-48 treated samples in comparison with the untreated control. According to this

analysis, we obtained four lists, two lists for the genes over- and under-expressed after 4 hours of treatment and two other lists for the same comparison after 24 hours of treatment. These four lists of genes are recorded in the **Tables 9-12**, as follows:

Table 9: Differentially over-expressed genes after 4 hours of treatment with AS-48 (list A).

Gene name	control-4h	AS-48-4h	Relative Expression
vapB16	0.000	1.011	0.000
vapB7	3.656	4.775	0.766
PPE40	12.728	15.641	0.814
PE20	8.461	10.347	0.818
mmpL9	13.424	15.724	0.854
PPE48-1	5.408	6.230	0.868
PE29	3.558	4.020	0.885
PE7	5.259	5.903	0.891
moaD1	4.985	5.544	0.899
narK1	13.220	14.671	0.901
PPE31	8.359	9.247	0.904
fadE9	9.814	10.740	0.914
vapB17	6.125	6.650	0.921
PPE1	9.286	10.059	0.923
mazE7	4.385	4.721	0.929
relK	5.617	6.043	0.929
mbtH	11.859	12.721	0.932

Table 10: Differentially infra-expressed genes after 4 hours of treatment with AS-48 (list B).

Gene name	control-4h	AS-48-4h	Relative Expression
nusB	16.705	10.388	1.608
thiS	3.656	2.339	1.563
aroD	15.550	10.208	1.523
aglA	17.002	12.185	1.395
galK	5.688	4.721	1.205
esxE	6.776	5.802	1.168
PE_PGRS49	5.863	5.108	1.148
vapC7	5.756	5.065	1.137
moaB1	5.734	5.065	1.132
vapB42	7.396	6.575	1.125
uspB	5.641	5.020	1.124
dosT	13.632	12.230	1.115
PE_PGRS36-1	6.446	5.802	1.111
lppQ	8.101	7.352	1.102
PE10	6.073	5.512	1.102
cut1	7.323	6.650	1.101
esxF	7.247	6.591	1.100
vapB22	7.973	7.269	1.097
rpmD	12.853	11.797	1.090
parD1	12.159	11.163	1.089
PE_PGRS10	11.525	10.592	1.088
pfkB	13.858	12.838	1.079
pabB	13.808	12.804	1.078
PE_PGRS3	8.738	8.130	1.075
vapB27	8.867	8.259	1.074
moaR1	10.913	10.191	1.071
PE_PGRS61	6.787	6.343	1.070
PE_PGRS15	11.669	10.910	1.070
vapC34	7.880	7.370	1.069
vapB12	7.140	6.679	1.069

Table 11: Differentially over-expressed genes after 24 hours of treatment with AS-48 (list C).

Gene name	control-24h	AS-48-24h	Relative Expression
mazE7	3.449	5.445	0.633
PE20	9.068	12.901	0.703
PPE31	8.210	11.099	0.740
cyp121	11.060	14.703	0.752
PPE42	11.759	15.606	0.753
cdh	13.213	16.553	0.798
PPE29	8.010	9.788	0.818
phoH1	15.857	18.223	0.870
vapC42	7.489	8.578	0.873
cdd	5.920	6.767	0.875
PPE32	9.505	10.858	0.875
accD1	12.631	14.429	0.875
relK	5.208	5.917	0.880
PPE48-1	4.689	5.308	0.883
papA4	9.143	10.324	0.886
mazF7	5.108	5.767	0.886
accA1	12.634	14.259	0.886
dppC	7.227	8.079	0.895
moaC1	5.949	6.586	0.903
celA1	9.637	10.596	0.909
esxS	6.592	7.195	0.916
yrbE4B	9.400	10.250	0.917
mtc28	10.674	11.637	0.917
PPE33	10.751	11.679	0.921
mpg	6.394	6.928	0.923
thrB	11.064	11.962	0.925
lprJ	11.599	12.517	0.927
prpC	12.672	13.662	0.928
ctpJ	9.101	9.796	0.929
ugpE	7.489	8.041	0.931
mpt83	9.692	10.390	0.933
secE2	10.007	10.726	0.933
PE_PGRS29	10.286	11.016	0.934
prpD	14.191	15.184	0.935
galK	5.159	5.510	0.936

Gene name	control-24h	AS-48-24h	Relative Expression
ephC	8.814	9.399	0.938
uspA	7.887	8.408	0.938
PE_PGRS9	7.856	8.369	0.939
PPE39	6.213	6.615	0.939
mce2D	8.321	8.853	0.940
lpqC	9.967	10.598	0.940

Table 12: Differentially infra-expressed genes after 24 hours of treatment with AS-48 (list D).

Gene name	control-24h	AS-48-24h	Relative Expression
aglA	17.585	11.780	1.493
plcA	14.873	11.048	1.346
lipP	17.064	13.630	1.252
mbtI	11.737	9.567	1.227
vapB7	4.293	3.572	1.202
mbtL	9.467	7.905	1.198
hisE	7.364	6.290	1.171
dosT	13.873	11.871	1.169
mbtA	10.156	8.727	1.164
mbtD	11.195	9.633	1.162
mbtC	11.272	9.756	1.155
mbtB	13.404	11.636	1.152
mbtJ	10.024	8.717	1.150
vapC7	5.512	4.794	1.150
cydD	11.155	9.980	1.118
iniB	11.995	10.769	1.114
hycP	9.806	8.853	1.108
lprD	12.483	11.287	1.106
fas	17.614	15.963	1.103
hsp	13.610	12.339	1.103
cydB	10.606	9.621	1.102
PPE1	9.482	8.611	1.101
hycE	12.786	11.644	1.098
argD	10.673	9.761	1.094
mbtK	10.932	10.008	1.092
hycQ	12.505	11.474	1.090
cydC	11.490	10.587	1.085
PE10	5.551	5.115	1.085

Gene name	control-24h	AS-48-24h	Relative Expression
rpmG1	5.551	5.115	1.085
blaI	14.224	13.194	1.078
higB	12.278	11.425	1.075
sigC	10.849	10.102	1.074
PE25	15.060	14.038	1.073
vapC17	7.479	6.975	1.072
argR	8.961	8.365	1.071
PPE3	14.209	13.268	1.071
vapC14	11.335	10.589	1.070
ctpC	14.889	13.931	1.069
cobU	8.723	8.176	1.067
fadD10	11.127	10.439	1.066
hycD	11.612	10.897	1.066
ureA	10.395	9.762	1.065
rpsN2	6.994	6.571	1.064
vapC36	10.647	10.009	1.064
vapB4	8.744	8.224	1.063
PE34	14.489	13.637	1.062
mbtN	12.434	11.731	1.060
metA	13.018	12.285	1.060

In the four tables above, the second and third column contain the expression level of the gene normalized. And the fourth column contains the ratio between the expression level in cultures treated with AS-48 in comparison with expression levels in untreated cultures. This ratio is <1 for genes over-expressed after AS-48 treatment and >1 for genes under-expressed after AS-48 treatment.

We compared the four lists of differentially expressed genes during time. The number of genes that appeared in one single list or in two lists simultaneously (obviously there was no gene in common between three or the four lists) were represented in the following Venn diagram (**Image 22**). Considering this

comparison, we selected some genes for further qRT-PCR analysis to validate and quantify the relative level of expression.

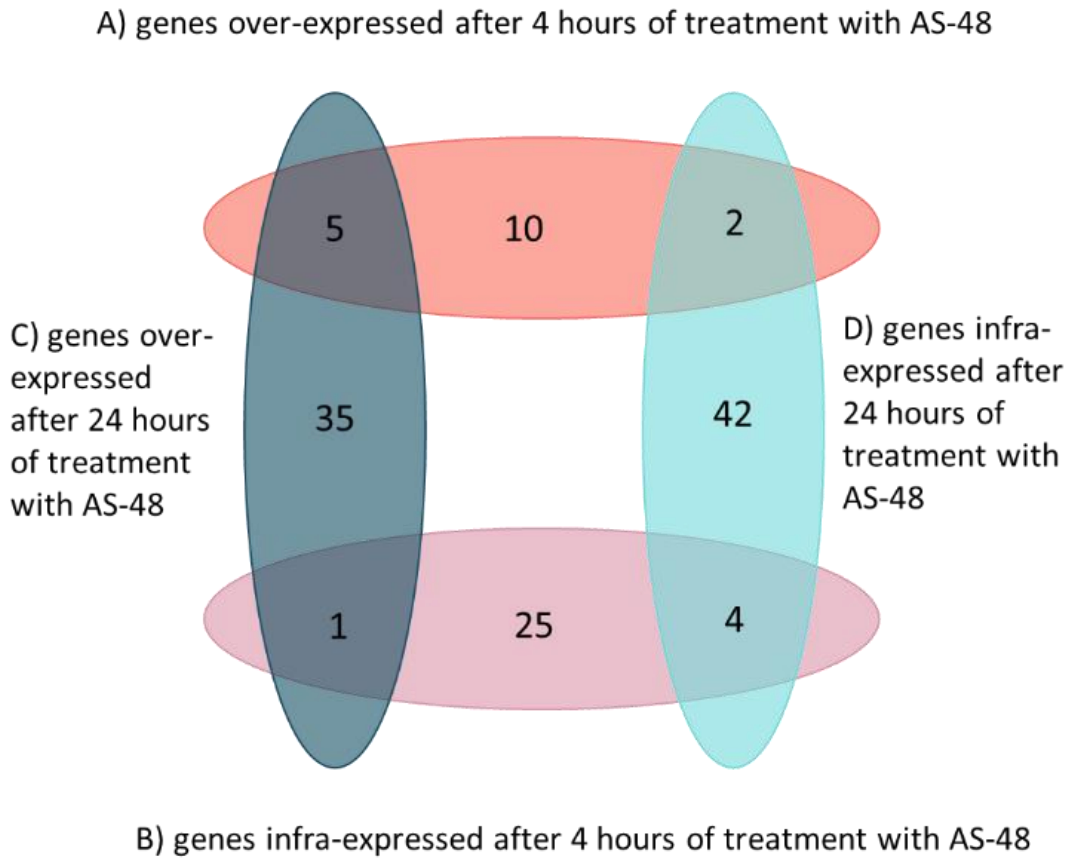

Image 22: Venn diagram with the four list of differentially expressed genes when *M. tuberculosis* is treated with AS-48. A) genes over-expressed after 4 hours of treatment with AS-48; B) genes infra-expressed after 4 hours of treatment with AS-48; C) genes over-expressed after 24 hours of treatment with AS-48; D) genes infra-expressed after 24 hours of treatment with AS-48.

The first group of pre-selected genes comprised those four genes that were found infra-expressed at both time points (i.e. common to lists B and D)*: aglA*, *vapC7*, *dosT* and *PE10.* Also, we pre-selected the five genes that are commonly over-expressed at the two-time points (i.e. common to lists A and C): *PE20*, *PPE48-1*, *PPE31*, *mazE7* and *relK.*

Second, we were intrigued by those genes that apparently inverted their expression upon time: the gen *galK*, seems infra-expressed after 4 hour of treatment but after 24 hours of treatment is over-expressed. In addition, genes

PPE1 and *vapB7* appeared over-expressed after 4 hours of treatment and infra-expressed after 24 hours.

Third, we have pre-selected other genes that were differentially expressed greatly in any single condition. This included a large number of genes; for example, we realized that there were 19 genes belonging to the Toxin-Antitoxin systems so we pre-selected at least one for each family (*maz*, *hig*, *par*, *rel* and *vap*); other genes, predicted to be in operons, were pre-selected also.

Finally, we added the rrs gene (encoding the 16S rRNA) as an internal control.

From the lists of pre-selected genes, PE and PPE genes were excluded from further analysis, since its function is still little known, so we could not relate with a possible mode of action of AS-48. We ended up with a list of 30 genes, selected for quantification of their relative expression by qRT-PCR (**Table 13**).

Table 13: List of genes selected from the RNAseq analysis for qRT-PCR.

Genes	List	Genes	List
accD1	C	*mbtN*	D
cydD	D	*mce2D*	C
cyp121	C	*metA*	D
dppC	C	*parD1*	B
ephC	C	*plcA*	D
esxS	C	*prpC*	C
fadD10	D	*relK*	A and C
fadE9	A	*rpmD*	B
fas	D	*rpsN2*	D
higB	D	*secE2*	C
hsp	D	*ugpE*	C
hycQ	D	*uspB*	B
lppQ	B	*vapB17*	A
mazE7	A and C	*vapC42*	C
mbtA	D	*vapC7*	B and D

Out of the 30 selected genes, four of them resulted in nonspecific retro-transcription amplification reaction (*metA, vapC42, fadD10* and *fadE9*), so they were left apart and the qRT-PCR validations for the different RNA extraction samples were done for remaining 26 genes. Technical triplicates were within 0.5 cycles and all the CTs values were under 35 cycles. In **Image 23**, we have compared the Relative Quantification (RQ) of each condition to the calibrator (Control 0 hours). An RQ value was considered as significant when there were more than 1.5 or less than 0.5, which is within the variations of the technique (49).

As we can observe in **Image 23**, the expression of *rrs* gene remains stable in all the conditions, so this housekeeping gene can be used to normalise the expression levels of the rest of the genes. Then when comparing the level of expression of genes obtained after the RNAseq analysis with those of relative quantification of qRT-PCR, the expected results should be:

1) We see that those genes that show over-expression or infra-expression (RQ<0.5 and RQ>1.5) in all the conditions are not reliable.
2) Those genes that appears in list A should be enhanced in the RQ of samples treated with AS-48 at 4 hours and diminished in the samples of control at 4 hours.
3) Genes in list B should be enhanced in the control at 4 hours and diminished in sample treated with AS-48 at 4 hours.
4) For list C, genes with a high RQ must be the ones highly expressed when treating with AS-48 during 24 hours and decreased in the control sample untreated after 24 hours.
5) And for the genes that appears in list D we expected an increase in the RQ of the untreated samples after 24 hours and a reduction in the ones treated with AS-48 during 24 hours.

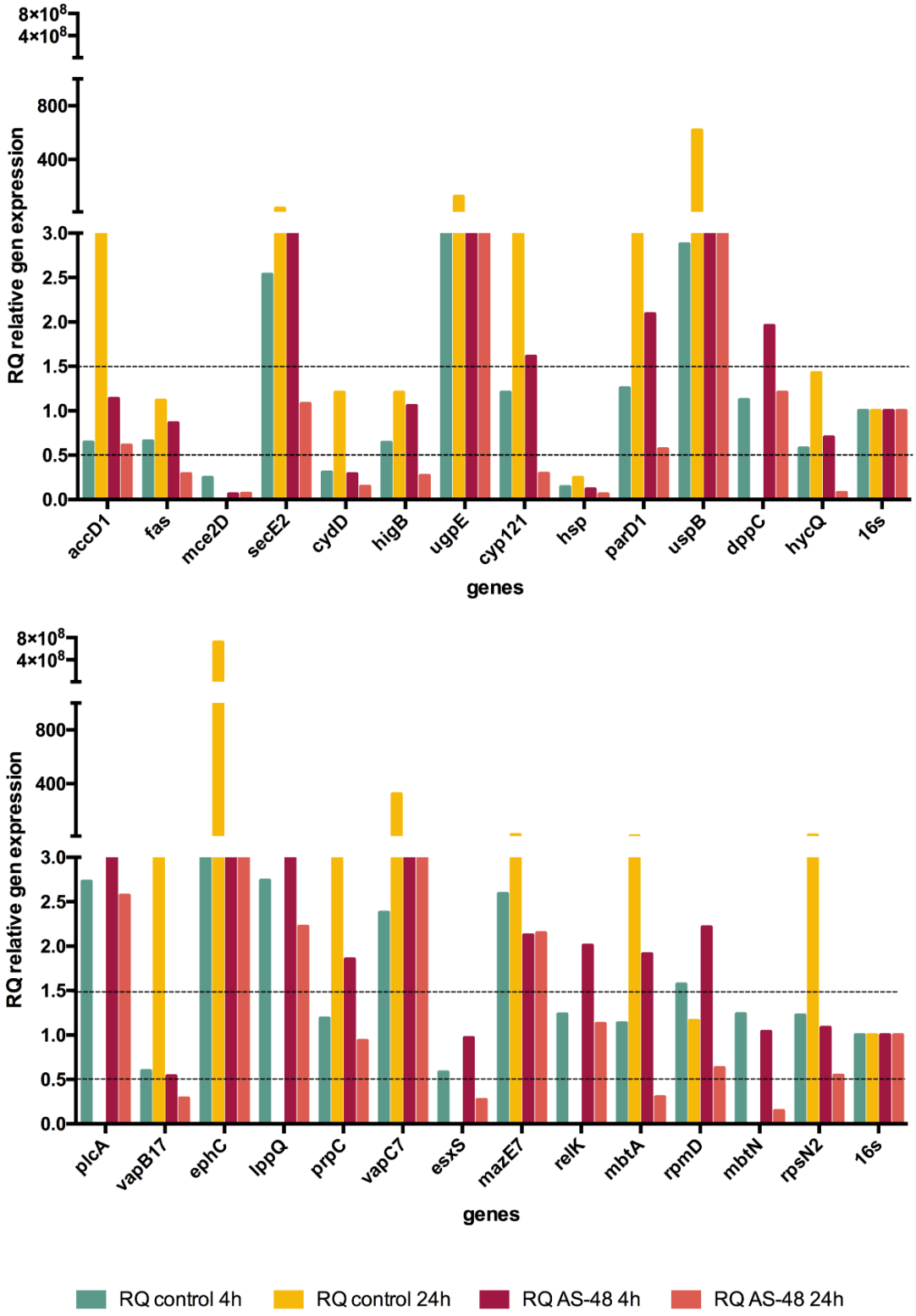

Image 23: Quantification of gene expression levels by qRT-PCR of those genes selected after the RNAseq analysis.

The final analysis obtained from the results of RNAseq was comparing the treatment with AS-48 in relation to its time control. In this way, we could be able to determinate which genes are really differentially expressed. In **Image 24** is represented the fold change of the treatment with AS-48 after 4 hours and after 24 hours normalized with the control at its respective time.

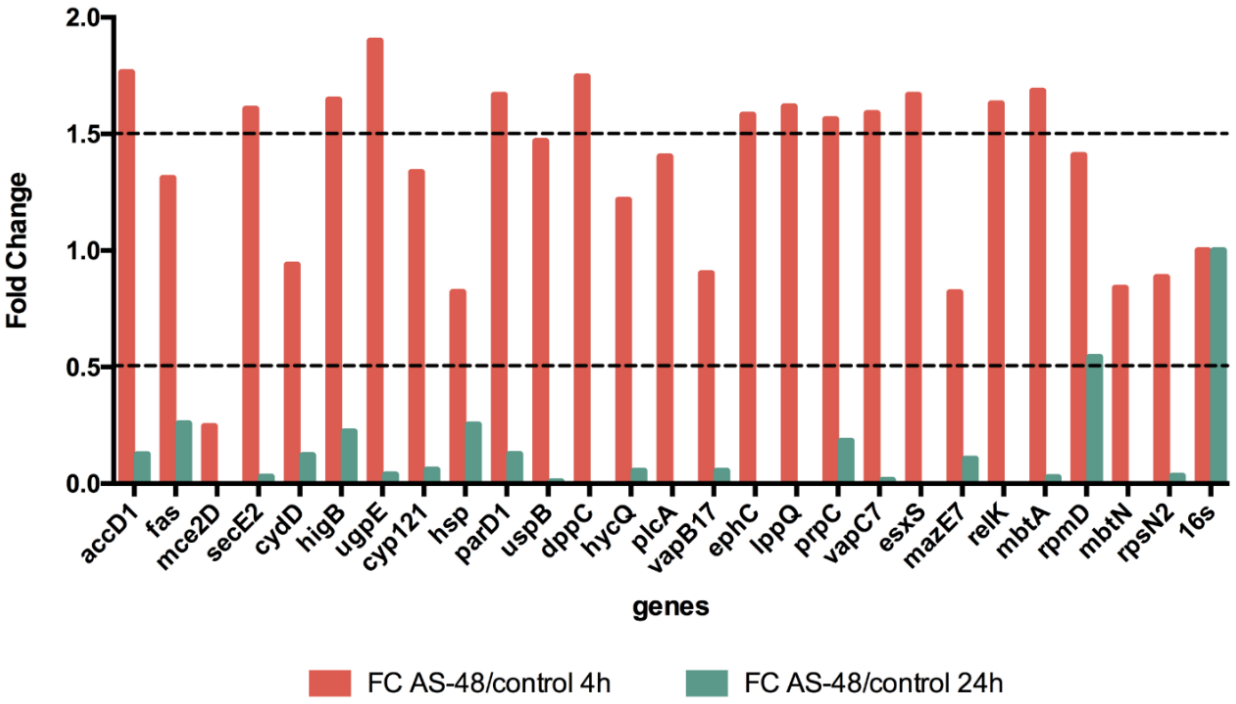

Image 24: Fold change of RQ (Relative Quantification) of treatment with AS-48 at different time points compared with its untreated time-dependent control sample.

From the Fold Change analysis, those genes that its fold change expression is higher than 1.5 and lower than 0.5 have been considered as differentially expressed. However, the fold change of the relative expression after 24 hours of treatment seems to be much lower than after 4 hours of treatment. We can speculate that the RNA samples obtained after 24 hours of treatment with AS-48 could start to be effected by the bactericidal action of AS-48, despite the fact that the O.D. of the culture correspond to a bacterial concentration higher than the used for the MIC.

As we have seen in CHAPTER 1, from the time-kill curve, AS-48 has a bactericidal effect after 48 hours of treatment, nevertheless a significant part of the bacterial population could be affected already after 24 hours. It is worth to remark that, the MIC of AS-48 is inoculum-dependent so the concentration of AS-48 used for treating the cultures prior to RNA extraction may not affect tuberculosis viability. In addition, the Fold Change and the RQ expression of the *rrs* housekeeping gene allow us to normalize the relative expression of each gene.

Those genes that are differentially expressed by both methods, RNAseq and qRT-PCR, could be modulating its expression due to the AS-48 effect, and we could consider that if a mutation in those genes happen could generate resistant bacilli to AS-48. In **Table 14** is shown the concordance of the results of both methods, if the result of qRT-PCR in terms of the relative expression of the Fold Change match with the RNAseq.

Table 14: Comparison of the Relative Gen expression of the selected genes by RNAseq and qRT-PCR.

	RNAseq				qRT-PCR				
Gene	OE_4h	IE_4h	OE_24h	IE_24h	OE_4h	IE_4h	OE_24h	IE_24h	**Concordance**
accD1			X		X			X	NO
cydD				X				X	**YES**
cyp121			X					X	NO
dppC			X		X			X	NO
ephC			X		X			X	NO
esxS			X		X			X	NO
fas				X				X	**YES**
higB				X				X	**YES**
hsp				X				X	**YES**
hycQ				X				X	**YES**
lppQ		X			X			X	NO
mazE7	X		X					X	NO
mbtA				X	X			X	NO(4h) **YES(24h)**
mbtN				X				X	**YES**
mce2D			X			X		X	NO
parD1		X			X			X	NO
plcA				X				X	**YES**
prpC			X		X			X	NO
relK	X		X		X			X	**YES(4h)** NO(24h)
rpmD		X							-
rpsN2				X				X	**YES**
secE2			X		X			X	NO
ugpE			X		X			X	NO
uspB		X						X	NO
vapB17	X							X	NO
vapC7		X		X	X			X	NO(4h) **YES(24h)**

Note: OE_4h: Over Expression at 4h hours; IE_4h: Infra Expression at 4h; OE_24h: Over Expression at 24h hours; IE_24h: Infra Expression at 24h.

The genes that show a differential expression by the two methods are: *cydD*, *fas*, *higB*, *hsp*, *hycQ*, *mbtN*, *plcA* and *rspN2*. For *mbtA* and *vapC7* there are concordance but only confirmed after 24 hours, and for *relK* only after 4 hours of treatment. We can see that the expression of these genes appears to be changed due to the effect of AS-48. For the other genes we cannot confirm the results obtained by RNAseq.

TARGETING DNA MOBILITY

It has been proposed that antimicrobial peptides could interact not only with the microbial membrane but also with its genetic material (50). In order to test this possibility, we performed a mobility shift assay to check if AS-48 is able to bind directly bacterial DNA. **Image 25** shows the electrophoresis gel with the samples of *M. tuberculosis* DNA treated with a concentration gradient of AS-48 to allow its interaction and binding with the DNA.

At concentrations below 40.625 µg/ml of AS-48, there is a normal migration of the DNA, equal to the one in the untreated control. But at concentrations of AS-48 from 81.25 µg/ml and above, the DNA stayed in the well. These concentrations of AS-48 are in the range of the MIC of AS-48 in *in vitro* cultures (64 µg/ml). We can hypothesize that bacteriocin AS-48 is binding the DNA due to electrostatic interactions, given that DNA is negatively charged and AS-48 is positively charged. If this were the case, after its interaction with AS-48, the DNA would have a reduced negative charge, which in turn would explain its reduced mobility in the electric field within the agarose gel. Then, we can consider that AS-48 may be targeting the membrane as well as the bacterial DNA.

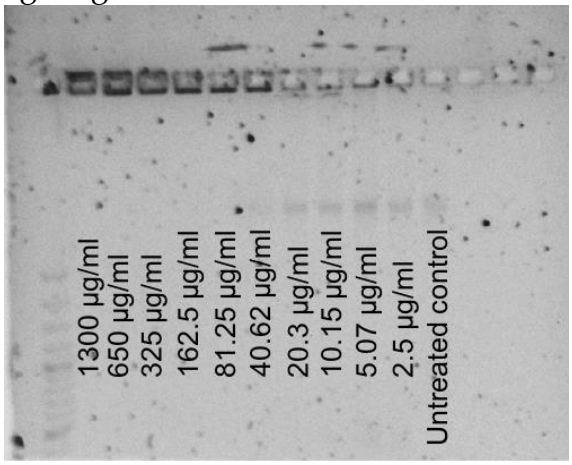

Image 25: DNA migration in electrophoretic gel with different concentrations of AS-48.

DISCUSSION

Natural or synthetic peptides are emerging as a promising source of novel antimicrobials (51). Currently, there are two AMPs in phase 2 of clinical development (murepavidin and brilacidin) for treating respectively *Pseudomonas aeruginosa* and *S. aureus* infections. As most AMPs, they both are targeting the bacterial membrane, an interesting new target for treating persistent infections as it is the case for tuberculosis (52). Other membrane-targeting compounds have been shown to be effective *in vitro* against *Clostridium difficile* (53). The interest of a possible application of AMPs in tuberculosis treatment has arisen since it was demonstrated that a high proportion of AMPs active against *P. aeruginosa* also showed activity against *M. tuberculosis* (54).

We conducted two experiments aimed at investigating the potential effect of AS-48 in the cell membrane. On the one hand, by determining the proportion of depolarized cells after AS-48 treatment, we found that this effect was both concentration and time dependent. On the other hand, in ethidium bromide accumulation assays, we monitored a time-course increase in fluorescence, and also an AS-48 concentration dependent effect. Then, we have demonstrated that AS-48 is acting on mycobacterial membranes, by using two independent methods. We have also observed the changes in the architecture of the bacilli by Electron Microscopy, however, to elucidate if the damage is either in the membrane or in the cell wall an analysis with Transmission Electron Microscopy could give a more precise image, as has been described in *M. marinum* by Smith J. *et al* (55).

Transcriptomics has evolved the study of the different molecular process in *Mycobacterium tuberculosis* but also has become an interesting and a useful tool for drug discovery and for getting a better understanding of the possible mechanism of resistance and its mode of action. Further validation is still needed to corroborate the vast information provided by the omics techniques, as well as the integration of phenotypic studies related with the role of the genes and proteins

being targeted. At this concern, bioinformatics tools and computer modelling are essential in order to make easy predictions, fast analysis of the massive data provided by omics techniques and consequently, improved drug discovery studies (56, 57). It could be also interesting to include the study of Tn-seq (phenotypic) data analysis, since it shows that there is a significant difference between transcriptionally relevant genes and the phenotypically important genes, i.e. those genes that the bacteria needs in order to keep its fitness when an environmental change happens (58).

From the transcriptomical analysis with RNAseq we noticed that those genes belonging to the antitoxin-toxin (TA) systems seem to be differentially expressed (in a ratio between 2 to 5 or even higher), when the *M. tuberculosis* cultures were treated with AS-48, in comparison with untreated control cultures. TA systems are composed of a stable protein, toxin, and a more labile antagonistic, antitoxin. *M. tuberculosis* has a very high number of TA systems, 79 in total, much higher than other mycobacteria. The systems belong to different families: VapBC (50 systems), MazEF (10 systems), YefM/YoeB (one system), RelBE (two systems), HigBA (two systems) and ParDE (two systems), one tripartite type II TAC (Toxin-Antitoxin-Chaperone) controlled by SecB-like chaperone, three potentially type IV systems and eight uncharacterized putative TA systems (59). It is thought that TA systems are involved in the control of growth, and in the persistence of *M. tuberculosis*, even though the signals that trigger activation of toxins are yet unknown (60). When *M. tuberculosis* persisters were induced by common antimicrobials, it was seen that TA systems were up-regulated (59), indeed the over-expression of *relE* has been shown that is related with the persister formation *in vivo* and the increase of the survival in the presence of rifampicin *in vitro* (61).

From the list of 11 genes that we have confirmed the expression by RNAseq and qRT-PCR, three of them are toxin producers (*higB*, *vapC7* and *relK*). In the case of *mbtN* and *mbtA* both genes could be repressed by iron and *IdeR* (62), then AS-48 could also be affecting this metabolic route. According to DeJesus *et al*. (63) a disruption of the genes, *rpsN2* and *higB*, provides a growth advantage in H37Rv.

Besides *higB* has been identified by DNA microarrays to be up-regulated at high temperatures as well as *hsp* (64), in this case we have not change any environmental condition.

However, *higB* is also up-regulated after 24 hours and 96 hours of starvation and *fas* is down regulated under the same conditions (65); some mechanism that happens in the cell under starvation conditions are similar to those when we have persister cells (59). From this we can hypothesize that AS-48, at short times exposures, is able to activate some mechanism that alters the production of persisters bacteria. We could also speculate about the infra expression of *cydD*, which is thought to be involved in the translocation of the substrate transport across the membrane, then the alteration of the membrane caused by AS-48 could also trigger the lack of nutrients and metabolic substrates for the normal growth of *M. tuberculosis*.

Besides the effect in the cell membrane we have demonstrated that AS-48 is a multitarget drug thus the possibility to acquire resistances is lower than targeting a unique mechanism. Indeed, we could not get any resistant mutants that is why we used a transcriptional analysis to assess the mode of action. We have validated the interaction of AS-48 with the mycobacterial membrane and with the DNA, nevertheless, other modes of action could be considered. We cannot decline the idea that AS-48 could be binding some regions of the DNA and the relative expression of genes would be modulated by the effect in the DNA instead by the effect of As-48 in the membrane.

To validate this hypothesis further transcriptomic studies should be needed, for example changing some of the culture conditions and time extraction. Moreover, the next step could be studying the combined effect of AS-48 and ethambutol and its transcriptomic changes in the cultures. The result of phenotipyc studies, generating knockouts, will give a precise idea of the real mechanism of action of AS-48.

REFERENCES

1. Nguyen L. 2016. Antibiotic resistance mechanisms in M-tuberculosis: an update. Archives of Toxicology 90:1585-1604.

2. Gygli SM, Borrell S, Trauner A, Gagneux S. 2017. Antimicrobial resistance in Mycobacterium tuberculosis: mechanistic and evolutionary perspectives. Fems Microbiology Reviews 41:354-373.

3. Kohanski MA, DePristo MA, Collins JJ. 2010. Sublethal Antibiotic Treatment Leads to Multidrug Resistance via Radical-Induced Mutagenesis. Molecular Cell 37:311-320.

4. Gao F, Hua Y, Korepanova A, Peskova Y, Rohal K, Nakamoto RK, Cross TA. 2003. Membrane protein structural genomics: Mycobacterium tuberculosis. Biophysical Journal 84:349a-349a.

5. Philalay JS, Palermo CO, Hauge KA, Rustad TR, Cangelosi GA. 2004. Genes required for intrinsic multidrug resistance in Mycobacterium avium. Antimicrobial Agents and Chemotherapy 48:3412-3418.

6. Ramon-Garcia S, Mick V, Dainese E, Martin C, Thompson CJ, De Rossi E, Manganelli R, Ainsa JA. 2012. Functional and Genetic Characterization of the Tap Efflux Pump in Mycobacterium bovis BCG. Antimicrobial Agents and Chemotherapy 56:2074-2083.

7. Danilchanka O, Pavlenok M, Niederweis M. 2008. Role of porins for uptake of antibiotics by Mycobacterium smegmatis. Antimicrob Agents Chemother 52:3127-34.

8. Monshupanee T, Johansen SK, Dahlberg AE, Douthwaite S. 2012. Capreomycin susceptibility is increased by TlyA-directed 2'-O-methylation on both ribosomal subunits. Mol Microbiol 85:1194-203.

9. Maus CE, Plikaytis BB, Shinnick TM. 2005. Mutation of tlyA confers capreomycin resistance in Mycobacterium tuberculosis. Antimicrobial Agents and Chemotherapy 49:571-577.

10. Ferber D. 2005. Biochemistry. Protein that mimics DNA helps tuberculosis bacteria resist antibiotics. Science 308:1393.

11. Comas I, Borrell S, Roetzer A, Rose G, Malla B, Kato-Maeda M, Galagan J, Niemann S, Gagneux S. 2012. Whole-genome sequencing of rifampicin-resistant Mycobacterium tuberculosis strains identifies compensatory mutations in RNA polymerase genes. Nature Genetics 44:106-U147.

12. Chen WJ, Biswas T, Porter VR, Tsodikov OV, Garneau-Tsodikova S. 2011. Unusual regioversatility of acetyltransferase Eis, a cause of drug resistance in XDR-TB. Proceedings of the National Academy of Sciences of the United States of America 108:9804-9808.

13. Zaunbrecher MA, Sikes RD, Metchock B, Shinnick TM, Posey JE. 2009. Overexpression of the chromosomally encoded aminoglycoside acetyltransferase eis confers kanamycin resistance in Mycobacterium tuberculosis. Proceedings of the National Academy of Sciences of the United States of America 106:20004-20009.

14. Bhat ZS, Rather MA, Maqbool M, Ahmad Z. 2018. Drug targets exploited in Mycobacterium tuberculosis: Pitfalls and promises on the horizon. Biomed Pharmacother 103:1733-1747.

15. Malik S, Willby M, Sikes D, Tsodikov OV, Posey JE. 2012. New insights into fluoroquinolone resistance in Mycobacterium tuberculosis: functional genetic analysis of gyrA and gyrB mutations. PLoS One 7:e39754.

16. Andre E, Goeminne L, Cabibbe A, Beckert P, Kabamba Mukadi B, Mathys V, Gagneux S, Niemann S, Van Ingen J, Cambau E. 2017. Consensus numbering system for the rifampicin resistance-associated rpoB gene mutations in pathogenic mycobacteria. Clin Microbiol Infect 23:167-172.

17. Meier A, Sander P, Schaper KJ, Scholz M, Bottger EC. 1996. Correlation of molecular resistance mechanisms and phenotypic resistance levels in streptomycin-resistant Mycobacterium tuberculosis. Antimicrob Agents Chemother 40:2452-4.

18. Beckert P, Hillemann D, Kohl TA, Kalinowski J, Richter E, Niemann S, Feuerriegel S. 2012. rplC T460C identified as a dominant mutation in linezolid-resistant Mycobacterium tuberculosis strains. Antimicrob Agents Chemother 56:2743-5.

19. Ye M, Xu L, Zou Y, Li B, Guo Q, Zhang Y, Zhan M, Xu B, Yu F, Zhang Z, Chu H. 2018. Molecular Analysis of Linezolid Resistant Clinical Isolates of Mycobacterium abscessus. Antimicrob Agents Chemother doi:10.1128/AAC.01842-18.

20. Njire M, Tan Y, Mugweru J, Wang C, Guo J, Yew W, Tan S, Zhang T. 2016. Pyrazinamide resistance in Mycobacterium tuberculosis: Review and update. Adv Med Sci 61:63-71.

21. Bhat ZS, Rather MA, Maqbool M, UL Lah H, Yousuf SK, Ahmad Z. 2017. Cell wall: A versatile fountain of drug targets in Mycobacterium tuberculosis. Biomedicine & Pharmacotherapy 95:1520-1534.

22. Machado D, Couto I, Perdigao J, Rodrigues L, Portugal I, Baptista P, Veigas B, Amaral L, Viveiros M. 2012. Contribution of Efflux to the Emergence of Isoniazid and Multidrug Resistance in Mycobacterium tuberculosis. Plos One 7.

23. Pawar A, Jha P, Konwar C, Chaudhry U, Chopra M, Saluja D. 2018. Ethambutol targets the glutamate racemase of Mycobacterium tuberculosis-an enzyme involved in peptidoglycan biosynthesis. Appl Microbiol Biotechnol doi:10.1007/s00253-018-9518-z.

24. Gler MT, Skripconoka V, Sanchez-Garavito E, Xiao H, Cabrera-Rivero JL, Vargas-Vasquez DE, Gao M, Awad M, Park SK, Shim TS, Suh GY, Danilovits M, Ogata H, Kurve A, Chang J, Suzuki K, Tupasi T, Koh WJ, Seaworth B, Geiter LJ, Wells CD. 2012. Delamanid for multidrug-resistant pulmonary tuberculosis. N Engl J Med 366:2151-60.

25. Chen XH, Hashizume H, Tomishige T, Nakamura I, Matsuba M, Fujiwara M, Kitamoto R, Hanaki E, Ohba Y, Matsumoto M. 2017. Delamanid Kills Dormant Mycobacteria In Vitro and in a Guinea Pig Model of Tuberculosis. Antimicrobial Agents and Chemotherapy 61.

26. Stover CK, Warrener P, VanDevanter DR, Sherman DR, Arain TM, Langhorne MH, Anderson SW, Towell JA, Yuan Y, McMurray DN, Kreiswirth BN, Barry CE, Baker WR. 2000. A small-molecule nitroimidazopyran drug candidate for the treatment of tuberculosis. Nature 405:962-6.

27. Matsumoto M, Hashizume H, Tomishige T, Kawasaki M, Tsubouchi H, Sasaki H, Shimokawa Y, Komatsu M. 2006. OPC-67683, a nitro-dihydro-imidazooxazole derivative

with promising action against tuberculosis in vitro and in mice. Plos Medicine 3:2131-2144.

28. Haver HL, Chua A, Ghode P, Lakshminarayana SB, Singhal A, Mathema B, Wintjens R, Bifani P. 2015. Mutations in genes for the F420 biosynthetic pathway and a nitroreductase enzyme are the primary resistance determinants in spontaneous in vitro-selected PA-824-resistant mutants of Mycobacterium tuberculosis. Antimicrob Agents Chemother 59:5316-23.

29. Chiarelli LR, Mori G, Orena BS, Esposito M, Lane T, de Jesus Lopes Ribeiro AL, Degiacomi G, Zemanova J, Szadocka S, Huszar S, Palcekova Z, Manfredi M, Gosetti F, Lelievre J, Ballell L, Kazakova E, Makarov V, Marengo E, Mikusova K, Cole ST, Riccardi G, Ekins S, Pasca MR. 2018. A multitarget approach to drug discovery inhibiting Mycobacterium tuberculosis PyrG and PanK. Sci Rep 8:3187.

30. Li K, Schurig-Briccio LA, Feng X, Upadhyay A, Pujari V, Lechartier B, Fontes FL, Yang H, Rao G, Zhu W, Gulati A, No JH, Cintra G, Bogue S, Liu YL, Molohon K, Orlean P, Mitchell DA, Freitas-Junior L, Ren F, Sun H, Jiang T, Li Y, Guo RT, Cole ST, Gennis RB, Crick DC, Oldfield E. 2014. Multitarget drug discovery for tuberculosis and other infectious diseases. J Med Chem 57:3126-39.

31. Campanico A, Moreira R, Lopes F. 2018. Drug discovery in tuberculosis. New drug targets and antimycobacterial agents. Eur J Med Chem 150:525-545.

32. Chen H, Nyantakyi SA, Li M, Gopal P, Aziz DB, Yang T, Moreira W, Gengenbacher M, Dick T, Go ML. 2018. The Mycobacterial Membrane: A Novel Target Space for Anti-tubercular Drugs. Front Microbiol 9:1627.

33. Cruz VL, Ramos J, Melo MN, Martinez-Salazar J. 2013. Bacteriocin AS-48 binding to model membranes and pore formation as revealed by coarse-grained simulations. Biochim Biophys Acta 1828:2524-31.

34. Hendrickson DG, Soifer I, Wranik BJ, Botstein D, Scott McIsaac R. 2018. Simultaneous Profiling of DNA Accessibility and Gene Expression Dynamics with ATAC-Seq and RNA-Seq. Methods Mol Biol 1819:317-333.

35. Haas BJ, Chin M, Nusbaum C, Birren BW, Livny J. 2012. How deep is deep enough for RNA-Seq profiling of bacterial transcriptomes? Bmc Genomics 13.

36. Wang Z, Gerstein M, Snyder M. 2009. RNA-Seq: a revolutionary tool for transcriptomics. Nat Rev Genet 10:57-63.

37. Sekyere JO, Asante J. 2018. Emerging mechanisms of antimicrobial resistance in bacteria and fungi: advances in the era of genomics. Future Microbiology 13:241-262.

38. Winglee K, Lun SC, Pieroni M, Kozikowski A, Bishai W. 2015. Mutation of Rv2887, a marR-Like Gene, Confers Mycobacterium tuberculosis Resistance to an Imidazopyridine-Based Agent. Antimicrobial Agents and Chemotherapy 59:6873-6881.

39. van Rensburg IC, Loxton AG. 2015. Transcriptomics: the key to biomarker discovery during tuberculosis? Biomark Med 9:483-95.

40. Malone KM, Rue-Albrecht K, Magee DA, Conlon K, Schubert OT, Nalpas NC, Browne JA, Smyth A, Gormley E, Aebersold R, MacHugh DE, Gordon SV. 2018. Comparative 'omics analyses differentiate Mycobacterium tuberculosis and Mycobacterium bovis and reveal distinct macrophage responses to infection with the human and bovine tubercle bacilli. Microb Genom doi:10.1099/mgen.0.000163.

41. Villarreal-Ramos B, Berg S, Whelan A, Holbert S, Carreras F, Salguero FJ, Khatri BL, Malone K, Rue-Albrecht K, Shaughnessy R, Smyth A, Ameni G, Aseffa A, Sarradin P, Winter N, Vordermeier M, Gordon SV. 2018. Experimental infection of cattle with Mycobacterium tuberculosis isolates shows the attenuation of the human tubercle bacillus for cattle. Scientific Reports 8.

42. Aguilar-Ayala DA, Tilleman L, Van Nieuwerburgh F, Palomino DDJC, Vandamme P, Gonzalez-Y-Merchand JA, Martin A. 2017. The transcriptome of Mycobacterium tuberculosis in a lipid-rich dormancy model through RNAseq analysis. Scientific Reports 7.

43. Rodrigues L, Viveiros M, Ainsa JA. 2015. Measuring efflux and permeability in mycobacteria. Methods Mol Biol 1285:227-39.

44. Trapnell C, Hendrickson DG, Sauvageau M, Goff L, Rinn JL, Pachter L. 2013. Differential analysis of gene regulation at transcript resolution with RNA-seq. Nat Biotechnol 31:46-53.

45. Tarazona S, Furio-Tari P, Turra D, Pietro AD, Nueda MJ, Ferrer A, Conesa A. 2015. Data quality aware analysis of differential expression in RNA-seq with NOISeq R/Bioc package. Nucleic Acids Res 43:e140.

46. Love MI, Huber W, Anders S. 2014. Moderated estimation of fold change and dispersion for RNA-seq data with DESeq2. Genome Biol 15:550.

47. Vansoolingen D, Dehaas PEW, Hermans PWM, Vanembden JDA. 1994. DNA-Fingerprinting of Mycobacterium-Tuberculosis. Bacterial Pathogenesis, Pt A 235:196-205.

48. Gonzalez C, Langdon GM, Bruix M, Galvez A, Valdivia E, Maqueda M, Rico M. 2000. Bacteriocin AS-48, a microbial cyclic polypeptide structurally and functionally related to mammalian NK-lysin. Proc Natl Acad Sci U S A 97:11221-6.

49. Bustin SA, Benes V, Garson JA, Hellemans J, Huggett J, Kubista M, Mueller R, Nolan T, Pfaffl MW, Shipley GL, Vandesompele J, Wittwer CT. 2009. The MIQE Guidelines: Minimum Information for Publication of Quantitative Real-Time PCR Experiments. Clinical Chemistry 55:611-622.

50. Jindal HM, Zandi K, Ong KC, Velayuthan RD, Rasid SM, Samudi Raju C, Sekaran SD. 2017. Mechanisms of action and in vivo antibacterial efficacy assessment of five novel hybrid peptides derived from Indolicidin and Ranalexin against Streptococcus pneumoniae. PeerJ 5:e3887.

51. da Cunha NB, Cobacho NB, Viana JF, Lima LA, Sampaio KB, Dohms SS, Ferreira AC, de la Fuente-Nunez C, Costa FF, Franco OL, Dias SC. 2017. The next generation of antimicrobial peptides (AMPs) as molecular therapeutic tools for the treatment of diseases with social and economic impacts. Drug Discov Today 22:234-248.

52. Hurdle JG, O'Neill AJ, Chopra I, Lee RE. 2011. Targeting bacterial membrane function: an underexploited mechanism for treating persistent infections. Nat Rev Microbiol 9:62-75.

53. Wu X, Cherian PT, Lee RE, Hurdle JG. 2013. The membrane as a target for controlling hypervirulent Clostridium difficile infections. J Antimicrob Chemother 68:806-15.

54. Ramon-Garcia S, Mikut R, Ng C, Ruden S, Volkmer R, Reischl M, Hilpert K, Thompson CJ. 2013. Targeting Mycobacterium tuberculosis and other microbial pathogens using improved synthetic antibacterial peptides. Antimicrob Agents Chemother 57:2295-303.

55. Smith J, Manoranjan J, Pan M, Bohsali A, Xu J, Liu J, McDonald KL, Szyk A, LaRonde-LeBlanc N, Gao LY. 2008. Evidence for pore formation in host cell membranes by ESX-1-secreted ESAT-6 and its role in Mycobacterium marinum escape from the vacuole. Infect Immun 76:5478-87.

56. Fallahi-Sichani M, El-Kebir M, Marino S, Kirschner DE, Linderman JJ. 2011. Multiscale Computational Modeling Reveals a Critical Role for TNF-alpha Receptor 1 Dynamics in Tuberculosis Granuloma Formation. Journal of Immunology 186:3472-3483.

57. Butcher EC, Berg EL, Kunkel EJ. 2004. Systems biology in drug discovery. Nature Biotechnology 22:1253-1259.

58. Jensen PA, Zhu Z, van Opijnen T. 2017. Antibiotics Disrupt Coordination between Transcriptional and Phenotypic Stress Responses in Pathogenic Bacteria. Cell Reports 20:1705-1716.

59. Keren I, Minami S, Rubin E, Lewis K. 2011. Characterization and transcriptome analysis of Mycobacterium tuberculosis persisters. MBio 2:e00100-11.

60. Sala A, Bordes P, Genevaux P. 2014. Multiple toxin-antitoxin systems in Mycobacterium tuberculosis. Toxins (Basel) 6:1002-20.

61. Singh R, Barry CE, 3rd, Boshoff HI. 2010. The three RelE homologs of Mycobacterium tuberculosis have individual, drug-specific effects on bacterial antibiotic tolerance. J Bacteriol 192:1279-91.

62. Rodriguez GM, Voskuil MI, Gold B, Schoolnik GK, Smith I. 2002. ideR, An essential gene in mycobacterium tuberculosis: role of IdeR in iron-dependent gene expression, iron metabolism, and oxidative stress response. Infect Immun 70:3371-81.

63. DeJesus MA, Gerrick ER, Xu W, Park SW, Long JE, Boutte CC, Rubin EJ, Schnappinger D, Ehrt S, Fortune SM, Sassetti CM, Ioerger TR. 2017. Comprehensive Essentiality Analysis of the Mycobacterium tuberculosis Genome via Saturating Transposon Mutagenesis. MBio 8.

64. Stewart GR, Wernisch L, Stabler R, Mangan JA, Hinds J, Laing KG, Young DB, Butcher PD. 2002. Dissection of the heat-shock response in Mycobacterium tuberculosis using mutants and microarrays. Microbiology 148:3129-38.

65. Betts JC, Lukey PT, Robb LC, McAdam RA, Duncan K. 2002. Evaluation of a nutrient starvation model of Mycobacterium tuberculosis persistence by gene and protein expression profiling. Mol Microbiol 43:717-31.

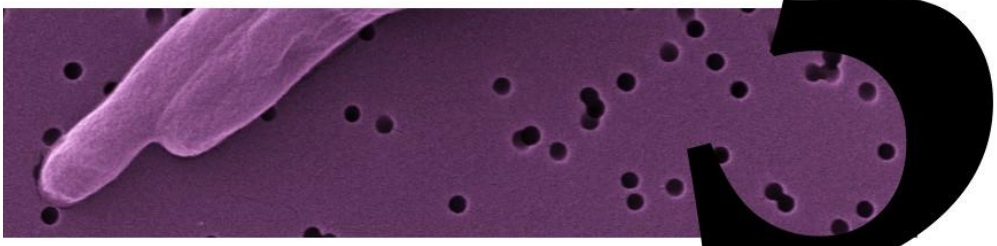

Chapter 3

In vivo approach of the antimicrobial activity of AS-48 against *M. tuberculosis*

INTRODUCTION

THE USEFULNESS OF ANIMAL MODELS IN ANTIMICROBIAL DRUG RESEARCH

In general, the *in vivo* approach to an infection is one of the key factors in researching new therapies and new antimicrobial treatments. Animal models exhibit a complexity that is almost impossible to achieve with an *in vitro* model and provide a unique environment to study the interaction of the bacterial infection, the host and the drug to be tested. Consequently, the information that could be obtained in these *in vivo* experiments is massive compared with other *in vitro* approaches of drug testing. Then, the use of animal models of infection is a first step for the design and development of preclinical assays, which in turn are the previous step of a clinical trial that has to be done in humans. Therefore, the use of suitable animal models provides an advantage in drug discovery and in new therapies to improve treatments. With animal models, it is possible to adjust several aspects such as dose schedule, drug concentration, assessments on toxicity, side effects and bacterial load.

These factors must be duly justified in animal models according to the Basic Principles of the Declaration of Helsinki by the World Medical Association (1). In this document, it is say that "Clinical research conform to the moral and scientific principles that justify medical research and should be based on laboratory and animal experiments or other scientifically established facts", so, always paying attention to ethical considerations, to improve human global health, it is mandatory to perform animal experiments.

DIVERSE ANIMAL MODELS IN TUBERCULOSIS RESEARCH

Particularly, in tuberculosis research, we have to take into account that there is no animal reservoir of *M. tuberculosis*. Although apparently, this could seem a disadvantage (since no suitable animal model, close to human infection, could be easily implemented), the fact is that several animal models (2, 3) provide a highly representative panorama of the infection development in the human being, in terms of virulence, response to antitubercular drugs, etc.

1. Guinea pig: Guinea pig was the first animal model used in tuberculosis research since the discovery of the etiologic agent of *M. tuberculosis* by Robert Koch. Nowadays, it is still considered as the reference model for vaccine testing, due to its similarity in the immunopathology with that of tuberculosis infected human beings (4). At early stage of the antibiotic research, guinea pig was also the reference animal model in drug susceptibility of the different first line drugs used in the treatment of tuberculosis (5-7). Recently, it has been demonstrated the activity of delamanid, one of the most recently discovered drugs against tuberculosis, against non-replicating and dormant bacilli of *M. tuberculosis* in the guinea pig model of infection (8). Chen X. and their colleges have also confirmed, in the guinea pig model, the previous studies performed in mice (9) to evaluate the activity of delamanid against dormant bacilli of tuberculosis; and showed the enhanced effect of delamanid in the common therapy for tuberculosis.

2. Rabbits: Similarly to guinea pigs, rabbits have been also used as a preclinical approach to tuberculosis and for drug susceptibility studies. Both models, guinea pigs and rabbits share the advantage of being close to the pathology in humans due to the formation of granuloma and caseation in response to tuberculosis infection (2).

3. Rats: In the case of rats, they are nearly considered as resistant to tuberculosis, the amount of bacterial inoculum required to infect them is higher than for guinea pig. Despite the fact that rats are the major model used for drug

testing and pharmacokinetic, this model cannot be considered for tuberculosis infection due to an adaptive response and a gradual clearance of the infection (10).

4. Non-human primates (NHPs): These animal models commonly are used after a first approach in other animals models, such as mouse or guinea pig. But, recently, the interest in the scientific community for these models has been increased. Some of the NHP used for tuberculosis-drug testing or detention are the squirrel monkey (*Saimiri sciureus*)(11); the genera of the Aotus monkey (12), that was thought to be less sensitive to tuberculosis infection; the marmoset (*Callithrix jacchus*) (13), which present the advantage of their small size comparing with others NHPs and the baboons (*Papio ursinus*) (14). Finally, the different kinds of macaques (15, 16), that shows a great similarity with the human anatomy and physiology: rhesus macaque (*Macaca fascicularis*) (17) or cynomolgus macaque (*Macaca mulatta*)(18) have been also widely used for tuberculosis research.

5. Others: Other animal's models like hamsters are also able to develop caseous granulomas, necrosis and fibrosis. Lately, minipig (19), zebra fish (*Danio rerio*) (20) have been also assayed as tuberculosis models.

THE MOUSE MODEL IN TUBERCULOSIS RESEARCH

Nevertheless, the mouse (21)model is one of the best characterized models for preclinical assays related with activity of drugs in general and in tuberculosis infection in particular. It has been demonstrated that the efficiency of different combined antimicrobial therapies in mouse models are coherent with that of the subsequent results of clinical trials in humans. Moreover, the mouse model can help to elucidate the toxicity of the drug in different organs after long periods of exposure, such as those that are required for tuberculosis treatment (22). The murin model is less expensive than rabbit and guinea pig models, in terms of price of the animals but also in space requirements in the animal facilities and in the

quantity of compound needed. Moreover the literature (**Image 26**) is more abundant than for guinea pig and rabbit, which are the most commonly used animal models (23).

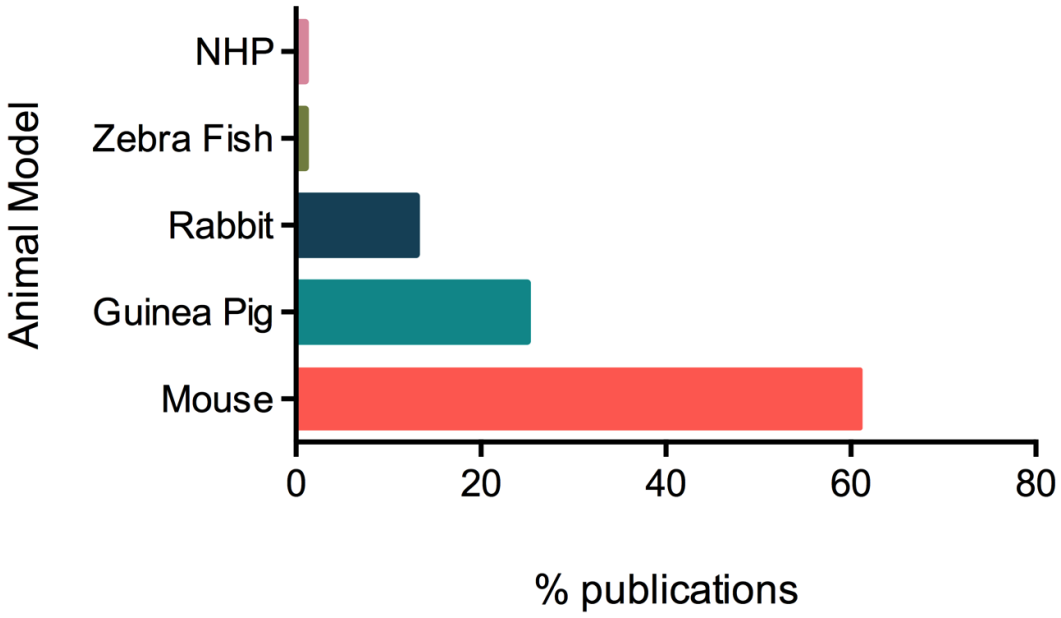

Image 26: Percentage of publications for each animal models in tuberculosis research. Based on the data published by Fonseca *et al*. (24).

Recently, a model of infection that mimics the development of necrotic granulomas and the formation of caseation in the C3HeB/FeJ mice has been developed, the also called Kramnik mouse model. This mice strain reaches a plateau of infection, which allows to get a subchronic infection, later than other commonly used strains such as BALB/c. It has been proved that the necrotic core of the caseum granuloma of C3HeB/FeJ mice constitutes a hypoxic environment (25, 26). This model, in addition to present a caseous granuloma, is greatly heterogenic in terms of bacterial subpopulations and types of lesion, becoming an improved mouse model (27).

For all these reasons, it is considered that the mouse model is the best option for animal studies in the infection of tuberculosis, hence, this is the *in vivo* model that we have used for our research on the activity of AS-48.

DESIGN OF *IN VIVO* MOUSE EXPERIMENTS

There are several aspects that need to be determined prior to the design of an *in vivo* mouse infection experiment. These are the mouse genetic lineage, the bacterial strain, selected for the infection process, the route of infection and the drug administration via.

1. It is necessary to choose carefully the genetic origin of the animals, and to decide whether using either inbred or outbred strains. Using inbred strains has some advantages (28): they are isogenic, which means that the animals are genetically identic individuals, and generally this results in a phenotypic uniformity, hence ensuring that the possible variability among different experiments (i.e. different response after a treatment) would not be due to genetic factors. Furthermore, the use of inbred strains allows a reduction in the number of mice needed for the experiments, which is an important ethical issue considering the three R's (Reduction, Replacement and Refinement) recommended in animal experimentation. In contrast, an outbred strain model would use genetically heterogeneous animals; although this situation is closer to a normal human population, hence ensuring that results will be independent of particular genetic traits. It has as a drawback that the number of mice needed to have statistically significant results would be larger than with an inbred population.

2. The bacterial strain. In many studies, the bacterial strain used for the infection was *M. tuberculosis* H37Rv, one of the international reference and mostly used strain in drug susceptibility either *in vitro* or *in vivo*. Other strains such as CDC1551, has been described as less virulent than H37Rv but the immune response seems to be faster and stronger than for H37Rv, *in vivo* (29, 30). To emulate a central nervous system of tuberculosis infection (which is the most aggressive form of extrapulmonary tuberculosis) *M. tuberculosis* clinical strain C3 has been used (31). Even in some cases, only the cord factor (trehalose 6'6-dimycolate) has been used to produce a granulomatous pathology (32).

3. Infection route: Mouse model is not the natural host of *M. tuberculosis*, then the route of administration is not determined and several options are available. Given that tuberculosis infection commonly occurs through the respiratory tract, the best way to get a pulmonary infection in animals is performing the infection directly throw the respiratory system, which can be emulated by the use of aerosol (33) or performing the infection by the intranasal route or intratracheal route. However other routes have to be taken into account, like the intravenous route, commonly in the tail vein (31).

4. Drug administration via. For drug administration any route could be used, but the most preferably one is the oral route (34), by oral gavage or by beverage or food intake. Specially, in the case of MDR-TB drug development is highly recommended to find an oral administration of drugs (35). But others routes could be implemented, such as the subcutaneous route (36), intraperitoneal or parenteral route (37). In the case of vaccination, it has been demonstrated that the intratracheal route for vaccination is more active than the subcutaneous route (33). Currently, the treatment mainly include oral drug administration and parenteral drug delivery, but, the delivery of dry powder by inhalation is increasing the interest by the scientific and medical community (38-40).

OBJECTIVES

The objectives of the animal experiments have been the following:

1) To test the possible *in vivo* toxicity (acute and subchronic) of AS-48 in the murine models, as well as the toxicity associated to particular administration routes. During the experiments, we observed the behavior or the response of the animals to the use of AS-48. For this, we have obtained tissues (brain, spleen, lungs, liver and kidneys) and blood from treated mice, and have analyzed them at different levels, either macroscopically, histologically or biochemically.
2) To determine the maximal dosage that could be administered to treat the tuberculosis infection in mice without causing major toxic effects.
3) To evaluate the antimycobacterial activity of the bacteriocin AS-48 either in monotherapy or in its synergistic combination with ethambutol (EMB) in a model of tuberculosis infected mice.
4) Finally, we have considered the effect of this peptide in the normal faecal microbiota of the mice in order to expand our knowledge of how this peptide works in *in vivo* environment.

MATERIALS AND METHODS

ANIMALS

Females specific pathogen free C57BL/6 JRj mice and both, females and males specific pathogen free BALB/c JRj mice (Janvier Labs, Saint Berthevin Cedex, France) were used for the *in vivo* experiments. Mice were allowed to acclimatize for one week before experiments, and were eight-weeks-old when the experiments started. Food and water were provided *ad libitum*. Lighting was artificial in cycles of 12-hours light-dark. Mice for toxicity assays were kept in the animal facilities of the *Centro de Investigaciones Biomédicas de Aragón* (CIBA) (ES 50 297 0012 011), and for the efficacy assay (upon infection with *M. tuberculosis*) were allocated in BLS3 animal facilities of *Centro de Encefalopatías y Enfermedades Transmisibles Emergentes* (ES 50 279 0012 009), at the University of Zaragoza. Sterile food, water and bed were provided for infected mice, they were lodged in ventilated cages. All the experiments that we have performed have taken into account the three R's principles. The aim was to minimize the number of animals required to assay the different conditions. For designing each protocol, the previous experiments were taken into account, and additionally, toxicological data of similar substances have been considered for the design of every experiment. All the procedures were accepted by the *Comisión Ética Asesora para la Experimentación Animal* of Aragón.

For all the experiments, mice were randomly divided into the different groups. All mice were weighted at reception and ear-labelled. The body weight of the groups was calculated as an average of all the individuals. All dosages (drugs, anesthesia…) were adapted to the body weight of each group. Mice were weighted and examined thoroughly every day before and during drug administration, and every abnormality in the behavior was recorded. Mice were treated according to the experimental design of every assay (acute toxicity, administration route

toxicity, subchronic toxicity, *M. tuberculosis* infection, and efficacy experiments) as detailed in the following sections.

Mice were euthanatized according to the standards and following a humanely procedure. Cervical dislocation was performed for the majority of the mice. Those mice for which the collection of blood was critical for biochemical and hematological test were euthanatized by using a carbon dioxide camera.

After euthanatizing the mice, a necropsy was performed. The general look of the external surface of the body, skin, orifices, internal organs and digestive tract was examined carefully, and every single abnormality was recorded.

ACUTE TOXICITY

When for a particular compound no information about toxicity is available, the Organisation for Economic Co-operation and Development **(**OECD) guidelines recommend to start acute toxicity assays with a default value of 175 mg/kg orally, and when toxic effects are observed, to reduce gradually the dose and test toxicity again. It is considered that, testing acute toxicity in one sex (commonly females) is enough. The sample size must be small due to the severity of the process, accordingly to the OECD.

Then, for our assays, since little previous information on the toxicity of AS-48 was available, the dose of the antimicrobial peptide AS-48 for acute toxicity assays was selected based on such indications in order to calculate the LD50. The concentrations of AS-48 assayed were 127.27, 65, 26, 15, 10, 5 and 2.5 mg/Kg of body weight, administered intraperitoneally in 200 µl in seven adult C57BL/6 JRj female mice respectively (41). All the doses were administered and calculated for each mouse individually, according to its initial weight.

ADMINISTRATION ROUTE TOXICITY ASSAY

Once the highest concentration of AS-48 that could be tested was determined in the acute toxicity assay, the different routes for treatment were assayed. The mice were divided in two groups of C57BL/6 JRj eight-weeks-old female mice, and received bacteriocin AS-48 by intraperitoneal or intranasal administration route, respectively. In these two groups, negative control mice were treated with sterile PBS through the respective administration route. For each administration route, two concentrations of AS-48 were assayed: two mice were treated with 2 mg/Kg body weight and two other mice with 1 mg/Kg body weight. All mice were weighted before starting the experiment and every time before the administration of each dosage. The dosing schedule were three times per week during two weeks.

For the intranasal route, mice were anesthetized by inhalation of isofluorane mixed with 5-3% of oxygen and kept asleep between the two applications of 20 µl needed to get the final concentration of AS-48. For the intraperitoneal route, the final volume injected was 100µl (41). After the sacrifice, necropsy was performed, and blood and organs were also analyzed. The organs extracted for further histological examination were: brain, spleen, lungs, liver and kidneys (42).

SUBCHRONIC TOXICITY

We stablished four groups of four BALB/c JRj eight-weeks-old mice: two groups of males and two of females. Within each group, mice were treated every day during 9 days with 4, 2 and 1 mg/Kg of body weight of AS-48, and PBS as a control, respectively. Every concentration was assayed then in duplicated for both sexes, as well as the negative PBS control (**Table 15**). All the AS-48 preparations were dissolved in sterile PBS and administered via intraperitoneal. Prior to administrations, mice were anesthetized with isofluorane mixed with 5-3% of oxygen. After the final point, on day 10 of the experiment, mice were euthanatized

and necropsy was done. Blood was obtained via cardiac puncture, collected in tubes with 0.8% of EDTA and hematological test was done. Organs (kidneys, lungs, brain, liver and spleen) were collected and kept in formalin for subsequent histopathology examinations.

Table 15: Groups of mice to assay the subchronic toxicity of AS-48 in BALB/c JRj intraperitoneally.

Group	Treatment	Sex
1	PBS	Male
	4mg/Kg of AS-48	Male
	2mg/Kg of AS-48	Male
	1mg/Kg of AS-48	Male
2	PBS	Male
	4mg/Kg of AS-48	Male
	2mg/Kg of AS-48	Male
	1mg/Kg of AS-48	Male
3	PBS	Female
	4mg/Kg of AS-48	Female
	2mg/Kg of AS-48	Female
	1mg/Kg of AS-48	Female
4	PBS	Female
	4mg/Kg of AS-48	Female
	2mg/Kg of AS-48	Female
	1mg/Kg of AS-48	Female

M. TUBERCULOSIS INFECTION IN MICE

In order to infect mice chronically with *M. tuberculosis*, eight-weeks-old BALB/c JRj mice were first anesthetized with isofluorane and then two instillations of 20 µl of a bacterial suspension (containing 200 cfu of *M. tuberculosis* H37Rv in total) were inoculated by the intranasal route to each mouse. The bacterial suspension was added drop-by-drop in the nasal orifices of each mouse

leaving time to assimilate the whole volume in the breathing, this protocol was adapted from Uranga S. *et al* (43). After two weeks, the infection of tuberculosis was evolved enough to represent a model of chronic infection, then specific treatments (as described in the following sections) were applied to the mice. It has been demonstrated that the volume of bacterial suspension used to infect mouse intranasally correlates with the efficiency of the infection: when the bacterial inoculum is contained in 40 µl, the percentage of colonization is higher than if the volume is 10 µl; in the latter case, the efficiency of the bacterial infection could decrease up to 80% of what expected (43).

EFFICACY EXPERIMENTS IN MICE

Groups of 8-weeks old BALB/c JRj female mice, with six animals each, were done in order to assay the efficacy of different treatments containing bacteriocin AS-48, either alone or in combination with ethambutol. A total of seven different groups were formed, which received the following treatments: the untreated control group received PBS only, a group was treated with therapeutic dosage of isoniazid (10 mg/Kg), two groups were treated with bacteriocin AS-48 only at two different concentrations (2 mg/Kg and 1 mg/kg respectively), another two groups were treated with the same concentration of AS-48 and a subinhibitory concentration of ethambutol (10 mg/Kg), and the last group was treated with the subinhibitory concentration of ethambutol only (**Table 16**).

The treatment was administered for five days per week during four weeks, and the dosages were administered by the intraperitoneal route. Mice were thoroughly observed after treatment and weight control was performed once a week. The mice whose weight loss was higher than the 20% of their initial weight, were euthanatized. After the final point of the experiment, animals were euthanatized by cervical dislocation, lungs were collected and kept frozen at least 24 hours in order to avoid contaminations when plating.

In order to quantify the number of CFUs allocated in the lungs, they were lysed in 1 ml of sterile water with tissue homogenizer and plated. For this, tubes containing lysed lungs were centrifuged 5 min at 1000 rpm to collect all the homogenized tissue. Serial 1:20 dilutions were done in PBS supplemented with 0.1% tyloxapol. A volume of 100µl of the corresponding dilution were plated in Middlebrook 7H10 media supplemented with albumin, dextrose, and catalase (ADC). Plates were incubated for 20 days at 37°C, and after this period the number of CFUS were counted. To prevent dissication, plates were sealed with Parafilm™ and covered with aluminum paper.

Table 16: Groups of six BALB/c JRj female mice for the efficacy assay.

Group	Treatment
1	PBS
2	10 mg/Kg of INH
3	2 mg/Kg of AS-48
4	1 mg/Kg of AS-48
5	2 mg/Kg of AS-48 + 10 mg/Kg of EMB
6	1 mg/Kg of AS-48 + 10 mg/Kg of EMB
7	10 mg/Kg of EMB

HEMATOLOGICAL AND BIOCHEMICAL ANALYSIS

For hematological analysis, whole blood samples were collected from the animals once the subchronic toxicity assay was finished. In order to avoid coagulation 1.5-2.2 mg of EDTA/ml of blood were added. The parameters measured were: white blood cells (WBC), lymphocytes (Lym), monocytes (Mon), granulocytes (Gran), red blood cells (RBC), hemoglobin (HGB), hematocrit (HCT), mean corpuscular volume (MCV), mean corpuscular hemoglobin (MCH), mean corpuscular hemoglobin concentration (MCHC), reed cell distribution width (RDW), platelet count (PLT), mean platelet volume (MPV), platelet distribution width (PDW) and procalcitonin (PCT). The blood samples were analyzed with the in the animal facilities at CIBA.

HISTOPATHOLOGICAL EXAMINATION

Several organs were collected (liver, spleen, lungs, brain and kidneys) from mice after the subchronic toxicity assays. Whole organs were fixed in formalin (4% formaldehyde) during 24 hours and included in paraffin. Samples were cut in slices, dehydrated and stained with hematoxylin-eosin (HE), sections were prepared by the Service of Pathological Anatomy at CIBA. Organ preparations were scanned with Aperio AT2 (Leica) and examined and photographed with Aperio eSlide Manager (Leica).

RESULTS

C57BL6 MICE EXHIBIT ACUTE TOXICITY WHEN THE CONCENTRATION OF AS-48 IS ≥ 2.5 MG/KG BODY WEIGHT

To assess the highest dose of AS-48 that could be used, in terms of toxicity, we firstly performed one experiment with a series of seven doses of AS-48 ranging from 127.27 to 2.5 mg/Kg body weight. Seven adult C57BL/6 JRj female mice received intraperitoneally a single dose each of AS-48 at a different concentration.

Mice who received doses of AS-48 at concentrations higher than or equal to 10 mg/Kg body weight deceased in 15-20 minutes after administration. The other two mice, that had received 5 mg/kg and 2.5 mg/Kg body weight of AS-48, presented depressed appearance, dyspnea and slowed movements; they were monitorized during a couple of hours and left in the cage. After 12 hours post-administration, they were found to be dead. We could appreciate that in several cases the duodenum showed an irritated surface and distention. No other alterations in other organs were observed. In the two mice that received 15 mg/Kg and 10 mg/Kg body weight of AS-48, respectively, we could appreciate a slightly haemorrhagic tissue in the subcutaneous area of the armpit.

In conclusion, the concentrations of AS-48 assayed seemed to be toxic for this mice lineage and through this administration route.

INTRAPERITONEAL VS. INTRANASAL ROUTE: TOXICITY ASSAY

In the previous experiment, we had determined that AS-48 resulted in acute toxicity when administered intraperitoneally at concentrations equal to or above 2.5 mg/Kg of body weight. We wanted to test next whether toxicity could depend on the administration route in the same mouse strain. For this, different groups of C57BL/6 JRj female mice were divided according to the administration route and the treatment received (**Table 17**). Bacteriocin AS-48 was administered at concentrations lower than 2.5 mg/Kg of body weight.

Table 17: Groups of mice for testing the different administration routes in the toxicity of AS-48.

Group	Administration route	Treatment
1	IP	PBS
2	IP	2mg/Kg of AS-48
3	IP	1mg/Kg of AS-48
4	IN	PBS
5	IN	2mg/Kg of AS-48
6	IN	1mg/Kg of AS-48

IP: intraperitoneal; IN: intranasal; PBS: phosphate buffer saline.

On one hand, for the intraperitoneal route, the two mice in group 2 received the highest dose (2 mg/Kg body weight) and deceased 40 minutes after the first administration. Before dying, they showed depressed behavior, eyelid partially closed and slow breathing. In the necropsy, we observed a dark region in the distal segment of the spleen and the jejunum with an orange coloring. We continued with the treatment of the control group (group 1) and the group treated with 1 mg/Kg body weight (groups 3) after 36 hours. The two mice of the group 3, treated with 1 mg/Kg body weight, showed eyelid partially closed, back bend and reduced mobility after the first administration of bacteriocin AS-48; however, they died after the second dosage. The intraperitoneal control group (group 1, receiving PBS) was euthanatized; no significant abnormality was observed macroscopically in the organs.

On the other hand, the intranasal treatment was prolonged for two weeks, administering a total of six doses, as scheduled. All mice in groups 5 and 6 showed a weight decrease and typical sign of suffering, such as hunched posture, piloerection, eyelids partially closed and low mobility, but after around 10 minutes they recovered the normality. Mice belonging to group 5 (2 mg/Kg of AS-48) were not administered the second dosage due to their weight loss observed after administration of the first dosage. These mice finally recovered their original

weight and could receive the third, fourth, fifth and sixth dosages. At the end of the experiment mice treated by the intranasal route, were euthanatized and blood and organs were collected (**Image 27**). Besides, the macroscopic observation of the different tissues and organs, lungs, kidneys, liver, spleen and brain were analysed by its histopathology.

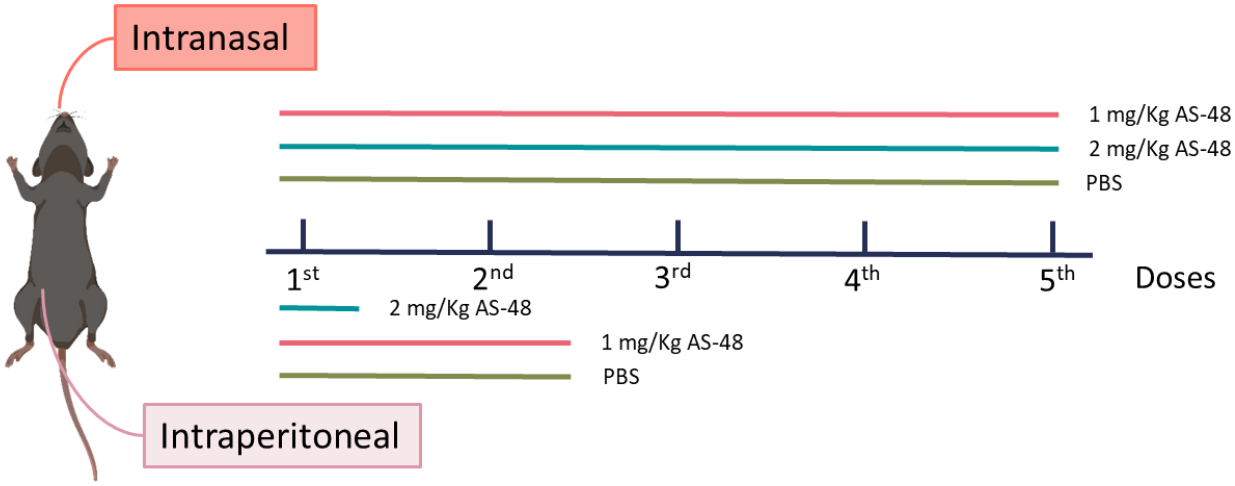

Image 27: Scheme of the experiments to evaluate the different routes of administration.

Furthermore, haematological analysis was performed (the different haematological parameters are listed in **Table 18**). In general, we could not determine a common pattern of the different altered values associated to the treatment with AS-48. The platelets (PLT) also appeared to be lower than the standard values in the PBS control of both administration routes, and in the groups treated with 1 mg/Kg of AS-48. Low values of PLT indicate thrombocytopenia, although no abnormal bleeding were observed during the sacrifice.

On the contrary we observed that the values of red blood cells (RBC), haemoglobin (HGB) and haematocrit (HCT) are higher than the standards in mice treated with PBS, treated with 2 mg/Kg of AS-48 in the intraperitoneal treatment and just in the group treated with 1 mg/Kg of AS-48, in the intranasal treatment. High values of RBC could cause their agglomeration in the vessel and capillary, which conclude in a lack of oxygen in the different tissues. The HCT measures the volume that take up the red blood cells in the blood; high HTC values indicate

dehydration or hypoxia, this could be related to the fact that we also have high values of RBC and the possibility of not good distribution of oxygen. .

Table 18: Haematological parameters measured in mice of the administration route experiment.

		Intraperitoneal treatment			Intranasal treatment		
PARAMETERS	RANGE	Control PBS	2 mg/Kg AS-48	1 mg/Kg AS-48	Control PBS	2 mg/Kg AS-48	1 mg/Kg AS-48
White Blood Cells (x10 9/L)	0.8 - 6.8	3.1	5.25	4.1	5.4	4.1	6.4
Lymphocytes (x10 9/L)	0.7 - 5.7	2.05	4.15	3	3.65	2.65	4.3
Monocytes (x10 9/L)	0.0 - 0.3	0.05	0.15	0.15	0.2	0.15	0.25
Granulocytes (x10 9/L)	0.1 - 1.8	1	0.95	0.95	1.55	1.3	1.85
Lymphocytes (%)	55.8 - 90.6	70.35	76.7	74.85	69.6	64.25	69.4
Monocytes (%)	1.8 - 6.0	2.2	3.05	3.5	3.6	3.95	3.95
Granulocytes (%)	8.6 - 38.9	27.45	25.25	21.65	26.8	31.8	26.65
Red Blood Cells (x10 12/L)	6.36 - 9.42	11.55	10.095	8.8	9.23	7.84	10.335
Hemoglobin (g/dL)	11.0 - 14.3	17.95	14.6	13.65	14.1	12.15	16.2
Hematocrit (%)	34.6 - 44.6	57.2	49.3	43.85	44.55	38.05	51.2
Mean corpuscular volume (fL)	48.2 - 58.3	49.55	48.9	50.05	48.3	48.6	49.5
Mean corpuscular hemoglobin (pg)	15.8 - 19.0	15.5	14.3	15.45	15.25	15.4	15.6
Mean corpuscular hemoglobin concentration (g/dL)	30.2 - 35.3	31.3	29.3	31	31.6	31.35	31.6
Red blood cell distribution width (%)	13.0 - 17.0	14.05	14.45	14.25	12.95	13.7	14.2
Platelets (x10 9/L)	450 - 1590	240	514	298.5	333	837.5	248
Mean platelet volume (fL)	3.8 - 6.0	5.35	5.9	5.45	5.3	5.15	5.4
Platelet distribution width		16	16.6	16.25	15.85	15.85	11.1
Procalcitonin (%)		0.1235	0.288	0.1555	0.1765	0.4305	0.1325

In the necropsy of each mouse, besides of the carefully examination of the tissues, several organs were collected, fixed, stained and histologically examined. We observe that brain and kidneys have a normal histological structure, we did not observe any signs of edema, hyperplasia or dysplasia, inflammation or atypical cells. In the case of the spleen, the white pulp is slightly hyperplasic in all the mice, we hypothesised that is due to the characteristic of the strain. We could not observe any difference between the control group and the treated ones in terms of the spleen histology. In some of the lungs we observe some areas with haemorrhages and swelling but with a conserved architecture and without fibrinoid tissues. We did not observe a relation between these changes in the lungs and the treatments.

In the case of the liver they present some differences in the histology between each group of treatment. First, in the intraperitoneal treatment group, we noticed that mice of the control treated with PBS have a correct structure of the organ, with very few accumulated lymphocytes (arrow in **Image 28, D)**) and

hepatocytes with a slightly vegetal-like deformation (clear cytoplasm and polygonal edges). In contrast, the livers of the mice treated with 2mg/Kg of AS-48 showed sinusoidal dilatation (arrows in **Image 28, E)**) , vegetal-like deformation of the parenchyma, and slightly patched in the panoramic view. We observe several binuclear cells or with prominent nuclei (cirlces in **Image 28, G)**), this could be due to a process of regeneration or repair. Mice treated with 1mg/Kg of AS-48 show a diffuse patched in the general histology of the liver and vegetal-like changes in the hepatocytes (**Image 28, F)**).

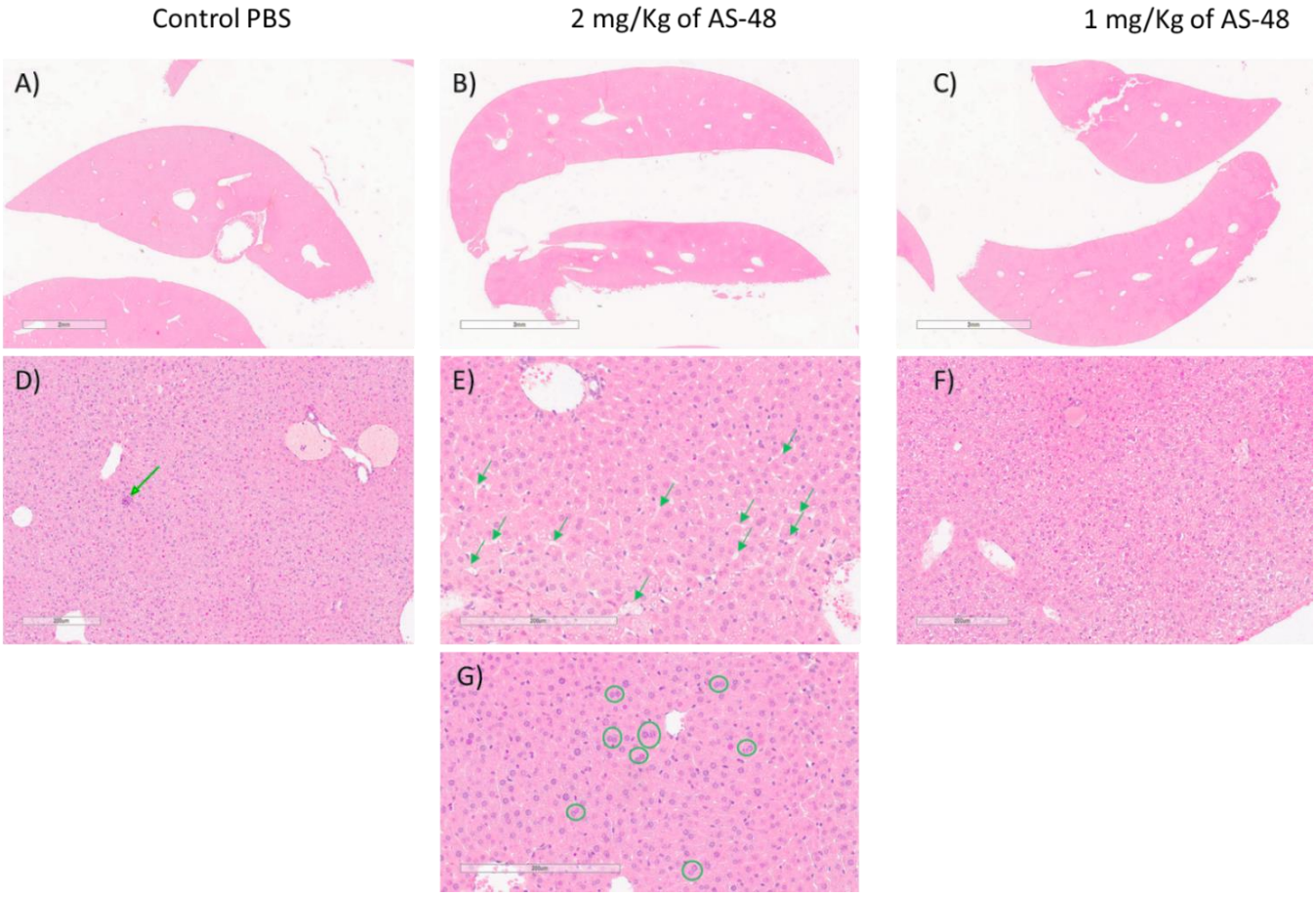

Image 28: Pictures of histological slices of mice livers from the experiment of intraperitoneal treatment with AS-48. A), B) and C) Panoramical view of the liver of mice treated with PBS, 2 mg/Kg of AS-48 and 1 mg/Kg of AS-48, respectively. D) Higher augment of liver treated with PBS; arrow: lymphocyte accumulated. E) and G) Higher augment of liver treated with 2 mg/Kg of AS-48; arrows: dilated sinusoids; circles: binuclear cells. And F) Higher augment of liver treated with 1 mg/Kg of AS-48, detail of vegetal-like changes in the hepatocytes.

Second, in the intranasal treatment group, livers of mice of the control treated with PBS have very few mixed infiltrate (lymphocytes and eosinophils) but a general healthy aspect (**Image 29, A) and D)**). Also the group treated with 1mg/Kg of AS-48 show a healthy appearance with no vegetal-like changes (**Image 29, C) and F)**). On the contrary, the liver of the mice treated with 2mg/Kg of AS-48 show a ballon cell degeneration (at a high augment, **Image X, E)**), vegetal-like changes. We also noticed that there is a loss of nuclei in the centrilobular cells that could means the beginning of a necrosis process (green circle, **Image 29, E)**).

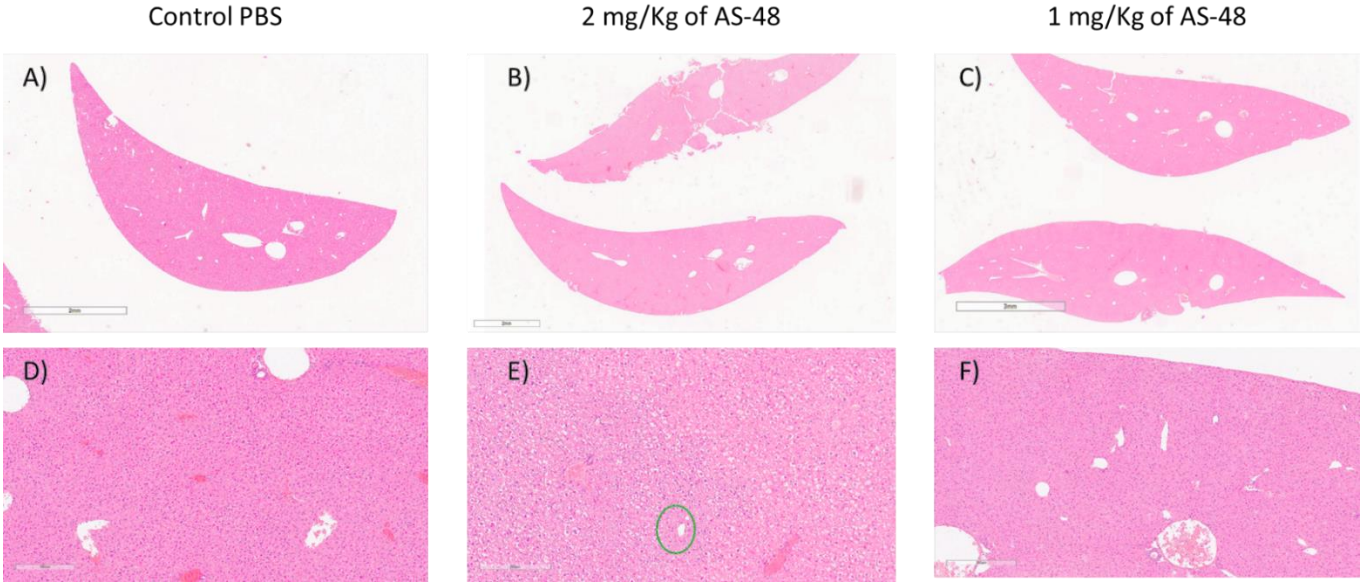

Image 29: Histological slices of mice liver from the experiment of intranasal treatment with AS-48. A), B) and C) Panoramical view of the liver of mice treated with PBS, 2 mg/Kg of AS-48 and 1 mg/Kg of AS-48, respectively. D), E) and F) Higher augment of liver treated with PBS, 2 mg/Kg of AS-48 and 1 mg/Kg of AS-48 respectively. Circle in panel E) indicates the centrilobular necrosis.

We could conclude that AS-48 at 1 or 2 mg/Kg of body weight is toxic for C57BL/6 JRj female mice when administered by the intraperitoneal route, but it seems to be better tolerated when administered by the intranasal route.

NO TOXICITY OBSERVED *IN VIVO* WHEN TREATING BALB/C MICE WITH AS-48 DURING 10 DAYS

Given the results of the acute toxicity assay, we considered whether the toxicity could be linked to the mouse strain. Then, we designed a pilot probe with a mouse of the lineage BALB/c, which received intraperitoneally two doses of AS-48 at 218 mg/Kg (i.e. the same concentration as used in the acute toxicity assay with the C57BL6 mice). In these conditions, we observed an absence of toxicity. In consequence, we decided to proceed further experiments with BALB/c mice only.For the subchronic toxicity assay, the following concentrations of AS-48 were administered to BALB/c mice: 4, 2 and 1 mg/Kg body weight. The doses were administered via intraperitoneal in a volume of 200 µl daily during 10 days (**Table 15**).

All the mice treated with 4mg/Kg of AS-48 were euthanatized (Humane Endpoint), after two days of administration, due to the evidence of suffering and distress consisting in abnormal posture and movement, depressed look, loss of normal temperature, piloerection and eyelids partially closed.

The rest of the mice (receiving either PBS or AS-48 at 2 or 1 mg/Kg) continued the procedure with normality. In general, female mice (groups 3 and 4; Table 2??) looked groomed than males (groups 1 and 2). During the ten days of the experiment, none of the animals showed any alteration in the movement and in the behaviour and their breathing and food uptake was completely normal (**Image 30**).

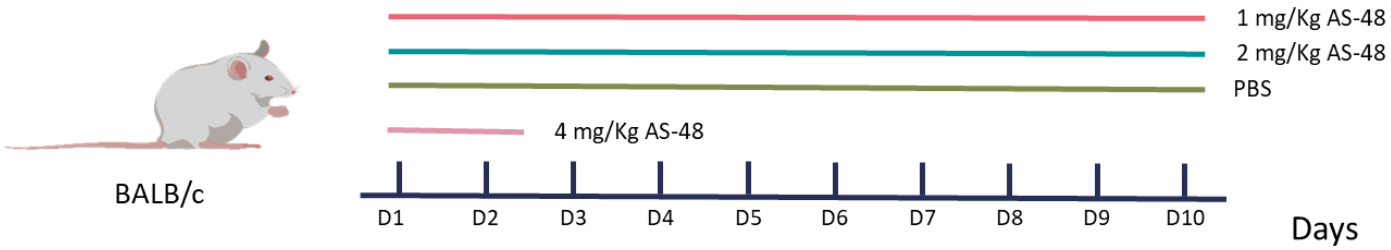

Image 30: Scheme of the *in vivo* subchronic toxicity of AS-48.

They were euthanatized by CO_2 camera for a complete extraction of the blood for further analysis. In the necropsy, mice did not show any abnormality, and all organs and epithelia looked healthy macroscopically.

In conclusion, AS-48 is toxic intraperitoneally after two administrations of 4 mg/Kg in BALB/c mice. When 2 or 1 mg/Kg of AS-48 was administered, no toxicity was observed after 10 consequently days. Moreover, weight of the mice did not vary along the process, **Image 31**, indicating the wellness of the mice. In females body weight varied slightly more between groups of treatment than in males, although females looked smarter than males. They all also showed a great variation between individuals particularly in groups treated with 1 mg/Kg of AS-48.

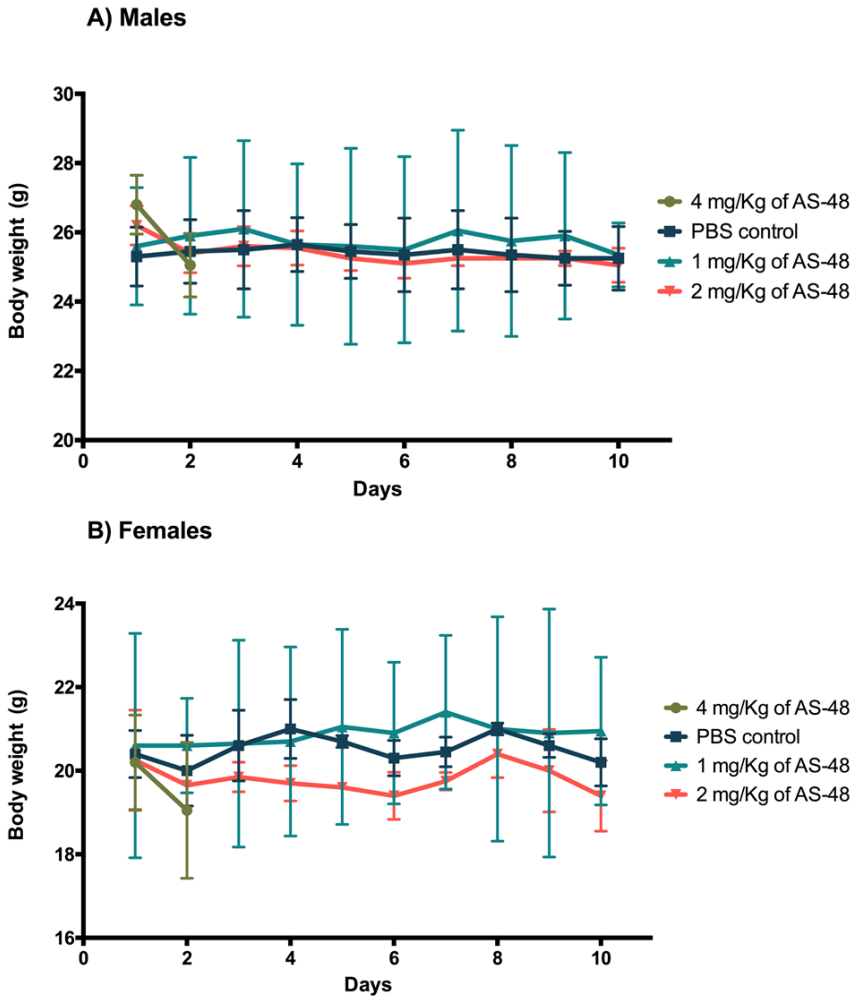

Image 31: Body weight of male mice in subchronic toxicity assay. A) Body weight of males and B) body weight of females

In the haematological study of the blood samples obtained after the subchronic toxicity assay, we observed also heterogeneous values (**Table 19**; it was not possible to obtain the blood of one male treated with 2 mg/kg of AS-48). With the exception of one mice from the control group, the mean platelet volume (MPV) presented high values which. In some cases, imply certain types of diabetes, but in this case, we have to pay a special attention to the low values of PLT observed in mice treated with 2 mg/Kg of AS-48. When these two events happen, low values of PLT and high of MPV, could indicate that AS-48 is toxic for example it occurs when a chemotherapy is administered in cancer patients.

We also could observe that RBC, HGB and HCT are generally higher than the standards. Also, the values of white blood cells (WBC), lymphocytes (Lym), Monocytes (Mon) and Granulocytes (Gran) seems to be higher than the standards, mainly in females. This may mean that the mice could be fighting off an infection, although we did not observe any sign of infection during the treatment neither in the necropsy. In this case females show values more altered than males, but during the experiment the general behaviour and appearance were better than the males, they did not show any distress sign and smarten up better than males.

Table 19: Haematological parameters measured in the subchronic toxicity assay.

		MALES			FEMALES		
PARAMETERS	RANGE	PBS	1mg/kg AS-48	2mg/kg AS-48	PBS	1mg/kg AS-48	2mg/kg AS-48
White Blood Cells (x10 9/L)	0.8 - 6.8	8.35	4.65	7.1	9.7	13.9	12.3
Lymphocytes (x10 9/L)	0.7 - 5.7	6.15	3.35	3.8	8	10.5	8.85
Monocytes (x10 9/L)	0.0 - 0.3	0.35	0.2	0.7	0.2	0.4	0.5
Granulocytes (x10 9/L)	0.1 - 1.8	1.85	1.1	2.6	1.5	3	2.95
Lymphocytes (%)	55.8 - 90.6	78.85	70.85	53.3	81.3	76.2	71.1
Monocytes (%)	1.8 - 6.0	3.1	4.35	9.8	2.75	3.1	4.25
Granulocytes (%)	8.6 - 38.9	18.05	24.8	36.9	15.95	20.7	24.65
Red Blood Cells (x10 12/L)	6.36 - 9.42	9.235	12.275	10.27	11.68	11.915	10.295
Hemoglobin (g/dL)	11.0 - 14.3	13.7	17.05	15.5	18.05	18.95	15.9
Hematocrit (%)	34.6 - 44.6	45.1	60.45	50.4	57.4	58.9	50.9
Mean corpuscular volume (fL)	48.2 - 58.3	48.7	49.05	49.1	49.1	49.45	49.35
Mean corpuscular hemoglobin (pg)	15.8 - 19.0	14.55	14.1	15	15.3	15.85	15.3
Mean corpuscular hemoglobin concentration (g/dL)	30.2 - 35.3	29.95	28.95	30.7	31.15	32.1	31.05
Red blood cell distribution width (%)	13.0 - 17.0	13.45	14.2	13.4	14.05	13.55	13.25
Platelets (x10 9/L)	450 - 1590	376	521	361	540	386	363
Mean platelet volume (fL)	3.8 - 6.0	6.25	7.65	6.2	7.55	6.65	6.85
Platelet distribution width		18.45	17.85	17.4	17.35	16.75	17.2
Procalcitonin (%)		0.256	0.406	0.223	0.4	0.2635	0.2475

Furthermore, we have analysed the possible toxicity through histology examinations. Those mice that were treated with 4mg/Kg of AS-48 (death after two administrations) exhibits a great toxicity in the liver, we can observe a great patched appearance in panel A) of **Image 32**. In the case of the males, the damage were more severe than in females: liver present subcapsular necrosis (arrows and bracket, **Image 32, B)**) and, portal and periportal necrosis building bridges between portal spaces (**Image 32, C)**). We observed several haemorrhagic focus and some cells with nuclei lost (**Image 32, D)**). In females, do not exhibits that severe necrosis, but the parenchyma present a hydropic degeneration in the centrolobular area.

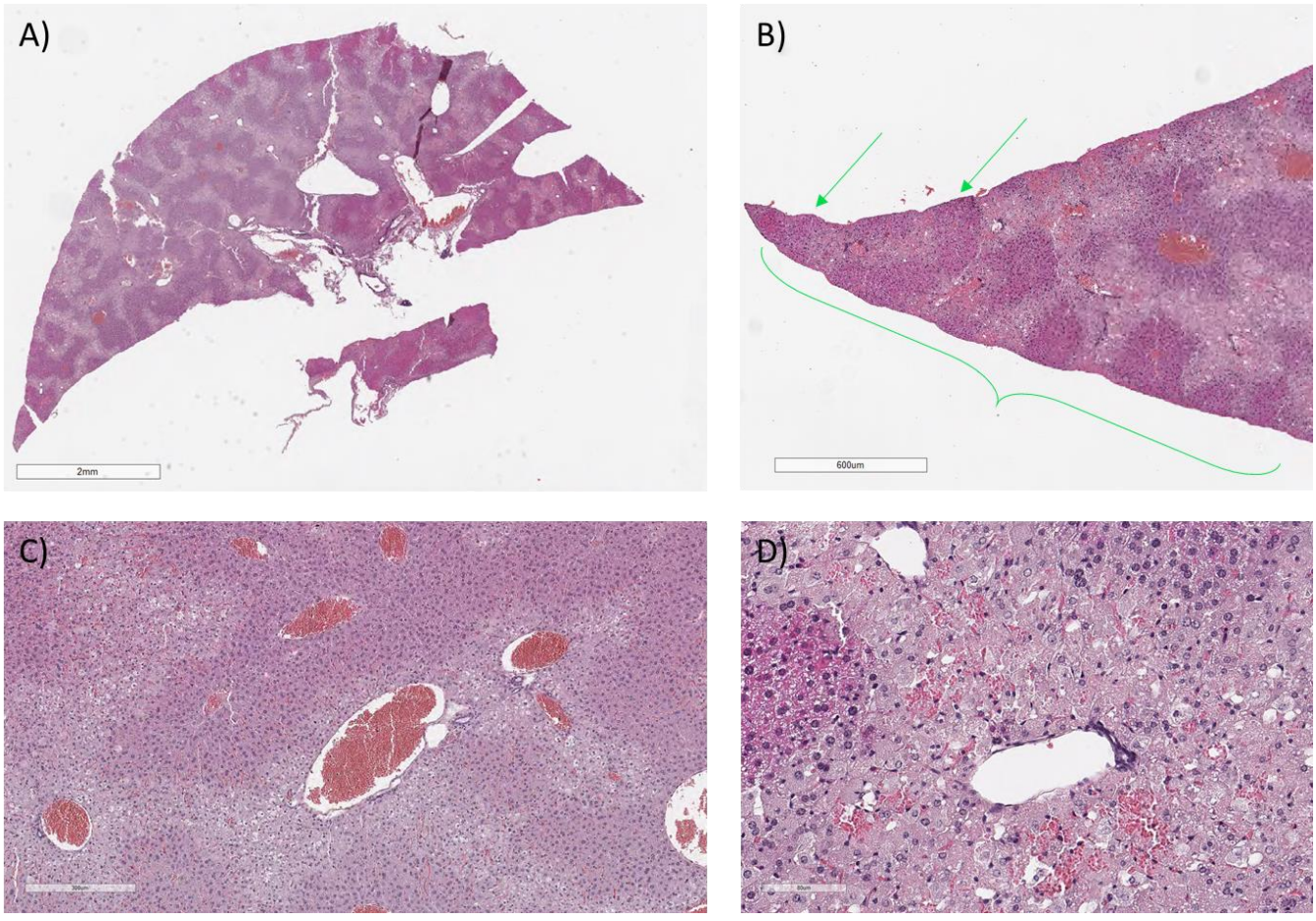

Image 32: Pictures from the histological slices of mice livers treated with 4 mg/Kg of AS-48 in the sucbhronic toxicity assay. A) Panoramical view of a live with patched necrosis; B) Arrows and bracket indicates the subcapsular necrosis area; C) Detail of the hepatic parenchyma with portal and periportal necrosis forming bridges; D) Higher augment of the necrotic area, hepatocytes with loss of nuclei.

In the livers of the mice treated with 2 mg/Kg of AS-48, 1 mg/Kg of AS-48 and the control group with PBS, we did not observe any abnormality. Just one of the males treated with 2 mg/Kg of AS-48 have slightly modifications in the normal appearance of the hepatic parenchyma.

We also have observed the histology of kidneys, spleen, brain and lungs. In the case of the lungs some of them presented some alterations such as some haemorrhagic areas, but without any fibrinoid appearance or red blood organization, so the haemorragic is not due to a thrombus and could be due to the process of euthanasia and/or due to the extraction. The rest of the organs present a normal architecture, and there were not any sign of toxicity or tissue damage.

IN VIVO EFFICACY OF AS-48 AND SYNERGISTIC COMBINATIONS OF AS-48 AND ETHAMBUTOL

The main objective was to test the efficacy of AS-48 against *M. tuberculosis* infected mice. The efficacy of treatments containing AS-48 were compared with that of the reference antituberculosis drug isoniazid. In addition, we explored *in vivo* the potential synergistic relationship between AS-48 (at two concentrations that presented synergism in *in vitro* conditions and were within the limits of the subchronic toxicity *in vivo)* and a sub-inhibitory dose of ethambutol (a first-line antituberculosis drug), and compared the efficacy of such combined treatment of AS-48 and ethambutol versus the bacteriocin as a mono-therapy (**Table 16**). For comparing data from the *in vitro* MIC determinations and the *in vivo* toxicity, we assumed that one kilogram of body weight is equivalent to one liter; this estimation allowed us to correlate also the MIC *in vitro* with the possible MIC *in vivo*.

Mice belonging to the group treated with 2mg/Kg of AS-48 alone were deceased after the first 10 days of treatment. Along treatment, mice that were treated with AS-48 only, mainly group 3 and 4 (2 mg/Kg and 1 mg/Kg of AS-48), showed an altered behavior, in terms of depression, piloerection, isolation and

reduction of the movement, for the period starting right after administration up to one hour after treatment. Interestingly, mice from groups 3, 4, 5 and 6 (treated with 2 mg/Kg of AS-48, 1 mg/kg of AS-48, 2 mg/kg of AS-48 + 10 mg/Kg of EMB and 1 mg/Kg of AS-48 +10 mg/Kg of EMB, respectively), i.e. all mice receiving bacteriocin AS-48 looked depressed after inoculation but their aspect improved considerably during the last two weeks of treatment compared with the first administrations. We can speculate that after several inoculations of bacteriocin AS-48, an immune adaptation happens and this could mitigate the adverse effects of the administration of AS-48.

After the final point of this experiment all animals were sacrificed, spleen and lungs were collected, examined in order to determine the lesions provoked by the tuberculosis infection and frozen. From the macroscopic appearance of both organs we could determine the evolution of the infection and estimate the dilutions that would be needed to plate in order to determine the exact bacterial load in lungs. Every mouse showed formation of granulomas in their lungs, but in the case of the group treated with isoniazid those lesions were much smaller than the rest of the groups, as expected.

In the untreated control, the bacterial load reached a value of 6.5 log cfu/ml. Animals in groups 3 and 4, which were treated with only AS-48, had higher bacterial loads than the ones in the untreated control group, 7.5 log cfu/ml and 6.6 log cfu/ml respectively. In the case of group 3 (treated with 2 mg/Kg of AS-48), mice deceased before the experiment was completed, so the high bacterial load in these animals could be due to the fact that the treatment was given for a much shorter time than the other groups. The only groups in which we could observe a slight decrease were groups 5 and 6, i.e. those in which treatment was a combination of AS-48 and ethambutol (**Image 33**); for these groups, bacterial loads were 6.3 log cfu/ml and 5.98 log cfu/ml respectively.

We can speculate that the concentration of ethambutol in combination with AS-48, even at subinhibitory concentrations, could provide certain improvement in mice health in the infected animals, in comparison with the groups receiving

only AS-48. Nevertheless, since in the control group (group 7) treated only with ethambutol, the number of cfu was slightly lower (5.91 log cfu/ml) than in the groups treated with both EMB and AS-48, it can be concluded that no synergy was observed when the combined treatment was applied in these conditions.

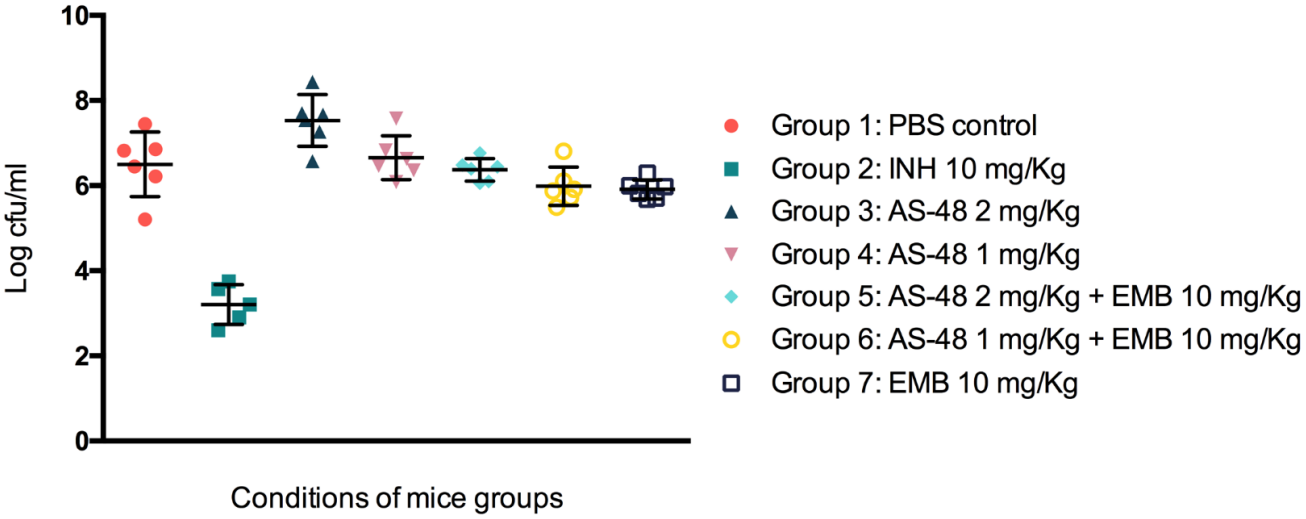

Image 33: Representation of the efficacy assay of the different concentrations of AS-48 alone or in combination with EMB against M. tuberculosis in Balb/c JRj mice.

On the other hand, the isoniazid efficiently reduced the number of cfus in lungs, resulting in a decrease of three log compared with the untreated control. In the case of the group treated with ethambutol only, given that this drug was administered at a subinhibitory dose, it was not expected to reduce significantly the number of cfu in the lung of infected mice.

The percent survival graph with the data obtained from the efficacy assay helps to understand the effect of AS-48 in infected mice (**Image 34)**. All mice in group 2 (treated with 10 mg/Kg of isoniazid), group 7 (treated with subinhibitory concentration (10 mg/Kg) of ethambutol), and the untreated group survived all along the experiment. Survival of mice in group 5 (treated with 2 mg/Kg of AS-48 and 10 mg/Kg of ethambutol) was higher (80%) than that in the other groups where AS-48 was administered. The group treated with 1 mg/Kg of AS-48 and 10 mg/Kg of ethambutol (group 6) had a percentage of survival of 60%. Comparing group 5 and 3 (both receiving AS-48 at 2 mg/Kg, with or without ethambutol,

respectively), the group in which the treatment includes ethambutol (group 5) had a much higher survival rate than the group treated with monotherapy with AS-48. We can observe the same phenomenon when we compare groups 4 and 6, both with the same concentration of AS-48 (1 mg/Kg) but group 6 receiving also 10 mg/Kg of ethambutol. In general, those groups that were treated with a combined therapy exhibited higher survival percentage than the ones receiving the same amount of AS-48 in monotherapy.

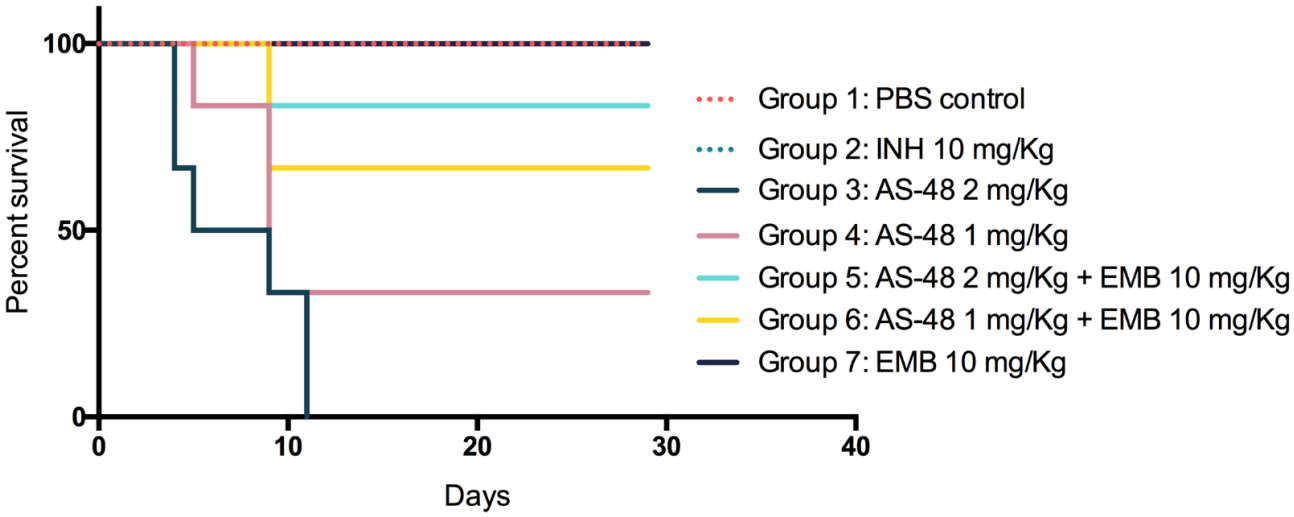

Image 34: Survival of the different treatments groups of mice in the efficacy assay (groups 1, 2 and 7 have the same tendency).

At different points, body weights were recorded and plotted (**Image 35)**. We can observe that at the beginning of the experiment there was little variability in body weigh between groups but at the end of the experiment, differences in body weigh between groups had increased and also within each group variability between animals had also increased. Body weight of animals in group treated with 2 mg/Kg of AS-48 only confirm the distress suffered by the mice: the weight decreased (and also the survival) reaching a diminution of the 20% in the body weight which is one of the aspects considered as humane final point.

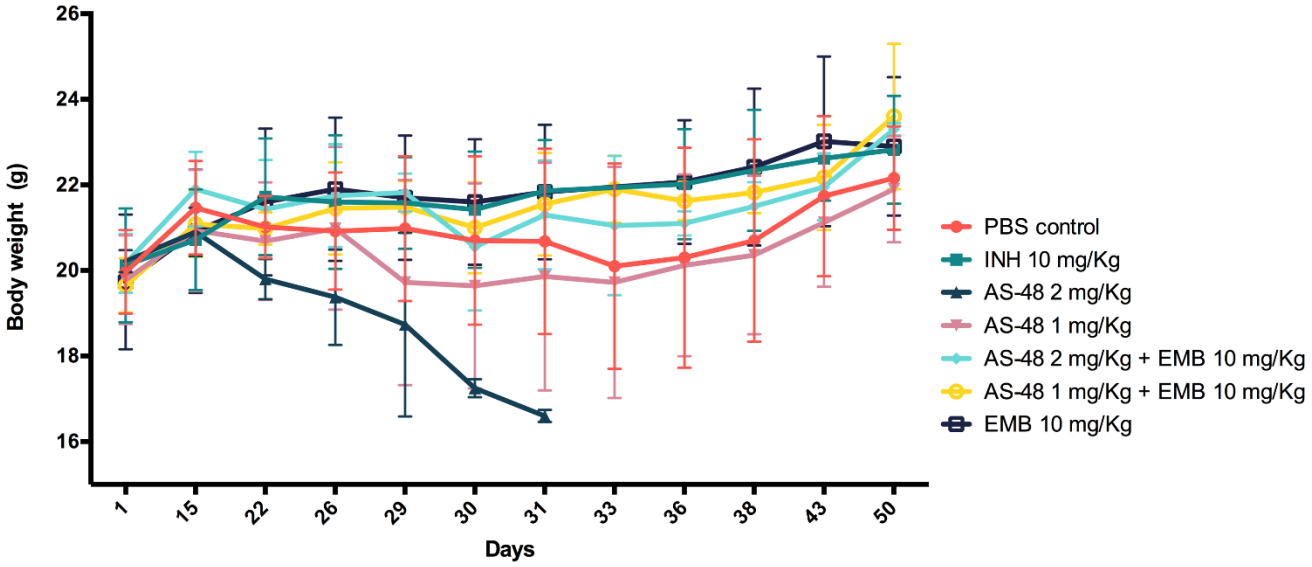

Image 35: Body weight recorded during the efficacy assay in all the mice groups.

In the necropsy of mice, we could highlight that all of them presented granuloma and lesions in both lungs. We could also notice that, due to the infection process, the spleen increased considerably its size. Nevertheless, the lesions observed in mice of group 2, treated with isoniazid, were less severe than the other groups. According to the extent of the lesions observed in the necropsy of lungs, we estimated the dilutions needed for determining accurately the number of cfu.

In conclusion, we could understand that, even the dose of ethambutol is in a subinhibitory concentration, this would help to mitigate the adverse effects caused by the accompanying drug AS-48. Those treatments in which both drugs, ethambutol and AS-48 were combined, showed slighty better results, in terms of percentage of survival and cfu reduction, than those in which AS-48 was administered alone. Despite that, we could not reach a significant decrease in the number of cfu in lungs obtained from the infected animals.

DISCUSSION

The main objective of this work has been to determine the toxicity of bacteriocin AS-48 in mice, in order to define the concentrations that could be used safely for treating *M. tuberculosis* infection in this experimental model, as well as to do a preliminary assessment on the efficacy of AS-48 to reduce bacterial burden in the lungs of infected mice. In general, the results of our experiments have revealed that AS-48 has important toxicity issues, given the high concentrations that would be needed in order to be effective against *M. tuberculosis*, and under the conditions assayed, AS-48 contributed very little to reduce bacterial load in infected animals. At the same time, these experiments have revealed potential approaches to further explore the usefulness of bacteriocin AS-48, opening interesting perspectives that will be explored in the future.

TOXICITY

According to the ODCE, a product is considered as safe when there is an absence of toxicity up to a dose of 2 g/L(44). We looked in the literature for data on toxicity of other antimicrobial peptides, in order to have a reference for designing our experiments with AS-48. For example, the lipophilic peptide YV11455 (45) was tested against *Staphylococcus aureus* (MRSA) in murine models, and resulted between 54-270-fold more effective than its analogue, the glycopeptide antibiotic vancomycin. Peptide YV11455, which targets the bacterial membrane, does not cause any sign of acute toxicity at a maximum dose of 12 mg/Kg body weight, since it resulted in a biochemical analysis similar to those of untreated animals, and no severe modifications in the histology of the organs was observed.

Due to the low solubility of AS-48 in aqueous solvents (maximum concentration reached has been 2.5 mg/ml) we were not able to test 2 g/L as this

is the concentration recommended by the ODCE. Then, we used much lower concentrations of AS-48 for the toxicity assays, starting with 127 mg/Kg, a value close to that recommended by OEDC, and this quantity was reduced stepwise until no toxicity was found.

Even with such low concentrations, according to the result of the acute toxicity assay, AS-48 resulted highly toxic presented clear signs of morbidity in our experiment in C57BL/6 mice. However, in BALB/c mice, they showed no toxicity at the same concentrations. We have to consider the genetic and physiological differences between both mice strains to elucidate why AS-48 is more toxic for one strain than for the other. Both strains are inbred mice and are commonly used for toxicity assays, and there are many factors such as levels of gene expression, allelic variants and/or the interaction with the environment, that result in different phenotypes between them. For example, Su S.H. *et al*. (46) demonstrated that the activity of the bronchoalveolar macrophages was differentially regulated in C57BL/6 and in BALB/c in terms of the immunological response in response to physical exercise. They showed that C57BL/6 presents a higher phagocytic activity than BALB/c, but also, C57BL/6 exhibits a high expression of the macrophage receptor with collagenous structure (MARCO) and this factor could imply the innate resistance of C57BL/6 to tuberculosis infection (46).

Moreover, both strains do not respond in the same way at different environmental stress stimuli. It has been demonstrated that BALB/c strain increases the metabolic rate when is exposed to high altitude indicating a minor adaptation to the hypoxic stress compared with the C57BL/6 strain (47). On the contrary, under a social defeat, BALB/c mice reduce their metabolic efficiency and their body weight, but C57BL/6 increase their food intake and present invariably metabolic changes compared with BALB/c (48). In the histology, we have observed that livers of C57BL/6 mice presented more damages than the livers of BALB/c mice, with the same dose of AS-48.

However, the mice that received the highest dose of AS-48 (4 mg/Kg) shows and appearance of necrosis more severe than the others doses. With this, we can confirm the toxicity of that concentration of AS-48 in this conditions. We also hypothesize that the damages observed in the lungs could be due to the euthanasia method, CO_2, which could cause a collapse and haemorrhage in the lungs. In some cases the damages observed in lungs could also be due to the extraction from the thoracic cavity, generating some bleeding in the areas to be studied.

From our experiments, we can conclude that C57BL/6 mice are more labile to AS-48 than BALB/c, although the determination of the mode of action of AS-48 in the organism or how the toxicity appears is beyond the scope of this work. For further understanding, it would be necessary to perform pharmacokinetic and pharmacodynamic studies.

While testing the toxicity associated to different administration routes, the toxicity observed in the group treated intraperitoneally was severe, and toxicity observed after the intranasal route was milder. Among the reasons that could explain this lower toxicity, we cannot exclude the fact that a fraction of the bacteriocin given intranasally would have been "redirected" to the gastric route, and could be degraded by digestive enzymes. If so, the final concentration absorbed would be less than the one theoretically assayed. According to the work of del Castillo-Santaella T. *et al.* (49) the gastric enzyme, pepsin, only degrades AS-48 partially, but a further degradation occurs in the duodenum with the action of trypsin and chymotrypsin, this phenomenon occurs in a time-depend manner.

Nevertheless, it was observed that a fraction of AS-48 keep intact under these conditions and are able to avoid digestive degradation, possibly due to the different conformation that AS-48 can have or the domains that expose in certain media (49). Given that in the discovery of new antituberculosis drugs, one of the preferences is to develop a drug that can be administered orally, this would be the Achilles's heel of bacteriocin AS-48.

On the other hand, the intranasal route for administering an antituberculosis agent has the advantage of the direct delivery of the antimicrobial to the lung (50). However, for the intranasal administration, we anesthetized mice and the effect of the anesthesia during a prolonged treatment could imply an increase of the toxicity and a decrease in the effectiveness of the treatment. As a first approximation, in the subchronic toxicity test and consequently in the efficacy test, we used the intraperitoneal route as this can be done with shorter anesthesia time. It is evident that comparing other administration routes would give us more information about which administration route would be the optimal one for administering bacteriocin AS-48 while minimizing its toxicity.

EFFICACY

For the efficacy assays, the administration of the antituberculosis agents with the aim of decreasing the bacterial load in the infected lungs could be given either through intranasal administration or by aerosol. Again, we have to consider the high exposure to anaesthesia with isoflurane, given that the treatment of tuberculosis would last for one month under our experimental conditions. The aerosol delivery has the limitation that a great concentration of compound is needed to allow the drug to reach the lungs in an effective concentration. Moreover, in comparison with other administration routes, the amount of drug dispensed to each mouse could vary and the exact drug load could not be calculated accurately.

Usually, both, isoniazid and ethambutol are administered orally, and the concentrations used in our efficacy experiment were calculated considering the indications for the oral administration (51) as well as other studies. For example, according to Plinke *et al.*(52) in female 8-week-old C57BL/6 there is a positive effect in the reduction of the CFUs in majority of the organs when the mice were treated with 25-50 mg/Kg body weight of ethambutol. To boost the effect of

ethambutol with AS-48 we decided to use subinhibitory concentrations of ethambutol *in vivo* as shown in the *in vitro* assays.

Jindal *et al*. (42) assayed the efficacy of antimicrobial synthetic peptides derived from indolicin and ranalexin in a murine model of *Streptococcus pneumoniae* infection. These studies demonstrated the antimicrobial action of these peptides against a systemic infection (pneumococcal pneumonia) and also the synergy effect between different peptides and between peptides and antibiotics such as ceftriaxone and erythromycin, resulting in an efficient combined therapy (42). The lipophilic peptide YV11455 (45) was tested against *Staphylococcus aureus* (MRSA) in murine models, and resulted between 54-270-fold more effective than its analogue, vancomycin.

Other peptides, such as the microcin J25 that targets the bacterial RNA polymerase, have been tested against *Salmonella* infections, showing a great reduction in the number of CFUs in spleen and liver, and more interestingly demonstrated an antimicrobial effect in the whole organism (53).

Although all the infected mice in the efficacy assay formed granuloma, the heterogeneity of the vascularity in granuloma could decrease blood irrigation and consequently the accessibility of the drug to the site of infection and to the compartments where non-proliferative bacteria reside. If we would have achieved a good decrease in bacterial load in the infected mice it would be highly relevant to perform new assays with the Kramnik model as well as a murine model of acute infection, as described by Rullas J. *et al*. (54). As the vascular architecture is destroyed in the caseous centre of necrotic lesions and cavities, this leads also to failed immune response due to poor access of circulating T lymphocytes, a reduction of oxygen and nutrient supply and the consequent metabolic quiescence of bacterial cells.

Then, to reach the caseum, where quiescence bacilli are, drugs must diffuse from the cellular border of the necrotic area to the centre of the caseous region without the assistance of active or facilitated transport mechanisms (55). In the

Kramnik (C3HeB/FeJ strain) model, with caseous formation, it is also shown that the survival rate decreases when it is compared with a common model such as BALB/c (26). Therefore in this study we decided to perform a traditional chronic infection for the efficacy assay and check if AS-48 could have an antitubercular effect as it has been demonstrated *in vitro*.

We have to take in consideration that this is the first time that in vivo experiments have being done in mammals. Recently, Baños *et al*. (56) described experiments carried out in rainbow trout (*Oncorhynchus mykiss*) with a protective result of the treatment against *Lactococcus garvieae*, reducing the mortality caused by this pathogen. They also have taken into consideration the use of the producer strain of AS-48, UGRA10, in the diet as a preventive action against this pathogen. For this animal model, they reached a reduction in the bacterial load and an increase of the survival (100µg intraperitoneally and 12.5µg/ml in baths). As we have said before, the tuberculosis infection is extremely difficult to emulate in an *in vivo* model, due to the lack of natural reservoir (besides the human) so, the absence of a succesful effect of AS-48 in this experiments could be linked to the conditions.

Further experiments with other animal models will be needed to explore the possible applications that AS-48 could have against infectious diseases.To enhance the access of the drug to the target in an *in vivo* model we also have to consider the drug vehicle, in this case we have used PBS as a common harmless vehicle. This system could also be improved with the use of nanoformulation, for example in the case of rifampicin/poly (lactic-co-glycolic acid), Ohashi K.*et al*. (57) described that nanoparticles containing mannitol microspheres increased the rifampicin uptake by inhalation in the pulmonary macrophages.

As we have seen, the intranasal route is less harmful for mice, so the treatment using an aerosol application could enhance its effect and reduce the possible *in vivo* toxicity.

We also propose, other drugs combination such as including AS-48 to the complete treatment against *M.tuberculosis*, the use of isoniazid, rifampicin, ethambutol and pyrazinamide together with AS-48 could boost the effectiveness of the common treatment and result in a reduction of the time and second side-effects.

REFERENCES

1. Williams JR. 2008. The declaration of Helsinki and public health. Bulletin of the World Health Organization 86:650-651.
2. Gupta UD, Katoch VM. 2005. Animal models of tuberculosis. Tuberculosis (Edinb) 85:277-93.
3. Singh AK, Gupta UD. 2018. Animal models of tuberculosis: Lesson learnt. Indian J Med Res 147:456-463.
4. Orme IM, Ordway DJ. 2016. Mouse and Guinea Pig Models of Tuberculosis. Microbiology Spectrum 4.
5. Karlson AG, Feldman WH. 1952. Isoniazid in Experimental Tuberculosis of Guinea Pigs Infected with Tubercle Bacilli Resistant to Streptomycin and to Para-Aminosalicylic Acid. American Review of Tuberculosis 66:477-485.
6. Karlson AG. 1961. Therapeutic Effect of Ethambutol (Dextro-2,2'-[Ethylenediimino]-Di-1-Butanol) on Experimental Tuberculosis in Guinea Pigs. American Review of Respiratory Disease 84:902-&.
7. Dickinson JM, Mitchison DA. 1976. Bactericidal Activity Invitro and in Guinea-Pig of Isoniazid, Rifampicin and Ethambutol. Tubercle 57:251-258.
8. Chen XH, Hashizume H, Tomishige T, Nakamura I, Matsuba M, Fujiwara M, Kitamoto R, Hanaki E, Ohba Y, Matsumoto M. 2017. Delamanid Kills Dormant Mycobacteria In Vitro and in a Guinea Pig Model of Tuberculosis. Antimicrobial Agents and Chemotherapy 61.
9. Matsumoto M, Hashizume H, Tomishige T, Kawasaki M, Tsubouchi H, Sasaki H, Shimokawa Y, Komatsu M. 2006. OPC-67683, a nitro-dihydro-imidazooxazole derivative with promising action against tuberculosis in vitro and in mice. Plos Medicine 3:2131-2144.
10. Singhal A, Aliouat EM, Herve M, Mathys V, Kiass M, Creusy C, Delaire B, Tsenova L, Fleurisse L, Bertout J, Camacho L, Foo D, Tay HC, Siew JY, Boukhouchi W, Romano M, Mathema B, Dartois V, Kaplan G, Bifani P. 2011. Experimental Tuberculosis in the Wistar Rat: A Model for Protective Immunity and Control of Infection. Plos One 6.
11. da Silva DA, Rego AM, Ferreira NV, de Andrade MAS, Campelo AR, Caldas PCS, Pereira MAS, Redner P, de Pina LC, Resende FC, Pissinatti TA, Lopes CAA, Kugelmeier T, Perea JAS, de Souza IV, da Silva FA, Campos CF, Fandinho Montes FCO, Antunes LCM. 2017. Detection of mycobacterial infection in non-human primates using the Xpert MTB/RIF molecular assay. Tuberculosis (Edinb) 107:59-62.
12. Obaldia N, 3rd, Nunez M, Montilla S, Otero W, Marin JC. 2018. Tuberculosis (TB) outbreak in a closed Aotus monkey breeding colony: Epidemiology, diagnosis and TB screening using antibody and interferon-gamma release testing. Comp Immunol Microbiol Infect Dis 58:1-10.
13. Via LE, England K, Weiner DM, Schimel D, Zimmerman MD, Dayao E, Chen RY, Dodd LE, Richardson M, Robbins KK, Cai Y, Hammoud D, Herscovitch P, Dartois V, Flynn JL, Barry CE, 3rd. 2015. A sterilizing tuberculosis treatment regimen is associated with faster

clearance of bacteria in cavitary lesions in marmosets. Antimicrob Agents Chemother 59:4181-9.

14. Parsons SD, Gous TA, Warren RM, de Villiers C, Seier JV, van Helden PD. 2009. Detection of Mycobacterium tuberculosis infection in chacma baboons (Papio ursinus) using the QuantiFERON-TB gold (in-tube) assay. J Med Primatol 38:411-7.

15. Pena JC, Ho WZ. 2016. Non-Human Primate Models of Tuberculosis. Microbiol Spectr 4.

16. Cadena AM, Hopkins FF, Maiello P, Carey AF, Wong EA, Martin CJ, Gideon HP, DiFazio RM, Andersen P, Lin PL, Fortune SM, Flynn JL. 2018. Concurrent infection with Mycobacterium tuberculosis confers robust protection against secondary infection in macaques. PLoS Pathog 14:e1007305.

17. Sibley L, Dennis M, Sarfas C, White A, Clark S, Gleeson F, McIntyre A, Rayner E, Pearson G, Williams A, Marsh P, Sharpe S. 2016. Route of delivery to the airway influences the distribution of pulmonary disease but not the outcome of Mycobacterium tuberculosis infection in rhesus macaques. Tuberculosis (Edinb) 96:141-9.

18. White AG, Maiello P, Coleman MT, Tomko JA, Frye LJ, Scanga CA, Lin PL, Flynn JL. 2017. Analysis of 18FDG PET/CT Imaging as a Tool for Studying Mycobacterium tuberculosis Infection and Treatment in Non-human Primates. J Vis Exp doi:10.3791/56375.

19. Ramos L, Obregon-Henao A, Henao-Tamayo M, Bowen R, Lunney JK, Gonzalez-Juarrero M. 2017. The minipig as an animal model to study Mycobacterium tuberculosis infection and natural transmission. Tuberculosis 106:91-98.

20. Fenaroli F, Repnik U, Xu YT, Johann K, Van Herck S, Dey P, Skjeldal FM, Frei DM, Bagherifam S, Kocere A, Haag R, De Geest BG, Barz M, Russell DG, Griffiths G. 2018. Enhanced Permeability and Retention-like Extravasation of Nanoparticles from the Vasculature into Tuberculosis Granulomas in Zebrafish and Mouse Models. Acs Nano 12:8646-8661.

21. Anonymous. <OECD_Chronic Toxicity Studies.pdf>.

22. Franzblau SG, DeGroote MA, Cho SH, Andries K, Nuermberger E, Orme IM, Mdluli K, Angulo-Barturen I, Dick T, Dartois V, Lenaerts AJ. 2012. Comprehensive analysis of methods used for the evaluation of compounds against Mycobacterium tuberculosis. Tuberculosis (Edinb) 92:453-88.

23. Nuermberger E. 2008. Using animal models to develop new treatments for tuberculosis. Semin Respir Crit Care Med 29:542-51.

24. Fonseca KL, Rodrigues PNS, Olsson IAS, Saraiva M. 2017. Experimental study of tuberculosis: From animal models to complex cell systems and organoids. PLoS Pathog 13:e1006421.

25. Harper J, Skerry C, Davis SL, Tasneen R, Weir M, Kramnik I, Bishai WR, Pomper MG, Nuermberger EL, Jain SK. 2012. Mouse model of necrotic tuberculosis granulomas develops hypoxic lesions. J Infect Dis 205:595-602.

26. Lanoix JP, Lenaerts AJ, Nuermberger EL. 2015. Heterogeneous disease progression and treatment response in a C3HeB/FeJ mouse model of tuberculosis. Dis Model Mech 8:603-10.

27. Irwin SM, Driver E, Lyon E, Schrupp C, Ryan G, Gonzalez-Juarrero M, Basaraba RJ, Nuermberger EL, Lenaerts AJ. 2015. Presence of multiple lesion types with vastly

different microenvironments in C3HeB/FeJ mice following aerosol infection with Mycobacterium tuberculosis. Dis Model Mech 8:591-602.

28. Festing MF. 2010. Inbred strains should replace outbred stocks in toxicology, safety testing, and drug development. Toxicol Pathol 38:681-90.

29. Barczak AK, Domenech P, Boshoff HI, Reed MB, Manca C, Kaplan G, Barry CE, 3rd. 2005. In vivo phenotypic dominance in mouse mixed infections with Mycobacterium tuberculosis clinical isolates. J Infect Dis 192:600-6.

30. Manca C, Tsenova L, Barry CE, 3rd, Bergtold A, Freeman S, Haslett PA, Musser JM, Freedman VH, Kaplan G. 1999. Mycobacterium tuberculosis CDC1551 induces a more vigorous host response in vivo and in vitro, but is not more virulent than other clinical isolates. J Immunol 162:6740-6.

31. Husain AA, Gupta UD, Gupta P, Nayak AR, Chandak NH, Daginawla HF, Singh L, Kashyap RS. 2017. Modelling of cerebral tuberculosis in BALB/c mice using clinical strain from patients with CNS tuberculosis infection. Indian J Med Res 145:833-839.

32. Hwang SA, Kruzel ML, Actor JK. 2017. Oral recombinant human or mouse lactoferrin reduces Mycobacterium tuberculosis TDM induced granulomatous lung pathology. Biochem Cell Biol 95:148-154.

33. Perdomo C, Zedler U, Kuhl AA, Lozza L, Saikali P, Sander LE, Vogelzang A, Kaufmann SH, Kupz A. 2016. Mucosal BCG Vaccination Induces Protective Lung-Resident Memory T Cell Populations against Tuberculosis. MBio 7.

34. Mdluli K, Kaneko T, Upton A. 2015. The tuberculosis drug discovery and development pipeline and emerging drug targets. Cold Spring Harb Perspect Med 5.

35. Weyer K, Falzon D, Jaramillo E. 2018. Towards all-oral and shorter treatment regimens for drug-resistant tuberculosis. Bull World Health Organ 96:667-667A.

36. Dutt M, Khuller GK. 2001. Chemotherapy of Mycobacterium tuberculosis infections in mice with a combination of isoniazid and rifampicin entrapped in Poly (DL-lactide-co-glycolide) microparticles. J Antimicrob Chemother 47:829-35.

37. Tiwari D, Park SW, Essawy MM, Dawadi S, Mason A, Nandakumar M, Zimmerman M, Mina M, Ho HP, Engelhart CA, Ioerger T, Sacchettini JC, Rhee K, Ehrt S, Aldrich CC, Dartois V, Schnappinger D. 2018. Targeting protein biotinylation enhances tuberculosis chemotherapy. Sci Transl Med 10.

38. Das SC, Stewart PJ, Tucker IG. 2018. The respiratory delivery of high dose dry powders. Int J Pharm 550:486-487.

39. Mehta P, Bothiraja C, Kadam S, Pawar A. 2018. Potential of dry powder inhalers for tuberculosis therapy: facts, fidelity and future. Artif Cells Nanomed Biotechnol doi:10.1080/21691401.2018.1513938:1-16.

40. Miranda MS, Rodrigues MT, Domingues RMA, Torrado E, Reis RL, Pedrosa J, Gomes ME. 2018. Exploring inhalable polymeric dry powders for anti-tuberculosis drug delivery. Mater Sci Eng C Mater Biol Appl 93:1090-1103.

41. Diehl KH, Hull R, Morton D, Pfister R, Rabemampianina Y, Smith D, Vidal JM, van de Vorstenbosch C. 2001. A good practice guide to the administration of substances and removal of blood, including routes and volumes. Journal of Applied Toxicology 21:15-23.

42. Jindal HM, Zandi K, Ong KC, Velayuthan RD, Rasid SM, Samudi Raju C, Sekaran SD. 2017. Mechanisms of action and in vivo antibacterial efficacy assessment of five novel hybrid peptides derived from Indolicidin and Ranalexin against Streptococcus pneumoniae. PeerJ 5:e3887.

43. Uranga S, Marinova D, Martin C, Aguilo N. 2016. Protective Efficacy and Pulmonary Immune Response Following Subcutaneous and Intranasal BCG Administration in Mice. Jove-Journal of Visualized Experiments doi:ARTN e5444010.3791/54440.

44. OECD. 2008. Test No. 425: Acute Oral Toxicity: Up-and-Down Procedure doi:doi:https://doi.org/10.1787/9789264071049-en.

45. Yarlagadda V, Konai MM, Manjunath GB, Prakash RG, Mani B, Paramanandham K, Ranjan SB, Ravikumar R, Chakraborty SP, Roy S, Haldar J. 2015. In vivo antibacterial activity and pharmacological properties of the membrane-active glycopeptide antibiotic YV11455. Int J Antimicrob Agents 45:627-34.

46. Su SH, Chen HI, Jen CJJ. 2001. C57BL/6 and BALB/c bronchoalveolar macrophages respond differently to exercise. Journal of Immunology 167:5084-5091.

47. Cramer NP, Xu X, Christensen C, Bierman A, Tankersley CG, Galdzicki Z. 2015. Strain variation in the adaptation of C57Bl6 and BALBc mice to chronic hypobaric hypoxia. Physiol Behav 143:158-65.

48. Razzoli M, Carboni L, Andreoli M, Ballottari A, Arban R. 2011. Different susceptibility to social defeat stress of BalbC and C57BL6/J mice. Behavioural Brain Research 216:100-108.

49. del Castillo-Santaella T, Cebrian R, Maqueda M, Galvez-Ruiz J, Maldonado-Valderrama J. 2018. Assessing in vitro digestibility of food biopreservative AS-48. Food Chemistry 246:249-257.

50. Gonzalez-Juarrero M, Woolhiser LK, Brooks E, DeGroote MA, Lenaerts AJ. 2012. Mouse model for efficacy testing of antituberculosis agents via intrapulmonary delivery. Antimicrob Agents Chemother 56:3957-9.

51. Anonymous. <142-18.pdf>.

52. Plinke C, Walter K, Aly S, Ehlers S, Niemann S. 2011. Mycobacterium tuberculosis embB codon 306 mutations confer moderately increased resistance to ethambutol in vitro and in vivo. Antimicrob Agents Chemother 55:2891-6.

53. Lopez FE, Vincent PA, Zenoff AM, Salomon RA, Farias RN. 2007. Efficacy of microcin J25 in biomatrices and in a mouse model of Salmonella infection. J Antimicrob Chemother 59:676-80.

54. Rullas J, Garcia JI, Beltran M, Cardona PJ, Caceres N, Garcia-Bustos JF, Angulo-Barturen I. 2010. Fast standardized therapeutic-efficacy assay for drug discovery against tuberculosis. Antimicrob Agents Chemother 54:2262-4.

55. Dartois V. 2014. The path of anti-tuberculosis drugs: from blood to lesions to mycobacterial cells. Nat Rev Microbiol 12:159-67.

56. Banos A, Ariza JJ, Nunez C, Gil-Martinez L, Garcia-Lopez JD, Martinez-Bueno M, Valdivia E. 2019. Effects of Enterococcus faecalis UGRA10 and the enterocin AS-48 against the fish pathogen Lactococcus garvieae. Studies in vitro and in vivo. Food Microbiol 77:69-77.

57. Ohashi K, Kabasawa T, Ozeki T, Okada H. 2009. One-step preparation of rifampicin/poly(lactic-co-glycolic acid) nanoparticle-containing mannitol microspheres using a four-fluid nozzle spray drier for inhalation therapy of tuberculosis. Journal of Controlled Release 135:19-24.

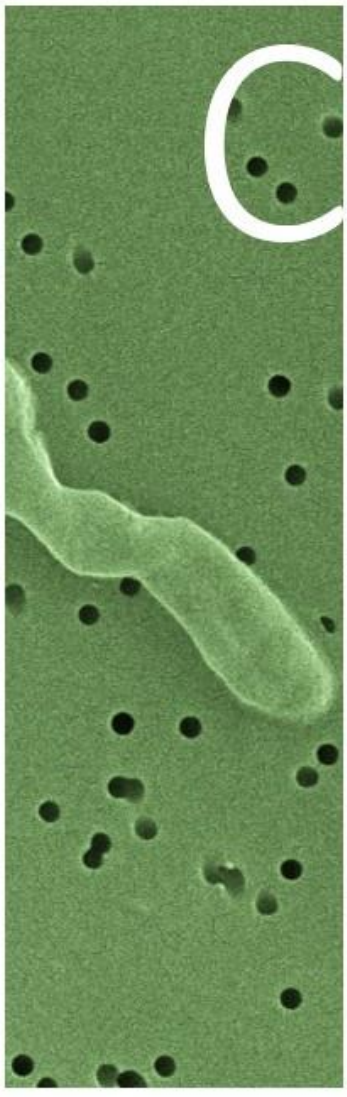

Conclusions

CONCLUSIONS

- Bacteriocin AS-48 shows bactericidal activity against *M. tuberculosis* complex, either laboratory and reference strains or clinical isolates.
- AS-48 has a variable activity against non-tuberculous mycobacteria.
- Synergy relationship between AS-48 and lysozyme.
- The modified bacteriocins from the wild type AS-48 have a lesser or equal bactericide activity against *M. tuberculosis* than the wild type.
- Porins mutants of *M. smegmatis* do not exhibit synergy between AS-48 and lysozyme, only the double porin mutant, ML10, has a synergy FICI of 0.5.
- Ethambutol and AS-48 exhibit a great synergy against *M. tuberculosis*.
- Antimicrobial concentrations of AS-48 are not cytotoxic in human and murine macrophage cell lines.
- Ethambutol and AS-48 also have a synergy activity in the infected macrophages against *M. tuberculosis*.
- *M. tuberculosis* exhibits more morphological damage with a synergistic combination than when AS-48 is acting alone.
- The activity of AS-48 is not mediated by efflux pumps.
- AS-48 is capable to depolarize the membrane potential, both, time and concentration dependent.
- AS-48 is targeting the mycobacterial membrane.

- The ratio of expression of Toxin-Antitoxin genes is 2-5 times higher than non-treated cultures.
- The activity of AS-48 also affect the mobility of DNA, thus the gene expression could be altered.
- AS-48 is a multitarget drug so, generate a resistant mutant is less probable than a unique-target drug. We have not been able to generate a resistant *M. tuberculosis* mutant against AS-48.
- The toxicity of AS in *in vivo* mice models is higher than the toxicity reached *in vitro*.
- BALB/c mice are less sensitive to AS-48 than C57BL/6, resulting hepatotoxic for this mice strain.
- The combined treatment of AS-48 and ethambutol is less toxic *in vivo* than the same concentration of AS-48 alone.
- The different treatments with AS-48 alone or in combination with subinhibitory concentrations of ethambutol do not reduce significantly bacteria burden in infected mice, treated by the intraperitoneal route.

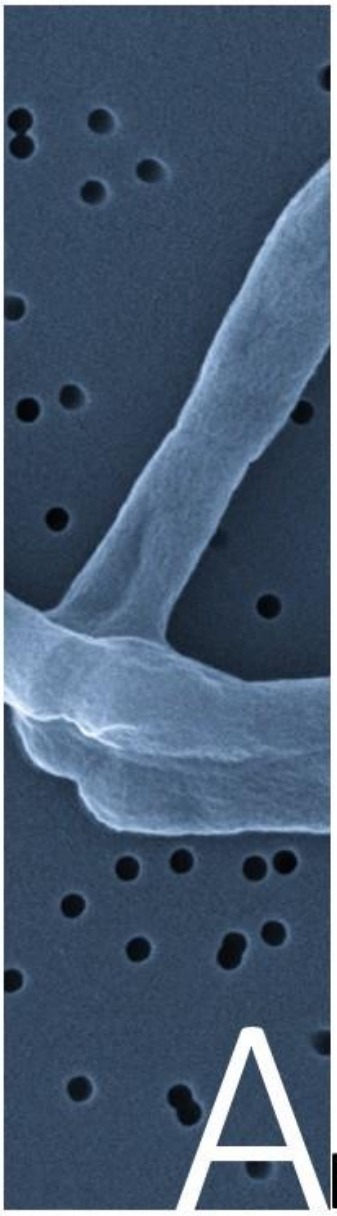

Annexes

ANNEX I: AS-48 PURIFICATION

The circular bacteriocin, AS-48, was purified according to Cebrian *et al*. (1). Briefly, 5L of reconstituted Esprion 300 (4% E-300, DMV Int., Veghel, Netherland) medium plus 1% glucose (E-300-G) were inoculated at 8% with a BHI (DIFCO) *Enterococcus faecalis* UGRA10 pre-inoculum. The culture was grown at 30˚C with shaking and controlled pH of 6.55 during 18-20h.

Once the culture was growth, it was directly mixed with reconstituted Sephadex CM-25 in 1:10 (v/v) proportion for ionic interchange purification. Matrix and culture were mixed for 1h and them the CM-25 was disposed of in a chromatography column. The matrix was washed with 1L of distillate water, and then, the peptide was eluted with 1L of NaCl 2M. 50ml fractions were collected and their antimicrobial activity tested against *Enterococcus faecalis* JH2-2.

Active fractions were concentrated and desalted using reverse-phase C-18 open columns. For this, 4 g of C-18 were reconstituted in an organic solvent (solvent B, Isopropanol: Acetonitrile, 2:1, 0.1% TFA) and equilibrated in the aqueous solvent (solvent A, distilled water +0.1% TFA). In this condition, the active fractions were applied to the column. The NaCl was removed from the column washing it with 5 column volumes, and the peptide was eluted in a solvent B gradient (20%, 40%, 60%, and 80%). The active fraction (60%) was lyophilized, resuspended in solvent A and purified to homogeneity by reverse phase-HPLC chromatography. The equipment includes a chromatographic (Agilent 1100 Series) with a degassing (G123779A), a manual injector (61328B), a quaternary bomb of high pressure (G1311A) and a wavelength detector. Semipreparative scale purification was performed using a C18 Vydac 218TP510 (10x250mm, 300Å; The Separation Group, Hesperia) column. The sample was load, and the peptide was eluted with a lineal gradient of solvent B in solvent A from 40% to 805 in 25 min at 3mL/min. The desired AS-48 peak was manually collected, lyophilized and stored until use.

REFERENCE

1. Cebrian R, Martinez-Bueno M, Valdivia E, Albert A, Maqueda M, Sanchez-Barrena MJ. 2015. The bacteriocin AS-48 requires dimer dissociation followed by hydrophobic interactions with the membrane for antibacterial activity. J Struct Biol 190:162-72.

ANNEX II: SYNERGY BETWEEN CIRCULAR BACTERIOCIN AS-48 AND ETHAMBUTOL AGAINST MYCOBACTERIUM TUBERCULOSIS

As part of this work we have published one paper referred to the first part of this thesis.

The title of the publication is: *Synergy between Circular Bacteriocin AS-48 and Ethambutol against Mycobacterium tuberculosis*. It was accepted the 26th of June of 2018 and published in the number of September 2018 in the journal of Antimicrobial Agents of Chemotherapy.

ANNEX III: THE EU APPROVED ANTIMALARIAL PYRONARIDINE SHOWS ANTITUBERCULAR ACTIVITY AND SYNERGY WITH RIFAMPICIN, TARGETING RNA POLYMERASE

During the period of developing this work I have collaborated performing some experiments detailed in the following paper: *The EU approved antimalarial pyronaridine shows antitubercular activity and synergy with rifampicin, targeting RNA polymerase*.

I performed some experiments of synergy between rifampicin and pyronaridine in vitro against *M. tuberculosis* and analysed the FICI results. This work was accepted the 5th of August of 2018 and published in the journal Tuberculosis in September of 2018.

AMERICAN SOCIETY FOR MICROBIOLOGY | Antimicrobial Agents and Chemotherapy®

MECHANISMS OF ACTION: PHYSIOLOGICAL EFFECTS

Synergy between Circular Bacteriocin AS-48 and Ethambutol against *Mycobacterium tuberculosis*

Clara Aguilar-Pérez,[a,b,c] Begoña Gracia,[a,b,c,d] Liliana Rodrigues,[a,b,c,d,e*] Asunción Vitoria,[a,b,c,d,h] Rubén Cebrián,[f*] Nathalie Deboosère,[g] Ok-ryul Song,[g] Priscille Brodin,[g] Mercedes Maqueda,[f] José A. Aínsa[a,b,c,d]

[a]Departamento de Microbiología, Facultad de Medicina, Universidad de Zaragoza, Zaragoza, Spain
[b]Instituto de Biocomputacion y Fisica de Sistemas Complejos, Universidad de Zaragoza, Zaragoza, Spain
[c]Instituto de Investigación Sanitaria de Aragón, Zaragoza, Spain
[d]CIBER de Enfermedades Respiratorias, Instituto de Salud Carlos III, Madrid, Spain
[e]Fundación Agencia Aragonesa para la Investigación y el Desarrollo, Zaragoza, Spain
[f]Departamento de Microbiología, Facultad de Ciencias, Universidad de Granada, Granada, Spain
[g]Université de Lille, CNRS, INSERM, CHU Lille, Institut Pasteur de Lille, U1019, UMR 8204, Center for Infection and Immunity of Lille, Lille, France
[h]Grupo de Estudio de Infecciones por Micobacterias de la SEIMC, Madrid, Spain

ABSTRACT The increasing incidence of multidrug-resistant *Mycobacterium tuberculosis* strains and the very few drugs available for treatment are promoting the discovery and development of new molecules that could help in the control of this disease. Bacteriocin AS-48 is an antibacterial peptide produced by *Enterococcus faecalis* and is active against several Gram-positive bacteria. We have found that AS-48 was active against *Mycobacterium tuberculosis*, including H37Rv and other reference and clinical strains, and also against some nontuberculous clinical mycobacterial species. The combination of AS-48 with either lysozyme or ethambutol (commonly used in the treatment of drug-susceptible tuberculosis) increased the antituberculosis action of AS-48, showing a synergic interaction. Under these conditions, AS-48 exhibits a MIC close to some MICs of the first-line antituberculosis agents. The inhibitory activity of AS-48 and its synergistic combination with ethambutol were also observed on *M. tuberculosis*-infected macrophages. Finally, AS-48 did not show any cytotoxicity against THP-1, MHS, and J774.2 macrophage cell lines at concentrations close to its MIC. In summary, bacteriocin AS-48 has interesting antimycobacterial activity *in vitro* and low cytotoxicity, so further studies *in vivo* will contribute to its development as a potential additional drug for antituberculosis therapy.

KEYWORDS AS-48, antimicrobial peptides, antituberculosis activity, synergism, antimycobacterial agents, bacteriocins, *Mycobacterium tuberculosis*, intracellular infection

Mycobacterium tuberculosis is the causal agent of tuberculosis, a disease that mainly affects the lungs and was responsible for 1.6 million deaths in 2016; it is the infectious disease with the highest mortality rate (1). *M. tuberculosis* is an intracellular pathogen residing in pulmonary macrophages within granulomas, where it is mostly kept in latent forms, the host defense mechanism against this pathogen. Infection progresses into active disease when the host immune system is suppressed and the granulomas cannot contain the bacilli. In this way, coinfection with HIV in tuberculosis patients is one of the key factors behind the increase in the incidence of tuberculosis, predominantly in countries where both diseases are endemic.

Tuberculosis is a curable disease, where the active forms are generally susceptible to diverse antimicrobials, such as the first-line drugs (isoniazid, pyrazinamide, ethambutol [EMB], rifampin, and streptomycin), which are prescribed as standard treatment for

Received 22 February 2018 **Returned for modification** 15 May 2018 **Accepted** 26 June 2018

Accepted manuscript posted online 9 July 2018

Citation Aguilar-Pérez C, Gracia B, Rodrigues L, Vitoria A, Cebrián R, Deboosère N, Song O-R, Brodin P, Maqueda M, Aínsa JA. 2018. Synergy between circular bacteriocin AS-48 and ethambutol against *Mycobacterium tuberculosis*. Antimicrob Agents Chemother 62:e00359-18. https://doi.org/10.1128/AAC.00359-18.

Address correspondence to Clara Aguilar-Pérez, clara.a@unizar.es, or José A. Aínsa, ainsa@unizar.es.

* Present address: Liliana Rodrigues, Global Health and Tropical Medicine, Unit of Medical Microbiology, Instituto de Higiene e Medicina Tropical, Universidade Nova de Lisboa, Lisbon, Portugal; Rubén Cebrián, Department of Molecular Genetics, University of Groningen, Groningen, The Netherlands.

tuberculosis. However, the huge incidence of multidrug-resistant (MDR) and extensively drug-resistant (XDR) *M. tuberculosis* strains (which are not responsive to standard treatment and need to be treated with second-line drugs such as aminoglycosides and fluoroquinolones, among others) has exacerbated the need for developing alternatives for an effective treatment. During 2016, about 490,000 cases of tuberculosis were caused by MDR strains, and 6.2% of them were caused by XDR strains (1).

In the context of drug resistance, not only in respect to tuberculosis but also in connection with many other bacterial pathogens, antimicrobial peptides (AMPs) may have great potential for use in treatment, either by themselves or in combination with other antimicrobials. AMPs are produced by prokaryotic or eukaryotic organisms. They are peptides and proteins, mostly cationic and with an amphiphilic nature, that are ribosomally synthesized. Most of the bacterial lineages can produce AMPs, called bacteriocins, that exhibit antimicrobial activity primarily against those species that are phylogenetically closely related with the producer species. Recently, a classification system of bacteriocins (2) was accepted whereby class I (less than 10 kDa) encompasses all the peptides that undergo enzymatic modification during biosynthesis, providing molecules with uncommon amino acids and structures that have an impact on their properties. Thus, there are lanthipeptides (class Ia), head-to-tail cyclized peptides (class Ib), sactibiotics that are sulfur–α-carbon-containing peptides (class Ic), and linear azol(in)e-containing peptides (class Id). Class II (less than 10 kDa) includes unmodified bacteriocins that do not require enzymes for their maturation; finally, class III consists of heat-labile bacteriocins without modifications that are larger than 10 kDa and with bacteriolytic or nonlytic mechanisms of action.

The prototype of the ribosomally synthesized and posttranslationally modified peptides (RiPPs) is the bacteriocin AS-48, which undergoes head-to-tail cyclization to render a circular molecule (class Ib). All of these cyclized peptides are synthesized as a linear precursor containing a leader sequence with a high molecular weight, and then they are posttranslationally modified. AS-48 is a 70-amino-acid, alpha-helical membrane-interacting peptide produced by *Enterococcus faecalis* that displays a broad antimicrobial spectrum against Gram-positive and Gram-negative bacteria. The mechanism of AS-48 antibacterial activity involves the accumulation of positively charged molecules at the membrane surface, leading to a disruption of the membrane potential (3, 4). The antimicrobial activity of AS-48 has already been proven in food products (5) and has been observed against numerous Gram-positive bacteria, including *Listeria monocytogenes* and enterotoxic *Staphylococcus aureus* (6).

Most of the studies on bacteriocins focus on their potential applications as food preservatives, and only a few of studies are focused on their potential biomedical applications and, specifically, antimicrobial or antituberculosis activity. Activity of nisin and lacticin 3147 has been shown against *Mycobacterium* strains such as *Mycobacterium kansasii*, *Mycobacterium avium* subsp. *paratuberculosis*, and *M. tuberculosis* H37Ra; in particular, lacticin 3147 exhibits greater antimycobacterial activity than nisin (7). The antimycobacterial activities of several bacteriocins were found to be similar to the activity of rifampin against *M. tuberculosis* (8).

In this work, we have investigated the antituberculosis activity of bacteriocin AS-48 alone and in combination with lysozyme and first-line drugs used in the treatment of tuberculosis, both in *in vitro* cultures and also in *M. tuberculosis*-infected macrophages. We report that AS-48 is active against *M. tuberculosis* and other mycobacterial species and synergizes with EMB. Bacteriocin AS-48 was not found to be cytotoxic at the doses required for inhibiting mycobacterial growth. Moreover, AS-48 caused depolarization of mycobacterial membranes and altered morphology of the bacilli. In conclusion, we demonstrate that bacteriocin AS-48 has positive features supporting its potential role in tuberculosis treatment.

RESULTS

Bacteriocin AS-48 showed bactericidal activity against *M. tuberculosis* complex. The activity of AS-48 was determined against several mycobacteria, including *M.*

TABLE 1 Mycobacterial strains used and MICs of AS-48 and lysozyme

Strain	MIC (μg/ml)		Source or reference
	AS-48	Lysozyme	
H37Rv	32–64	200–400	37
H37Ra	32	400	38
BCG Pasteur 1173	32	200–400	Laboratory collection
Mt103	64	400	39
CDC1551	64	400	40
GC 1237	16–32	400	41
H37Rv *phoP*	64	400	42
SS18b	32–64	>1,200	43
M. smegmatis mc²155[a]	64	400	44

[a]Fast-growing mycobacteria.

tuberculosis complex reference strains, clinical isolates, and other clinically relevant nontuberculous mycobacteria (NTM).

First, we tested AS-48 activity against *M. tuberculosis* complex clinical and reference strains. The MICs of AS-48 were quite uniform, between 16 and 64 μg/ml (Table 1; see also Table S1 in the supplemental material), and there was no difference in the MICs of AS-48 between active replicating cells and the nonreplicative strain SS18b of *M. tuberculosis*. We observed a similar MIC of AS-48 for *Mycobacterium smegmatis* and other NTM (see below).

The kill kinetics indicated that bacteriocin AS-48 is bactericidal since concentrations equal to the MIC and 2× MIC were capable of reducing the number of live bacteria in a culture of *M. tuberculosis* H37Rv. First, after 1 or 2 days of treatment, the number of CFU was reduced by almost 2 logs in comparison with levels in untreated cultures. After 6 days of treatment with 128 or 64 μg/ml of AS-48, no live bacteria could be detected (Fig. 1), and this was found to be statistically significant by a linear regression test (*P* values of 0.0005 and <0.0001, respectively).

Synergy between lysozyme and nisin was previously observed in Gram-positive bacteria (9, 10). Similarly, we have observed that the presence of lysozyme resulted in an increase in *M. tuberculosis* susceptibility to AS-48. First, we tested lysozyme activity against mycobacterial strains and found that different mycobacterial strains or species have more variability in the MICs of lysozyme (Tables 1 and S1) than the MIC obtained for AS-48. Notably, the nonreplicating strain SS18b of *M. tuberculosis* was found to be greatly resistant to lysozyme. Second, we tested the susceptibility of mycobacterial strains to AS-48 in the presence of lysozyme (Table 2). We found that, for most strains, susceptibility to AS-48 greatly increased (between 64- and 16-fold) in the presence of subinhibitory concentrations of lysozyme. In order to quantify the effect of lysozyme on growth inhibition by AS-48, we calculated the fractional inhibitory concentration index (FICI). The results of all strains assayed are indicated in Table 2. For reference strains,

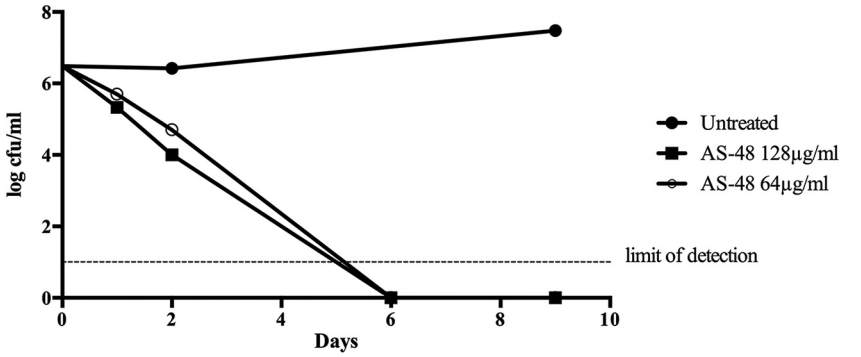

FIG 1 Kill kinetics of bacteriocin AS-48 at 64 and 128 μg/ml against cultures of *M. tuberculosis* H37Rv. Untreated cultures were used as controls.

TABLE 2 MIC of AS-48 in the presence of different concentrations of lysozyme and the fractional inhibitory concentration index

Strain	MIC of AS-48 (μg/ml) at the indicated lysozyme concn (μg/ml)						FICI[a]
	400	200	100	50	25	12.5	
H37Rv	<0.03125	0.0625	1	4	>32		0.25
H37Ra	<0.03125	2	4	16	>32		0.375
BCG Pasteur		<0.125	2	16	>32		0.3125
Mt103	<0.125	4	32	32	64	>64	0.5625
CDC1551		<0.125	16	32	64	>64	0.5
GC 1237	<0.03125	4	8	>32			0.375
H37Rv *phoP*		<0.125	8	32	64	>64	0.375
M. smegmatis mc²155	<0.125	32	64	>64			1
HMS 1500		<0.03125	8	>32			0.375
HMS 1531			<0.03125	0.5	4	8	0.375
HMS 1536		<0.03125	8	>32			0.5
HMS 1546			<0.03125	2	8	>32	0.5
HMS 1548	<0.03125	2	16	>32			0.5312
HMS 1292			<0.03125	4	16	>32	0.3125
HMS 1278		<0.03125	2	8	>32		0.5

[a]The fractional inhibitory index (FICI) is calculated as follows: $FICI = (MIC_{AS\text{-}48\ in\ the\ presence\ of\ lysozyme}/MIC_{AS\text{-}48\ alone}) + (MIC_{lysozyme\ in\ the\ presence\ of\ AS\text{-}48}/MIC_{lysozyme\ alone})$. An FICI of ≤0.5 indicates synergism, a value of 0.5 to 4 indicates no interaction, and a value of >4.0, indicates antagonism.

maximum synergism was observed for H37Rv and, to a lesser extent, for *Mycobacterium bovis* BCG, H37Ra, H37Rv *phoP*, GC 1237 (Beijing genotype), CDC1551, and Mt103. Although technically synergism is defined as an FICI of ≤0.5, we consider the strains Mt103 and HMS 1548, which resulted in FICIs slightly over 0.5, to have weak synergistic interactions. The synergy effect occurred in all of the *M. tuberculosis* complex strains analyzed.

Bacteriocin AS-48 has variable activity against NTM. In most NTM, the MIC of AS-48 is the same as that for *M. tuberculosis* (i.e., 64 μg/ml), with the exception of slow-growing mycobacterial species such as *Mycobacterium xenopi*, *Mycobacterium lentiflavum*, and *Mycobacterium gordonae*. For *M. xenopi* and *M. gordonae*, the value of the MIC of AS-48 was <2 μg/ml, and the MIC of lysozyme was <9.375 μg/ml. In contrast, the MIC of AS-48 against *M. lentiflavum* was higher than 256 μg/ml, and the MIC of lysozyme was also higher than 1,200 μg/ml, indicating that this mycobacterial species is less susceptible to AS-48 and to lysozyme (Table S1).

Synergy test between AS-48 and first-line antituberculosis drugs. AS-48 has been tested also in combination with the main first-line antituberculosis drugs, EMB, isoniazid, streptomycin, and rifampin. The combination of AS-48 and EMB was the only one to present a synergistic relation, with an FICI of 0.09375, which was the lowest FICI obtained in all the assays (Fig. 2).

Is AS-48 targeting the mycobacterial membrane? In order to explore whether bacteriocin AS-48 could be targeting the mycobacterial membrane, we carried out experiments for ethidium bromide accumulation, and we determined the ability of AS-48 for depolarizing the mycobacterial membrane.

It is assumed that AS-48 forms pores in the membrane (11), thus making the cell more permeable to compounds such as ethidium bromide. Therefore, in an ethidium bromide accumulation assay, we would expect that the fluorescence detected would be higher in the presence of AS-48, reflecting the increased accumulation of ethidium bromide as a result of the effect of AS-48 on the bacterial membrane. We compared the effect of AS-48 with that of verapamil, a well-known efflux inhibitor (12), which produces an increase in the accumulation of ethidium bromide. In the presence of AS-48, fluorescence due to accumulated ethidium bromide increased in a concentration-dependent manner although the kinetics of accumulation was rather distinct from that observed with verapamil (Fig. 3).

The determination of membrane potential was carried out using a BacLight kit according to the manufacturer's instructions using *M. smegmatis* mc²155 and *M. bovis*

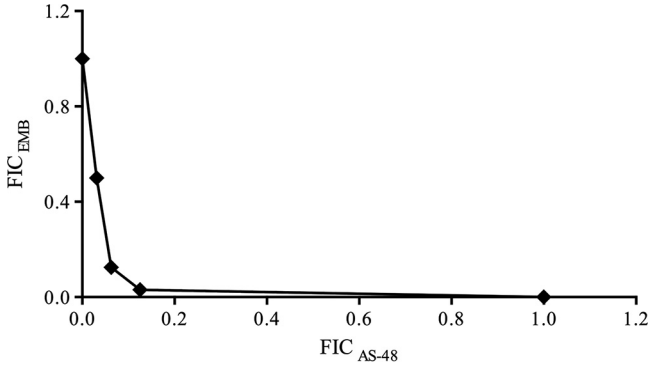

FIG 2 Synergism between AS-48 and EMB in *M. tuberculosis* H37Rv. For the reference strains CDC1551, Mt103, H37Ra, and H37Rv *phoP*, the plot had the same shape, indicating that synergy between AS-48 and EMB was very similar to that in H37Rv.

BCG cells. In a representative control experiment, in the untreated cells, 3.4% of cells were depolarized, whereas in the cells treated with the protonophore carbonyl cyanide *m*-chlorophenylhydrazone (CCCP), the percentage of depolarized cells was 94.93%. We assessed the effect of AS-48 at several concentrations and for different times of incubation (1 or 24 h). We observed that AS-48 depolarized cells in a concentration-dependent manner, and this effect was much higher in the cells incubated with AS-48 for 24 h than in those tested after 1 h of incubation. Data in Fig. 4 show that the percentage of depolarized cells after 24 h is 67.04% in the presence of 128 μg/ml of AS-48, 26.34% with 64 μg/ml, and 18.68% with 32 μg/ml. Again, this demonstrates that the depolarization of the cells is concentration dependent and increases with time.

Antimicrobial concentrations of AS-48 are not cytotoxic for macrophage cell lines. The cytotoxicity of AS-48 on human and mouse lung macrophage cell lines was carried out by MTT [3-(4,5-dimethyl-2-thiazolyl)-2,5-diphenyl-2H-tetrazolium bromide] and neutral red assays.

In both protocols, >70% cell viability was observed at concentrations of AS-48 below 128 μg/ml, which is considered noncytotoxic according to standard international protocols (13). Even when slight differences in cell viability were observed below 32 μg/ml of AS-48, they were not significant (Fig. 5). We did not observe a concentration-dependent cytotoxic effect in any of the cell lines assayed. At 128 μg/ml, <40% cell viability was observed (Fig. 5) (*P* value of <0.0001).

Lysozyme cytotoxicity was also analyzed, and, as expected, no cytotoxicity was observed in these cell lines. Finally, we assayed cytotoxicity of some of the synergistic combinations of AS-48 and lysozyme that showed great antimicrobial effect in *M.*

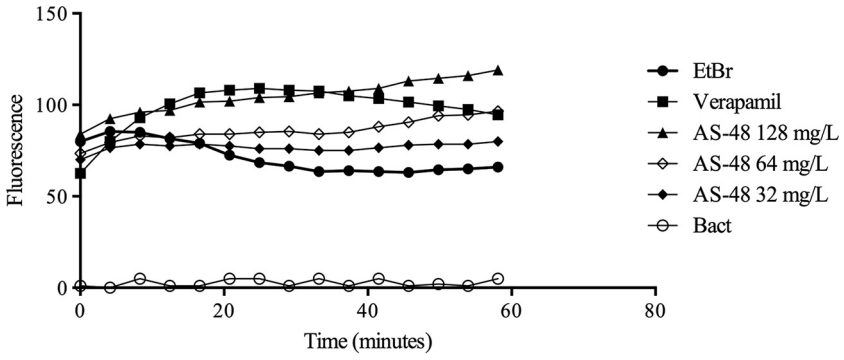

FIG 3 Assay of ethidium bromide (EtBr) accumulation in *M. smegmatis* cells in the presence of different concentrations of AS-48. VP, verapamil, used as control for the maximum accumulation of ethidium bromide; Bact, negative control with only a bacterial suspension.

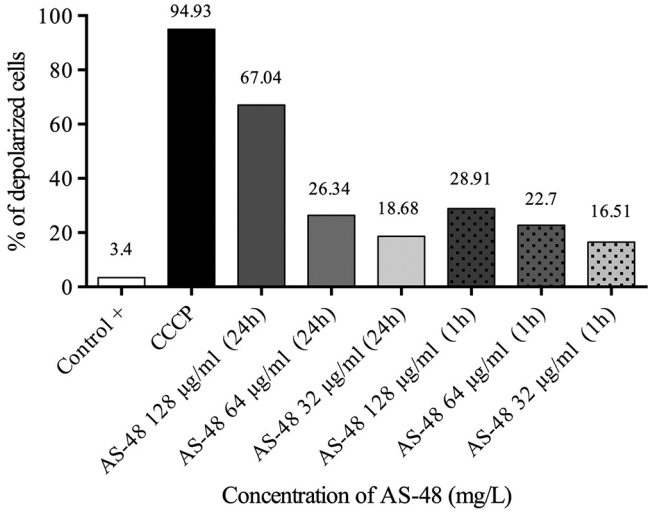

FIG 4 Flow cytometry assay for determination of membrane depolarization. The positive control contained just a bacterial suspension. CCCP, ionophore showing maximum membrane depolarization. The concentration of AS-48 and the time of exposure to AS-48 are shown below each bar.

tuberculosis, and we found that these combinations did not cause any cytotoxic effect (Fig. 5).

Treatment with AS-48 results in morphological changes in *M. tuberculosis*. We treated *M. tuberculosis* cells with AS-48, along with untreated cells as a control, and samples were taken at several time points for microscopic observation. We found that at short time exposures, cells were affected by AS-48 (Fig. 6): the morphology of cells treated with a concentration of AS-48 equal to the MIC after 48 h and 72 h was rougher than that of the control.

Moreover, we assayed the combination of 8 μg/ml of AS-48 with 25 μg/ml of lysozyme and analyzed cells at 24, 48, and 96 h after treatment. When bacterial cells were treated with a synergistic combination of AS-48 and lysozyme, they exhibited greater morphological damage (Fig. 7) than cells treated with AS-48 alone (Fig. 6).

Synergy between EMB and AS-48 in the infected macrophages. In the model of Raw 264.7 cells infected with *M. tuberculosis* H37Rv-green fluorescent protein (GFP), we

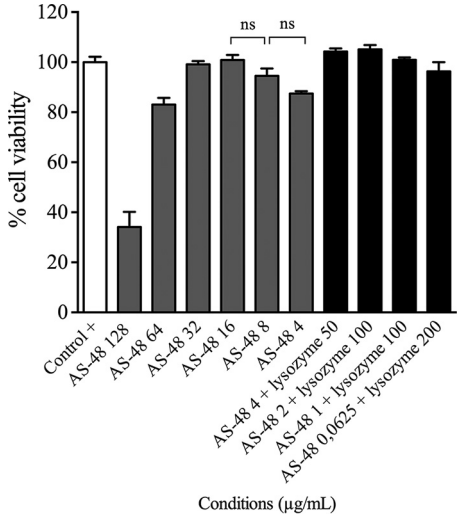

FIG 5 Representative results of the cell viability assays, as determined by neutral red uptake technique in cell cultures of J774.2 murine macrophages. Cell suspensions with no compounds added were used as a positive control. ns, not significant.

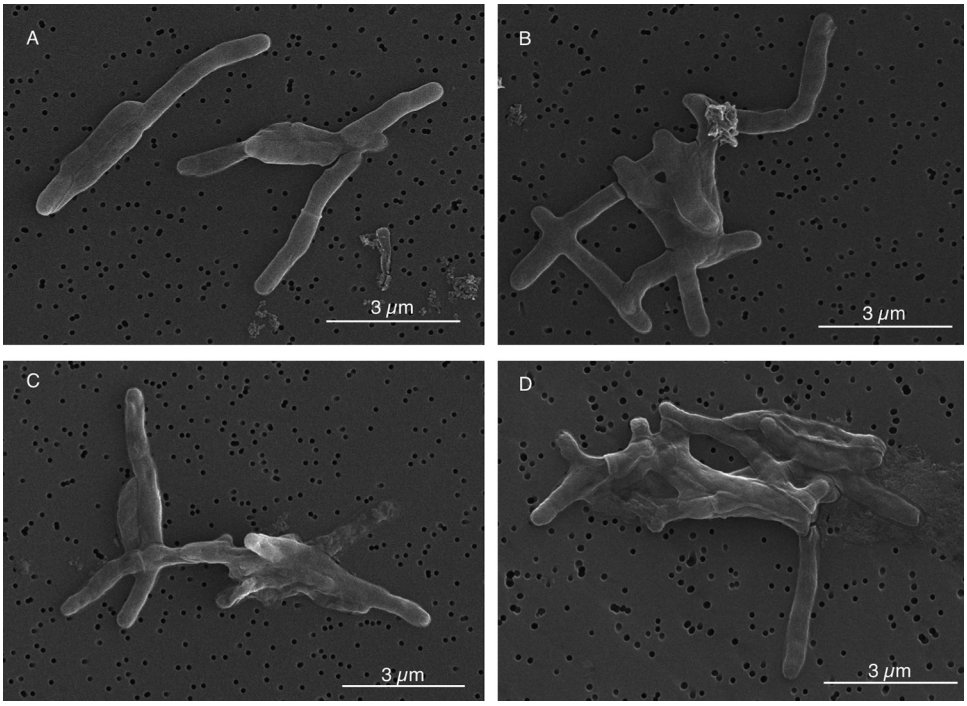

FIG 6 Scanning electron microscopy images of *M. tuberculosis* H37Rv under different conditions. (A and B) Positive control after 48 and 72 h of growth, respectively. (C and D) Cells treated with 64 μg/ml of AS-48 for 48 and 72 h, respectively.

observed low FICI values (Table 3) ranging from 0.5 and 0.18, which is indicative of synergism. These FICI values were similar to those obtained in the *in vitro* antimycobacterial assays. The combination of 2 μg/ml AS-48 and 2 μg/ml EMB resulted in the lowest FICI value. Other combinations also resulted in synergistic FICI values but to a lesser extent (Table 3). The determination of viable bacteria after treatment with EMB and AS-48 resulted in a reduction of CFU counts between 90 and 99.9% in comparison with totals in untreated controls. The efficacy of AS-48 for killing intracellular pathogens was previously proven by Abengózar et al. (14) when they showed the anti-leishmanial activity of AS-48 in Raw 264.7 infected macrophages. Despite the fact that the infection mechanism is different between *Leishmania* and mycobacteria, these experiments show that AS-48 is active against pathogens residing intracellularly in macrophages.

DISCUSSION

During recent years, we have witnessed a decline in the number of deaths and incidence of tuberculosis globally; however, recent reports estimate that 600,000

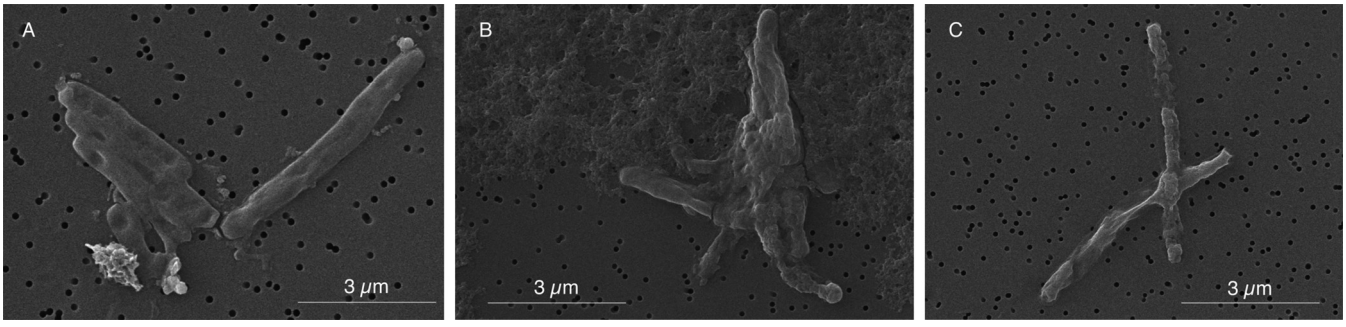

FIG 7 Scanning electron microscopy images of *M. tuberculosis* H37Rv treated with a synergistic combination of 8 μg/ml of AS-48 and 25 μg/ml of lysozyme after treatment for 24 h (A) 48 h (B), and 96 h (C).

TABLE 3 Intracellular MICs and FICs of AS-48 and EMB alone or in combination and FICIs[a]

MIC (μg/ml)		FIC		
AS-48	EMB	AS-48	EMB	FICI[b]
32				
16	0.125	0.5	0.007	0.50
8	0.5	0.25	0.03	0.28
2	2	0.06	0.12	0.18
	16			

[a]Values were determined in Raw 264.7 cells infected with *M. tuberculosis* H37Rv-GFP. EMB, ethambutol.
[b]The fractional inhibitory index (FICI) is calculated as follows: FICI = ($MIC_{AS\text{-}48\ in\ the\ presence\ of\ ethambutol}$/$MIC_{AS\text{-}48\ alone}$) + ($MIC_{ethambutol\ in\ the\ presence\ of\ AS\text{-}48}$/$MIC_{ethambutol\ alone}$). An FICI of ≤0.5 indicates synergism, a value of 0.5 to 4 indicates no interaction, and a value of >4.0 indicates antagonism.

people had MDR or rifampin-resistant (RR) tuberculosis in 2016, which represents a notable increase over the previous year (1). Drug-based treatment for MDR or RR tuberculosis is available only for 20% of these patients, and it is much longer, more expensive, and more toxic than treatment of drug-susceptible tuberculosis. More worryingly, the success rate of MDR tuberculosis treatment is around 50%. Altogether, these facts clearly mean that there is an imperative need for researching new drugs against tuberculosis and, more specifically, against MDR and RR tuberculosis.

The pipeline of new antituberculosis drugs in clinical development includes just seven new compounds (petromanid, delpazolid, SQ-109, GSK-3036656, Q-203, PBTZ-169, and OPC-167832), which, although promising, seems to be insufficient for the treatment of tuberculosis since it requires at least three drugs to be administered simultaneously (15).

Natural or synthetic peptides are emerging as a promising source of novel antimicrobials (16). Currently, there are two AMPs in phase 2 of clinical development (murepavadin and brilacidin) for treating, respectively, *Pseudomonas aeruginosa* and *S. aureus* infections. As with most AMPs, both target the bacterial membrane, an interesting new target for treating persistent infections such as tuberculosis (17). Other membrane-targeting compounds have been shown to be effective *in vitro* against *Clostridium difficile* (18). The interest in the possible application of AMPs in tuberculosis treatment has arisen since it was demonstrated that a high proportion of AMPs active against *P. aeruginosa* also showed activity against *M. tuberculosis* (19). Recently, the activity of antimicrobial peptides against several species of mycobacteria has been reviewed (20).

Bacteriocins are AMPs produced by certain genera of bacteria, such as lactic acid bacteria. Previously, antimicrobial activity of bacteriocin AS-48 has been reported (4). In this study, we report the activity of bacteriocin AS-48 against *M. tuberculosis*.

Susceptibility of *M. tuberculosis* strains to bacteriocin AS-48 ranged from 16 to 64 μg/ml, including reference strains and several clinical isolates of *M. tuberculosis* selected by their different spoligotype and restriction fragment length polymorphism (RFLP) profiles. We found that AS-48 is bactericidal against *M. tuberculosis*. Several other bacteriocins have been reported as effective against *M. tuberculosis* in *in vitro* assays (7, 21–23): colistin has a MIC of 16 μg/ml (24), and nisin showed a MIC of >60 μg/ml against *M. tuberculosis* H37Ra (7). The authors described variants of nisin with an enhanced antimicrobial activity (22) against *M. tuberculosis* as well as other naturally occurring bacteriocins such as lacticin 3147 (MIC_{90} of 7.5 μg/ml) (7). Bacteriocins capable of strongly inhibiting growth of *M. tuberculosis* at a concentration similar to that of rifampin have also been described (8).

The success in the improvement of antituberculosis activity of nisin derivatives (22) prompted us to explore whether variants of AS-48 (altered in residues important for maturation, conformation stability, etc.) could have reduced MICs in comparison with the MIC of wild-type AS-48. However, none of these variants resulted in a significant change of their MICs against *M. tuberculosis* (data not shown), similar to what has been described for other bacterial species (4).

We have also explored susceptibility of other mycobacterial species to AS-48 and

found that for some species (*M. smegmatis*, *Mycobacterium fortuitum*, and *Mycobacterium mucogenicum*, three fast-growing mycobacteria) the MIC of AS-48 did not change significantly from that of *M. tuberculosis*. Carroll et al. (22) also described a rather uniform susceptibility of nisin derivatives between *M. tuberculosis*, *M. kansasii*, and *M. avium*. For other mycobacterial species (slow-growing and chromogenic species), however, we obtained either very low MICs (<2 μg/ml for *M. xenopi* and *Mycobacterium gordonae*), or we could not detect any inhibition of growth up to 256 μg/ml (*M. lentiflavum*).

Lysozyme is an enzyme present in respiratory tract secretions as part of the body's defense mechanisms against microbes. It has been reported that the combination of lysozyme and bacteriocins such as nisin results in a synergistic effect against many bacterial pathogens such as *C. difficile* (25). This synergistic effect of lysozyme has also been described for AS-48 (10). Lysozyme acting on the cell wall could facilitate the access of AS-48 into the bacteria and increase its bactericidal effect. Through synergy tests, we have found that AS-48 strongly synergizes with lysozyme, as has been reported for other bacterial species (10).

From the early dates of antituberculosis treatment, it became evident that monotherapy results in the selection of drug-resistant strains, so a combination therapy was established as a gold standard for antituberculosis treatment, with decreased probabilities to develop resistance. Thus, for any new antituberculosis agent, it is interesting to investigate not only its own antimicrobial activity but also its interactions with other drugs in use against tuberculosis. We have investigated the interactions between AS-48 and first-line antituberculosis drugs by using a checkerboard assay, considered an accurate drug combination analysis method (26) that has been used for demonstrating synergism of drugs and drug candidates in *M. tuberculosis* (27, 28). We found that there is synergism between AS-48 and EMB. In fact, the synergism between AS-48 and EMB was stronger than that of AS-48 and lysozyme. We can hypothesize that EMB, by inhibiting biosynthesis of arabinogalactan in the cell wall, could facilitate the access of AS-48 to its potential target, the mycobacterial membrane. The work by Kalita et al. (29) reported synergism between the antimicrobial human neutrophil peptide 1 (HNP-1) and the antituberculosis drugs isoniazid and rifampin and, hence, proposed the use of this AMP as an adjuvant in antituberculosis chemotherapy.

We conducted two experiments aimed at investigating the potential effect of AS-48 on the cell membrane. On the one hand, by determining the proportion of depolarized cells after AS-48 treatment, we found that this effect was both concentration and time dependent. On the other hand, in ethidium bromide accumulation assays, we monitored a time course increase in fluorescence and also an AS-48 concentration-dependent effect. Thus, we have demonstrated by using two independent methods that AS-48 acts on mycobacterial membranes.

In the intracellular *M. tuberculosis* growth assays in macrophages, the combination of AS-48 and EMB readily showed strong synergism, and the FICI values obtained were similar to the ones found in *in vitro* cultures. However, when we tested the interaction between AS-48 and lysozyme in the intracellular model of infection, no synergistic effect was observed under any of the conditions tested, in contrast with what we have observed in *in vitro* cultures. We can speculate either that lysozyme could not get inside the macrophages and thus could not reach the intracellular bacteria residing in the phagosome or that it could have been degraded by the macrophage.

In summary, we have reported here the antituberculosis activity *in vitro* of circular bacteriocin AS-48 on both extracellular and intracellular bacteria. Interestingly, we have found that in both systems, AS-48 strongly synergizes with EMB, hence opening the way to further explore the interaction of other AMPs with antituberculosis drugs and their future potential use as adjuvants of current antituberculosis treatments or as part of a new, alternative therapeutic regimen.

MATERIALS AND METHODS

Bacterial strains and culture conditions. Mycobacterial strains used in this work for *in vitro* tests are listed in Table 1 (see also Table S1 in the supplemental material). All strains were cultured in Middlebrook 7H9 medium (Difco) supplemented with 10% albumin-dextrose-catalase (ADC) (BD) and 0.05% Tween 80. For drug susceptibility testing, Tween 80 was replaced by 0.5% glycerol. Cultures were incubated at 37°C in 25-cm^2 flasks. Cultures on solid medium were performed in Middlebrook 7H10 agar (Difco) supplemented with 10% ADC and 0.05% Tween 80.

For infection assays, a recombinant strain of *M. tuberculosis* H37Rv (ATCC 27294) constitutively expressing a green fluorescent protein (H37Rv-GFP) was used as a reporter for the intracellular mycobacterial replication assay (30). This strain was grown in Middlebrook 7H9 medium supplemented with 10% oleic acid-albumin-dextrose-catalase (OADC; Difco), 0.05% Tween 80 (Sigma-Aldrich), 0.5% glycerol (Euromedex), and 50 μg/ml hygromycin B (Invitrogen). Cultures were maintained at 37°C under static conditions for up to 14 days to reach the exponential phase of bacterial growth before being used for the intracellular mycobacterial replication assay.

Cell cultures. The following cell lines were used: murine macrophages MHS (Health Protection Agency [HPA] Culture Collections 95090612), J774.2 (European Collection of Authenticated Cell Cultures [ECACC] 85011428), Raw 264.7 (TIB-71), and human monocytes THP-1 (ECACC 88081201). MHS cells were cultured in Dulbecco's modified Eagle's medium (DMEM), and the rest were cultivated in RPMI 1640 medium with GlutaMAX (Gibco) and containing 10% heat-inactivated fetal bovine serum (FBS; Gibco). When cells were to be used for cytotoxicity assays, antibiotics (penicillin, streptomycin, and ciprofloxacin) were added to cell precultures. Cells were cultured in a controlled 5% CO_2 atmosphere at 37°C.

MIC. Serial broth microdilutions were made to determine the MIC of AS-48, which was purified to homogeneity from the *E. faecalis* UGRA10 strain (31) according to Ananou et al. (32), lysozyme (L3790; Sigma-Aldrich), and other antimicrobials (isoniazid, moxifloxacin, streptomycin, and EMB [Sigma-Aldrich]).

Dilutions of compounds were made in 100 μl of culture medium for mycobacterial strains in sterile 96-well polypropylene flat-bottom plates. Wells were inoculated with 1×10^5 CFU in 100 μl and incubated at 37°C for 7 days for slow-growing mycobacteria or for 4 days for fast-growing species. Then, 30 μl of 0.1 mg/ml filter-sterilized resazurin (Sigma-Aldrich) was added. The results were revealed after 48 h in the case of slow-growing mycobacteria or after 24 h for fast-growing species. Positive and negative controls were added in all the experiments, and moxifloxacin (Sigma) at 0.5 mg/ml was used in all the assays as a control (33).

Kill kinetics. We determined the kill kinetics in order to find out whether the antituberculosis effect of bacteriocin AS-48 could be bactericidal or bacteriostatic. For this, *Mycobacterium tuberculosis* H37Rv was grown in culture medium until exponential phase, then diluted to 10^6 CFU/ml, and separated in three flasks. Bacteriocin AS-48 was added to cultures to give final concentrations of 64 and 128 μg/ml, and the third culture was left untreated as a control. All cultures were incubated at 37°C. After 1, 2, 6, and 9 days of incubation, samples of 100 μl were taken, and serial 1:10 dilutions in phosphate-buffered saline (PBS) supplemented with tyloxapol (a nonionic surfactant) at 0.1% was added to avoid bacterial clumping. Dilutions were plated on Middlebrook 7H10 agar supplemented with ADC, in triplicate, and plates were incubated for 3 weeks at 37°C. The numbers of CFU for each time point and culture were determined and plotted as log CFU versus time, and results were analyzed for significance by a linear regression test.

Synergy test. The synergy assay blends gradients of two compounds to evaluate their activities and the interactions between them. In fresh medium for culturing mycobacteria, solutions at 4-fold the highest concentration to be tested were prepared for each compound. Then, both compounds were serially 2-fold diluted in sterile 96-well flat bottom plates; one of the compounds was diluted along the columns, and the other was diluted in the rows. The first column would then have just one of the compounds, and the last row would have the other; the rest of the plate would be a matrix of both gradients. Finally, wells were inoculated as described above and incubated and treated with resazurin as in a conventional MIC assay.

FIC index analysis. The fractional inhibitory concentration (FIC) index allows objective identification of any interaction between two compounds against a particular bacterial strain, indicating whether there is synergy, no interaction, or antagonism.

In the 96-well plate, the first column shows the MIC of one of the compounds (*X*), and the last row shows the MIC of the second compound (*Y*). For each well in which there is no growth next to a well with growth, the FIC must be calculated using the following formulas: $FIC_X = MIC_{X \text{ in the presence of } Y}/MIC_{X \text{ alone}}$ and $FIC_Y = MIC_{Y \text{ in the presence } X}/MIC_{Y \text{ alone}}$.

Both values, together with other points of inhibition, can be represented graphically, and a concave line will be indicative of synergy. Alternatively, the addition of FIC_X and FIC_Y indicates the FICI value. An FICI value up to 0.5 indicates synergy, a value between 0.5 and 4 indicates that there is no interaction between the compounds, and a value over 4 indicates antagonism (34, 35).

Ethidium bromide accumulation assay. The ethidium bromide assay assessed the capacity to accumulate ethidium bromide at increasing concentrations of bacteriocin AS-48. *M. smegmatis* was cultivated until the culture reached an optical density at 600 nm (OD_{600}) of 0.6 to 0.8 under the conditions mentioned above. The culture was centrifuged, and the pellet was washed in PBS supplemented with 0.05% Tween 80; then, the OD_{600} was adjusted to 0.8 in the same buffer further supplemented with 0.4 % glucose. Ethidium bromide was used at 1 μg/ml combined with inhibitory and subinhibitory concentrations of AS-48. Verapamil at 75 μg/ml was used as a positive control showing the highest accumulation of ethidium bromide. A control experiment was done with PBS-Tween 80 buffer

and no bacterial inoculum to set the values of fluorescence of the compounds by themselves. Other controls were done without ethidium bromide. Accumulation of ethidium bromide was measured by recording fluorescence at 530-nm excitation and 590-nm detection for 1 h (12).

Cytotoxicity assays. An MTT assay and neutral red assay (36) were used to determine AS-48 cytotoxicity in MHS and J774.2 murine macrophages and THP-1 human macrophages. Cells were cultured in 96-well flat-bottom plates with the appropriate medium. THP-1 monocytes were differentiated to macrophages by using 10 ng/ml of phorbol 12-myristate 13-acetate (PMA) (P1585-1MG; Sigma-Aldrich) for 72 h. The concentrations used for cytotoxicity assays were 15,000 cells/well (MHS) and 20,000 cells/well (J774.2) for mouse lung macrophages and 50,000 cells/well (THP-1) for human lung macrophages. They were cultured for 24 h, and then the compounds were added dissolved in fresh culture medium. Absorbance was measured in an MTT assay at 570 and 650 nm and by fluorescence in the case of neutral red at 530- and 645-nm excitation and emission wavelengths, respectively. Percent cell viability in comparison with that of untreated controls was determined, and treatments were considered to be cytotoxic or not according to the International Organization for Standardization (13). To check the lack of differences between samples treated with lower concentrations of AS-48, we performed one-way analysis of variance (ANOVA) tests.

Analysis of the bacterial membrane potential. *M. smegmatis* and *M. bovis* BCG membrane potentials were measured by a BacLight bacterial membrane potential kit (B34950; Thermo Fisher); integrity of the membrane potential results in fluorescence due to the accumulation of $DiOC_2$ (3) inside bacterial cells. Bacterial cells were treated with several concentrations of AS-48 for 24 h to assess its effect on membrane potential. The samples were analyzed by flow cytometry.

Samples for SEM. The effect of AS-48 on the morphology of *M. tuberculosis* H37Rv was analyzed by scanning electron microscopy (SEM). SEM images were acquired using an SEM Inspect F50 (FEI Company, Eindhoven, The Netherlands). Bacterial cultures treated with AS-48 at 64 μg/ml or with 8 μg/ml of AS-48 plus 25 μg/ml of lysozyme were diluted to 10^5 CFU/ml, and samples were first fixed with glutaraldehyde. Then, samples were washed three times with 10× PBS, filtered through a 0.1-μm-pore-size filter (0.1-μm VCTP Isopore membrane filter; Millipore), and then dehydrated with a graded ethanol series and kept in 100% ethanol. Finally, ethanol was evaporated at room temperature, and samples were covered with a thin layer of metal (Pt; 15 nm) and examined at 15,000 eV and different magnifications.

***M. tuberculosis* macrophage infection assay.** Cultures of H37Rv-GFP were maintained with stirring for 3 days before infection to ensure that bacterial cells were in exponential growth. Then, bacterial cells were washed twice with PBS without Mg^{2+} and Ca^{2+}, followed by a third wash with RPMI 1640 medium supplemented with 10% FBS (RPMI-FBS), and centrifuged at 70 × *g* for 2 min to pellet bacterial clumps; the supernatant corresponded to a homogenous suspension of bacteria. Bacterial titer was determined by measuring the optical density at 600 nm and by measuring enhanced GFP (EGFP) fluorescence on a Victor Multilabel Counter (PerkinElmer); the sample was further diluted in RPMI-FBS medium prior to infection. Raw 264.7 macrophages were used for the intracellular mycobacterial replication assay and harvested by using Versene (Life Technologies). Macrophages were prepared at a concentration of 5×10^5 cells/ml, infected at a multiplicity of infection (MOI) of 1:2 with H37Rv-GFP, and incubated in RPMI-FBS cell culture medium at 37°C with stirring at 120 rpm. After 2 h, cells were centrifuged at 160 × *g* for 5 min, resuspended in the same volume of fresh medium containing 50 μg/ml of amikacin to kill extracellular bacteria, and incubated for 1 h at 37°C with shaking at 120 rpm. Cells were washed and resuspended in the same volume of fresh medium. Infected cells were seeded in 384-well plates (Greiner Bio-One) at 2×10^4 cells/well containing compound (AS-48, EMB, and lysozyme diluted in water). Plates were incubated for 5 days at 37°C in 5% CO_2. Infected cells were stained for 30 min with Syto60 dye (Invitrogen) at a final concentration of 5 μM. Finally, images were acquired (as described below), and then cells were lysed with Dulbecco's PBS (DPBS)–0.1% Triton X-100 buffer for 1 min to release intracellular bacteria. The number of viable bacterial cells was determined by serially plating dilutions on Middlebrook 7H11 (Difco) agar plates, supplemented with 0.5% glycerol, 10% OADC, and 50 μg/ml hygromycin B. After 3 weeks of incubation at 37°C in 5% CO_2, the numbers of viable bacteria (CFU) were calculated.

Image acquisition and analysis. Images were acquired on an automated fluorescent confocal microscope (Opera; PerkinElmer), using a 20× water immersion lens. Syto60-labeled cells were detected using a 640-nm excitation laser coupled with a 690/70-nm detection filter, and GFP-labeled bacteria were detected using a 488-nm laser coupled with a 540/75-nm detection filter. A series of six images was taken per well, and each one was analyzed using the Columbus system (version 2.5.1; PerkinElmer) image analysis software. Briefly, the images were processed to determine the output image of GFP mask and remove background in that channel. Then, the output images corresponding to the Syto60 values were processed similarly to assess morphological parameters of cells. Properties of intensity and morphology were filtered to select the correct nuclear population. Spots corresponding to the bacteria infecting the cells were detected, and bacterial number and the area in pixels were determined for each cell. The intracellular bacterial growth was quantified by the total intracellular bacterial area (pixels) per well. In order to consider a cell infected, the number of bacteria within the cell area was set as ≥1. Efficiency of infection and effectivity of treatment with compounds were determined in terms of the percentage of infected cells and mean *M. tuberculosis* area per infected cell.

SUPPLEMENTAL MATERIAL

Supplemental material for this article may be found at https://doi.org/10.1128/AAC.00359-18.

SUPPLEMENTAL FILE 1, PDF file, 0.1 MB.

ACKNOWLEDGMENTS

We thank Ana Belén Gómez for technical support in the culture of eukaryotic cells and Nacho Aguiló for help in the interpretation of cytometry flow experiments and for helpful discussion on the manuscript. We thank Ainhoa Lucía for support with the cytotoxicity assays. We thank Alexandre Vandeputte and Isabelle Ricard for technical expertise in the infection assays.

This work was supported by grants from the Spanish Government (SAF2013-48971-C2-2-R to J.A.A. and SAF2013-48971-C2-1-R to M.M.). C.A.-P. is a recipient of a predoctoral fellowship (BES-2014-067962) from the Spanish Government and was funded by EMBO Short Term Fellowships (number 6986). P.B., N.D., and O.-R.S. received financial support from the European Community (ERC-STG INTRACELLTB grant number 260901 and MM4TB grant number260872), the EMBO Young Investigator Program, the Agence Nationale de la Recherche (ANR-10-EQPX-04-01), the Feder (12001407 [D-AL] Equipex Imaginex BioMed), and the Région Nord Pas de Calais (convention number 12000080).

The funders had no role in study design, data collection and interpretation, or the decision to submit the work for publication.

REFERENCES

1. World Health Organization. 2017. Global tuberculosis report 2017. World Health Organization, Geneva, Switzerland. http://www.who.int/tb/publications/global_report/en/.
2. Alvarez-Sieiro P, Montalban-Lopez M, Mu D, Kuipers OP. 2016. Bacteriocins of lactic acid bacteria: extending the family. Appl Microbiol Biotechnol 100:2939–2951. https://doi.org/10.1007/s00253-016-7343-9.
3. Sánchez-Barrena MJ, Martínez-Ripoll M, Gálvez A, Valdivia E, Maqueda M, Cruz V, Albert A. 2003. Structure of bacteriocin AS-48: from soluble state to membrane bound state. J Mol Biol 334:541–549. https://doi.org/10.1016/j.jmb.2003.09.060.
4. Sanchez-Hidalgo M, Montalban-Lopez M, Cebrian R, Valdivia E, Martinez-Bueno M, Maqueda M. 2011. AS-48 bacteriocin: close to perfection. Cell Mol Life Sci 68:2845–2857. https://doi.org/10.1007/s00018-011-0724-4.
5. Abriouel H, Lucas R, Omar NB, Valdivia E, Galvez A. 2010. Potential applications of the cyclic peptide enterocin AS-48 in the preservation of vegetable foods and beverages. Probiotics Antimicrob Proteins 2:77–89. https://doi.org/10.1007/s12602-009-9030-y.
6. Ananou S, Valdivia E, Martinez Bueno M, Galvez A, Maqueda M. 2004. Effect of combined physico-chemical preservatives on enterocin AS-48 activity against the enterotoxigenic Staphylococcus aureus CECT 976 strain. J Appl Microbiol 97:48–56. https://doi.org/10.1111/j.1365-2672.2004.02276.x.
7. Carroll J, Draper LA, O'Connor PM, Coffey A, Hill C, Ross RP, Cotter PD, O'Mahony J. 2010. Comparison of the activities of the lantibiotics nisin and lacticin 3147 against clinically significant mycobacteria. Int J Antimicrob Agents 36:132–136. https://doi.org/10.1016/j.ijantimicag.2010.03.029.
8. Sosunov V, Mischenko V, Eruslanov B, Svetoch E, Shakina Y, Stern N, Majorov K, Sorokoumova G, Selishcheva A, Apt A. 2007. Antimycobacterial activity of bacteriocins and their complexes with liposomes. J Antimicrob Chemother 59:919–925. https://doi.org/10.1093/jac/dkm053.
9. Chun W, Hancock RE. 2000. Action of lysozyme and nisin mixtures against lactic acid bacteria. Int J Food Microbiol 60:25–32. https://doi.org/10.1016/S0168-1605(00)00330-5.
10. Ananou S, Rivera S, Madrid MI, Maqueda M, Martínez-Bueno M, Valdivia E. 2018. Application of enterocin AS-48 as biopreservative in eggs and egg fractions: synergism through lysozyme. LWT Food Sci Technol 89:409–417. https://doi.org/10.1016/j.lwt.2017.11.018.
11. Gonzalez C, Langdon GM, Bruix M, Galvez A, Valdivia E, Maqueda M, Rico M. 2000. Bacteriocin AS-48, a microbial cyclic polypeptide structurally and functionally related to mammalian NK-lysin. Proc Natl Acad Sci U S A 97:11221–11226. https://doi.org/10.1073/pnas.210301097.
12. Rodrigues L, Viveiros M, Ainsa JA. 2015. Measuring efflux and permeability in mycobacteria. Methods Mol Biol 1285:227–239. https://doi.org/10.1007/978-1-4939-2450-9_13.
13. International Organization for Standardization. 2009. Biological evaluation of medical devices. Part 5: tests for *in vitro* cytotoxicity. ISO 10993-5:2009. International Organization for Standardization, Geneva, Switzerland.
14. Abengozar MA, Cebrian R, Saugar JM, Garate T, Valdivia E, Martinez-Bueno M, Maqueda M, Rivas L. 2017. Enterocin AS-48 as evidence for the use of bacteriocins as new leishmanicidal agents. Antimicrob Agents Chemother 61:e02288-16. https://doi.org/10.1128/AAC.02288-16.
15. World Health Organization. 2017. Antibacterial agents in clinical development. World Health Organization, Geneva, Switzerland.
16. da Cunha NB, Cobacho NB, Viana JF, Lima LA, Sampaio KB, Dohms SS, Ferreira AC, de la Fuente-Nunez C, Costa FF, Franco OL, Dias SC. 2017. The next generation of antimicrobial peptides (AMPs) as molecular therapeutic tools for the treatment of diseases with social and economic impacts. Drug Discov Today 22:234–248. https://doi.org/10.1016/j.drudis.2016.10.017.
17. Hurdle JG, O'Neill AJ, Chopra I, Lee RE. 2011. Targeting bacterial membrane function: an underexploited mechanism for treating persistent infections. Nat Rev Microbiol 9:62–75. https://doi.org/10.1038/nrmicro2474.
18. Wu X, Cherian PT, Lee RE, Hurdle JG. 2013. The membrane as a target for controlling hypervirulent Clostridium difficile infections. J Antimicrob Chemother 68:806–815. https://doi.org/10.1093/jac/dks493.
19. Ramon-Garcia S, Mikut R, Ng C, Ruden S, Volkmer R, Reischl M, Hilpert K, Thompson CJ. 2013. Targeting Mycobacterium tuberculosis and other microbial pathogens using improved synthetic antibacterial peptides. Antimicrob Agents Chemother 57:2295–2303. https://doi.org/10.1128/AAC.00175-13.
20. Gutsmann T. 2016. Interaction between antimicrobial peptides and mycobacteria. Biochim Biophys Acta 1858:1034–1043. https://doi.org/10.1016/j.bbamem.2016.01.031.
21. Carroll J, O'Mahony J. 2011. Anti-mycobacterial peptides: made to order with delivery included. Bioeng Bugs 2:241–246. https://doi.org/10.4161/bbug.2.5.16229.
22. Carroll J, Field D, O'Connor PM, Cotter PD, Coffey A, Hill C, Ross RP, O'Mahony J. 2010. Gene encoded antimicrobial peptides, a template for the design of novel anti-mycobacterial drugs. Bioeng Bugs 1:408–412. https://doi.org/10.4161/bbug.1.6.13642.
23. Montalban-Lopez M, Sanchez-Hidalgo M, Valdivia E, Martinez-Bueno M, Maqueda M. 2011. Are bacteriocins underexploited? Novel applications for old antimicrobials. Curr Pharm Biotechnol 12:1205–1220. https://doi.org/10.2174/138920111796117364.
24. van Breda SV, Buys A, Apostolides Z, Nardell EA, Stoltz AC. 2015. The antimicrobial effect of colistin methanesulfonate on Mycobacterium tuberculosis in vitro. Tuberculosis (Edinb) 95:440–446. https://doi.org/10.1016/j.tube.2015.05.005.
25. Chai C, Lee KS, Imm GS, Kim YS, Oh SW. 2017. Inactivation of Clostridium difficile spore outgrowth by synergistic effects of nisin and lysozyme. Can J Microbiol 63:638–643. https://doi.org/10.1139/cjm-2016-0550.
26. Jia J, Zhu F, Ma X, Cao Z, Cao ZW, Li Y, Li YX, Chen YZ. 2009. Mechanisms

of drug combinations: interaction and network perspectives. Nat Rev Drug Discov 8:111–128. https://doi.org/10.1038/nrd2683.
27. Makarov V, Lechartier B, Zhang M, Neres J, van der Sar AM, Raadsen SA, Hartkoorn RC, Ryabova OB, Vocat A, Decosterd LA, Widmer N, Buclin T, Bitter W, Andries K, Pojer F, Dyson PJ, Cole ST. 2014. Towards a new combination therapy for tuberculosis with next generation benzothiazinones. EMBO Mol Med 6:372–383. https://doi.org/10.1002/emmm.201303575.
28. Lechartier B, Hartkoorn RC, Cole ST. 2012. In vitro combination studies of benzothiazinone lead compound BTZ043 against Mycobacterium tuberculosis. Antimicrob Agents Chemother 56:5790–5793. https://doi.org/10.1128/AAC.01476-12.
29. Kalita A, Verma I, Khuller GK. 2004. Role of human neutrophil peptide-1 as a possible adjunct to antituberculosis chemotherapy. J Infect Dis 190:1476–1480. https://doi.org/10.1086/424463.
30. Christophe T, Jackson M, Jeon HK, Fenistein D, Contreras-Dominguez M, Kim J, Genovesio A, Carralot JP, Ewann F, Kim EH, Lee SY, Kang S, Seo MJ, Park EJ, Skovierova H, Pham H, Riccardi G, Nam JY, Marsollier L, Kempf M, Joly-Guillou ML, Oh T, Shin WK, No Z, Nehrbass U, Brosch R, Cole ST, Brodin P. 2009. High content screening identifies decaprenyl-phosphoribose 2′ epimerase as a target for intracellular antimycobacterial inhibitors. PLoS Pathog 5:e1000645. https://doi.org/10.1371/journal.ppat.1000645.
31. Cebrian R, Banos A, Valdivia E, Perez-Pulido R, Martinez-Bueno M, Maqueda M. 2012. Characterization of functional, safety, and probiotic properties of Enterococcus faecalis UGRA10, a new AS-48-producer strain. Food Microbiol 30:59–67. https://doi.org/10.1016/j.fm.2011.12.002.
32. Ananou S, Muñoz A, Gálvez A, Martínez-Bueno M, Maqueda M, Valdivia E. 2008. Optimization of enterocin AS-48 production on a whey-based substrate. Int Dairy J 18:923–927. https://doi.org/10.1016/j.idairyj.2008.02.001.
33. Palomino JC, Martin A, Camacho M, Guerra H, Swings J, Portaels F. 2002. Resazurin microtiter assay plate: simple and inexpensive method for detection of drug resistance in Mycobacterium tuberculosis. Antimicrob Agents Chemother 46:2720–2722. https://doi.org/10.1128/AAC.46.8.2720-2722.2002.
34. Odds FC. 2003. Synergy, antagonism, and what the chequerboard puts between them. J Antimicrob Chemother 52:1. https://doi.org/10.1093/jac/dkg301.
35. European Committee for Antimicrobial Susceptibility Testing (EUCAST) of the European Society of Clinical Microbiology and Infectious Diseases (ESCMID). 2000. Terminology relating to methods for the determination of susceptibility of bacteria to antimicrobial agents. Clin Microbiol Infect 6:503–508. https://doi.org/10.1046/j.1469-0691.2000.00149.x.
36. Repetto G, del Peso A, Zurita JL. 2008. Neutral red uptake assay for the estimation of cell viability/cytotoxicity. Nat Protoc 3:1125–1131. https://doi.org/10.1038/nprot.2008.75.
37. Cole ST, Barrell BG. 1998. Analysis of the genome of Mycobacterium tuberculosis H37Rv. Novartis Found Symp 217:160–172. https://doi.org/10.1002/0470846526.ch12.
38. Lee JS, Krause R, Schreiber J, Mollenkopf HJ, Kowall J, Stein R, Jeon BY, Kwak JY, Song MK, Patron JP, Jorg S, Roh K, Cho SN, Kaufmann SH. 2008. Mutation in the transcriptional regulator PhoP contributes to avirulence of Mycobacterium tuberculosis H37Ra strain. Cell Host Microbe 3:97–103. https://doi.org/10.1016/j.chom.2008.01.002.
39. Gonzalo Asensio J, Maia C, Ferrer NL, Barilone N, Laval F, Soto CY, Winter N, Daffe M, Gicquel B, Martin C, Jackson M. 2006. The virulence-associated two-component PhoP-PhoR system controls the biosynthesis of polyketide-derived lipids in Mycobacterium tuberculosis. J Biol Chem 281:1313–1316. https://doi.org/10.1074/jbc.C500388200.
40. Fleischmann RD, Alland D, Eisen JA, Carpenter L, White O, Peterson J, DeBoy R, Dodson R, Gwinn M, Haft D, Hickey E, Kolonay JF, Nelson WC, Umayam LA, Ermolaeva M, Salzberg SL, Delcher A, Utterback T, Weidman J, Khouri H, Gill J, Mikula A, Bishai W, Jacobs WR, Venter JC, Fraser CM. 2002. Whole-genome comparison of Mycobacterium tuberculosis clinical and laboratory strains. J Bacteriol 184:5479–5490. https://doi.org/10.1128/JB.184.19.5479-5490.2002.
41. Caminero JA, Pena MJ, Campos-Herrero MI, Rodriguez JC, Garcia I, Cabrera P, Lafoz C, Samper S, Takiff H, Afonso O, Pavon JM, Torres MJ, van Soolingen D, Enarson DA, Martin C. 2001. Epidemiological evidence of the spread of a Mycobacterium tuberculosis strain of the Beijing genotype on Gran Canaria Island. Am J Respir Crit Care Med 164:1165–1170. https://doi.org/10.1164/ajrccm.164.7.2101031.
42. Chesne-Seck ML, Barilone N, Boudou F, Gonzalo Asensio J, Kolattukudy PE, Martin C, Cole ST, Gicquel B, Gopaul DN, Jackson M. 2008. A point mutation in the two-component regulator PhoP-PhoR accounts for the absence of polyketide-derived acyltrehaloses but not that of phthiocerol dimycocerosates in Mycobacterium tuberculosis H37Ra. J Bacteriol 190:1329–1334. https://doi.org/10.1128/JB.01465-07.
43. Zhang M, Sala C, Hartkoorn RC, Dhar N, Mendoza-Losana A, Cole ST. 2012. Streptomycin-starved Mycobacterium tuberculosis 18b, a drug discovery tool for latent tuberculosis. Antimicrob Agents Chemother 56:5782–5789. https://doi.org/10.1128/AAC.01125-12.
44. Snapper SB, Melton RE, Mustafa S, Kieser T, Jacobs WR, Jr. 1990. Isolation and characterization of efficient plasmid transformation mutants of Mycobacterium smegmatis. Mol Microbiol 4:1911–1919. https://doi.org/10.1111/j.1365-2958.1990.tb02040.x.

Tuberculosis 112 (2018) 98–109

Contents lists available at ScienceDirect

Tuberculosis

journal homepage: www.elsevier.com/locate/tube

Drug Discovery and Resistance

The EU approved antimalarial pyronaridine shows antitubercular activity and synergy with rifampicin, targeting RNA polymerase

Giorgia Mori[a], Beatrice Silvia Orena[a], Clara Franch[b,1], Lesley A. Mitchenall[b], Adwait Anand Godbole[c], Liliana Rodrigues[d,e,f,2], Clara Aguilar-Pérez[d,e], Júlia Zemanová[g], Stanislav Huszár[g], Martin Forbak[g], Thomas R. Lane[h], Mohamad Sabbah[i], Nathalie Deboosere[j], Rosangela Frita[j], Alexandre Vandeputte[j], Eik Hoffmann[j], Riccardo Russo[k], Nancy Connell[k], Courtney Veilleux[k], Rajiv Kumar[c], Pradeep Kumar[k], Joel S. Freundlich[k,l], Priscille Brodin[j], Jose Antonio Aínsa[d,e], Valakunja Nagaraja[c,m], Anthony Maxwell[b], Katarína Mikušová[g], Maria Rosalia Pasca[a], Sean Ekins[h,n,*]

[a] Department of Biology and Biotechnology "Lazzaro Spallanzani", University of Pavia, 27100 Pavia, Italy
[b] Department of Biological Chemistry, John Innes Centre, Norwich Research Park, Norwich NR4 7UH, UK
[c] Department of Microbiology and Cell Biology, Indian Institute of Science, Bangalore 560012, India
[d] Departamento de Microbiología, Facultad de Medicina, and BIFI, Universidad de Zaragoza, and IIS-Aragón, 50009 Zaragoza, Spain
[e] CIBER Enfermedades Respiratorias (CIBERES), Instituto de Salud Carlos III, Spain
[f] Fundación ARAID, Zaragoza, Spain
[g] Department of Biochemistry, Faculty of Natural Sciences, Comenius University in Bratislava, Mlynská dolina, Ilkovičova 6, 84215, Bratislava, Slovakia
[h] Collaborations Pharmaceuticals, Inc., 840 Main Campus Drive, Lab 3510, Raleigh, NC 27606, USA
[i] Department of Chemistry, University of Cambridge, Lensfield Rd, Cambridge, CB2 1EW, UK
[j] Univ Lille, CNRS, INSERM, CHU Lille, Institut Pasteur de Lille, U1019 - UMR 8204 - CIIL - Center for Infection and Immunity of Lille, 1 rue du Professeur Calmette, 59000 Lille, France
[k] Division of Infectious Disease, Department of Medicine and the Ruy V. Lourenço Center for the Study of Emerging and Re-emerging Pathogens, Rutgers University - New Jersey Medical School, Newark, NJ 07103, USA
[l] Department of Pharmacology, Physiology, and Neuroscience, Rutgers University – New Jersey Medical School, Newark, NJ, 07103, USA
[m] Jawaharlal Nehru Centre for Advanced Scientific Research, Bangalore 560064, India
[n] Collaborative Drug Discovery, 1633 Bayshore Highway, Suite 342, Burlingame, CA 94403, USA

ARTICLE INFO

Keywords:
Antimalarial
Gyrase
Mycobacterium tuberculosis
Pyronaridine
Repurposing
Topoisomerase
Tuberculosis
RNA polymerase

ABSTRACT

The search for compounds with biological activity for many diseases is turning increasingly to drug repurposing. In this study, we have focused on the European Union-approved antimalarial pyronaridine which was found to have *in vitro* activity against *Mycobacterium tuberculosis* (MIC 5 μg/mL). In macromolecular synthesis assays, pyronaridine resulted in a severe decrease in incorporation of ^{14}C-uracil and ^{14}C-leucine similar to the effect of rifampicin, a known inhibitor of *M. tuberculosis* RNA polymerase. Surprisingly, the co-administration of pyronaridine (2.5 μg/ml) and rifampicin resulted in *in vitro* synergy with an MIC 0.0019–0.0009 μg/mL. This was mirrored in a THP-1 macrophage infection model, with a 16-fold MIC reduction for rifampicin when the two compounds were co-administered *versus* rifampicin alone. Docking pyronaridine in *M. tuberculosis* RNA polymerase suggested the potential for it to bind outside of the RNA polymerase rifampicin binding pocket. Pyronaridine was also found to have activity against a *M. tuberculosis* clinical isolate resistant to rifampicin, and when combined with rifampicin (10% MIC) was able to inhibit *M. tuberculosis* RNA polymerase *in vitro*. All these findings, and in particular the synergistic behavior with the antitubercular rifampicin, inhibition of RNA polymerase in combination *in vitro* and its current use as a treatment for malaria, may suggest that pyronaridine

* Corresponding author. Collaborations Pharmaceuticals, Inc., 840 Main Campus Drive, Lab 3510, Raleigh, NC 27606, USA.
E-mail address: sean@collaborationspharma.com (S. Ekins).
[1] Present address: Inspiralis Ltd., Norwich Research Park Innovation Centre, Colney Lane, Norwich NR4 7GJ, UK.
[2] Present address: Global Health and Tropical Medicine, GHTM, Unit of Medical Microbiology, Instituto de Higiene e Medicina Tropical, IHMT, Universidade Nova de Lisboa, UNL, Lisbon, Portugal.

https://doi.org/10.1016/j.tube.2018.08.004
Received 9 January 2018; Received in revised form 3 August 2018; Accepted 5 August 2018

could also be used as an adjunct for treatment against *M. tuberculosis* infection. Future studies will test potential for *in vivo* synergy, clinical utility and attempt to develop pyronaridine analogs with improved potency against *M. tuberculosis* RNA polymerase when combined with rifampicin.

1. Introduction

The search for new drugs that could be used as effective treatments for neglected diseases continues due to both the lack of effective treatments and drug resistance. In particular, *Mycobacterium tuberculosis* (*Mtb*), the causative agent of tuberculosis (TB), results in approximately 1.6 million fatalities out of 10.4 million new cases in 2016 [1]. For decades, there has been extensive research focused on developing molecules that could overcome drug resistance, shorten the duration of TB therapy and attempt to avoid drug-drug interactions with therapeutics used to treat patients co-infected with HIV infection [2–5]. For well over 70 years, compounds have been evaluated in the *in vivo* mouse model [6] and some of these could be suitable for reevaluation [7]. With a shortage of funding for future research [8] there is a need for enhancing the efficiency of TB drug discovery efforts. Increasingly, there has been some interest in using drug repurposing, namely taking drugs approved for another purpose and leveraging them for additional diseases [9]. This can be facilitated using high-throughput screening of libraries of approved drugs from the FDA or other regulatory agencies, computational or virtual screening using docking or pharmacophores, machine learning or combinations of methods, knowledge-based methods, gene-expression data or serendipity [9–14]. These approaches are particularly important for addressing neglected and rare diseases where the urgency is great and an already approved drug would shorten the path to the clinic and perhaps mitigate the treatment regimen length.

In this context we focus on tuberculosis, with an example being from a previously published medium-throughput screen of approved drugs which identified several compounds with previously unknown activity against *Mtb,* including the antimalarial compound primaquine (MIC = 5 μM) [15]. Moreover, numerous compounds with antimalarial activity *in vitro* have been found to have activity against *Mtb in vitro* [16], such as the 4-aminoquinoline antimalarials (e.g. mefloquine and its enantiomers [17,18]) (Fig. S1). Similarly, another recent repurposing example for *Mtb* identified from a high throughput screen is the proton pump inhibitor lansoprazole which has to be activated to the sulphide [19] to possess activity *in vitro* but this needs to be provided directly as the metabolite to obtain efficacious *in vivo* concentrations greater than the MIC [20].

Pyronaridine is a potent antimalarial (EC_{50} = 13.5 nM *versus Plasmodium falciparum*) with chemical similarity to the aminoquinolines that has been widely used in China [21]. It is currently used in combination with artesunate in the European Medicines Agency-approved Pyramax against *P. falciparum* and *Plasmodium vivax* infections [22] (Fig. S1). As an antimalarial compound, pyronaridine is active against the intraerythrocytic stage of the disease, with less toxicity than the antimalarial chloroquine, as well as activity against drug-resistant forms of the disease [22]. Pyronaridine-treated animals did not show behavioral disturbances or neurotoxicity. In rat and human liver microsomes, the major metabolite is the quinoneimine. Metabolite characterization based on the blood, urine, and feces samples obtained in a mass balance study, allowed for identification of nine primary and four secondary metabolites of pyronaridine [23].

In a previous study, following initial docking of pyronaridine to a homology model of *Mtb* topoisomerase I (Topo I) [24–26], pyronaridine was selected to evaluate its antitubercular activity *in vitro* because of its promising *in vivo* PK and antimalarial activity (and good selectivity index). In this work, our goals were to assess whether pyronaridine could then be considered an antitubercular and a starting point for further optimization or progression to future *in vivo* models of infection.

2. Methods

All the experiments were performed in a BSL-3 safety laboratory with trained researchers to avoid any risk of contamination.

2.1. Drugs and reagents

Pyronaridine tetraphosphate and additional antimalarial compounds (chloroquine, primaquine, quinine, mefloquine, halofantrine, amodiaquine, lumefantrine and quinoline) were obtained from Sigma Aldrich (Dorset, England and St. Louis, MO). Efflux inhibitors including carbonyl cyanide *m*-chlorophenylhydrazone (CCCP), thioridazine, verapamil, reserpine and phenylalanine-arginine beta-naphthylamide (PAβN) were purchased from Sigma-Aldrich (Madrid, Spain).

2.2. MIC determination in mycobacterial species

Mtb strains were grown at 37 °C in Middlebrook 7H9 broth (BD biosciences), supplemented with albumin-dextrose-catalase (10%), and a surfactant agent (Tween 80 or Tyloxapol) at 0.05%. MIC values for the compounds were determined by broth microdilution method using resazurin as an indicator of bacterial growth [27]. MIC values were also determined on solid Middlebrook 7H11 medium (BD biosciences) supplemented with oleic acid-albumin-dextrose-catalase (OADC), by incubating plates at 37 °C for about 21 days and the growth was visually evaluated. In both cases, culture media contained serial dilutions of drugs (1–40 μg/mL), and the MIC was taken as the lowest drug concentration that prevented visible growth on plates or resazurin color change. MICs are given as the average of at least three independent determinations.

The *Mtb* extensively drug resistant clinical strain was grown as above to OD_{595} 0.2–0.3 and diluted 1000-fold in Middlebrook 7H9 broth, supplemented with albumin-dextrose-catalase (10%). The test compound was dispensed in 384-well plates using Echo® 555 liquid handler (Labcyte, San Jose, CA) at selected concentration, 50 μl of diluted *Mtb* culture was added to each well and incubated for 7 days 37 °C followed by addition of AlamarBlue® (ThermoFisher Scientific). The plate was read using Cytation 3 multi-mode plate reader after 24–48 h incubation at 37 °C to determine MIC.

Mycobacterium smegmatis cells were grown in Middlebrook 7H9 broth supplemented with 0.2% glycerol and 0.05% Tween-80. Cultures were grown to OD_{600} = 0.6, diluted to a final OD_{600} of 0.05 with fresh media and aliquoted into a 100-well growth plate. Serial dilutions of the compounds were added to the culture. The untreated culture was taken as a control. The growth was monitored at 595 nm with continuous shaking at 200 rpm. The readings were analyzed by GraphPad Prism software (version 5.0) to determine growth kinetics and MIC of the compounds.

2.3. Growth inhibitory activity versus ESKAPE bacteria

Pyronaridine was assayed for its growth inhibitory ability of bacteria in the ESKAPE class, which were listed amongst the top global health priorities by the WHO in 2017 [28]. The MIC determination of pyronaridine versus relevant strains of *Enterobacter cloacae* (ATCC 13047), *Staphylococcus aureus* (ATCC 43300), *Klebsiella pneumoniae* (BAA 2146), *Acinetobacter baumannii* (ATCC 19606), *Pseudomonas aeruginosa* (HER 1018), and *Enterococcus faecium* (NCTC 7171) followed the liquid dilution method [29].

2.4. Combination studies with pyronaridine and other antitubercular drugs

The MICs of isoniazid, rifampicin, and ciprofloxacin for *Mtb* were assessed at a range of concentrations in the presence of pyronaridine at a sub-inhibitory concentration (2.5 μg/mL). As a control, the MICs of isoniazid, rifampicin, and ciprofloxacin were also determined in the absence of pyronaridine. All MIC determinations were done following the protocol described above.

For estimating more precisely the interaction between rifampicin and pyronaridine, we used the checkerboard assay, in which a range of concentrations of rifampicin was combined with a range of concentrations of pyronaridine, and calculated FIC and FICI (Fractional Inhibitory Concentration Index) [30,31]. For a drug, FIC is the ratio between its MIC in the combination and the MIC of the drug alone. For a pair of drugs, FICI is the addition of the two individual FIC values. A FICI value up to 0.5 indicates synergy, when it is between 0.5 and 4 indicates there is no interaction between the compounds, and a FICI value over 4 indicates antagonism.

2.5. Intracellular mycobacterial replication assay

72 h Phorbol-12-Myristate-13-Acetate (PMA, 50 ng/mL, Sigma-Aldrich) differentiated human THP-1 macrophages (ATCC#TIB-202) and murine RAW264.7 (ATCC#TIB-71) suspensions were infected with GFP-expressing *Mtb* H37Rv (MOI = 2) in RPMI-1640 Glutamax medium (Gibco) containing 10% heat-inactivated Fetal Bovine Serum (FBS, Gibco; RPMI-FBS) during 2 h under mild shaking (120 rpm) as previously described [32,33]. Cells were washed with RPMI-FBS and treated with amikacin (50 μg/mL, Sigma-Aldrich) for 1 h to kill bacteria still present in the culture medium. The infected cells were washed twice and 50 μL of cell suspension was added per well in 384-well assay plates containing Pyronaridine, as well as positives (isoniazid MIC x 100, and dose response curves (DRC) for rifampicin) and negative (DMSO 1%) controls. The MICs of rifampicin were assessed at a range of concentrations in combination with pyronaridine at 4 sub-inhibitory concentrations (ranged from 0.39 to 3.125 μg/mL) only on THP-1 cells. As a control, the MICs of rifampicin was also determined in the absence of pyronaridine. Microplates were incubated for 5 days at 37 °C with 5% CO_2.

The cells were stained with Syto60, 5 μM (Invitrogen) for 30 min at 37 °C with 5% CO_2 before imaging. Image acquisitions were performed on an automated confocal microscope (Opera, PerkinElmer) using a 20× water objective. Syto60-labeled cells were detected using excitation (Ex) at 640 nm and emission (Em) at 690 nm and GFP-bacteria were detected using Ex at 488 nm and Em at 540 nm. A series of 6 images was taken by well and each one was analyzed using the image-analysis software Columbus system (version 2.5.1, PerkinElmer) (Fig. 1A). Briefly, the two images were first segmented to remove background and normalize pixel intensities between images. Then, cell nuclei and cytoplasm were detected using an intensity detection algorithm applied on the Syto60 channel. Properties of intensity and morphology were filtered to correctly select the cell population. A spot detection algorithm based on the GFP channel was applied for the detection of *Mtb*-GFP in cells and in whole image, when cell lysis was observed for infected THP-1 cells. The bacterial intensity and area in pixels were measured. The image-based parameters that correlate to bacterial growth are the percentage of infected cells and the bacterial area (pixel) per cell and per well. The number of cells informed as to the cytotoxicity of the compound for effective concentrations. Typically, drugs demonstrated a dose-dependent decrease on both bacterial area and percentage of infected macrophages. In this study, the parameter used as a read-out was the area of bacteria present per cell and per well (expressed in px) for infected RAW264.7 and THP-1 macrophages, respectively. Normalizations were performed based on the average values obtained for the negative (DMSO 1%) and positive (isoniazid 10 μg/mL) controls. Inhibition of bacterial replication was determined for rifampicin alone and in combination with pyronaridine at different concentrations. Percentage of inhibition is plotted against the log10 of the compound concentration, determined in the absence or the presence of pyronaridine at different concentrations. Fitting was performed by Prism software using the sigmoidal dose-response (variable slope) model, constraining top and bottom values of the curve to 100% and 0% respectively. The MIC corresponded to the first concentration on the bottom of the curve.

2.6. Efflux studies with pyronaridine

The *in vitro* activity of pyronaridine was determined in *Mtb* mutants with deletions in genes encoding efflux pumps by using the protocol above. The MIC of pyronaridine in the presence of efflux inhibitors was determined to evaluate the contribution of efflux activity to *Mtb* susceptibility to this drug. For this, we initially determined the MIC of the efflux inhibitors CCCP, thioridazine, verapamil, reserpine and PAβN, according to the Middlebrook 7H9 broth microdilution protocol described above, and the results were recorded with resazurin dye [27]. Next, the impact of the efflux inhibitors (at one fourth of their MIC) on the MIC of pyronaridine was determined by the same method, in a range of two-fold pyronaridine concentrations from 80 to 0.6 μg/mL. The inoculated 96-well plates were incubated for 6 d at 37 °C and for an additional 2 d after the addition of the redox indicator (30 μl of a resazurin solution at 0.1 mg/ml). A change from blue to pink indicates reduction of resazurin and therefore bacterial growth. Thus, the MIC was defined as the lowest concentration of compound that prevented this color change.

Finally, the detection of ethidium bromide efflux on a real-time basis by the *Mtb* strains was performed using a fluorometric method previously described [34]. Briefly, *Mtb* strains were grown in 7H9-ADC medium at 37 °C until an OD_{600} of 0.6–0.8. Cultures were centrifuged at 2880 × g for 10 min, the supernatant was discarded, the pellet was washed in phosphate buffered saline (PBS; pH 7.4), and the OD_{600} was adjusted to 0.8 with PBS with 0.05% Tween 80. Aliquots of 100 μL of bacterial suspension were transferred into wells of a 96-well plate containing ethidium bromide at a concentration of 1 μg/mL. To determine the effect of pyronaridine and verapamil on the accumulation of ethidium bromide, 10 μL of each compound was added to the corresponding well of the 96-well plate. Each inhibitor was used at a maximum concentration of one-half of their MIC to not compromise the cellular viability. Relative fluorescence was acquired every 51 s for 60 min at 37 °C in a Synergy HT detection microplate reader (Biotek Instruments), using 530/25 nm and 590/20 nm as excitation and detection wavelengths, respectively.

2.7. In silico docking of pyronaridine

The development of the homology model created for *Mtb* topoisomerase I has been described previously [24,25]. Docking was performed on this model in Discovery Studio version 4.1 (Biovia, San Diego, CA) using libdock as described previously [26]. For this study we also docked pyronaridine into RNA polymerase (5UHG) at the D-AAP1 site [35], sphere size 8.36 Å, using the same protocol.

2.8. Gyrase enzymatic assays

Mtb and Escherichia coli DNA gyrase supercoiling assays were carried out as described previously [36,37]. For IC_{50} determinations, compounds, dissolved in DMSO, were included in supercoiling assays at a range of concentrations; the final DMSO concentration was kept < 5%.

2.9. Topoisomerase I assay

The relaxation of supercoiled pUC18 DNA was carried out as described previously [38]. Briefly, 500 ng DNA was incubated with 1 unit

of *Mtb* topoisomerase I (MttopoI) for 30 min at 37 °C in buffer containing 40 mM Tris·HCl (pH 8.0), 20 mM NaCl, 5 mM $MgCl_2$ and 1 mM EDTA. Enzyme inhibition assays were carried out with a preincubation of the enzyme and various concentrations of the compounds at 37 °C for 15 min, followed by the addition of the substrate DNA. After incubating at 37 °C for 30 min, the samples were electrophoresed in a 1.2% agarose gel for 12 h at 2.5 V/cm, stained with ethidium bromide (0.5 μg/mL), and the DNA bands were visualized using a gel documentation system (Bio-Rad, Hercules, CA, USA).

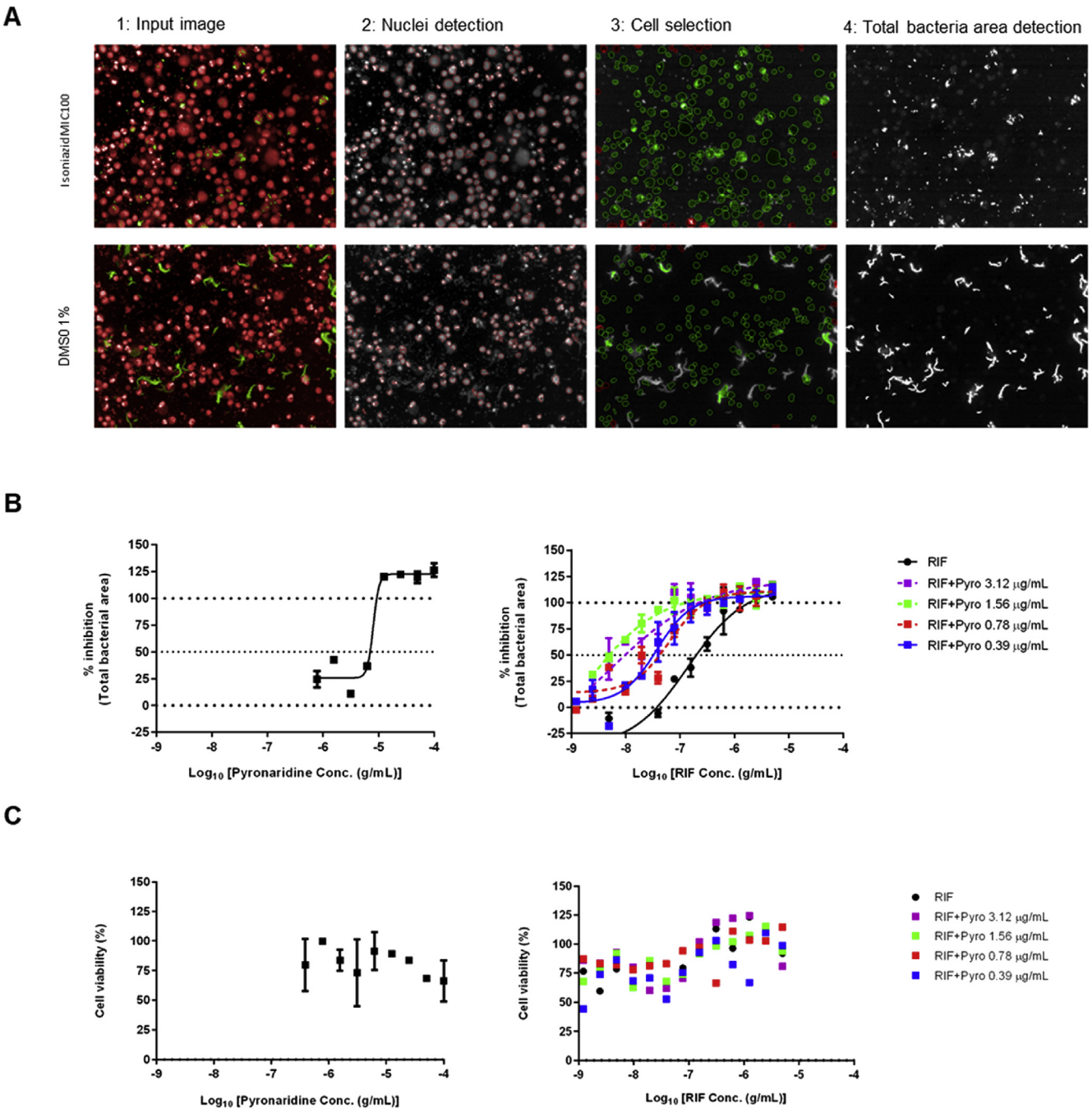

Fig. 1. High content phenotypic infection assay for the determination of pyronaridine effect on *Mycobacterium tuberculosis* replication in THP-1 human macrophages. (A) Steps of the multiparametric image analysis. Cells (nuclei and cytoplasm) were detected by an intensity detection algorithm applied on the Syto60 channel. A spot detection algorithm based on the GFP channel was applied for the detection of *Mtb*-GFP in whole image and in cells and the bacterial intensity and area in pixels were measured. The bacterial replication was quantified by the total bacterial area (pixel) per well. Experiments have been carried out in duplicate. Fitting was performed by Prism software using the sigmoidal dose – response (variable slope) model. 1: Typical 2-color image; 2 and 3: Circled objects correspond respectively to detected nuclei and detected cells, 4: Filled white objects correspond to total bacteria area. (B) Effects of rifampicin and pyronaridine combinations on inhibition of bacterial replication in PMA-differentiated THP-1 macrophages. The parameter used as a read-out was the area of bacteria present per well. Normalizations were performed based on the average values obtained for the negative (DMSO 1%) and positive (isoniazid 10 μg/mL) controls. Percentage of inhibition is plotted against the log10 of the rifampicin (RIF) concentration, determined in the absence or in the presence of pyronaridine (Pyro) at different concentrations. (C) Effects of rifampicin and pyronaridine combinations on THP-1 macrophage viability. Cell viability was measured by comparison to the average value obtained for the positive control (isoniazid 10 μg/mL). Experiments were carried out in duplicate.

2.10. RNA polymerase assay

The specific activity of *Mtb* RNA polymerase was determined by promoter non-specific transcription assay using calf thymus DNA as template. RNA polymerase and different concentration of compounds (rifampicin or/and pyronaridine) were preincubated at 37 °C for 10 min followed by addition of reaction buffer (40 mM Tris/HCl, pH 8.0, 10 mM MgCl $_2$, 1 mM Na_2 EDTA, 14 mM β-mercaptoethanol, 200 μM NTPs, 20 μCi (740 kBq) [^{3}H] UTP ml $^{-1}$ and 15 μg calf thymus DNA ml $^{-1}$). The reactions were carried out at 37 °C for 30 min and stopped by spotting on Na_2 EDTA-soaked DE81 filter papers. Filters were washed twice with 5% Na_2HPO_4 for 15 min each and then rinsed with ethanol. The filter paper was dried and the [^{3}H] UMP incorporation was measured by liquid scintillation counting. Specific activities of the RNA polymerases were expressed as nmoles [^{3}H] UMP incorporated per mg protein in 30 min [39].

2.11. InhA enzymatic assay

The expression and purification of recombinant *Mtb* InhA were performed as previously described [40]. The substrate 2-*trans*-octenoyl-CoA was synthesized from 2-*trans*-octenoic acid and coenzyme A via anhydride formation following acylation, as previously described [41]. Compounds were dissolved in 100% DMSO. The enzyme reaction contained 30 mM PIPES pH 7.5, 50 mM NaCl and 0.1 mM EDTA. InhA (100 nM) was preincubated for 10 min at room temperature with 0.250 mM NADH and compounds at a final concentration of 1% (v/v) DMSO in 150 μL reaction volume. The reaction was started by the addition of 2-*trans*-octenoyl-CoA at a final concentration of 1.5 mM. Depletion of NADH was followed by measuring the absorbance of NADH (340 nm) in the reaction for 20 min using a spectrophotometer plate reader (CLARIOstar - BMG LABTECH). Inhibition percentage and IC_{50} values were calculated based on the initial rates of reaction.

2.12. iniBAC promoter induction assay

A *Mycobacterium bovis* BCG strain harboring *iniBAC* promoter fused to mWasabi was grown to OD_{595} = 0.2. Pyronaridine was plated in 96-well black well plates in quadruplet at 0, 10, 50 and 100 μM using an Echo® 555 liquid handler (Labcyte, San Jose, CA) maintaining equal amounts of DMSO (0.5 μl) in each sample, followed by addition of 200 μl of BCG strain. The wasabi fluorescence was read at 0, 24 and 48 h post treatment. Fold induction was calculated as ratio with DMSO only control.

2.13. Metabolic labeling

Metabolic labeling was performed with *Mtb* H37Ra strain, for which the MIC for pyronaridine was established by REMA to be 37.5 μM. The macromolecular synthesis (MMS) assay was performed in a microplate format. Pre-culture of *Mtb* H37Ra was grown in complete Middlebrook 7H9 broth (BD biosciences), supplemented with albumin-dextrose-catalase (10%) and 0.05% Tween 80 to OD_{600} 0.4. After harvesting of the cells by 10 min centrifugation at 4000 × g and room temperature and their washing with Sauton medium under the same conditions, the bacteria were suspended to a final OD_{600} = 0.5 in Sauton medium. 100 μL of the culture was added to the wells of 96-well plate containing the drugs aliquoted in 2 μL DMSO (streptomycin was dissolved in water). The control drugs were used in 10 × MIC values for *Mtb* H37Ra; i.e., 0.05 μg/mL for rifampicin (RIF) and 5 μg/mL for streptomycin (STR), while pyronaridine was used at 8 × MIC and 4 × MIC. This was followed by the addition of the radioactive substrates ^{14}C-uracil (ARC, specific activity 53 mCi/mmol), ^{14}C-L-leucine (Moravek Biochemicals, specific activity 328 mCi/mmol) or ^{14}C-acetate (ARC, specific activity 106 mCi/mmol), in the final concentrations 1.5 μCi/ml, 0.5 μCi/ml and 1.0 μCi/ml, respectively. After 3 h of incubation at 37 °C the cultures were transferred from the wells into equal volume of ice-cold 10% TCA and the mixtures were precipitated on ice for 1 h. The precipitates were collected by 20 min centrifugation at 14,000 × g and 4 °C and washed 2 times with 5% TCA. The final pellets were suspended in 100 μL of water and incorporated radioactivity was quantified by scintillation counting.

Large-scale ^{14}C-acetate metabolic labeling of *Mtb* H37Ra was performed in Middlebrook 7H9 broth (BD biosciences), supplemented with albumin-dextrose-catalase (10%) and 0.05% Tyloxapol at 37 °C. The culture was grown until OD_{600} reached ~0.2. Pyronaridine in the final concentration 8 × MIC was then added from DMSO stock (final concentration of DMSO in the culture was 1%). Radiolabelling with ^{14}C-acetate (ARC, specific activity 106 mCi/mmol) in the final concentration 0.5 μCi/ml was performed for 3 or 24 h, after 1 or 24 h of drug pretreatment. Three aliquots corresponding to 2 mL of culture of OD_{600} 0.5 were harvested from each control and drug-treated cultures and these were used for extraction of DNA, proteins and lipids.

DNA was extracted by Bacterial DNA extraction Kit (BioTeke Corporation, Beijing, China) according to the manual with a few modifications: (i) the cells were inactivated by heating 10 min at 95 °C prior to each extraction; (ii) incubation with Lysozyme was performed at 37 °C for 2 h and deproteinisation with Proteinase K at 70 °C for 1 h; (iii) DNA was eluted with 50 μL of elution buffer. Extracted DNA was dried in a vacuum concentrator and resuspended in 20 μL ddH_2O. 2 μL were used for scintillation counting and the rest was loaded onto a 0.7% agarose gel. After separation, DNA was transferred on a nylon membrane (Hybond^{TM}-N$^+$ (Amersham)) by an alkaline transfer using 0.4 M NaOH. Dried membranes were exposed to autoradiography film Biomax MR-1 (Kodak) at −80 °C for 1 month.

Proteins were precipitated with 10% TCA as described above. Final pellets were suspended in 500 μL of ddH_2O and 10 μL were analyzed by SDS-PAGE followed by Western blotting. The membrane was exposed to autoradiography film Biomax MR-1 (Kodak) at −80 °C for 8 d. The proteins were visualized by staining with Ponceau S.

Lipids were extracted as described previously [42] and dissolved in 100 μL of Solvent I (see below). 5 μL aliquots of the lipid extracts were analyzed by TLC on silica gel plates (Merck) in Solvent I: $CHCl_3$/CH_3OH/NH_4OH/H_2O (65:25:0.5:4); Solvent II $CHCl_3$/CH_3OH/H_2O (20:4:0.5); and Solvent III: petroleum ether/ethyl acetate (98:2; 3 times). After chromatography, the plates were exposed to autoradiography film (BioMax MR) at −80 °C for 8 d.

2.14. Protein expression reporter assay

Mycobacterium bovis BCG expressing mWasabi under constitutive *hsp60* promoter was grown (OD_{595} = 0.3–0.4). The compounds were plated in 96-well black clear bottom plates using Echo® 555 liquid handler in quadruplicates. To each well 200 μl of BCG culture was added and mWasabi fluorescence was read at 0 h and subsequent time points using Synergy Neo 2 multi-mode plate reader (BioTek, Winooski, VT, USA).

3. Results

3.1. In vitro activity of pyronaridine against mycobacteria and ESKAPE bacteria

Several antimalarial compounds (mefloquine, pyronaridine, chloroquine and amodiaquine) were tested for their *in vitro* activity against *Mtb* alongside isoniazid as a positive control. Pyronaridine had weaker activity against *Mtb* than isoniazid, with an MIC of 5 μg/mL, whilst the other compounds were not active with an MIC ≥ 20 μg/mL (Fig. S1; Table 1). The MIC of pyronaridine against *M. smegmatis* was 15.54–31.08 μg/mL (Table 1, Fig. S2) [26]. Additionally, we found that pyronaridine exhibited an MIC > 25 μg/mL versus relevant strains of *E. cloacae*, *S. aureus*, *K. pneumoniae*, *A. baumannii*, *P. aeruginosa*, and *E. faecium*.

Table 1
In vitro activity against *Mtb* H37Rv and *M. smegmatis* of selected antimalarial compounds.

Compounds	MIC in *M. tuberculosis* H37Rv (μg/ml)
Mefloquine	20
Pyronaridine	5
Chloroquine	> 20
Amodiaquine	> 20
Isoniazid (Control)	0.05

3.2. Ex vivo activity of pyronaridine

The efficacy of pyronaridine was next investigated with an intracellular model of *Mtb* infection. To this end, we resorted to a fluorescence image-based assay for the monitoring of pyronaridine activity against a 5-day growth of *Mtb* H37Rv-GFP within human PMA-differentiated THP-1 and murine RAW264.7 macrophages. As expected [32], the MIC of rifampicin was 0.1 μg/mL (Fig. 1B and Fig. S4A). Pyronaridine displayed an MIC of.12.5 μg/mL in human THP-1 macrophages (Fig. 1B) and was devoid of cytotoxicity in human macrophages (Fig. 1C). On the other side, it did not have any effect on intracellular growth up to 3.1 μM in murine macrophages (Fig. S4A) and showed cytotoxicity for higher concentrations (Fig. S4B).

Interestingly, the presence of sub-inhibitory concentrations of pyronaridine (1.56 and 3.12 μg/ml) increased the *Mtb* susceptibility to rifampicin in human macrophages, resulting in a 16-fold decrease in the MIC. The FICI was calculated to quantify the effect of pyronaridine on growth inhibition by rifampicin. And FICI values ranging from 0.19–0.31 were obtained indicating a synergistic relationship (synergy when FICI < 0.5). We also performed BRAID analysis with these data [43] (Fig. S5), which also suggests this combination is synergistic (κ = 3.91).

3.3. Efflux studies

First, we determined the MIC of pyronaridine against three *Mtb* knockout mutants, each carrying a deletion in a specific gene encoding an efflux pump protein previously reported to be involved in drug susceptibility, virulence and other bacterial processes: Tap [44–48], P55 [49,50], and Mmr [51]. All these efflux mutants presented the same level of susceptibility to pyronaridine as the parental WT strain *Mtb* H37Rv, hence excluding any likely role of Tap, P55 or Mmr efflux pumps in the transport of this drug.

Since *Mtb* has many other putative drug efflux pumps [52] we next explored the possibility of general inhibition of efflux pumps to check whether this could lead to an increase of the activity of pyronaridine [53]. We found that all five efflux pump inhibitors that were tested were incapable of decreasing the whole-cell activity of pyronaridine. This suggested that efflux does not play a major role in susceptibility to this drug.

Pyronaridine has been described as a modulator of the activity of P-glycoprotein [54]. Other compounds having inhibitory activity of P-glycoprotein, such as reserpine and verapamil, are frequently used as global efflux inhibitors in laboratory conditions [53]. Hence, we tested whether pyronaridine could modulate efflux. Pyronaridine at concentrations equal to one-half and one-fourth of its MIC decreased the accumulation of ethidium bromide, whereas verapamil at the same concentrations readily increased the accumulation of ethidium bromide (Fig. S3). This suggests that pyronaridine is not likely to be an efflux inhibitor.

3.4. Searching for the pyronaridine target(s)

To find the pyronaridine target, spontaneous *Mtb* colonies resistant to pyronaridine (ranging from 5 to 10-fold MIC) were isolated, but unfortunately the resistance profile was not confirmed (data not shown).

Table 2
Pyronaridine activity against wild type and drug resistant mutants of *Mtb*.

Mtb strains	MIC (μg/mL)		References
	Pyronaridine	INH	
H37Rv	5–10	0.025	–
NTB1 (*dprE1*, G387S)	5–10	0.025	[55]
DR1 (*mmpL3*, V681I)	5–10	0.025	[56]
88.7 (*pyrG*, V186G)	5–10	0.025	[57]
53.3 (*Rv2466c*, W28S)	5–10	0.025	[58]
Ty1 (*Rv3405c*, c190t)	5–10	0.025	[87]
81.10 (*ethA*, D1109-37)	5–10	0.025	[57]
IC1 (resistant to STR, INH, RIF, EMB)	40	> 0.2	[59]
IC2 (resistant to STR, INH, RIF, EMB, PZA, ETH, CAP)	40	> 0.2	[59]

Table note: STR: streptomycin, INH: isoniazid, RIF: rifampicin, EMB: ethambutol, PZA: pyrazinamide, ETH: ethionamide, CAP: capreomycin, FQ: fluoroquinolones.

With the same purpose, a panel of *Mtb* mutants (Table 2) harboring different known mutations in genes encoding for drug targets (NTB1, DR1, 88.7) [55–57], activators (53.3 and 81.10) [57,58], and inactivator (Ty1) [58] was used to study the mechanism of action of pyronaridine. All *Mtb* mutants were sensitive to pyronaridine suggesting that the mechanism of action was different than that investigated.

Finally, pyronaridine was tested against two MDR *M. tuberculosis* clinical isolates, resistant to isoniazid, rifampicin, ethambutol and streptomycin [59]. Interestingly, these clinical isolates were fully resistant to pyronaridine. An additional clinical MDR strain resistant to all four first line drugs harboring the rpoB-S450L mutation in the rifampicin resistance determining region (RRDR) was fully susceptible to pyronaridine on its own and showed comparable growth inhibition curve (Fig. S6). Further enzymatic and metabolic assays were performed to try to elucidate the mechanisms of action and resistance to pyronaridine in *Mtb*.

3.5. Enzymatic assay with InhA

As the initial MDR clinical isolates (Table 2) were resistant to both pyronaridine and INH we considered enoyl-ACP reductase (InhA) as a possible target for pyronaridine. Inhibition of purified InhA by pyronaridine was studied in triplicate at a final concentration of 100 μM using triclosan as a positive control [60]. InhA was ruled out as a target for pyronaridine, as the compound did not show any inhibitory effect at this concentration.

3.6. iniBAC promoter induction assay

The *iniBAC* promoter has been shown to be induced by cell wall inhibitors in *Mtb*. We tested pyronaridine for induction of *iniBAC* using a promoter-reporter strain. We did not observe any significant induction of the *iniBAC* promoter with this compound suggesting a mechanism of action that may not be involving effects on cell wall biosynthesis.

3.7. Enzymatic assay with topo I

Pyronaridine was previously docked in the homology model of topo I (LibDock score 126.85) and when tested *in vitro* exhibited a weak inhibition of the relaxation activity of MttopoI at IC_{50} 25.9 μg/mL (Fig. 2). This value is higher than the MIC for pyronaridine.

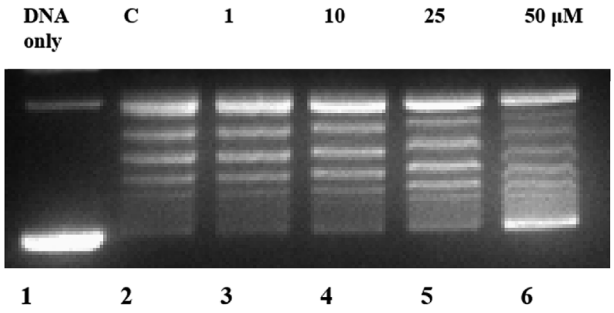

Fig. 2. Inhibitory activity of pyronaridine. 1 unit of MttopoI was incubated with increasing concentrations of the molecule at 37 °C for 15 min following which, 500 ng of supercoiled pUC18 was added. The incubation was further continued at 37 °C for 30 min and the reaction was terminated by addition of 0.6% SDS-agarose dye. The reaction products were resolved on a 1.2% agarose gel followed by staining with EtBr. Lane 1, supercoiled pUC18; lane 2, relaxation control; lanes 3–6, increasing concentration of pyronaridine.

3.8. Enzymatic assays with DNA gyrase

DNA gyrase was explored as a possible pyronaridine target using a series of antimalarial aminoquinoline compounds and testing their ability to inhibit the supercoiling reaction of DNA gyrases from *Mtb* and *E. coli* (Fig. 3, Table 3 and Supplemental Table 1). We found that pyronaridine is modestly active (IC_{50} 25 μM; 23 μg/mL) against *Mtb* gyrase. The compound was similarly active *versus E. coli* gyrase. An approximate five-fold increase in IC_{50} from the MIC for pyronaridine suggests that DNA gyrase is not the pyronaridine primary target. Mefloquine showed the same activity *versus E. coli* gyrase as pyronaridine (IC_{50} = 25 μM; 10 μg/mL), but was relatively inactive against *Mtb* gyrase (IC_{50} > 100 μM; > 40 μg/mL). Chloroquine, primaquine, quinine, halofantrine, amodiaquine, lumefantrine and quinoline and several other analogs were inactive against gyrase like isoniazid, which was used as a negative control (IC_{50} > 100 μM).

Under appropriate conditions, quinolone drugs, such as ciprofloxacin, can stabilize a cleaved complex between gyrase and DNA [61,62]. We have assessed whether pyronaridine can stabilize a cleavage complex between gyrase and DNA and have found no evidence that it does (data not shown). This suggests that pyronaridine does not bind the enzyme at the quinolone pocket, i.e. its weak activity likely results from binding elsewhere on the enzyme, potentially suggesting a novel binding site outside of the well-known quinolone pocket.

3.9. Metabolic labeling with ^{14}C precursors

For evaluation of potential interference of pyronaridine with the metabolism of nucleic acids, which could be caused by inhibition of DNA gyrase, we performed macromolecular synthesis assays with ^{14}C precursors in *Mtb* H37Ra. In the initial experiment, we monitored the incorporation of ^{14}C-uracil, ^{14}C-leucine and ^{14}C-acetate into TCA-precipitated material after 3 h of radiolabeling. A severe decrease in incorporation of ^{14}C-uracil into the TCA-precipitated material, similar to the effect of rifampicin, a known inhibitor of RNA polymerase, indeed pointed to inhibition of metabolism of nucleic acids (Fig. 4A). Streptomycin was used as a control inhibitor affecting protein synthesis. While it did not show any effects on ^{14}C-uracil incorporation, the antibiotic decreased radiolabeling of proteins with ^{14}C-leucine by about 50% (Fig. 4B). Although pyronaridine caused even higher inhibition of ^{14}C-leucine-radiolabeling of the cells, rifampicin triggered a similar response. Therefore, we attributed these changes to secondary effects of these drugs. ^{14}C-acetate radiolabeling can be considered as a tool for monitoring overall metabolic activity in the treated bacteria. As shown in Fig. 4C, under the conditions used for radiolabeling, there was only a minor inhibition of incorporation of this precursor to the mycobacterial cells treated with the drugs, and thus we consider the changes observed for pyronaridine and the control drugs in the ^{14}C-uracil and ^{14}C-leucine radiolabeling experiment related to their cellular targets.

To investigate the effects of pyronaridine on *Mtb* H37Ra in more detail we performed ^{14}C-acetate labeling under three different conditions: (i) 1 h drug treatment followed by 3 h radiolabeling; (ii) 1 h drug treatment followed by 24 h radiolabeling; and (iii) 24 h drug treatment followed by 24 h radiolabeling. While 3 h of ^{14}C-acetate treatment did not appear to label DNA, 24 h incubation of mycobacteria in the presence of ^{14}C-acetate resulted in its incorporation to DNA and revealed its inhibition in the presence of pyronaridine (Fig. S7A). At the same time, we confirmed severe inhibition of labeling of the proteins in all three conditions (Fig. S7B). Lipids extracted from the radiolabeled cultures were analyzed by TLC. The gradual decrease in incorporation of ^{14}C-acetate into lipids with the duration of exposure to the drug very likely reflects down-stream effects caused by prolonged treatment of the cells with the drug, which affects primarily synthesis of nucleic acids and consequently also proteins (Fig. S7C). These macromolecular synthesis assays directed us to explore RNA polymerase as a potential target for pyronaridine.

3.10. Protein reporter assays

M. bovis strain constitutively expressing mWasabi reporter was exposed to pyronaridine and time-dependent effects of fluorescence were studied. The time course experiment showed that pyronaridine treatment abrogated synthesis of new mWasabi molecules similar to inhibition by rifampicin, a known inhibitor of RNA Polymerase (Fig. S8) suggesting that this compound may putatively inhibit a step in protein biosynthesis and was consistent with inhibition of ^{14}C-Leucine incorporation (Fig. 4B).

3.11. Is RNA polymerase the cellular target of pyronaridine?

The crystal structure of *Mtb* RNA polymerase shows the potential for two ligands, with rifampicin and the non-rifampicin-related compound Nα-aroyl-N-aryl-phenylalaninamide (AAP) D-AAP1 bound to two independent sites (Fig. 5) [35]. Docking of pyronaridine in the same site as D-AAP1 showed multiple potential interactions, including a cation-π and two parallel displaced π-stacking interactions with residues R834 and F350/H854, respectively, along with other hydrophobic interactions.

Following this docking study, we tested pyronaridine as a potential inhibitor of *Mtb* RNA polymerase *in vitro*. Pyronaridine on its own showed no inhibition of this enzyme (Fig. S9). However, when pyronaridine is combined with rifampicin at 10% MIC approximately ~50% inhibition of *Mtb* RNA-polymerase activity is observed (Fig. 6). This suggests that both compounds can bind RNA polymerase simultaneously, likely in different binding pockets.

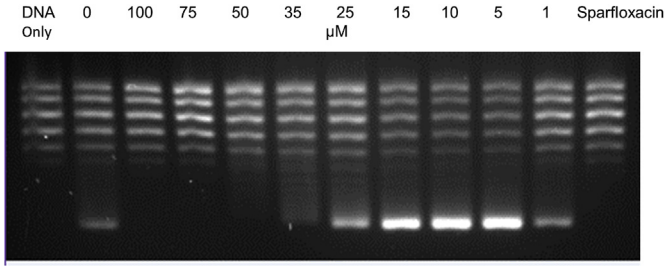

Fig. 3. Inhibition of DNA supercoiling by *Mtb* gyrase by pyronaridine. DNA supercoiling assays were carried out as described previously [36]; the amount of enzyme used was adjusted to give incomplete supercoiling to increase the sensitivity of the assay. All lanes contain gyrase except the first, which contains substrate only (relaxed pBR322 DNA). The last lane contains a control inhibitor (sparfloxacin (200 μM); concentrations of pyronaridine are indicated above the lanes.

Table 3
Screening of select antimalarial compounds against DNA gyrase.

Compound	Gyrase IC_{50} μM (μg/ml)[a]	
	Mtb	*E. coli*
Pyronaridine	25 (23)	25 (23)
Chloroquine	> 100 (> 50)	> 100 (> 50)
Mefloquine	> 100 (> 40)	25 (10)
Amodiaquine	> 100 (> 45)	> 100 (> 45)
Isoniazid (Control)	> 100 (> 15)	> 100 (> 15)

[a] IC50 values for inhibition of gyrase-catalyzed supercoiling for compounds are given in μM and μg/mL (in parentheses); isoniazid is included as a control.

3.12. Drug combination studies

Combination studies were performed using pyronaridine at 2.5 μg/mL to check any impact of this drug on the MICs of isoniazid, rifampicin or ciprofloxacin (Table 4). In the case of isoniazid and ciprofloxacin, no changes in the MICs were observed versus the MIC of either drug alone suggesting a lack of interaction between pyronaridine and InhA and gyrase inhibitors. Interestingly, pyronaridine at 2.5 μg/mL reduced the MIC of rifampicin between 2- and 4-fold. This interaction between rifampicin and pyronaridine was further investigated by using the checkerboard assay; calculated FICI index ranged between 0.355 and 0.748, indicating a rather moderate synergism between these two drugs *in vitro*. These FICI values are on the same range as those obtained in *Mtb* infected macrophages, hence corroborating that both drugs synergize to a moderate level.

4. Discussion

Pyronaridine is a potent [21,63,64] antimalarial that is approved in the EU as part of a combination therapy [22]. There have been several efforts to ascertain the target of pyronaridine in malaria (including: interference with the digestive system in *P. falciparum* and *Plasmodium berghei* [65], inhibition of β-haematin to enhance haematin-induced human blood cell lysis [66,67], inhibition of glutathione-dependent haem degradation [66,68]) and hemozoin synthesis which have all been reviewed [22]. These mechanisms are shared by aminoquinolines such as chloroquine [69]. Interestingly, while several groups work on both malaria and tuberculosis [70], the literature is silent on the activity of pyronaridine against *Mtb* and potential targets for it. Recent studies have demonstrated that pyronaridine possesses *in vivo* activity against *Trypanosoma cruzi*, the causative agent of Chagas disease [22] and that in human peripheral blood monocytes from controls and Chagas disease patients it results in increased TNFα $+CD8^+$, IL-10 + and $CD8^+$ [71]. Pyronaridine is also active against *Babesi*a spp. parasite [72] and against the Ebola virus [73]. As this molecule has already been approved in the EU this may have a more direct path to clinical testing for these and potentially other diseases.

In this study, it was demonstrated that pyronaridine has modest to weak activity against *Mtb in vitro* (Table 1, Table 2, Fig. 1), but no activity against ESKAPE pathogens. The possible *Mtb* inhibition mechanism of action was studied. Two *Mtb* clinical isolates resistant to isoniazid, rifampicin, ethambutol and streptomycin were found to be resistant to pyronaridine, while a clinical MDR strain resistant to all four first line drugs harboring rpoB-S450L mutation in the rifampicin resistance determining region (RRDR) retained its sensitivity to pyronaridine. Interestingly, in macromolecular synthesis assays, treatment with pyronaridine resulted in a severe decrease in incorporation of ^{14}C-uracil and ^{14}C-leucine similar to the effect seen with rifampicin (Fig. 4). This finding could point to the interference with the metabolism of nucleic acids in mycobacteria (Table 2).

Most bacteria contain two type II topoisomerases: DNA gyrase and DNA topoisomerase IV; *Mtb* being an exception: it only has a gyrase, which exhibits topoisomerase IV-like properties (e.g. higher decatenation activity compared with other gyrases) [74,75]. As *E. coli* possesses both gyrase and topoisomerase IV we also tested pyronaridine (and other selected aminoquinoline compounds) against *E. coli* topoisomerase IV and found higher activity against this enzyme (IC_{50} = ~0.1 μM for pyronaridine) than was found for gyrase. The interaction of aminoquinolines with Gram-negative topoisomerase IVs will be the subject of future work. Interestingly, pyronaridine has been previously suggested to possess decatenation activity (11 μM) against *Plasmodium falciparum* DNA topoisomerase II activity *in vitro* [76]. Recent work has also suggested that DNA gyrase in *Mtb* functions as a decatenase and that RNA polymerase and topoisomerases have a functional association [77]. Our work perhaps provides some evidence for the importance of targeting (even at a very low level) DNA gyrase and DNA topoisomerase I [78], as their IC_{50} values were broadly similar. Additionally, pyronaridine and rifampicin similarly decrease the incorporation of ^{14}C-uracil and ^{14}C-leucine eluding to a similar mechanism (Fig. 4). This initially suggested to us the potential that pyronaridine may target RNA polymerase as this is also the known target of rifampicin. The targeting of RNA polymerase is important because mutations in the rifampicin binding site can lead to resistance to this widely used drug. A recent study has described RNA polymerase transcription initiation complexes with rifampicin and a non-rifampicin RNA polymerase inhibitor [35]. The non-rifampicin molecule binds on the N-terminus of the RNA polymerase bridge helix and aromatic residues interacted with three subsites. When the residues in these sites were substituted rifampicin resistance was observed. Pyronaridine when docked into this pocket was found to overlap this non-rifampicin compound (Fig. 5B) with a Libdock score of 144.1 which surpasses the best dock in the rifampicin site (126.6). The potential for directly targeting *Mtb* RNA polymerase was experimentally verified with the combination of pyronaridine and

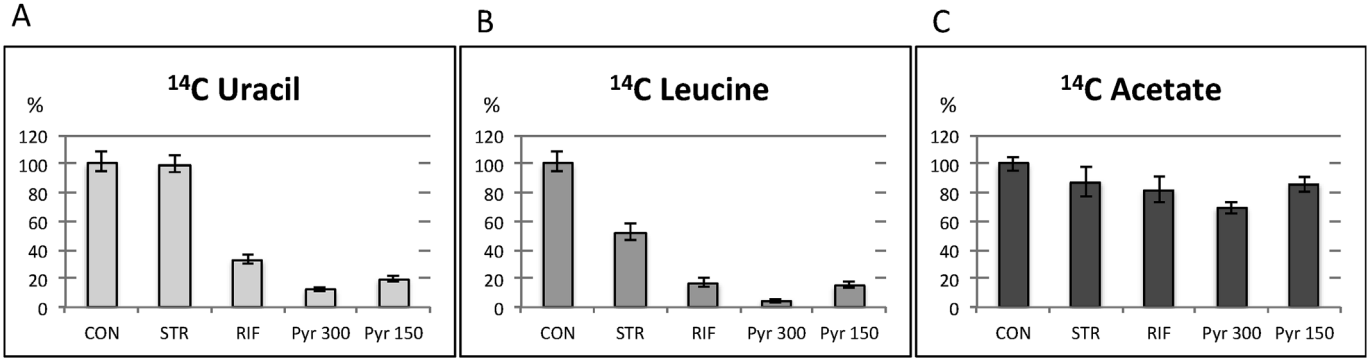

Fig. 4. Macromolecular synthesis assays with *Mtb* H37Ra. The experiment was performed in 96-well plates. ^{14}C-uracil and ^{14}C-L-leucine labeling was carried out in triplicates and ^{14}C-acetate in duplicates, the values represent averages with standard errors. Pyronaridine (Pyr) was used in the final concentrations 300 μM (8 × MIC) and 150 μM (4 × MIC), streptomycin (STR) at 5 μg/ml (10 × MIC) and rifampicin (RIF) at 0.05 μg/ml (10 × MIC).

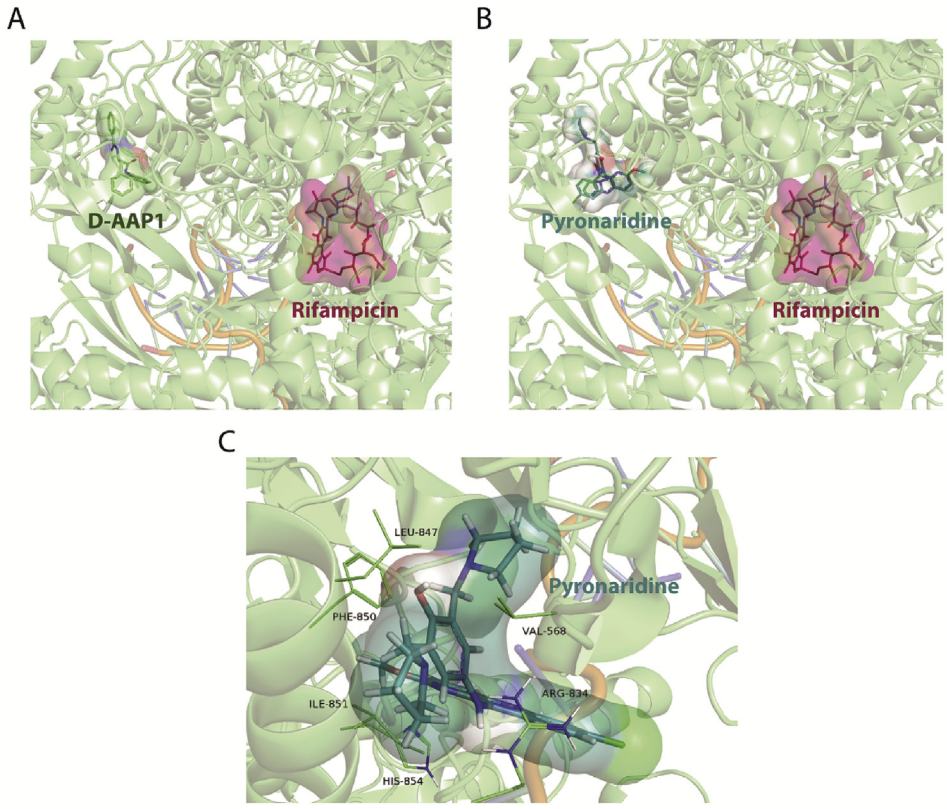

Fig. 5. Docking of pyronaridine in RNA-polymerase. The crystal structure of Mtb RNA-polymerase (5UHG, green) shows the potential for two ligands, rifampicin (red) and the non-Rif-related compounds-Nα-aroyl-N-aryl-phenylalaninamide (AAP) D-AAP1 (light green), to bind to two independent sites (A). Rifampicin and pyronaridine (cyan) are synergistic, in a similar manner as rifampicin and D-AAP1, so if Mtb RNA-polymerase is the target of pyronaridine it is likely to bind to the D-AAP1 site (B). The rigid docking of pyronaridine into RNA-polymerase using the program libdock generated a score of 144.10, suggesting numerous interactions between the ligand and the enzyme. The dock of pyronaridine proposes several potential interactions with RNA-polymerase, including a cation-π and two parallel displaced π-stacking interactions with residues R834 and F350/H854, respectively, along with other hydrophobic interactions (C).

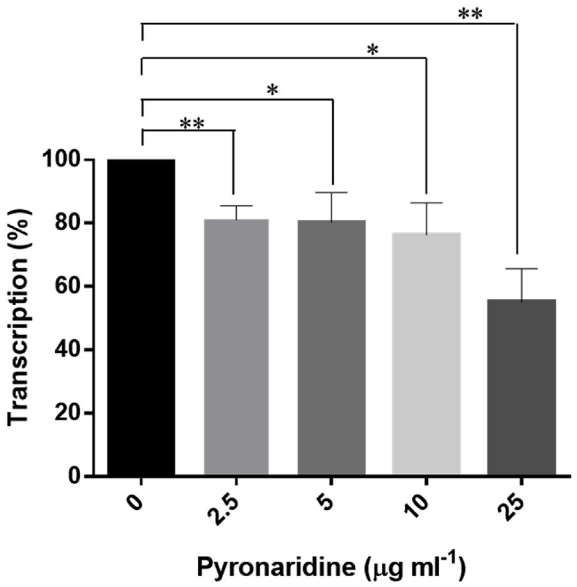

Fig. 6. Inhibition of *M. tuberculosis* RNAP activity by Pyronaridine in the presence of Rifampicin (10% MIC). Transcription assays carried out in the presence of rifampicin (10% MIC) along with increasing concentration of pyronaridine (0–25 μg/ml). The transcription in the presence of 10% MIC of rifampicin without pyronaridine is considered as 100%. The experiment was carried out three times and error bars indicate sd. Unpaired *t*-test was used for statistical analysis. P-value < 0.05 was considered as significant. * ≤ 0.05, ** ≤ 0.01.

rifampicin (Fig. 6) versus the lack of activity of pyronaridine on its own (Fig. S9) at concentrations up to 100 μg/ml. Different binding pockets in RNA polymerase are also supported by our MDR mutant resistant to all four first line drugs harboring the rpoB-S450L mutation (Fig. S6) which retained pyronaridine activity. While rifampicin alone was not effective against this isolate at the concentrations tested (Fig. S6), pyronaridine has a slightly reduced EC_{50} in the clinical strain as compared to the wild-type H37Rv strain. Taken as a whole, these data suggest that when rifampicin and pyronaridine are administered simultaneously they both act by inhibiting RNA polymerase via binding to unique binding pockets. This is similar to data found with rifampicin and DAAP-1, which were additive and bound to unique sites within RNAP [35]. Pyronaridine therefore represents a compound that is already clinically accessible, compared with DAAP-1, and thus could be used to test the viability of a therapy to suppress rifampicin resistance emergence as well as potentially return rifampicin sensitivity to resistant strains.

Following these observations, the most interesting finding of this current work was the *in vitro* and *ex vivo* synergy between rifampicin and pyronaridine. It remains to be seen whether this will also be reflected *in vivo,* but if so it could lower the effective dose of rifampicin (e.g. as shown in Fig. 6), mitigating side effects, and the length of treatment. This represents an example of drug repurposing to lead to a potential clinical candidate in the form of pyronaridine when used in conjunction with rifampicin. There are other examples of compounds showing synergy with rifampicin although their targeting of RNA polymerase is unknown (biapenem [79], faropenem [80], 2-(quinolin-4-yloxy)acetamides [81], 2(5H)-furanone-based compounds [82], Indole-2-carboxamide-based MmpL3 Inhibitors [83], timcodar [84], thioridazine [85] and 7-amino-4-methyl-2H-chromen-2-one [86]) and these show FICI values that are in line with what we observed with pyronaridine (Supplemental Table 2).

This work therefore represents a starting point in the study of pyronaridine as new, more active derivatives could be potentially synthesized in order to use them alone or in combination with rifampicin.

Conflicts of interest

SE is founder, owner and an employee of Collaborations Pharmaceuticals Inc.

Table 4
Combination study of pyronaridine and isoniazid, rifampicin or ciprofloxacin.

COMPOUND	MIC (μg/ml)
INH	0.025
INH + PYR (2.5 μg/ml)	0.05
CIPRO	0.125
CIPRO + PYR (2.5 μg/ml)	0.125
RIF	0.0039
RIF + PYR (2.5 μg/ml)	0-0019 - 0.0009

Abbreviations: INH: isoniazid, CIPRO: ciprofloxacin, RIF: rifampicin, PYR: pyronaridine.

Acknowledgments

The work was supported by a grant from the European Community's Seventh Framework Program (Grant 260872). V.N. is a J.C. Bose fellow of Department of Science and Technology, Government of India. Work in A.M.'s lab is also funded by the Biotechnology and Biosciences Research Council (UK) Institute Strategic Programme Grants BB/J004561/1 and BB/P012523/1. K.M. acknowledges support by Ministry of Education, Science, Research and Sport of the Slovak Republic (grant 0395/2016 for Slovak/Russian cooperation in science 2015-15075/33841:1-15E0) and by the Research and Development Operational Programme funded by European Regional Development Fund (Contract ITMS 26240120027). Work in PB.'s lab is also supported from the European Community (ERC-STG INTRACELLTB Grant n° 260901), the Agence Nationale de la Recherche (ANR-10-EQPX-04-01), the Feder (12001407 (D-AL) Equipex Imaginex BioMed) and the Région Nord Pas de Calais (convention n°12000080). J.A. acknowledges support by Ministry of Economy and Competitiveness of Spain (grant SAF-2013-48971-C2-2-R). None of these sponsors had any role in study design; in the collection, analysis and interpretation of data; in the writing of the report; and in the decision to submit the article for publication. S.E. Kindly acknowledges several collaborators for their continued work on pyronaridine including Dr. Mary Lingerfelt, Dr. Peter Madrid, Dr. Robert Davey, Dr. Jair Lage de Siqueira-Neto as well as Dr. Iain Old, Dr. Stewart Cole and our MM4TB colleagues for support and encouragement.

Appendix A. Supplementary data

Supplementary data related to this article can be found at https://doi.org/10.1016/j.tube.2018.08.004.

References

[1] Anon. Global tuberculosis report 2016. 2016http://www.who.int/tb/publications/global_report/en/.
[2] Zignol M, Dean AS, Falzon D, van Gemert W, Wright A, van Deun A, Portaels F, Laszlo A, Espinal MA, Pablos-Méndez A, Bloom A, Aziz MA, Weyer K, Jaramillo E, Nunn P, Floyd K, Raviglione MC. Twenty years of global surveillance of antituberculosis-drug resistance. N Engl J Med 2016;375:1081–9.
[3] Zhang Y. The magic bullets and tuberculosis drug targets. Annu Rev Pharmacol Toxicol 2005;45:529–64.
[4] Ballel L, Field RA, Duncan K, Young RJ. New small-molecule synthetic antimycobacterials. Antimicrob Agents Chemother 2005;49:2153–63.
[5] Zumla AI, Gillespie SH, Hoelscher M, Philips PP, Cole ST, Abubakar I, McHugh TD, Schito M, Maeurer M, Nunn AJ. New antituberculosis drugs, regimens, and adjunct therapies: needs, advances, and future prospects. Lancet Infect Dis 2014;14:327–40.
[6] Ekins S, Perryman AL, Clark AM, Reynolds RC, Freundlich JS. Machine learning model analysis and data visualization with small molecules tested in a mouse model of Mycobacterium tuberculosis infection (2014-2015). J Chem Inf Model 2016;56:1332–43.
[7] Mikusova K, Ekins S. Learning from the past for TB drug discovery in the future. Drug Discov Today 2017;22:534–45.
[8] Riccardi G, Old IG, Ekins S. Raising awareness of the importance of funding for tuberculosis small-molecule research. Drug Discov Today 2016;22:487–91.
[9] Ekins S, Williams AJ, Krasowski MD, Freundlich JS. In silico repositioning of approved drugs for rare and neglected diseases. Drug Discov Today 2011;16:298–310.
[10] Ekins S, Williams AJ. Finding promiscuous old drugs for new uses. Pharm Res 2011;28:1786–91.
[11] Aliper A, Plis S, Artemov A, Ulloa A, Mamoshina P, Zhavoronkov A. Deep learning applications for predicting pharmacological properties of drugs and drug repurposing using transcriptomic data. Mol Pharm 2016;13:2524–30.
[12] Djaout K, Singh V, Boum Y, Katawera V, Becker HF, Bush NG, Hearnshaw SJ, Pritchard JE, Bourbon P, Madrid PB, Maxwell A, Mizrahi V, Myllyjallio H, Ekins S. Predictive modeling targets thymidylate synthase ThyX in Mycobacterium tuberculosis. Sci Rep 2016;6:27792.
[13] Lamb J, Crawford ED, Peck D, Modell JW, Blat IC, Wrobel MJ, Lerner J, Brunet JP, Subramanian A, Ross KN, Reich M, Hieronymus H, Wei G, Armstrong SA, Haggarty SJ, Clemons PA, Wei R, Carr SA, Lander ES, Golub TR. The Connectivity Map: using gene-expression signatures to connect small molecules, genes, and disease. Science 2006;313:1929–35.
[14] Lamb J. The Connectivity Map: a new tool for biomedical research. Nat Rev Cancer 2007;7:54–60.
[15] Lougheed KE, Taylor DL, Osborne SA, Bryans JS, Buxton RS. New anti-tuberculosis agents amongst known drugs. Tuberculosis (Edinb) 2009;89:364–70.
[16] Ekins S, Reynolds R, Kim H, Koo M-S, Ekonomidis M, Talaue M, Paget SD, Woolhiser LK, Lenaerts AJ, Bunin BA, Connell N, Freundlich JS. Bayesian models leveraging bioactivity and cytotoxicity information for drug discovery. Chem Biol 2013;20:370–8.
[17] Bermudez LE, Meek L. Mefloquine and its enantiomers are active against Mycobacterium tuberculosis in vitro and in macrophages. Tuberc Res Treat 2014;2014:530815.
[18] Danelishvili L, Wu M, Young LS, Bermudez LE. Genomic approach to identifying the putative target of and mechanisms of resistance to mefloquine in mycobacteria. Antimicrob Agents Chemother 2005;49:3707–14.
[19] Rybniker J, Vocat A, Sala C, Busso P, Pojer F, Benjak A, Cole ST. Lansoprazole is an antituberculous prodrug targeting cytochrome bc1. Nat Commun 2015;6:7659.
[20] Mdanda S, Baijnath S, Shobo A, Singh SD, Maguire GEM, Kruger HG, Arvidsson PI, Naicker T, Govender T. Lansoprazole-sulfide, pharmacokinetics of this promising anti-tuberculous agent. Biomed Chromatogr 2017:31.
[21] Chang C, Lin-Hua T, Jantanavivat C. Studies on a new antimalarial compound: pyronaridine. Trans R Soc Trop Med Hyg 1992;86:7–10.
[22] Croft SL, Duparc S, Arbe-Barnes SJ, Craft JC, Shin CS, Fleckenstein L, Borghini-Fuhrer I, Rim HJ. Review of pyronaridine anti-malarial properties and product characteristics. Malar J 2012;11:270.
[23] Morris CA, Dueker SR, Lohstroh PN, Wang LQ, Fang XP, Jung D, Lopez-Lazaro L, Baker M, Duparc S, Borghini-Fuhrer I, Pokorny R, Shin JS, Fleckenstein L. Mass balance and metabolism of the antimalarial pyronaridine in healthy volunteers. Eur J Drug Metab Pharmacokinet 2015;40:75–86.
[24] Godbole AA, Ahmed W, Bhat RS, Bradley EK, Ekins S, Nagaraja V. Inhibition of Mycobacterium tuberculosis topoisomerase I by m-AMSA, a eukaryotic type II topoisomerase poison. Biochem Biophys Res Commun 2014;446:916–20.
[25] Godbole AA, Ahmed W, Bhat RS, Bradley EK, Ekins S, Nagaraja V. Targeting Mycobacterium tuberculosis topoisomerase I by small-molecule inhibitors. Antimicrob Agents Chemother 2015;59:1549–57.
[26] Ekins S, Godbole AA, Keri G, Orfi L, Pato J, Bhat RS, Verma R, Bradley EK, Nagaraja V. Machine learning and docking models for Mycobacterium tuberculosis topoisomerase I. Tuberculosis (Edinb) 2017;103:52–60.
[27] Palomino JC, Martin A, Camacho M, Guerra H, Swings J, Portaels F. Resazurin microtiter assay plate: simple and inexpensive method for detection of drug resistance in Mycobacterium tuberculosis. Antimicrob Agents Chemother 2002;46:2720–2.
[28] WHO. Global priority list of antibiotic-resistant bacteria to guide research, discovery, and development of new antibiotics. 2017http://www.who.int/medicines/publications/WHO-PPL-Short_Summary_25Feb-ET_NM_WHO.pdf?ua=1.
[29] Balouiri M, Sadiki M, Ibnsouda SK. Methods for in vitro evaluating antimicrobial activity: a review. J Pharmaceut Anal 2016;6:71–9.
[30] Odds FC. Synergy, antagonism, and what the chequerboard puts between them. J Antimicrob Chemother 2003;52:1.
[31] (ESCMID) ESoCMaID. EUCAST Definitive Document E.Def 1.2, May 2000: terminology relating to methods for the determination of susceptibility of bacteria to antimicrobial agents. Clin Microbiol Infect 2000;6:503–8.
[32] Christophe T, Jackson M, Jeon HK, Fenistein D, Contreras-Dominguez M, Kim J, Genovesio A, Carralot JP, Ewann F, Kim EH, Lee SY, Kang S, Seo MJ, Park EJ, Skovierova H, Pham H, Riccardi G, Nam JY, Marsollier L, Kempf M, Joly-Guillou ML, Oh T, Shin WK, No Z, Nehrbass U, Brosch R, Cole ST, Brodin P. High content screening identifies decaprenyl-phosphoribose 2' epimerase as a target for intracellular antimycobacterial inhibitors. PLoS Pathog 2009;5:e1000645.
[33] Song OR, Deboosere N, Delorme V, Queval CJ, Deloison G, Werkmeister E, Lafont F, Baulard A, Iantomasi R, Brodin P. Phenotypic assays for Mycobacterium tuberculosis infection. Cytometry A 2017;91:983–94.
[34] Rodrigues L, Viveiros M, Ainsa JA. Measuring efflux and permeability in mycobacteria. Methods Mol Biol 2015;1285:227–39.
[35] Lin W, Mandal S, Degen D, Liu Y, Ebright YW, Li S, Feng Y, Zhang Y, Mandal S, Jiang Y, Liu S, Gigliotti M, Talaue M, Connell N, Das K, Arnold E, Ebright RH. Structural basis of Mycobacterium tuberculosis transcription and transcription inhibition. Mol Cell 2017;66:169–179 e8.
[36] Karkare S, Yousafzai F, Mitchenall LA, Maxwell A. The role of Ca(2)(+) in the activity of Mycobacterium tuberculosis DNA gyrase. Nucleic Acids Res 2012;40:9774–87.
[37] Reece RJ, Maxwell A. Tryptic fragments of the Escherichia coli DNA gyrase A protein. J Biol Chem 1989;264:19648–53.
[38] Bhaduri T, Bagui TK, Sikder D, Nagaraja V. DNA topoisomerase I from

Mycobacterium smegmatis. An enzyme with distinct features. J Biol Chem 1998;273:13925–32.
[39] Malshetty V, Kurthkoti K, China A, Mallick B, Yamunadevi S, Sang PB, Srinivasan N, Nagaraja V, Varshney U. Novel insertion and deletion mutants of RpoB that render Mycobacterium smegmatis RNA polymerase resistant to rifampicin-mediated inhibition of transcription. Microbiology 2010;156:1565–73.
[40] Quemard A, Sacchettini JC, Dessen A, Vilcheze C, Bittman R, Jacobs Jr. WR, Blanchard JS. Enzymatic characterization of the target for isoniazid in Mycobacterium tuberculosis. Biochemistry 1995;34:8235–41.
[41] He X, Alian A, Stroud R, Ortiz de Montellano PR. Pyrrolidine carboxamides as a novel class of inhibitors of enoyl acyl Carrier protein reductase from Mycobacterium tuberculosis. J Med Chem 2006;49:6308–23.
[42] Esposito M, Szadocka S, Degiacomi G, Orena BS, Mori G, Piano V, Boldrin F, Zemanova J, Huszar S, Barros D, Ekins S, Lelievre J, Manganelli R, Mattevi A, Pasca MR, Riccardi G, Ballell L, Mikusova K, Chiarelli LR. A phenotypic based target screening approach delivers new antitubercular CTP synthetase inhibitors. ACS Infect Dis 2017;3:428–37.
[43] Twarog NR, Stewart E, Hammill CV, Shelat AA. BRAID: a unifying paradigm for the analysis of combined drug action. Sci Rep 2016;6:25523.
[44] Lee RE, Hurdle JG, Liu J, Bruhn DF, Matt T, Scherman MS, Vaddady PK, Zheng Z, Qi J, Akbergenov R, Das S, Madhura DB, Rathi C, Trivedi A, Villellas C, Lee RB, Rakesh, Waidyarachchi SL, Sun D, McNeil MR, Ainsa JA, Boshoff HI, Gonzalez-Juarrero M, Meibohm B, Bottger EC, Lenaerts AJ. Spectinamides: a new class of semisynthetic antituberculosis agents that overcome native drug efflux. Nat Med 2014;20:152–8.
[45] Villellas C, Aristimuno L, Vitoria MA, Prat C, Blanco S, Garcia de Viedma D, Dominguez J, Samper S, Ainsa JA. Analysis of mutations in streptomycin-resistant strains reveals a simple and reliable genetic marker for identification of the Mycobacterium tuberculosis Beijing genotype. J Clin Microbiol 2013;51:2124–30.
[46] Ramon-Garcia S, Mick V, Dainese E, Martin C, Thompson CJ, De Rossi E, Manganelli R, Ainsa JA. Functional and genetic characterization of the tap efflux pump in Mycobacterium bovis BCG. Antimicrob Agents Chemother 2012;56:2074–83.
[47] Ainsa JA, Blokpoel MC, Otal I, Young DB, De Smet KA, Martin C. Molecular cloning and characterization of Tap, a putative multidrug efflux pump present in Mycobacterium fortuitum and Mycobacterium tuberculosis. J Bacteriol 1998;180:5836–43.
[48] Adams KN, Takaki K, Connolly LE, Wiedenhoft H, Winglee K, Humbert O, Edelstein PH, Cosma CL, Ramakrishnan L. Drug tolerance in replicating mycobacteria mediated by a macrophage-induced efflux mechanism. Cell 2011;145:39–53.
[49] Ramon-Garcia S, Martin C, Thompson CJ, Ainsa JA. Role of the Mycobacterium tuberculosis P55 efflux pump in intrinsic drug resistance, oxidative stress responses, and growth. Antimicrob Agents Chemother 2009;53:3675–82.
[50] Martinot AJ, Farrow M, Bai L, Layre E, Cheng TY, Tsai JH, Iqbal J, Annand JW, Sullivan ZA, Hussain MM, Sacchettini J, Moody DB, Seeliger JC, Rubin EJ. Mycobacterial metabolic syndrome: LprG and Rv1410 regulate triacylglyceride levels, growth rate and virulence in Mycobacterium tuberculosis. PLoS Pathog 2016;12:e1005351.
[51] Rodrigues L, Villellas C, Bailo R, Viveiros M, Ainsa JA. Role of the Mmr efflux pump in drug resistance in Mycobacterium tuberculosis. Antimicrob Agents Chemother 2013;57:751–7.
[52] De Rossi E, Ainsa JA, Riccardi G. Role of mycobacterial efflux transporters in drug resistance: an unresolved question. FEMS Microbiol Rev 2006;30:36–52.
[53] Rodrigues L, Parish T, Balganesh M, Ainsa JA. Antituberculosis drugs: reducing efflux = increasing activity. Drug Discov Today 2017;22:592–9.
[54] Qi J, Wang S, Liu G, Peng H, Wang J, Zhu Z, Yang C. Pyronaridine, a novel modulator of P-glycoprotein-mediated multidrug resistance in tumor cells in vitro and in vivo. Biochem Biophys Res Commun 2004;319:1124–31.
[55] Makarov V, Manina G, Mikusova K, Mollmann U, Ryabova O, Saint-Joanis B, Dhar N, Pasca MR, Buroni S, Lucarelli AP, Milano A, De Rossi E, Belanova M, Bobovska A, Dianiskova P, Kordulakova J, Sala C, Fullam E, Schneider P, McKinney JD, Brodin P, Christophe T, Waddell S, Butcher P, Albrethsen J, Rosenkrands I, Brosch R, Nandi V, Bharath S, Gaonkar S, Shandil RK, Balasubramanian V, Balganesh T, Tyagi S, Grosset J, Riccardi G, Cole ST. Benzothiazinones kill Mycobacterium tuberculosis by blocking arabinan synthesis. Science 2009;324:801–4.
[56] Poce G, Bates RH, Alfonso S, Cocozza M, Porretta GC, Ballell L, Rullas J, Ortega F, De Logu A, Agus E, La Rosa V, Pasca MR, De Rossi E, Wae B, Franzblau SG, Manetti F, Botta M, Biava M. Improved BM212 MmpL3 inhibitor analogue shows efficacy in acute murine model of tuberculosis infection. PLoS One 2013;8:e56980.
[57] Mori G, Chiarelli LR, Esposito M, Makarov V, Bellinzoni M, Hartkoorn RC, Degiacomi G, Boldrin F, Ekins S, de Jesus Lopes Ribeiro AL, Marino LB, Centarova I, Svetlikova Z, Blasko J, Kazakova E, Lepioshkin A, Barilone N, Zanoni G, Porta A, Fondi M, Fani R, Baulard AR, Mikusova K, Alzari PM, Manganelli R, de Carvalho LP, Riccardi G, Cole ST, Pasca MR. Thiophenecarboxamide derivatives activated by EthA kill Mycobacterium tuberculosis by inhibiting the CTP synthetase PyrG. Chem Biol 2015;22:917–27.
[58] Albesa-Jove D, Chiarelli LR, Makarov V, Pasca MR, Urresti S, Mori G, Salina E, Vocat A, Comino N, Mohorko E, Ryabova S, Pfieiffer B, Lopes Ribeiro AL, Rodrigo-Unzueta A, Tersa M, Zanoni G, Buroni S, Altmann KH, Hartkoorn RC, Glockshuber R, Cole ST, Riccardi G, Guerin ME. Rv2466c mediates the activation of TP053 to kill replicating and non-replicating Mycobacterium tuberculosis. ACS Chem Biol 2014;9:1567–75.
[59] Menendez C, Rodriguez F, Ribeiro AL, Zara F, Frongia C, Lobjois V, Saffon N, Pasca MR, Lherbet C, Baltas M. Synthesis and evaluation of alpha-ketotriazoles and alpha,beta-diketotriazoles as inhibitors of Mycobacterium tuberculosis. Eur J Med Chem 2013;69:167–73.
[60] Parikh SL, Xiao G, Tonge PJ. Inhibition of InhA, the enoyl reductase from Mycobacterium tuberculosis, by triclosan and isoniazid. Biochemistry 2000;39:7645–50.
[61] Gellert M, Mizuuchi K, O'Dea MH, Itoh T, Tomizawa JI. Nalidixic acid resistance: a second genetic character involved in DNA gyrase activity. Proc Natl Acad Sci U S A 1977;74:4772–6.
[62] Sugino A, Peebles CL, Kreuzer KN, Cozzarelli NR. Mechanism of action of nalidixic acid: purification of Escherichia coli nalA gene product and its relationship to DNA gyrase and a novel nicking-closing enzyme. Proc Natl Acad Sci U S A 1977;74:4767–71.
[63] Okombo J, Kiara SM, Mwai L, Pole L, Ohuma E, Ochola LI, Nzila A. Baseline in vitro activities of the antimalarials pyronaridine and methylene blue against Plasmodium falciparum isolates from Kenya. Antimicrob Agents Chemother 2012;56:1105–7.
[64] Vivas L, Rattray L, Stewart L, Bongard E, Robinson BL, Peters W, Croft SL. Antimalarial efficacy of pyronaridine and artesunate in combination in vitro and in vivo. Acta Trop 2008;105:222–8.
[65] Wu LJ, Rabbege JR, Nagasawa H, Jacobs G, Aikawa M. Morphological effects of pyronaridine on malarial parasites. Am J Trop Med Hyg 1988;38:30–6.
[66] Auparakkitanon S, Chapoomram S, Kuaha K, Chirachariyavej T, Wilairat P. Targeting of hematin by the antimalarial pyronaridine. Antimicrob Agents Chemother 2006;50:2197–200.
[67] Dorn A, Vippagunta SR, Matile H, Jaquet C, Vennerstrom JL, Ridley RG. An assessment of drug-haematin binding as a mechanism for inhibition of haematin polymerisation by quinoline antimalarials. Biochem Pharmacol 1998;55:727–36.
[68] Famin O, Krugliak M, Ginsburg H. Kinetics of inhibition of glutathione-mediated degradation of ferriprotoporphyrin IX by antimalarial drugs. Biochem Pharmacol 1999;58:59–68.
[69] Sullivan Jr. DJ, Gluzman IY, Russell DG, Goldberg DE. On the molecular mechanism of chloroquine's antimalarial action. Proc Natl Acad Sci U S A 1996;93:11865–70.
[70] Okombo J, Chibale K. Insights into integrated lead generation and target identification in malaria and tuberculosis drug discovery. Acc Chem Res 2017;50:1606–16.
[71] Otta DA, de Araujo FF, de Rezende VB, Souza-Fagundes EM, Eloi-Santos SM, Costa-Silva MF, Santos RA, Costa HA, Siqueira Neto JL, Martins-Filho OA, Teixeira-Carvalho A. Identification of anti-trypanosoma cruzi lead compounds with putative immunomodulatory activity. Antimicrob Agents Chemother 2018 Mar 27;62(4).
[72] Rizk MA, El-Sayed SA, Terkawi MA, Youssef MA, El Said el Sel S, Elsayed G, El-Khodery S, El-Ashker M, Elsify A, Omar M, Salama A, Yokoyama N, Igarashi I. Optimization of a fluorescence-based assay for large-scale drug screening against Babesia and theileria parasites. PLoS One 2015;10:e0125276.
[73] Ekins S, Freundlich J, Clark A, Anantpadma M, Davey R, Madrid P. Machine learning models identify molecules active against Ebola virus in vitro. F1000Res 2015;4:1091.
[74] Aubry A, Fisher LM, Jarlier V, Cambau E. First functional characterization of a singly expressed bacterial type II topoisomerase: the enzyme from Mycobacterium tuberculosis. Biochem Biophys Res Commun 2006;348:158–65.
[75] Manjunatha UH, Dalal M, Chatterji M, Radha DR, Visweswariah SS, Nagaraja V. Functional characterisation of mycobacterial DNA gyrase: an efficient decatenase. Nucleic Acids Res 2002;30:2144–53.
[76] Chavalitshewinkoon P, Wilairat P, Gamage S, Denny W, Figgitt D, Ralph R. Structure-activity relationships and modes of action of 9-anilinoacridines against chloroquine-resistant Plasmodium falciparum in vitro. Antimicrob Agents Chemother 1993;37:403–6.
[77] Ahmed W, Sala C, Hegde SR, Jha RK, Cole ST, Nagaraja V. Transcription facilitated genome-wide recruitment of topoisomerase I and DNA gyrase. PLoS Genet 2017;13:e1006754.
[78] Nagaraja V, Godbole AA, Henderson SR, Maxwell A. DNA topoisomerase I and DNA gyrase as targets for TB therapy. Drug Discov Today 2017;22:510–8.
[79] Kaushik A, Ammerman NC, Tasneen R, Story-Roller E, Dooley KE, Dorman SE, Nuermberger EL, Lamichhane G. In vitro and in vivo activity of biapenem against drug-susceptible and rifampicin-resistant Mycobacterium tuberculosis. J Antimicrob Chemother 2017;72:2320–5.
[80] Gurumurthy M, Verma R, Naftalin CM, Hee KH, Lu Q, Tan KH, Issac S, Lin W, Tan A, Seng KY, Lee LS, Paton NI. Activity of faropenem with and without rifampicin against Mycobacterium tuberculosis: evaluation in a whole-blood bactericidal activity trial. J Antimicrob Chemother 2017;72:2012–9.
[81] Giacobbo BC, Pissinate K, Rodrigues-Junior V, Villela AD, Grams ES, Abbadi BL, Subtil FT, Sperotto N, Trindade RV, Back DF, Campos MM, Basso LA, Machado P, Santos DS. New insights into the SAR and drug combination synergy of 2-(quinolin-4-yloxy)acetamides against Mycobacterium tuberculosis. Eur J Med Chem 2017;126:491–501.
[82] Ngwane AH, Panayides JL, Chouteau F, Macingwana L, Viljoen A, Baker B, Madikane E, de Kock C, Wiesner L, Chibale K, Parkinson CJ, Mmutlane EM, van Helden P, Wiid I. Design, synthesis, and in vitro antituberculosis activity of 2(5H)-Furanone derivatives. IUBMB Life 2016;68:612–20.
[83] Stec J, Onajole OK, Lun S, Guo H, Merenbloom B, Vistoli G, Bishai WR, Kozikowski AP. Indole-2-carboxamide-based MmpL3 inhibitors show exceptional antitubercular activity in an animal model of tuberculosis infection. J Med Chem 2016;59:6232–47.
[84] Grossman TH, Shoen CM, Jones SM, Jones PL, Cynamon MH, Locher CP. The efflux pump inhibitor timcodar improves the potency of antimycobacterial agents. Antimicrob Agents Chemother 2015;59:1534–41.
[85] de Knegt GJ, Ten Kate MT, van Soolingen D, Aarnoutse R, Boeree MJ, Bakker-Woudenberg IA, de Steenwinkel JE. Enhancement of in vitro activity of tuberculosis drugs by addition of thioridazine is not reflected by improved in vivo therapeutic efficacy. Tuberculosis (Edinb) 2014 Dec;94(6):701–7.
[86] Tandon R, Ponnan P, Aggarwal N, Pathak R, Baghel AS, Gupta G, Arya A, Nath M,

Parmar VS, Raj HG, Prasad AK, Bose M. Characterization of 7-amino-4-methylcoumarin as an effective antitubercular agent: structure-activity relationships. J Antimicrob Chemother 2011;66:2543–55.

[87] Neres J, Hartkoorn RC, Chiarelli LR, Gadupudi R, Pasca MR, Mori G, Venturelli A, Savina S, Makarov V, Kolly GS, Molteni E, Binda C, Dhar N, Ferrari S, Brodin P, Delorme V, Landry V, de Jesus Lopes Ribeiro AL, Farina D, Saxena P, Pojer F, Carta A, Luciani R, Porta A, Zanoni G, De Rossi E, Costi MP, Riccardi G, Cole ST. 2-Carboxyquinoxalines kill mycobacterium tuberculosis through noncovalent inhibition of DprE1. ACS Chem Biol 2015;10:705–14.

Esta tesis se terminó de imprimir el 24 de marzo de 2019,

día que conmemora la primera descripción

de la bacteria *Mycobaterium*

tuberculosis

en 1882 por

Robert

Koch